

# **Separation of Azeotropic Mixtures: Tools for Analysis and Studies on Batch Distillation Operation**

Eva-Katrine Hilmen

*A Thesis Submitted for the Degree of Dr. Ing.*

Norwegian University of Science and Technology  
Department of Chemical Engineering

November 2000



## Abstract

Separation of azeotropic mixtures is a topic of great practical and industrial interest. Most liquid mixtures of organic components form nonideal systems. The presence of some specific groups, particularly polar groups (oxygen, nitrogen, chlorine and fluorine), often results in the formation of azeotropes. Azeotropic mixtures may often be effectively separated by distillation by adding a liquid material (entrainer) to the system.

For the development of separation processes for azeotropic mixtures, there is a need for insight into the fundamental phenomena of nonideal and azeotropic phase equilibria. This thesis includes a detailed survey on azeotropic phase equilibrium diagrams of ternary mixtures. Diagram analysis is shown to be an efficient tool for prediction of feasible separations. As a simplifying concept it is proposed that all feasible structures of ternary azeotropic phase equilibrium diagrams can be qualitatively represented by a few elementary cells of which only four have so far been reported to exist. This greatly reduces the complexity of azeotropic distillation analysis and is a key to a simple evaluation of the possibilities and limitations of azeotropic mixtures separation.

Insights gained from continuous azeotropic distillation is extended to the operation of batch distillation with focus on the dynamics and control of multivessel and extractive batch distillation as processes for separating azeotropic mixtures. Practical implications of this renewed insight for the fine- and specialty chemical industries are given in the concluding pages of the thesis.

## Preface

This thesis is submitted in partial fulfillment of the requirements for the degree *doktor ingeniør* at the Norwegian University of Science and Technology (NTNU). The majority of the work has been carried out during the period from 1994 to 1999 at the Department of Chemical Engineering, NTNU with Professor Sigurd Skogestad as main advisor. Since 1997, Dr. Valeri N. Kiva from Karpov Institute of Physical Chemistry in Moscow has been a co-advisor of the thesis.

I spent the academic year 1995-96 in the group of Professor Michael F. Doherty and Professor Michael F. Malone at the Department of Chemical Engineering at the University of Massachusetts in Amherst. The following academic year 1996-97, Dr. Valeri N. Kiva was a visiting researcher in our group at NTNU. I had one year maternity leave in 1999-2000.

The work is a part of an industrial project on solvent recovery in fine and specialty chemical industries in cooperation with Borregaard, Nycomed Imaging, Norsk Hydro and Dyno Industries. The project has been organized through the Fine and Specialty Chemicals and PROSMAT programs of the Research Council of Norway. The efforts of the industrial participants is greatly appreciated. My visits to the plants and production facilities were very fortunate. Special thanks to Thor Alvik at Borregaard and Joachim Schmidt at Nycomed Imaging for their contributions.

I would like to thank my advisor Professor Sigurd Skogestad for his invaluable advice and contributions to this work. His insights and high standards have definitely helped to shape this work. It is a pleasure to have an advisor being so joyful in his work and creative in his research.

I am in particular indebted to Dr. Valeri N. Kiva for his significant impact on the course of this work. His insight to the field of azeotropic distillation and to practical distillation operation has been most valuable. Many achievements of his research are included in this thesis. Thanks also for being a man of strong character. Our discussions have been most amusing and enlightening.

My thanks goes to Professor Michael F. Doherty and Professor Michael F. Malone for a great and inspiring year in their group at the University of Massachusetts in Amherst, introducing me to the many aspects of azeotropic distillation and nonideal thermodynamics.

Thanks to former and present colleagues at NTNU for making an enjoyable working environment. Stewart Clark, Stathis, Hilde, Lucie and Jan are thanked for proofreading parts of the thesis. Ingvild for being my confidant. I acknowledge the assistance of Dr. Bella Alukhanova in drawing the figures for the survey on azeotropic phase equilibrium diagrams (Chapter 3) in this thesis.

Finally, I want to express gratitude to my parents, sister and grandparents for their unconditional support and encouragement. My warmest thanks goes to my husband Erik for putting up with me during what must have been demanding times. Without his immense support and patience this work would not have resulted. Our beloved daughter Tone was born in June 1999 and the thesis completed in November 2000, beginning a new era in our lives.

Financial support from the Research Council of Norway, Borregaard, Nycomed Imaging, Norsk Hydro, Dyno Industries, PROST and the Fulbright Foundation is gratefully acknowledged.

# Contents

<b>Abstract</b>	<b>i</b>
<b>Preface</b>	<b>ii</b>
<b>1 Introduction</b>	<b>1</b>
1.1 Motivation and industrial relevance . . . . .	1
1.2 Thesis overview . . . . .	4
1.3 The reader's guide to the thesis . . . . .	5
<b>I Principles and Tools for Analysis</b>	<b>7</b>
<b>2 Methods of Azeotropic Mixtures Separation: General Considerations</b>	<b>9</b>
2.1 Introduction . . . . .	9
2.2 Azeotropy . . . . .	10
2.2.1 What is <i>azeotropy</i> ? . . . . .	10
2.2.2 Vapor-liquid phase equilibrium, nonideality and azeotropy . . . . .	11
2.2.3 Nonideality and separation by distillation . . . . .	13
2.2.4 Physical phenomena leading to nonideality and azeotropy . . . . .	14
2.3 General separation processes . . . . .	16
2.3.1 Membrane-distillation hybrids . . . . .	17
2.3.2 Pressure-swing distillation . . . . .	20
2.3.3 Entrainer-addition distillation methods . . . . .	21
2.3.4 Discussion . . . . .	22
2.4 Entrainer-addition distillation methods . . . . .	25
2.4.1 Feasibility analysis . . . . .	25
2.4.2 Feasibility analysis for azeotropic mixtures . . . . .	26

2.4.3	Homogeneous azeotropic distillation . . . . .	27
2.4.4	Heteroazeotropic distillation . . . . .	32
2.4.5	Extractive distillation . . . . .	35
2.4.6	Entrainer selection . . . . .	40
2.5	Summary and conclusions . . . . .	41
<b>3</b>	<b>Azeotropic Phase Equilibrium Diagrams: A Survey</b>	<b>43</b>
3.1	Introduction . . . . .	43
3.2	Thermodynamic basis . . . . .	48
3.3	Isotherm maps of ternary mixtures . . . . .	52
3.4	Open evaporation . . . . .	55
3.4.1	Residue curves . . . . .	55
3.4.2	Properties of residue curves' singular points . . . . .	57
3.4.3	Rule of azeotropy . . . . .	60
3.4.4	Structure of residue curve maps . . . . .	62
3.4.5	Separatrices of residue curves and flexure of the boiling temperature surface	65
3.4.6	Structure of distillate curve maps . . . . .	67
3.5	Other simple equilibrium phase transformations . . . . .	67
3.5.1	Open condensation . . . . .	67
3.5.2	Repeated equilibrium phase mapping and distillation lines . . . . .	68
3.5.3	Relationship between residue curves, distillation lines and condensation curves . . . . .	71
3.6	Heterogeneous mixtures . . . . .	73
3.6.1	Simple phase transformations in heterogeneous mixtures . . . . .	74
3.6.2	Examples of simple equilibrium phase transformation maps . . . . .	75
3.7	Ternary VLE diagrams. Classification, occurrence and structure determination . .	79
3.7.1	Classifications of ternary VLE diagrams . . . . .	79
3.7.2	Completeness of classifications . . . . .	83
3.7.3	Occurrence of predicted structures . . . . .	83
3.7.4	Determination of the structure . . . . .	88
3.8	Unidistribution and univolatility lines . . . . .	95
3.8.1	Distribution coefficient and relative volatility . . . . .	95
3.8.2	Univolatility and unidistribution line diagrams . . . . .	96
3.8.3	Structure of unidistribution and univolatility line diagrams . . . . .	103
3.9	Conclusions . . . . .	117
	Definitions of Terms . . . . .	118

<b>4</b>	<b>On the Topology of Ternary VLE Diagrams: Elementary Cells</b>	<b>123</b>
4.1	Introduction . . . . .	123
4.2	Classification of ternary VLE diagrams . . . . .	124
4.3	Elementary cells . . . . .	126
4.4	Occurrence in nature . . . . .	128
4.5	Use of elementary cells . . . . .	131
4.5.1	The album . . . . .	131
4.5.2	Multiple steady states . . . . .	132
4.6	Pseudo-component subsystem . . . . .	133
4.7	Conclusion . . . . .	134

## **II Studies on Batch Distillation Operation** **137**

<b>5</b>	<b>Holdup Effect in Residue Curve Map Prediction of Batch Distillation Products</b>	<b>139</b>
5.1	Introduction . . . . .	139
5.2	Model and data . . . . .	142
5.3	Results and discussion . . . . .	145
5.4	Conclusion . . . . .	150
	Appendix 5A . . . . .	151
<b>6</b>	<b>Batch Distillation Columns and Operating Modes: Comparison</b>	<b>153</b>
6.1	Introduction . . . . .	153
6.2	Batch distillation column configurations . . . . .	154
6.2.1	Regular and inverted columns . . . . .	154
6.2.2	Middle vessel and multivessel columns . . . . .	154
6.3	Operating policies . . . . .	157
6.3.1	Open operation (conventional) . . . . .	158
6.3.2	Closed operation . . . . .	158
6.3.3	Cyclic operation . . . . .	159
6.3.4	Semicontinuous operation . . . . .	159
6.4	Comparison of cyclic and closed middle vessel columns . . . . .	159
6.4.1	Results . . . . .	161
6.4.2	Discussion . . . . .	162
6.4.3	Comparison with integrated continuous distillation . . . . .	163
6.4.4	Conclusion . . . . .	164

<b>7</b>	<b>Closed Multivessel Batch Distillation of Ternary Azeotropic Mixtures</b>	<b>169</b>
7.1	Introduction . . . . .	169
7.2	Columns and operating modes for ternary separation . . . . .	171
7.3	VLE diagrams and steady state composition profiles . . . . .	173
7.4	Mixtures studied . . . . .	174
7.5	Mathematical model . . . . .	176
7.6	Simulation results . . . . .	177
7.6.1	Results on ternary zeotropic mixture (Cell I) . . . . .	179
7.6.2	Results on ternary azeotropic mixture (Cell II) . . . . .	183
7.6.3	Results on ternary azeotropic mixture with one distillation boundary . . . . .	194
7.7	Discussion and suggestions for further research . . . . .	200
7.8	Conclusion . . . . .	202
	Appendix 7A . . . . .	203
<b>8</b>	<b>Extractive Batch Distillation: Column Schemes and Operation</b>	<b>207</b>
8.1	Introduction . . . . .	207
8.2	Mixtures studied . . . . .	211
8.3	Mathematical model and assumptions . . . . .	213
8.4	Extractive batch distillation in the conventional column . . . . .	214
8.4.1	Process description . . . . .	214
8.4.2	Simulation results for System 1 (ethanol - water - ethylene glycol) . . . . .	215
8.4.3	Simulation results for System 2 (acetone - methanol - water) . . . . .	219
8.4.4	Summary: Extractive batch distillation . . . . .	226
8.5	Extractive batch distillation in the middle vessel column . . . . .	226
8.5.1	Process description . . . . .	226
8.5.2	Simulation results with simultaneous separation (Scheme I) . . . . .	229
8.5.3	Summary: Extractive middle vessel batch distillation . . . . .	233
8.6	Conclusion . . . . .	233
	Appendix 8A . . . . .	234
<b>9</b>	<b>Control Strategies for Extractive Middle Vessel Batch Distillation</b>	<b>237</b>
9.1	Introduction . . . . .	237
9.2	Important considerations for control . . . . .	239
9.3	Two-point composition control . . . . .	240
9.4	Simulation model . . . . .	242
9.5	Closed loop simulation results . . . . .	242



9.5.1 Closed loop simulation results (Scheme I: simultaneous) . . . . . 245  
9.5.2 Closed loop simulation results (Scheme II: sequential) . . . . . 251  
9.6 Discussion and further work . . . . . 255  
9.7 Conclusion . . . . . 255

**III Conclusions 257**

**10 Practical Implications, Conclusions and Suggestions for Future Work 259**

10.1 Practical implications . . . . . 259  
10.2 Conclusions . . . . . 262  
10.3 Suggestions for future work . . . . . 263

**Note Concerning the References 267**

**References 269**



# Chapter 1

## Introduction

How should a given liquid mixture be separated? Let the nature of the mixture determine its way of separation, my advisor Valeri N. Kiva would say, meaning that one needs to consider the properties of each particular mixture. Nature seldom behaves ideally. Complexities like the formation of azeotropes may introduce an obstacle for the separation. Yet, it may be used to promote or enhance separation too. In this thesis, possibilities and limitations imposed by the formation of azeotropes in liquid mixtures are investigated. Distillation-based separation techniques are focused and flexible batch operation is promoted for the particular example of solvent recovery in the fine- and specialty chemical industries.

### 1.1 Motivation and industrial relevance

Industrial production of chemicals involves purification and recovery of the products, by-products and unreacted raw materials. Distillation is clearly the dominating separation process, accounting for more applications than all the others combined (extraction, adsorption, crystallization, membrane-based technologies and so forth). In fact, distillation columns consume more than 95% of the total energy used in separations in chemical process industries Worldwide (Ognisty, 1995).

*“It is not easy to put a new face on a technology as old as that of distillation. And yet, the economic impact of even minor, but general, improvements in the method can be most substantial. We workers in the area have a responsibility to make distillation a more efficient and effective separation method – while striving always to recognize those instances when it really is not the best way to take the mixture apart.”*

Fair (1987)

All liquid mixtures have forces of intermolecular attraction. That is why they form liquids and not gases. The molecular interactions when two or more components are mixed may cause the mixture to form certain “inseparable” compositions where the vapor and liquid compositions at equilibrium are equal within a given pressure and temperature range. These specific mixture compositions are called azeotropes. Azeotropy is not a rare phenomena.

Azeotropy plays an important role in vapor-liquid equilibrium separation processes such as distillation, similar to eutetics and peretetics in liquid-solid systems such as crystallization. To be able to develop separation processes for azeotropic mixtures, there is a need for insight into the fundamental phenomena of azeotropic phase equilibria. The vapor-liquid envelope of the equilibrium temperature surfaces defines the feasible operating region in which any real distillation process must operate. The existence of azeotropes complicates the structure of this operating envelope, and the resulting distillation behavior of multicomponent azeotropic mixtures may be very complex. The main interest behind azeotropic phase equilibrium diagrams is to reveal all the physiochemical restrictions imposed on the separation process by the nature of the mixture in question. Diagram analysis provides important insight for the optimal choice of separation method and the design and synthesis of azeotropic distillation separation systems. Thus, there is an incentive to look more carefully into the field of vapor-liquid equilibrium diagrams and the so-called *thermodynamic topological analysis* of azeotropic mixtures.

### **Tools for analysis: graphical methods**

Nonideal and azeotropic phase equilibrium diagrams like residue curve maps are sometimes nicknamed the *McCabe-Thiele of azeotropic distillation* (Kunesh *et al.*, 1995), indicating its importance as a graphical design tool in distillation separation of azeotropic mixtures. The term *analysis-driven synthesis* is used by Westerberg and Wahnschafft (1996) to emphasize that the real work in synthesis of nonideal separation sequences is to establish enough information to begin the synthesis process. Such pre-synthesis analysis involves determination of the nonideal behavior of the mixture (finding azeotropes, discovering liquid-liquid behavior, pressure dependencies, distillation behavior and so forth). Graphical representations of the vapor-liquid equilibrium with material balance lines, operating lines and distillation composition trajectories drawn into the diagram are commonly used for such analysis.

The power of graphical representation is it gives insight and understanding. Human beings have the ability to identify problems and see patterns, and extract information from these. On a graph one can see the effects of changes clearly and often sources of a particular problem becomes obvious.

Using azeotropic phase equilibrium diagrams (like residue curve maps), we can immediately identify infeasible specifications and alternative distillation sequences can be proposed without trial and error. The shapes of the distillation lines (or residue curves) are very useful in the design of real finite reflux distillation columns since they give a qualitative picture of the composition profiles in actual staged distillation columns (Wasylkiewicz *et al.*, 1999a).

In retrofit operations, graphical VLE diagrams can help to understand the behavior of the azeotropic system when attempting to change operating conditions, and can be used to ensure that it is

thermodynamically possible to move from the initial state to the final state (Wasylkiewicz *et al.*, 1999a). By analyzing the residue curve map topology, troubleshooting process difficulties, reasons for controllability and purity problems can be quickly identified (Wasylkiewicz *et al.*, 1999a).

### Solvent recovery in fine- and specialty chemical industries

As waste regulations are becoming more stringent, the economical benefits of having recovery systems that allow for recycling and reuse of the solvents within the process are significant. Recovery and reuse of organic solvents is generally practiced because of increased solvent costs and potential solvent shortages and because disposal often results in violation of air-, water- or land-pollution regulations.

The work presented in this paper is connected to an industrial project on solvent recovery in four Norwegian fine- and specialty chemical plants. The production facilities under consideration process high-value products at moderate to low volumes. The process feed stocks often vary both in size and quality from one day to another, which favors flexible processing equipment. The existing equipment is mainly conventional batch distillation columns. The solvent recovery typically involves purification of low-boiling organic solvents that form minimum-boiling homoazeotropes with water. Azeotropy and the highly nonideal behavior during distillation complicates the recovery of the solvents. As a contradiction to this, high purities above azeotrope composition are usually required in order to reuse the waste solvents in the bulk synthesis operations. Often solvent mixtures that cannot be fully recovered end up as toxic waste crossing the plant boundary.

*“Designing equipment for such [azeotropic] separations is a real challenge to the distillation engineer. Often, sufficient data are not available for complete calculation so that the process must be developed in the laboratory, or, at least, assumptions checked. Combinations of continuous and batch distillations, decanting, multistage extraction, and chemical treatment may often be combined in a successful process.”*

Drew as quoted by Schweitzer (1997)

The thesis focus is on various batch distillation configurations for separating azeotropic mixtures. Interest in batch processes has increased with the growing importance of specialty chemicals, characterized by high-value, low-capacity, short-term production and strongly nonideal liquid mixtures. These high value-added products often require high purity and this makes the separation step an important part of the process. The use of solvents is unavoidable to many processes in the fine- and special chemical industries.

*“An understanding of azeotropes is desirable for two reasons. First, they often occur in distillation and make a given separation impossible by ordinary distillation. Secondly, they may be utilized to separate mixtures not ordinarily separable by straight distillation.”*

Ewell *et al.* (1944)

This statement clearly sets the perspective in which the work presented in this thesis has been conducted. Dealing with solvent recovery distillation systems this inevitable includes azeotropic

mixtures. Further, some of the established and very powerful separation methods for solvent mixtures, even those solvent mixtures that do not form azeotropes, utilize the formation of azeotropes to increase the effectiveness of the distillation separation.

## 1.2 Thesis overview

The thesis contents is twofold as the title indicates. First, general aspects of azeotropic mixtures separation and tools for the analysis of their thermodynamic behavior during distillation are considered. Second, extensions to batch distillation operation are made, which include simulation studies of multivessel and extractive batch distillation with emphasis on operation and control.

The thesis is organized in three parts: Part I (Chapter 2 - 4) comprises theory on separation methods for azeotropic mixtures and structural properties of ternary phase equilibrium diagrams, Part II (Chapter 5 - 9) involves studies on azeotropic batch distillation and Part III (Chapter 10) gives practical implications for an industrial project connected to the thesis and overall conclusions. The thesis chapter-by-chapter:

### Part I Principles and Tools for Analysis

**Chapter 2** gives an *introduction* to the phenomenon of azeotropy and the various methods by which azeotropic mixtures can be separated. The possibilities to separate azeotropic mixtures by entrainer-addition distillation, and in particular extractive distillation, are considered.

**Chapter 3** comprises a *survey* of vapor-liquid equilibrium (VLE) diagrams which reveal the basic thermodynamic phenomena of nonideal and azeotropic mixtures. The survey is a result of a cooperation performed in parallel with more specific studies on azeotropic batch distillation. The main contributor of the survey is Valeri N. Kiva.

**Chapter 4** presents the novel concept of *elementary topological cells* of ternary VLE diagrams and discuss the occurrence of the thermodynamic feasible structures in nature. Some uses of the elementary cells in azeotropic distillation presynthesis analysis are included.

### Part II Studies on Batch Distillation Operation

**Chapter 5** includes a study on the *effect of holdup* in azeotropic batch distillation product prediction based on residue curve map analysis.

**Chapter 6** gives an introduction and overview of various batch distillation columns and modes of operation, along with a *comparative study* on two alternative operating policies for the multivessel batch distillation column. This chapter only considers ideal (constant relative volatility) mixtures.

**Chapter 7** considers the direct application of VLE diagram tools in *closed multivessel batch distillation* analysis. The chapter includes dynamic simulation of the cyclic batch column and the closed middle vessel column for the separation of ternary azeotropic mixtures. An indirect level control strategy is implemented that eliminates the need for pre-calculated vessel holdups. VLE

diagram information is used for operation and control considerations.

**Chapter 8** considers *extractive batch distillation* schemes and operation. Extension of extractive distillation insights to batch operation is performed. Simulation studies on extractive distillation in the conventional batch column and extractive distillation in the middle vessel batch column with three modifications of the middle vessel configuration are presented.

**Chapter 9** presents *control strategies* for extractive distillation in the middle vessel batch column with closed loop simulations. This is the first study reported on control of this process.

### Part III Conclusions

**Chapter 10** provides practical guidelines on *how to approach* a given liquid mixture separation task, and overview of the overall conclusions of the thesis and suggestions for future work.

SpeedUp inputfiles for the dynamic simulation models used in Chapters 5-9, and MATLAB m-files for the vapor-liquid equilibrium calculation of isotherms and distillation lines, are available at <http://www.chembio.ntnu.no/users/skoge/distillation/> under *Speedup and Matlab files*.

## 1.3 The reader's guide to the thesis

The thesis span a broad field of research. Not all the topics are of interest to every reader. Here is the author's proposal of highlights for the readers involved in the following three areas:

Process synthesis (azeotropic distillation): Chapter 3 and 4

Process control (azeotropic and batch): Chapter 4 and 9

Industrial separation of azeotropic mixtures: Chapters 2 and 10

An alphabetical listing with definitions of central terms as they are used in the thesis is given in *Definitions of terms* (p. 118). An overview (quick reference) of alternative terms found in English-language, Russian and German literature is given in Table 3.1 (p. 46).





## **Part I**

# **Principles and Tools for Analysis**



## Chapter 2

# Methods of Azeotropic Mixtures Separation: General Considerations

In most cases, azeotropic mixtures require special methods to facilitate their separation. There is a need to search for a separating agent other than energy, and this agent might be a membrane material for pervaporation or an entrainer for extractive distillation.

This chapter gives an introduction to the phenomena of azeotropy and outlines various methods to separate homogeneous azeotropic mixtures. Distillation methods based on the addition of an entrainer for extractive and heteroazeotropic distillation are described in more detail.

### 2.1 Introduction

In spite of the intensive research in the field of azeotropic mixtures separation, especially during the last 15 years, there seems to be no clear vision of the possibilities and applicability of the methods. This is the motivation for the present chapter. An introduction to the phenomena of azeotropy and nonideal vapor-liquid equilibrium behavior is given before we consider various methods to separate azeotropic mixtures.

In general, separation of homogeneous liquid mixtures requires the creation or addition of another phase within the system. The most common method is repeated vaporization and condensation - distillation - where the vapor phase becomes gradually enriched in the more volatile component(s) compared to the liquid. Alternatives to distillation are adsorption, membrane separation, crystallization, liquid-liquid extraction, chromatography and others (Smith, 1995).

Separation of a liquid mixture by distillation is dependent on the fact that even when a liquid is partially vaporized, the vapor and liquid compositions differ. The vapor phase becomes enriched in the more volatile components and is depleted in the less volatile components with respect to its equilibrium liquid phase. By segregating the phases and repeating the partial vaporization, it is often possible to achieve the desired degree of separation.

An azeotrope cannot be separated by ordinary distillation since no enrichment of the vapor phase occurs at this point. Therefore, in most cases, azeotropic mixtures require special methods to facilitate their separation. Such methods utilize a mass separating agent other than energy that causes or enhances a selective mass transfer of the azeotrope-forming components. This agent might be a membrane material for pervaporation or an entrainer for extractive distillation. Extractive and heteroazeotropic distillation are the most common methods, and are described in more detail in a separate section in this chapter.

## 2.2 Azeotropy

### 2.2.1 What is azeotropy?

The term *azeotrope* means “nonboiling by any means” (Greek: *a* - non, *zeo* - boil, *tropos* - way/mean), and denotes a mixture of two or more components where the equilibrium vapor and liquid compositions are equal at a given pressure and temperature. More specifically, the vapor has the same composition as the liquid and the mixture boils at a temperature other than that of the pure components’ boiling points. Azeotropes have sometimes been mistaken for single components because they boil at a constant temperature. However, for an azeotrope a variation in pressure changes not only the boiling temperature, but also the composition of the mixture, and this easily distinguishes it from a pure component.

The term *azeotropy* was introduced by Wade and Merriman in 1911 to designate mixtures characterized by a minimum or a maximum in the vapor pressure under isothermal conditions, or, equivalently, with an extremal point in the boiling temperature at constant pressure (Swietoslawski, 1963; Malesinski, 1965). Since then the term has been used for liquid systems forming one or several azeotropes. The mixture whose composition corresponds to an extremal point is called an *azeotrope*. If at the equilibrium temperature the liquid mixture is homogeneous, the azeotrope is a *homoazeotrope*. If the vapor phase coexists with two liquid phases, it is a *heteroazeotrope*. Systems which do not form azeotropes are called *zeotropic* (Swietoslawski, 1963). A brief history of the first observations of azeotropy is given in, for example, Gmehling *et al.* (1994).

The defining conditions of an azeotropic mixture and the physical phenomena leading to nonideality and azeotropy are questions that are addressed in more detail in the next sections.

### 2.2.2 Vapor-liquid phase equilibrium, nonideality and azeotropy

At low to moderate pressures and temperatures away from the critical point, the vapor-liquid phase equilibrium for a multicomponent mixture may be expressed as:

$$y_i P = x_i \gamma_i(T, \mathbf{x}) P_i^{sat}(T), \quad i = 1, 2, \dots, n \quad (2.1)$$

where  $y_i$  and  $x_i$  are the vapor and liquid compositions of component  $i$ , respectively,  $P$  and  $T$  are the system pressure and temperature,  $\gamma_i$  is the activity coefficient of component  $i$  in the liquid phase, and  $P_i^{sat}$  is the saturated vapor pressure of component  $i$ . The activity coefficient  $\gamma_i$  is a measure of the nonideality of a mixture and changes both with temperature and composition. When  $\gamma_i = 1$ , the mixture is said to be ideal and Equation (8.2) simplifies to Raoult's law:

$$y_i P = x_i P_i^{sat}(T), \quad i = 1, 2, \dots, n \quad (2.2)$$

Nonideal mixtures exhibit positive ( $\gamma_i > 1$ ) or negative ( $\gamma_i < 1$ ) deviations from Raoult's law. If these deviations become so large that the vapor pressure exhibits an extremal point at constant temperature, or, equivalently, an extremal point in the boiling temperature at constant pressure, the mixture is *azeotropic*. At azeotropic points, the liquid phase and its equilibrium vapor phase have the same composition  $\mathbf{x} = \mathbf{y}$ , and the condensation and boiling temperature curves are tangential with zero slope (see Figure 2.1a). If the positive deviations are sufficiently large ( $\gamma_i > 4$ ,

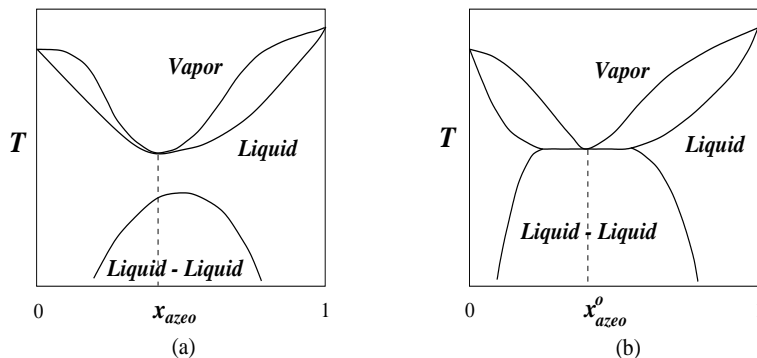


Figure 2.1: Azeotropes may be homogeneous or heterogeneous. Binary phase diagram with minima in the condensation and boiling temperatures at constant pressure (positive deviation): (a) minimum-boiling homoazeotrope; (b) heteroazeotrope.

typically), phase splitting may occur and form a heteroazeotrope where the vapor phase is in equilibrium with two liquid phases (see Figure 2.1b). In the heteroazeotropic point the overall liquid composition  $x_{azeo}^o$  is equal to the vapor composition, and the vapor and liquid temperature surfaces are tangential with zero slope, but the three coexisting phases have distinct compositions. In ternary and multicomponent systems *saddle* azeotropes may occur, which Swietoslowski (1963) call *positive-negative* azeotropes. The first reported ternary saddle azeotrope was the acetone,

chloroform and methanol mixture shown in Figure 2.2, which was examined by Ewell and Welch (1945). Saddle azeotropic mixtures exhibit a hyperbolic point in the temperature isobar which is

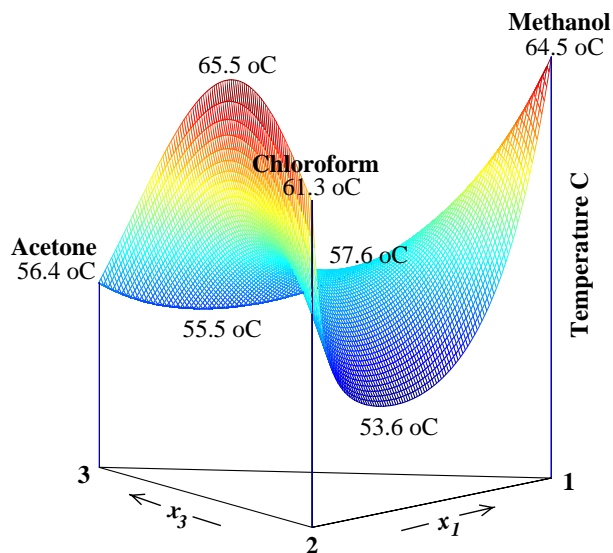


Figure 2.2: Complex azeotropic behavior of a ternary mixture. Boiling temperature surface as a function of liquid composition for the mixture of acetone, chloroform and methanol forming three binary azeotropes and one ternary saddle azeotrope at atmospheric pressure.

neither a minimum nor a maximum in either boiling temperature or vapor pressure (see Figure 2.2, saddle point at 57.6 °C). The corresponding residue curve diagram is shown in Figure 2.3.

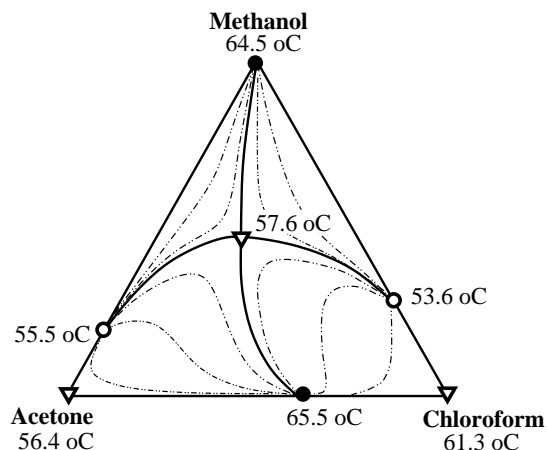


Figure 2.3: Residue curve map for the mixture in Figure 2.2. The residue curves' singular points are indicated by ● (stable node), ○ (unstable node) and ∇ (saddle), and boundaries by bold lines.

A mixture is said to be *tangentially azeotropic* if the boiling temperature isobar exhibits an extremal point located at the pure component edges, i.e., at zero concentration for one or several of the components in the mixture (Swietoslawski, 1963). A mixture is said to be *tangentially zeotropic* if the boiling temperature at constant pressure exhibits a *nearly* extreme point at zero concentration for one or several of the components. This phenomenon is also called a *tangent pinch* (Doherty and Knapp, 1993). Such mixtures are of great practical importance (Serafimov, 1987). Examples of common tangentially zeotropic mixtures are acetic acid and water and acetone and water. The binary phase diagram for the acetone and water mixture is given in Figure 2.4. The mixture exhibits a tangent pinch at the acetone edge.

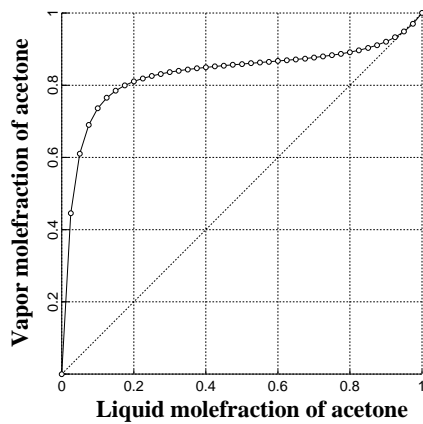
### 2.2.3 Nonideality and separation by distillation

One measure of the degree of enrichment, or, the ease of separation, is the relative volatility between pair of the components, derived from Equation (8.2):

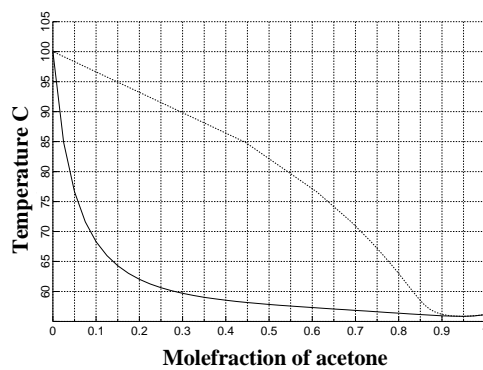
$$\alpha_{ij} = \frac{y_i/x_i}{y_j/x_j} = \frac{\gamma_i P_i^{sat}}{\gamma_j P_j^{sat}} \quad (2.3)$$

The relative volatility of most mixtures changes with temperature, pressure and composition. The more  $\alpha_{ij}$  deviates from unity, the easier it is to separate component  $i$  from component  $j$ . At an azeotropic point, the relative volatility of the azeotrope-forming components equals one ( $\alpha_{ij} = 1$ ) and it is impossible to further enrich the vapor. Thus azeotropes can never be separated into pure components by ordinary distillation. However, *heteroazeotropes* may be separated into its two liquid phases by other methods such as decantation. Similarly, any mixture where the relative volatilities are close to unity is difficult to separate by ordinary distillation since little enrichment occurs with each partial vaporization step. Typically, conventional distillation becomes uneconomical when  $0.95 < \alpha_{ij} < 1.05$  (there are exceptions), since a high reflux ratio and a large number of theoretical equilibrium stages are required (Van Winkle, 1967). The special methods used to facilitate the separation of azeotropic mixtures may also be applied to close-boiling zeotropic mixtures.

Note that ternary and multicomponent mixtures may have a locus in the composition space where the relative volatility between a pair of the components is equal to unity without forming any azeotropes. The presence of such *univolatility lines* does not hinder separation of the mixture by ordinary distillation. It only means that the relative volatility order of the components changes within the composition space and this is common for nonideal mixtures. Therefore, the terms “light”, “intermediate” and “heavy” that are often used to indicate the relative volatility order of the pure components in ternary mixtures have limited meaning for nonideal and azeotropic mixtures.



(a)



(b)

Figure 2.4: Tangent pinch is a common phenomenon. Binary phase diagram for acetone and water mixture at atmospheric pressure: (a) vapor and liquid equilibrium compositions; (b) condensation and boiling temperatures as a function of composition.

## 2.2.4 Physical phenomena leading to nonideality and azeotropy

Why are azeotropes formed? Azeotropy is merely a characteristic of the highly nonlinear phase equilibria of mixtures with strong molecular interactions. Azeotropes are formed due to differences in intermolecular forces of attraction among the mixture components (hydrogen bonding



and others). The particular deviation from ideality is determined by the balance between the physiochemical forces between identical and different components. Briefly, we have three groups:

1. *Positive deviation from Raoult's law*: The components “dislike” each other. The attraction between identical molecules (A-A and B-B) is stronger than between different molecules (A-B). This may cause the formation of a minimum-boiling azeotrope and heterogeneity.
2. *Negative deviation from Raoult's law*: The components “like” each other. The attraction between different molecules (A-B) is the strongest. This may cause the formation of a maximum-boiling azeotrope.
3. *Ideal mixture obeys Raoult's law*: The components have similar physiochemical properties. The intermolecular forces between identical and different molecules (A-A, B-B and A-B) are equal.

For simplicity, the above explanation is given for binary mixtures. The main difference for ternary and multicomponent mixtures is that an azeotropic point is not necessarily an absolute extreme (minimum or maximum point) of the boiling temperature at isobaric condition, but it may be a local extreme (saddle).

The tendency of a mixture to form an azeotrope depends on two factors: (i) the difference in the pure component boiling points, and (ii) the degree of nonideality (Horsley, 1973; King, 1980). The closer the boiling points of the pure components and the less ideal mixture, the greater the likelihood of an azeotrope. A heuristic rule is given in Perry and Chilton (1973) that azeotropes occur infrequently between compounds whose boiling points differ by more than about 30 °C. An important exception to this rule is heteroazeotropic mixtures where the components may have a large difference in the boiling points of the pure components, and still exhibit strong nonideality and immiscibility regions. In heterogeneous mixtures the different components may even repel each other (Group 1 in the above list). This is why only minimum-boiling heteroazeotropes occur in nature.

Swietoslawski (1963) emphasizes that most mixtures of organic compounds form nonideal systems. The presence of some specific groups, particularly polar groups (oxygen, nitrogen, chlorine and fluorine), often results in the formation of azeotropes. Roughly half of the 18 800 binary systems collected in Gmehling *et al.* (1994) are azeotropic. More than 90 % of the known azeotropes show positive azeotropy, that is, minimum-boiling azeotropes in the binary case (Lecat, 1949; Rousseau, 1987; Gmehling *et al.*, 1994). Further, more than 80 % of these are homoazeotropic (Gmehling *et al.*, 1994).

Ideal or nearly ideal behavior is encountered in mixtures formed by closely related chemical substances such as heptane and hexane, or butyl alcohol and hexyl alcohol. However, there are exceptions to this heuristic rule as well. If there is a point in the composition space in which the vapor pressures of the two components are equal at a given temperature (in the region of the normal boiling-points of the pure components), this may correspond to an azeotropic point which is called a Bancroft point, illustrated in Figure 2.5. This is referred to as Bancroft's rule (Malesinski, 1965). The intermolecular forces in the mixture may be similar, but the mixture still

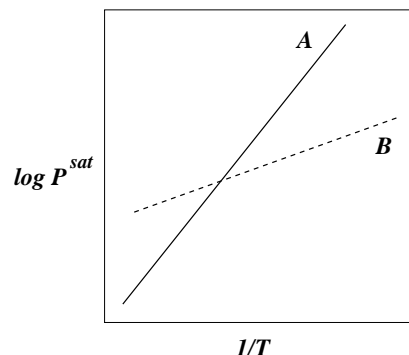


Figure 2.5: Bancroft point. Intersection of the vapor pressure curves of the pure components A and B at a given temperature.

exhibits an azeotropic behavior. An example of such an azeotrope-forming mixture of nonpolar substances is benzene and cyclohexane. Note that many exceptions to Bancroft's rule are found (Swietoslowski, 1963; Malesinski, 1965) and it should be used only as an indication. Out of 972 mixtures examined by Rechenberg (1921, 1923) and Lecat (1929), 489 (50 %) have a Bancroft point, but only 377 (40 %) form azeotropes (Malesinski, 1965). Bancroft's rule is neither a necessary nor a sufficient condition for the formation of an azeotrope, and, thus, does not play an important role in determining whether a mixture forms azeotropes or not.

## 2.3 General separation processes

There are various methods for separating liquid mixtures that form one or more homoazeotropes. Distillation methods are the oldest and most exploited, either by pressure variation or the addition (and subsequent separation) of an agent, called an entrainer, that alters the phase equilibrium of the mixture. Other alternative separation techniques for azeotropic mixtures, such as membrane separation, are usually combined with distillation. Augmenting distillation with complementary separation technologies are commonly referred to as *hybrid distillation* systems. Enhanced distillation is another common term used for distillation systems that utilize mass separating agents other than energy. This term means the use of entrainers, or, the use of other separating techniques to complement distillation, and it does not necessarily involve azeotropes (Stichlmair *et al.*, 1989; Fair, 1987).

Our considerations are limited to the separation of homoazeotropic mixtures. However, multiple phases and heteroazeotropes may be introduced by the separation technique applied. A well-known commercial example is the purification of ethanol to an anhydrous product. Ethanol and water form a binary minimum-boiling homoazeotrope of about 96 weight % ethanol at atmospheric pressure. This system is used as a reference example throughout this section. Its

separation is most commonly done by *heteroazeotropic distillation* using cyclohexane or benzene as entrainer, but applications of distillation coupled with membranes or adsorption are also seen (Fair, 1987). There is also the possibility of using liquid extraction coupled with a simple flash concentration step.

In the following we outline two promising methods that do not depend on the introduction of an additional liquid component to the system, that is, *membrane-distillation hybrids* and *pressure-swing distillation*, before we focus on the more utilized *entrainer-addition distillation methods*. The section is summed up in a collective discussion of the advantages and disadvantages of these alternative separation processes.

### 2.3.1 Membrane-distillation hybrids

The separation of liquid and gas mixtures with membranes as separating agents is an emerging separation operation. Industrial applications were greatly accelerated in the 1980s (Seader and Henley, 1998). The membrane itself acts as the mass separating agent, preferentially absorbing and diffusing one of the azeotrope-forming components. The feed mixture is partially separated by means of a semipermeable barrier (the membrane) into a *retentate*, that part of the feed that does not pass through the membrane (i.e., is retained), and, a *permeate*, that part of the feed that does pass through the membrane (Seader and Henley, 1998).

#### *Pervaporation*

The most commonly used membrane technology for liquid azeotropic mixtures is *pervaporation* with low pressure on the permeate side of the membrane so as to evaporate the permeate (Pettersen and Lien, 1995; Seader and Henley, 1998). A composite membrane is used that is selective for one of the azeotrope constituents. *Vapor permeation* is a similar technology, where the feed enters as saturated vapor. This is specially used in combination with distillation processes, where saturated vapor streams are readily available (Pettersen and Lien, 1995). One important limitation of vapor permeation, however, (which does not exist for pervaporation) is that the vapor permeation fluxes are very sensitive to superheating. Even small degrees of superheating can result in a significant flux decrease (Rautenbach and Vier, 1995). Pervaporation is reported to account for 3.6 % of the total membrane separation applications in chemical and pharmaceutical production (Knauf *et al.*, 1998). Pervaporation is considered to be expensive both in terms of investment and processing costs (at high throughput) as discussed later. Because of its high selectivity, however, pervaporation is of interest in cases where conventional separation processes either fail or result in a high specific energy consumption or high investment costs. The most important category of separation tasks for which pervaporation is promising, is in fact mixtures with a homoazeotrope or close-boiling characteristics (Rautenbach and Albrecht, 1989).

One often distinguishes between two different types of pervaporation-distillation hybrids: (a) where the task of the pervaporation (or vapor permeation) stage is limited to azeotrope separation only, and (b) where the pervaporation stage (membrane unit) is designed for azeotrope separation and for achieving the product specifications. Figure 2.6 illustrates typical configurations for these

two processes. The azeotropic mixture withdrawn from the top of the columns ( $A_{12}$ ) is supplied

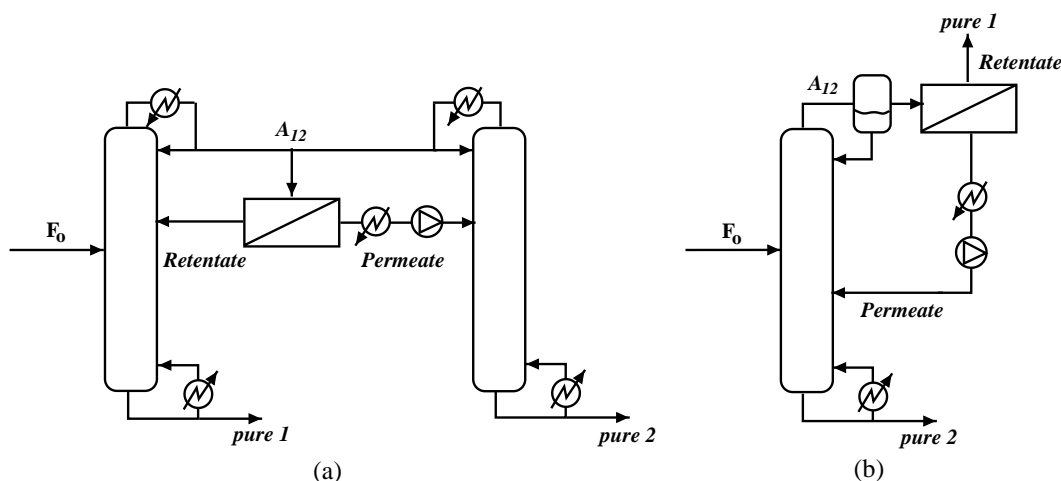


Figure 2.6: Membrane-distillation hybrids. Separation of a binary homoazeotropic mixture: (a) pervaporation unit between two distillation columns; (b) distillation column augmented with a vapor permeation unit where the retentate has sufficient purity to be a final product.

to the membrane modules. There are many other membrane-distillation hybrid configurations. The key to an efficient and economic membrane separation process is the membrane. It must have good permeability (high mass-transfer flux), high selectivity, stability, freedom from fouling (defect-free), and a long life (two or more years) (Seader and Henley, 1998). The membranes used to separate organic solvent and water mixtures are mostly organic polymers, but also ceramic inorganic membranes are seen (Li and Xu, 1998). Polyvinyl alcohol membranes provide a high driving force just in the ethanol-water azeotrope composition region, and have a high selectivity for water (Guerreri, 1992). Pervaporation membrane materials suitable for various mixture systems can be found in the “Membrane Handbook” (Flemming and Slater, 1992). Pervaporation is applicable to separations over the entire composition range, but the phase change requires considerable more energy than other pressure driven membrane techniques like reverse osmosis (Goldblatt and Gooding, 1986).

The main industrial applications of pervaporation separation processes include (Rautenbach and Albrecht, 1989; Seader and Henley, 1998):

- removal of water from organic solvents (e.g., dehydration of alcohols, ketones and esters);
- removal of organics from water (e.g., removal of volatile organic compounds (VOCs), toluene and trichloroethylene from wastewater); and
- separation of organic-organic azeotropes (e.g., benzene-cyclohexane) and isomers.

An illustration of an industrial process for dehydration of ethanol using membrane pervaporation in combination with a continuous distillation column is given in Figure 2.7. By integrating

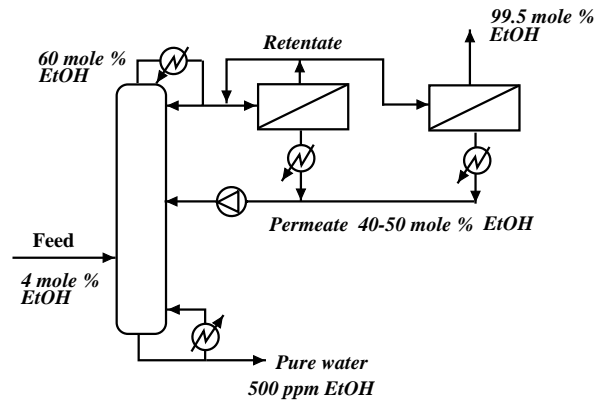


Figure 2.7: Industrial ethanol dehydration using two pervaporation modules and one distillation column (Goldblatt and Gooding, 1986).

the two separation techniques, the separation task is switched among the technologies in such a way that each operates in the region of the composition space where it is most effective (Pressly and Ng, 1998). Goldblatt and Gooding (1986) performed experiments and simulations to evaluate the pervaporation-distillation hybrid process in Figure 2.7. Their study indicates a reduction of production costs by 50 % over conventional heteroazeotropic distillation for dehydration of ethanol using benzene as entrainer. They concluded that high selectivity and moderate flux membranes are necessary for the system to be economically attractive compared to the conventional heteroazeotropic distillation process. Guerreri (1992) reports about 25 % energy savings for this hybrid process compared to traditional heteroazeotropic distillation process.

Pervaporation is best applied when the feed solution is diluted in the main permeant (Seader and Henley, 1998). Permeate fluxes decrease significantly with decreasing feed concentrations. There is a trade-off between the permeate flux and selectivity. Membrane modules can be arranged in series or in parallel cascades in order to increase the obtainable degree of separation. A number of membrane stages may be needed, with a small amount of permeant produced per stage and re-heating of the retentate between stages (Seader and Henley, 1998). The example of ethanol dehydration has an azeotrope concentration that favors the membrane pervaporation process, since only a single-stage pervaporation with a moderate specific membrane area is needed for the azeotrope separation. A question that still remains to be answered is the performance of such membrane separation systems for other binary homoazeotropes that have less concentrated azeotrope compositions.

Pervaporation-distillation hybrids are commercially used for the dehydration of isopropanol too. Rautenbach and Vier (1995) considered a combination of batch distillation and vapor permeation for removal of isopropanol from water. The constant distillate composition policy was

implemented, thus the distillate product flowrate decreases during the operation. Therefore, the membrane area of the subsequent vapor permeation unit is determined by the distillate product flowrate at the beginning of the production period. Rautenbach and Vier (1995) found this hybrid pervaporation-batch distillation process for separating isopropanol and water superior to extractive distillation using ethylene glycol as the entrainer. However, no attempt was made to compare the process with the conventional process of heteroazeotropic distillation-decanter hybrid.

### 2.3.2 Pressure-swing distillation

Pressure changes can have a large effect on the vapor-liquid equilibrium compositions of azeotropic mixtures and thereby affect the possibilities to separate the mixture by ordinary distillation. By increasing or decreasing the operating pressure in individual columns we can move distillation boundaries in the composition space or even make azeotropes appear or disappear (or transform into heteroazeotropes). For some mixtures, a simple change in pressure can result in a significant change in the azeotrope composition and enable a complete separation by pressure-swing distillation illustrated in Figure 2.8. A binary homoazeotropic mixture is introduced as feed  $F_o$  to the

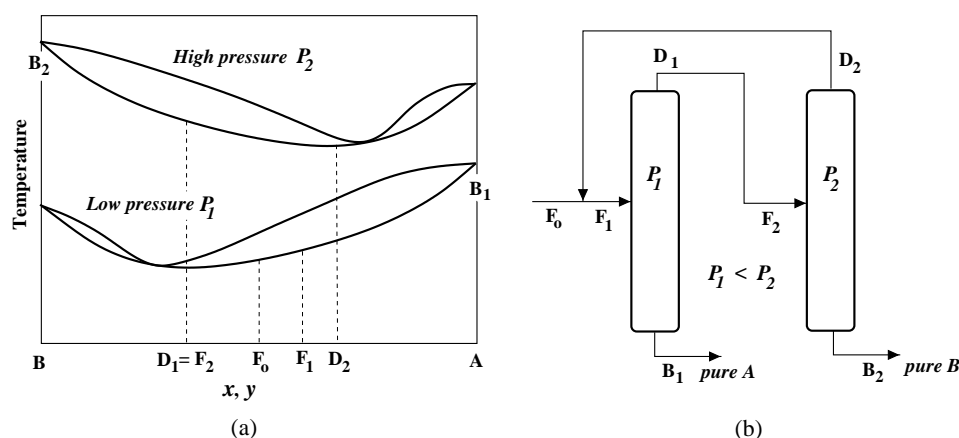


Figure 2.8: Pressure-swing distillation: (a) temperature-composition diagram for a minimum-boiling binary azeotrope that is sensitive to changes in pressure; (b) distillation sequence.

low-pressure column. The bottom product from this  $P_1$  column is relatively pure A, whereas the overhead is an azeotrope with  $x_{D_1}$ . This azeotrope is fed to the high-pressure column, which produces relatively pure  $B_2$  in the bottom and an azeotrope with composition  $x_{D_2}$  in the overhead. This azeotrope is recycled into the feed of the low-pressure column. The smaller the change in azeotropic composition with pressure, the larger is the recycle in Figure 2.8b. According to Smith (1995), a change in azeotropic composition of at least 5 percent with a change in pressure is usually required. Examples of industrial mixtures that can be separated by pressure-swing distillation are given by Schweitzer (1979). For example, the tetrahydrofuran-water azeotrope

may be separated by using two columns operated at  $P_1 = 1$  atm and  $P_2 = 8$  atm. Our example of the ethanol-water azeotrope is not considered to be sufficiently pressure sensitive for the pressure-swing distillation process to be competitive. However, it is interesting to mention that a hybrid system of pressure-swing adsorption (PSA) and distillation is reported to be a competitive alternative to the conventional methods (Humphrey and Seibert, 1992).

Although changing the vapor-liquid equilibrium (VLE) properties of an azeotropic mixture by purely physical means (pressure or temperature changes) is an attractive and definite possibility, it is generally not an option and such processes are often uneconomical (Van Winkle, 1967).

### 2.3.3 Entrainer-addition distillation methods

Physiochemical changes of the VLE behavior of an azeotropic mixture by the addition of an extra-neous liquid component offers a number of possibilities. We name the mixture to be separated as the *original mixture*, and the added component that facilitates the separation the *entrainer*. For the purpose of ease of visualization, we limit our considerations to binary homoazeotropic original mixtures and one-component entrainers. The same separation techniques apply to multicomponent mixtures where the key components form characteristic mixtures falling into the categories discussed, and the entrainer may be a mixture of components. We distinguish between three different conventional entrainer-addition based distillation methods depending on the properties and role of the entrainer and the organization (scheme) of the process:

***Homogeneous azeotropic distillation*** (ordinary distillation of homoazeotropic mixtures):

- The entrainer is completely miscible with the components of the original mixture. It may form homoazeotropes with the original mixture components.
- The distillation is carried out in a conventional single-feed column.

***Heteroazeotropic distillation*** (decanter-distillation hybrids that involve heteroazeotropes):

- The entrainer forms a heteroazeotrope with at least one of the original mixture components.
- The distillation is carried out in a combined column and decanter system.

***Extractive distillation:***

- The entrainer has a boiling-point that is substantially higher than the original mixture components and is selective to one of the components.
- The distillation is carried out in a two-feed column where the entrainer is introduced above the original mixture feed point.
- The main part of the entrainer is removed as bottom product.

We actually prefer an even broader definition of extractive distillation, as discussed later, that includes the symmetrical process of separating maximum-boiling azeotropes using a low-boiling

entrainer (*re-extractive distillation*), and combined heteroazeotropic and extractive distillation schemes (*heteroextractive distillation*). There are other more exotic methods that may also be called entrainer-addition distillations, including:

*Reactive distillation*: The entrainer reacts preferentially and reversibly with one of the original mixture components. The reaction product is distilled out from the non-reacting component and the reaction is reversed to recover the initial component. The distillation and reaction is usually carried out in one column (catalytic distillation).

*Chemical drying (chemical action and distillation)*: The volatility of one of the original mixture components is reduced by chemical means. An example is dehydration by hydrate formation. Solid sodium hydroxide may be used as an entrainer to remove water from tetrahydrofuran (THF). The entrainer and water forms a 35-50 % sodium hydroxide solution containing very little THF (Schweitzer, 1997).

*Distillation in the presence of salts*: The entrainer (salt) dissociates in the mixture and alters the relative volatilities sufficiently so that the separation becomes possible. A salt added to an azeotropic liquid mixture will reduce the vapor pressure of the component in which it is more soluble. Thus extractive distillation can be applied using a salt solution as the entrainer. An example is the dehydration of ethanol using potassium acetate solution (Furter, 1968).

Obviously, the various methods may be combined and modified. For example, an entrainer may form a pressure-sensitive azeotrope that makes it possible to utilize entrainer-addition and pressure-swing distillation. The three conventional entrainer-addition distillation methods outlined in this section; homogeneous azeotropic distillation, heteroazeotropic distillation and extractive distillation, are described in more detail in Section 2.4.

### 2.3.4 Discussion

In the overview of separation processes given by Smith (1995), the basic advantages of distillation are listed as: potential for high throughput, any feed concentration, and high purity. Because of these advantages compared with other thermal separation processes, distillation is used in 90 % of cases for the separation of binary and multicomponent liquid mixtures (Gmehling *et al.*, 1994). The distillation technique itself is a mature technology, that is, we have confidence in its design, operation and control, in contrast to other promising technologies such as membranes. On the negative side, distillation tends to use large amounts of energy (low thermodynamic efficiency) and the introduction of an additional liquid entrainer to the mixture system causes additional complexities. Distillation is particularly energy intensive when the heat of vaporization of the mixture to be separated is high, such as for water and alcohols, and it is for these particular separation tasks that pervaporation-distillation hybrids are said to be competitive.

Augmenting distillation with, for example, pervaporation can simplify the overall process structure, reduce the energy consumption and avoid entrainers (Hömmerich and Rautenbach, 1998).



The main advantage of using membranes as mass separating agents is that the selectivity is independent of the vapor-liquid equilibria. For example a pervaporation unit can be used for the azeotrope separation only. This allows the distillation column to be designed for less stringent operating conditions, while the subsequent pervaporation stage pushes the separation to completion. But, pervaporation and vapor permeation are expensive because of relatively low permeate fluxes and the usually low condensation temperature (Rautenbach and Vier, 1995). In case of pervaporation, processing costs are further increased by the required re-heating energy and the integration of heat exchangers into the process. Industrial applications of pervaporation have generally been limited to moderate volumes, because the prices of the membrane modules tend to be high for large capacities. While the capital investments for distillation as a function of capacity scales according to the “six-tenths power rule”, membranes tend to scale linearly with capacity (Kunesh *et al.*, 1995). Thus, distillation often has a distinct economic advantage at large throughput.

The fact that many of the alternative separation technologies to distillation can only handle low throughput may not be a limitation. For example, pervaporation-distillation hybrids may be well suited in small to moderate volume production and batchwise operation, such as in pharmaceutical and specialty chemical industries. Dehydration of organic solvents by a pervaporation-batch distillation hybrid has significant advantages when batch units are required for subsequent treatment of a variety of spent solvents (Rautenbach *et al.*, 1992). Membrane units only handle relatively pure feeds, that is, liquid mixtures dilute in one component and without heavy contaminants like salts and tar. Solvent recovery from “mother liquors” may require pretreatment (e.g. filtration and distillation) before the membrane unit.

Membrane units have little flexibility to variations in feed composition. Distillation, and in particular batch distillation, is based on robust and flexible equipment that can handle a wide range of compositions and frequent changes of the feed mixture components. In addition, distillation is able to achieve high-purity of the separation products. Many of the alternatives to distillation only carry out partial separation and cannot produce pure end-products. Thus, several of the other alternative separation methods can be used only in combination with distillation, while distillation itself can be used as a stand-alone operation.

Let us go back to the commercial example of ethanol dehydration. The conventional method of heteroazeotropic distillation using cyclohexane or benzene as entrainer produces absolute ethanol (> 99.5 mole %). The entrainer forms a heteroazeotrope that is easily recovered by decantation. Still, some of the entrainer (about 50 ppm, typically) remains in the ethanol product, precluding its use in pharmaceutical, medical, food or beverage products. Alternatively, the ethanol-water azeotrope may be separated by molecular sieves (adsorption) or membrane pervaporation. In combination with ordinary distillation these hybrid processes produce absolute ethanol without other contaminants than the initial water. The advantages that are highlighted are that these processes generate safer products and give significant energy savings. Sometimes the membrane material must be regenerated using chemical solvents and the same added aspects as for entrainer-addition distillations applies.

Bergdorf (1991) studied several membrane-distillation hybrids for dehydration of azeotrope-forming solvents. Interestingly, a combined system of pervaporation and pressure-swing distilla-

tion was found to be economically favorable in one case. No particular separation technique was concluded to be more promising than others, as Bergdorf (1991) formulated “*each dehydration process finds its range of application*”.

It is important to consider the separation sequence as a whole, including the regeneration of the separating agent. Exploiting pressure sensitivity should usually be considered before the use of an extraneous liquid component. In the choice between an entrainer that forms a new homoazeotrope, and an entrainer that forms a heteroazeotrope, the latter is normally preferred since a heteroazeotrope can be separated simply by decantation in combination with distillation. Occasionally, a component that already exists in the process (or production site) can be used as an entrainer. These options should be investigated first. In pharmaceutical production, a common requirement is that the products must be completely entrainer-free. As mentioned, the latter may be unavoidable in entrainer-addition distillation methods and causes such methods to be entirely excluded from consideration. This issue may even be the main incentive to look more carefully into alternatives to the conventional entrainer-addition distillation methods.

Brown (1963) compared the economics of nine separation processes for the separation of acetic acid and water (a zeotropic close-boiling mixture). These included ordinary distillation, heteroazeotropic distillation, extraction with low-boiling, and extraction with high-boiling entrainers. They concluded that the most economical process varied with the concentration of the original mixture feed composition. Extraction processes gave the greatest return for 2 to 60 mole % feeds and azeotropic distillation processes greater return at above 75 mole % feed concentration. According to Gmehling *et al.* (1994) a general comparison of extractive and heteroazeotropic distillation favors the latter because extractive distillation has the disadvantage that the entrainer must be vaporized and a higher energy requirement is therefore necessary. Another industrial mixture example is tetrahydrofuran and water which form a minimum-boiling azeotrope. Chang and Shih (1989) compared heteroazeotropic distillation using n-pentane as entrainer to the pressure-swing distillation scheme, which is the conventional method for separation of this mixture. The proposed n-pentane heteroazeotropic distillation scheme was found to be competitive with the low/high pressure distillation scheme, but with “*no technical or economical edge*”, that is, with slightly higher investment costs and a lower operating cost.

According to Tassios (1972), azeotropic distillation separation methods like extractive- and heteroazeotropic distillation have not been used as frequently as they should in industry, even if the often used reasons of high investment and high operating costs are usually weak when one does an in-depth study. Roche [in Tassios (1972)] claims that the real reason lies with the time and money required to obtain a satisfactory process design. Today, simple tools based on graphical analysis of vapor-liquid equilibrium diagram structures are established providing a rapid method for evaluating the possibilities to separate a given azeotropic mixture, choose a suitable separation (distillation) method and process scheme and predict the achievable distillation products compositions. Together with more advanced distillation synthesis tools and simulation software, this dramatically change the way distillation processes for complex nonideal mixtures can be analyzed, understood and designed. Significant improvements over conventional process designs have been shown using these relatively new tools (Wahnschafft, 1997; Serafimov and Frolkova, 1997).

## 2.4 Entrainer-addition distillation methods

Given an original binary mixture with one homoazeotrope we search for an entrainer that forms a ternary mixture that is separable, either by conventional distillation or by the special distillation methods outlined in Section 2.3. The distillation behavior of ternary azeotropic mixtures may be very complex and the decision whether the resulting mixture is separable by distillation is not straightforward. Therefore, we need a tool for the evaluation of the possibilities to separate ternary azeotropic mixtures at the presynthesis stage.

### 2.4.1 Feasibility analysis

Ternary VLE diagrams, such as distillation line map and residue curve map, provide a graphical tool for the prediction of feasible distillation product compositions. Here, we only consider the simple  $\infty/N$  analysis for such prediction (Stichlmair, 1988), that is, the *infinite reflux* bounding of the feasible product composition regions with a finite number of equilibrium stages. From this quick graphical method we can immediately identify the limited separations achievable by distillation.

For an introduction to graphical methods for azeotropic distillation feasibility analysis and separation synthesis the reader is referred to Westerberg and Wahnschafft (1996) and Stichlmair and Fair (1998). It is desirable to depict the regions in which the distillate and bottom products are confined. Triangular diagrams of *distillation lines* or *residue curves* are particularly suited to identify feasible products at the limiting operating condition of infinite and total reflux (that is, the reflux ratio  $R = L/D$  in Figure 2.10 is very high or equal to infinity). The *distillation lines* coincide exactly with the infinite reflux steady state composition profiles of equilibrium staged distillation columns, that is, the operating line at infinite reflux ratio. The *residue curves* coincide exactly with the infinite reflux steady state liquid composition profiles of packed distillation columns when all the resistance to mass transfer is in the vapor phase (perfectly mixed liquid phase) (Serafimov *et al.*, 1973; Pöllmann and Blass, 1994). For a feasible separation, the material balances have to be fulfilled:

$$\begin{aligned} F &= D + B \\ F x_F &= D x_D + B x_B \end{aligned}$$

That is, the distillate and bottom product compositions must lie on the straight material balance line through  $F$ , and, due to the assumption of infinite reflux, on the same distillation line. The resulting (infinite reflux) feasible distillation product regions are illustrated in Figure 2.9. The regions are bounded by the distillation line through the feed and the two material balance lines for pure distillate and pure bottom product, respectively. These two material balance lines correspond to the direct and indirect sharp splits (with an infinite number of equilibrium stages). The distillation line through the feed represents the separation with minimum number of equilibrium stages. Note in particular that it is impossible to achieve a saddle ( $\nabla$ ) as a pure product in a

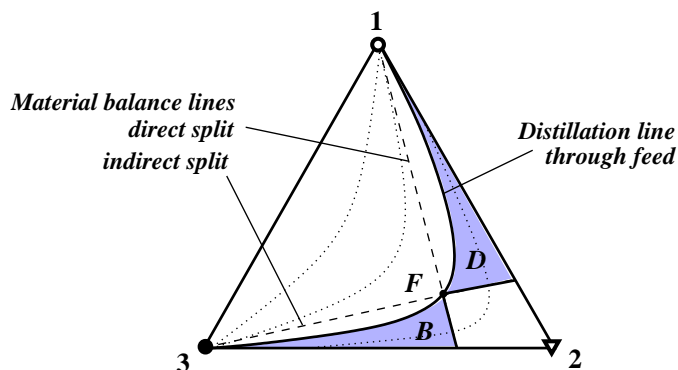


Figure 2.9: Feasible product regions for a ternary zeotropic mixture with feed  $F$  determined by infinite reflux analysis. The possible distillate  $D$  and bottom  $B$  product compositions (shaded) are limited by the distillation line through the feed  $F$ , and by the straight material balance line through  $F$  and the initial and final points of the distillation lines, respectively. Pure components indicated by  $\bullet$  (stable node),  $\circ$  (unstable node) and  $\nabla$  (saddle). (The diagram corresponds to Class 0.0-1 (Cell I), see Chapter 4).

single-feed zeotropic distillation column. The nodes ( $\circ$  and  $\bullet$ ) determines the potential distillate and bottom products for a given feed (for each column in a separation sequence).

## 2.4.2 Feasibility analysis for azeotropic mixtures

Unlike zeotropic distillation, the product compositions of azeotropic distillation depend on the feed composition and its position relative to distillation line (or residue curve) boundaries. As a first approximation, we assume that the composition trajectories of the distillation column operating at *finite* reflux cannot cross the infinite reflux distillation boundaries. Then, the feasible product regions for azeotropic mixtures are limited by distillation lines boundaries too, if any. However, small deviations occur for finite reflux. Advanced approaches for the prediction of feasible product compositions at real operating conditions have been developed (Petlyuk, 1978; Nikolaev *et al.*, 1979; Kiva *et al.*, 1993; Wahnschafft *et al.*, 1992; Pöllmann and Blass, 1994; Castillo *et al.*, 1998; Thong *et al.*, 2000). These approaches give some refinements of the feasible product regions even for zeotropic mixtures (additional product compositions reachable at finite reflux), and additional possibilities for certain types of azeotropic diagrams. But, the main conclusions are the same as for the simple infinite reflux approach; that is, the possibilities of separating (ternary) azeotropic mixtures by ordinary distillation are very limited. An important exception is mixtures with curved distillation line boundaries which can be crossed at finite reflux if the feed is located in the concave region of the boundary (Marchenko *et al.*, 1992; Wahnschafft *et al.*, 1992).

### 2.4.3 Homogeneous azeotropic distillation

Here we consider *ordinary distillation* of ternary mixtures with at least one binary homoazeotrope (that is, the one that stems from the original mixture). The entrainer may or may not form new azeotropes in the system. The only criteria is that the resulting ternary system should form a VLE diagram structure that is promising for separation. This statement may seem obvious, but we find it necessary to emphasize that no other limitations or criteria are necessary to pose at this stage. The entrainer selection criteria given by several authors such as Van Winkle (1967), Doherty and Calderola (1985) and Stichlmair and Fair (1998) are discussed later. The distillation is carried out in a conventional single-feed column as illustrated in Figure 2.10. The entrainer  $F_E$  is introduced

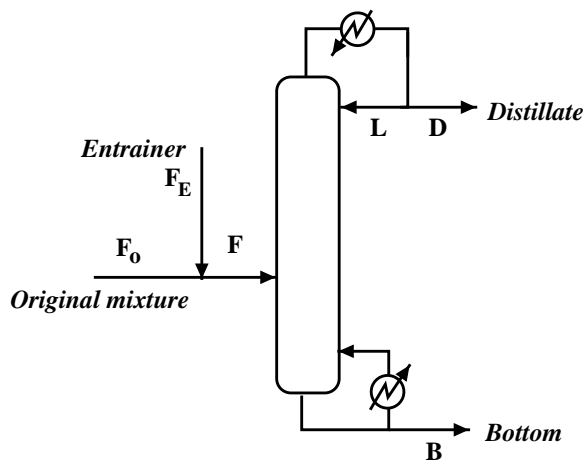


Figure 2.10: Homogeneous azeotropic distillation in a single-feed column.

to the original mixture feed  $F_o$  to form a ternary mixture feed  $F$ . The separation sequence alternatives are similar to the various schemes of ordinary zeotropic distillation of ternary mixtures (direct, indirect, prefractionator and so forth).

We distinguish between two broad cases of the entrainer properties: (1) the entrainer is zeotropic, and (2) the entrainer is azeotropic. Our presentation here does not consider all the resulting feasible diagram structures, but we give selected examples to illustrate the ideas.

If the entrainer does not form any new azeotropes (zeotropic entrainer) the resulting ternary mixtures are shown in Figure 2.11. We refer to Chapter 4 for an overview of the classifications of feasible VLE diagrams for ternary azeotropic mixtures. The terms “light”, “intermediate” and “heavy” entrainer are used here in reference to the boiling temperature of the pure components that forms the mixture. The relative volatility of the components in the mixture vary within the composition diagram and may be identified by univolatility lines and K-ordered regions (Chapter 3). Note the symmetry between the “antipodal diagrams” of minimum-boiling binary azeotropes and maximum-boiling binary azeotropes. For simplicity, we only consider an

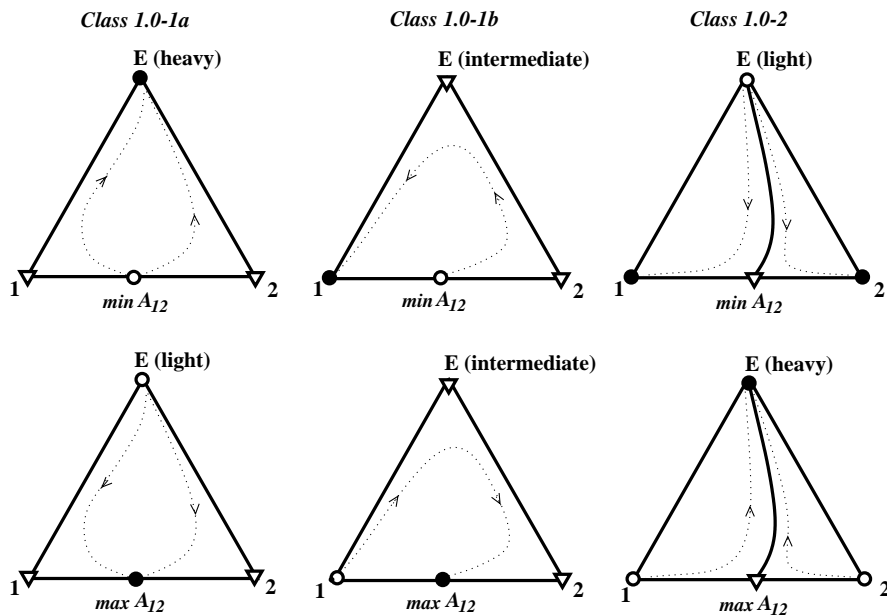


Figure 2.11: Zeotropic entrainer. Structures of the resulting ternary VLE diagrams of the original binary azeotropic mixture of components 1 and 2, and the entrainer E. The singular points are indicated by  $\bullet$  stable node,  $\circ$  unstable node and  $\nabla$  saddle.

original mixture with a minimum-boiling azeotrope. The same arguments applies to the opposite case of maximum-boiling binary azeotrope, but with inverted schemes for the distillation separation (and some additional aspects due to the different volatility behavior in the column).

For a quick analysis of the possibilities and limitations of the distillation of the resulting ternary mixtures (original mixture + entrainer) we use the infinite reflux approach:

*Heavy zeotropic entrainer:* The analysis illustrated in Figure 2.12 shows that it is not possible to separate the original mixture into pure components 1 and 2 (both saddles) by a sequence of ordinary single-feed distillation columns, and the azeotrope  $A_{12}$  is an inevitable product. A more detailed (finite reflux) analysis gives the same conclusion (Wahnschafft and Westerberg, 1993). (However, the special method of *extractive distillation* may be used to separate mixtures of this structure in a two-feed column scheme as presented later.)

*Intermediate zeotropic entrainer:* The analysis illustrated in Figure 2.13 shows that we can achieve pure components 1 and 2 and E by ordinary single-feed distillation columns depending on the feed composition (and operating conditions), even though one of the original mixture components is a saddle. An intermediate zeotropic entrainer thus seems very promising. However, there is a possibility for multiple steady states for certain operating conditions, which may cause operational problems, and care must be taken when designing

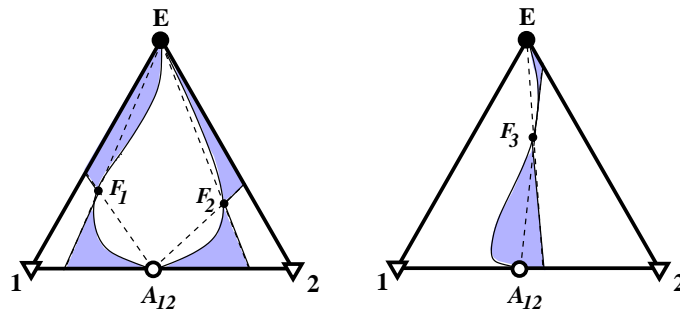


Figure 2.12: Feasible product regions for mixture with heavy entrainer. It is impossible to obtain pure components 1 and 2 in a sequence of single-feed distillation columns. (Corresponds to Class 1.0-1a, Cell II.)

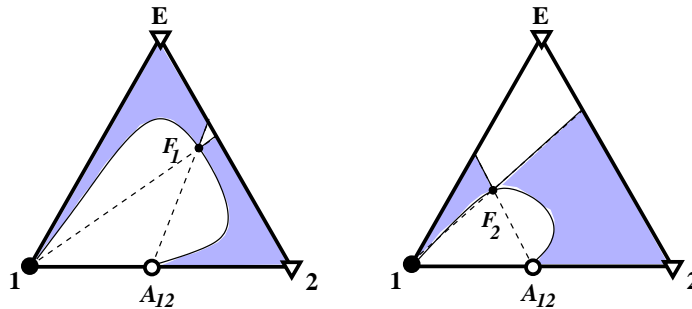


Figure 2.13: Feasible product regions for mixture with intermediate entrainer. Pure components 1 and 2 (and E for specific feed compositions) may be obtained. (Corresponds to Class 1.0-1b, Cell III.)

such processes (Laroche *et al.*, 1992b; Bekiaris *et al.*, 1993; Güttinger and Morari, 1996; Kiva and Alukhanova, 1997). Furthermore, finding an entrainer that forms this diagram structure is difficult as its occurrence in nature is limited. In addition, because of the requirement that the entrainer has a boiling-point between the original mixture components, the relative volatilities in the resulting mixture are usually close to unity and the separation often uneconomical. However, the often referred mixture of acetone-heptane-benzene is an example for which this process is economical (Stichlmair and Fair, 1998).

*Light zeotropic entrainer:* The analysis is illustrated in Figure 2.14. This diagram class has a distillation boundary that splits the composition space into two distillation regions. The original mixture components 1 and 2 are located in two different distillation regions and if the boundary is linear the separation is impossible. If we view the diagram as a combination of two cells, we see that the feasible regions (Figure 2.14 left) are as showed in Figure 2.9. However, for curved boundaries the answer is not so obvious (Figure 2.14 right).

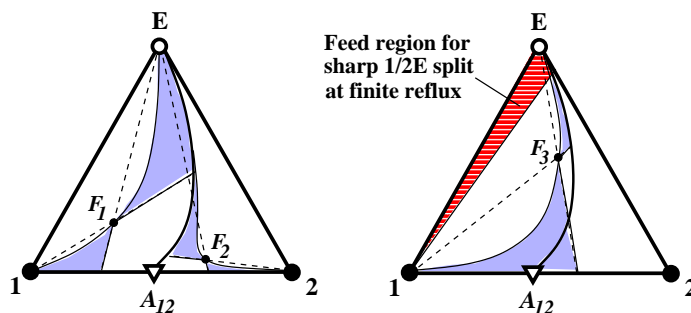


Figure 2.14: Feasible product regions for mixture with light entrainer. Some possibility for obtaining pure components 1 and 2. (Corresponds to Class 1.0-2 consisting of two Cell I's.)

Complete separation may be achieved by a scheme with recycle for feed compositions located in the concave region of the distillation line boundary (Wilson *et al.*, 1955; Balashov *et al.*, 1970; Kiva and Serafimov, 1976b; Doherty and Caldarola, 1985; Stichlmair, 1988; Wahnschafft *et al.*, 1992; Wahnschafft *et al.*, 1993). This scheme may be economical for the separation of a maximum-boiling azeotrope using an entrainer (antipodal diagram) where the heavy entrainer recycle does not have to be evaporated. Detailed analysis show that there is a feed region (striped) where the sharp separation  $1/2E$  can be achieved at finite reflux ratio (Marchenko *et al.*, 1992; Kiva *et al.*, 1993; Wahnschafft *et al.*, 1992; Wahnschafft *et al.*, 1993). For feeds located in this narrow region, pure components 1 and 2 can be achieved through a sequence of ordinary single-feed distillation columns (that is, the distillation line boundary is crossed by the given distillation trajectory at finite reflux). In practice, however, it is difficult to find an entrainer that gives sufficient curvature of the boundary and large enough relative volatilities.

If the entrainer forms new azeotropes, there are numerous possible diagrams structures of the resulting ternary mixture. Selected examples are shown in Figure 2.15. Analysis of the feasible product regions of all possible ternary VLE diagram structures with an evaluation of the possibilities to separate each structure is beyond the scope of this thesis. For a quick estimate of the possibilities to separate resulting ternary diagrams with several distillation line regions, we propose to use the concept of *elementary topological cells* presented in Chapter 4. The idea is that, based on our knowledge about the simple diagrams given above, we can qualitatively predict the behavior of other more complex diagrams by looking at them as combinations of these simple structures. For example (from Figure 2.15):

*Class 2.0-2a:* This diagram includes the promising Cell III (with the characteristic U-shaped distillation lines) adjoining the original mixture edge. That is, the lower region of this diagram is similar to the Class 1.0-1b in Figure 2.13, where the new azeotrope  $A_{2E}$  acts as an “intermediate” entrainer. The separation into pure components 1 and 2 is possible (Foucher *et al.*, 1991).



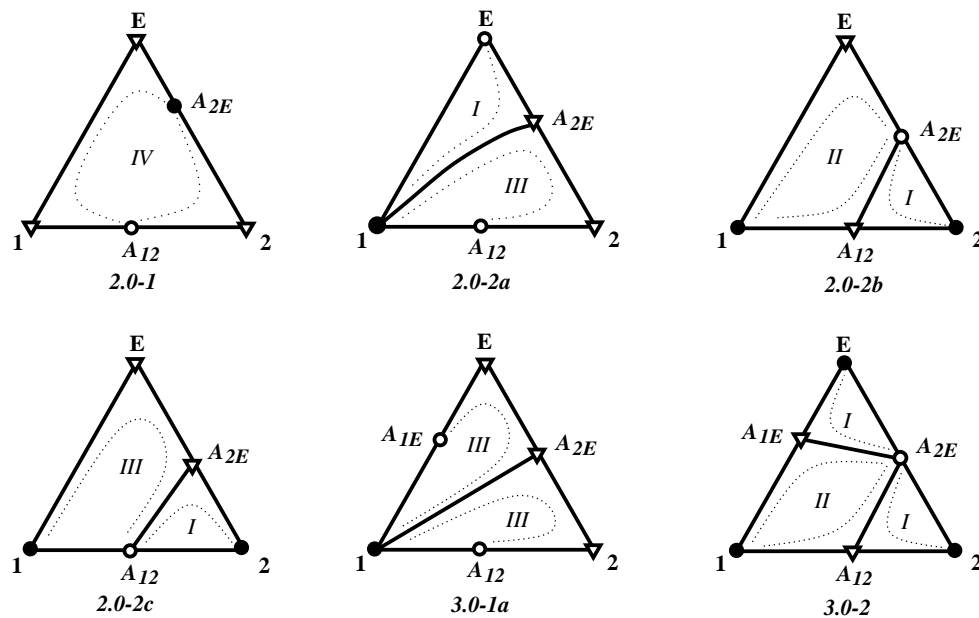


Figure 2.15: Azeotropic entrainer. Selected structures of the resulting ternary VLE diagrams of the original mixture 1 and 2, and the entrainer E. Elementary cells indicated by I, II, III and IV.

*Class 2.0-2b:* This diagram may be viewed as a combination of two subsystems: Cell I (pseudo ternary zeotropic mixture similar to the structure in Figure 2.9) and Cell II (similar to the Class 1.0-1a in Figure 2.12). Separation into pure components 1 and 2 is not possible due to the distillation boundary between the components 1 and 2, unless the boundary is (highly) curved. Then, the scheme with recycle can be implemented where the azeotrope  $A_{2E}$  acts as the entrainer (Stichlmair and Fair, 1998).

*Class 3.0-1a:* The same arguments as for Class 2.0-2a applies.

*Class 3.0-2:* The same arguments as for Class 2.0-2b applies.

Doherty and Caldarola (1985) give the condition that the separation is possible if both the original mixture components 1 and 2 belong to the same distillation line region (as is the case for the Classes 2.0-1, 2.0-2a and 3.0-1a in Figure 2.15). An important exception is the crossing of curved distillation line boundaries (as might be a possibility for the Classes 2.0-2b and 3.0-2 in Figure 2.15). Here, the condition given by Stichlmair and Fair (1998) is more appropriate; that is, the separation is possible if the points of the original mixture components 1 and 2 are nodes of two neighboring regions (with curved boundary).

Even though some of the resulting structures with an azeotropic entrainer are promising, the overall conclusion is that the possibilities of separating azeotropic mixtures in ordinary single-

feed columns are limited and therefore special distillation methods need to be applied.

#### 2.4.4 Heteroazeotropic distillation

Heteroazeotropic (VLLE) distillation, often referred to as azeotropic distillation (but we do not recommend this nomenclature), involves the formation of a heteroazeotrope (or the use of an existing heteroazeotrope) to effect the desired separation. The crucial difference compared to homoazeotropic distillation is that a heteroazeotrope can be separated easily by decantation. This also makes the process scheme simpler. First, for illustration purposes, we consider in Figure 2.16 a particular example of heteroazeotropic distillation where the original mixture is ternary mixture of Class 1.0-2 with a saddle heteroazeotrope that splits the diagram into two distillation regions. The distillation boundary is "crossed" by the liquid-liquid phase splitting (decantation)

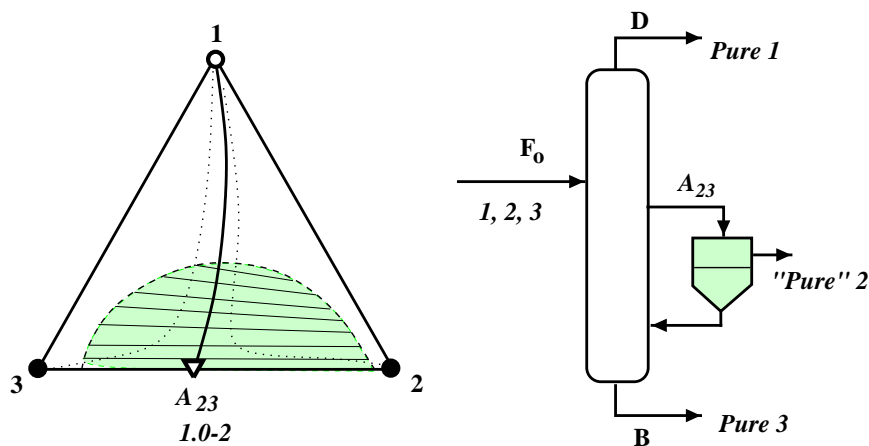


Figure 2.16: Heteroazeotropic distillation with side-stream decanter.

of the heteroazeotrope, and the separation into the three original mixture components is feasible. An example mixture of this type is acetone - water - 1-butanol (Stichlmair and Fair, 1998).

Given that the original mixture is binary and includes a homoazeotrope, there are many possible VLLE diagrams that result from adding an entrainer that forms a binary heteroazeotrope with one of the original mixture components, or, a ternary heteroazeotrope. The most common structure is Class 3.1-2 with three binary minimum-boiling azeotropes and a ternary heterogeneous azeotrope. The entrainer may be mixed with the original feed or introduced to the column as a separate second feed. If the entrainer has a volatility near that of the feed, it is usually mixed with the feed to form a single stream. If volatility is below that of the feed, the entrainer is usually added above the feed stage (Schweitzer, 1997). A typical heteroazeotropic distillation process scheme is shown in Figure 2.17. Relatively pure component 2 is removed as the bottom product. The ternary heteroazeotrope is distilled overhead. Part of the condensate  $D$  is refluxed to the

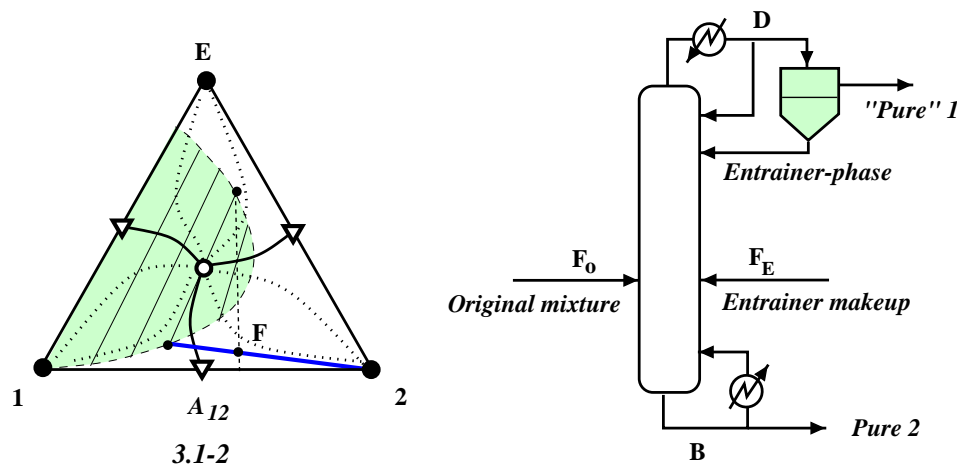


Figure 2.17: A more common heteroazeotropic distillation scheme with distillate decanter.

column, if necessary, to achieve a satisfactory separation of the heteroazeotrope, and the remainder is separated into two liquid phases in the decanter. One liquid phase contains the bulk of the entrainer (and component 2) which is returned as reflux. The other liquid phase contains the bulk of component 1. If this layer contains a significant amount of entrainer, then it may be fed to an additional column to separate and recycle the entrainer and produce pure 1. Promising VLE diagrams of the resulting ternary system (original mixture + entrainer) are structures where the heteroazeotrope formed by the entrainer is an unstable node ( $\circ$ ). The diagram is then split into at least two distillation regions. The original mixture components 1 and 2 are stable nodes ( $\bullet$ ) of these regions. The feed composition is located in one region and one end of the liquid-liquid tie-line is located in the other.

*Ethanol dehydration:* The earliest example of heteroazeotropic distillation is the dehydration of ethanol using benzene as entrainer that was presented by Young in 1902 (Pratt, 1967). Ethanol (2) - water (1) - benzene (E) forms a ternary VLE diagram of Class 3.1-2 in Figure 2.17. Pure (anhydrous) ethanol is produced in the bottom. The ternary heteroazeotrope is removed as distillate and separated into an organic-phase containing only 1 mole % water and a water-phase containing 36 mole % water in the decanter. The organic-phase is recycled to the column. The water-phase is sent to recovery columns for removal of water and recovery of benzene and ethanol. Today, cyclohexane is a more common entrainer for ethanol dehydration by heteroazeotropic distillation.

An interesting example, given by Wilson *et al.* (1955), is the dehydration of hydrazine, which form a maximum-boiling homoazeotrope with water  $A_{12}$ , by using aniline as an entrainer. Aniline is a "heavy" entrainer that forms a binary heteroazeotrope with water  $A_{2E}$ . The resulting ternary VLLE diagram is of Class 2.0-2a with a curved distillation boundary as illustrated in Figure 2.18. The previously described scheme with recycle (moving the feed composition of Column 1 into the concave region of the curved distillation boundary) was implemented.

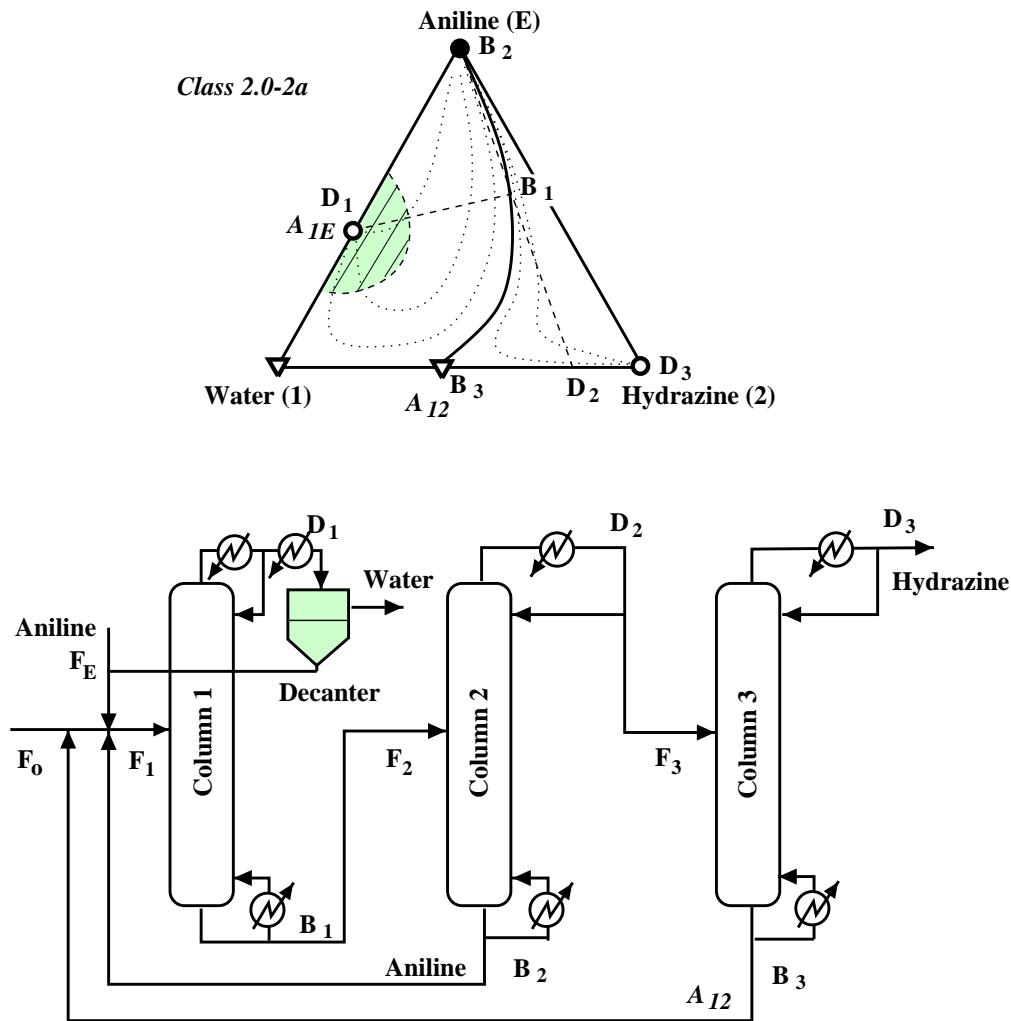


Figure 2.18: *Heteroazeotropic distillation scheme with recycle* (Wilson et al., 1955).

For more details about heteroazeotropic distillation processes in general the reader is referred to the literature, e.g. Doherty and coworkers (1990a; 1990b; 1990c), ?, and Widagdo and Seider and coworkers (1992; 1996).

The possible entrainers for heteroazeotropic distillation are limited, but if one can be found then it is usually preferred compared to an entrainer for extractive distillation.

- It is generally possible to find a heteroazeotropic entrainer when the original mixture con-

sists of hydrophilic and hydrophobic organic components (such as ethanol and water);

- It is very difficult to find an entrainer when the original mixture consists of only hydrophilic (or only hydrophobic) components (such as benzene and cyclohexane).

### 2.4.5 Extractive distillation

Extractive distillation is the oldest known method for separating azeotropic mixtures. Benedict and Rubin (1945) give the following definition of extractive distillation:

*“Distillation in the presence of a substance which is relatively non-volatile compared to the components to be separated and which, therefore, is charged continuously near the top of the distilling column so that an appreciable concentration is maintained on all plates of the column.”*

The basic principle is that the extractive entrainer interacts differently with the components of the original mixture and thereby alters their relative volatility. These interactions occur predominantly in the liquid phase and the entrainer is introduced above the original mixture feed point to ensure that the entrainer remains in appreciable concentration in the liquid phase in the column section below.

The definition of extractive distillation given above is much broader than the traditional one found in most textbooks and encyclopedia (Hoffman, 1964; Van Winkle, 1967; Perry, 1997). A common restriction on the “extractive distillation” is that the entrainer should not introduce new azeotropes in the system, that is, no distillation boundaries (Stichlmair *et al.*, 1989; Doherty and Knapp, 1993; Gmhelng and Möllmann, 1998). However, this restriction seems unnecessary. The entrainer may well form new azeotropes and this may even be preferably as in the process of *heteroextractive distillation* where the entrainer forms a heteroazeotrope with one of the original mixture components and is miscible and selective to the other. Furthermore, the extractive distillation scheme may operate within one distillation region of the ternary mixture composition space, and still achieve a desirable separation (in terms of the original mixture product specifications).

Let us first consider the simplest example of extractive distillation where the original mixture is a binary minimum-boiling homoazeotrope and the entrainer is miscible and zeotropic. The main conditions that a candidate extractive entrainer must satisfy in order to make the separation feasible are:

#### First condition:

The resulting ternary system of the binary minimum-boiling azeotrope and the entrainer should form a VLE diagram (or cell) of the structural type shown in Figure 2.19.

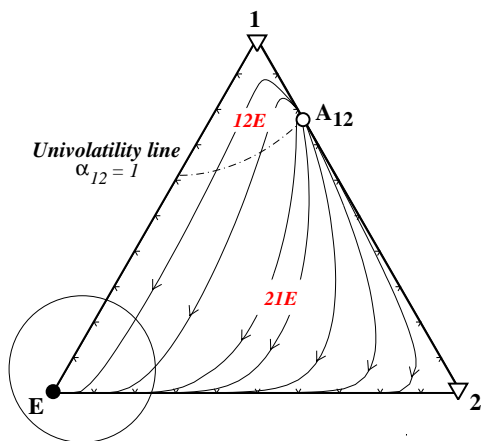


Figure 2.19: Promising VLE diagram for extractive distillation (Class 1.0-1a, Cell II). The univolatility line  $\alpha_{12}=1$  indicates the change in volatility order of the mixture components.

Second condition:

The entrainer must cause a substantial change in the relative volatility between the azeotrope-forming components 1 and 2. Typically, the relative volatility  $\alpha_{12}$  at infinite dilution in the entrainer should be larger than 2.

Third condition:

The entrainer must have a higher boiling-point than the original mixture components. Typically,  $\Delta T_{E-1,2} > 30^{\circ}C$ . The relative volatility between the entrainer and the component that is recovered in the distillate should preferably be large (typically,  $\alpha_{1E} > 3.0$ ). The larger the boiling-point difference between the entrainer and the distillate component, the less reflux and less number of trays needed in the rectifying section (typically,  $\Delta T_{E-1,2} = 50 - 150^{\circ}C$ ).

The most important feature of the diagram in Figure 2.19 is the shape of the residue curves near the entrainer stable node (circled). The presence of a univolatility line deforms the residue curves according to the entrainer selectivity (here causing S-shaped residue curves). The shape of the residue curves in Figure 2.19 indicates that the entrainer has strongest affinity to component 2. The entrainer must be miscible with the component removed in the bottom product, but there are no special requirements to the miscibility with the other component removed as distillate (that is, the entrainer can be miscible, partly miscible or immiscible with the distillate component).

### Process scheme

An illustration of extractive distillation is shown in Figure 2.20. Extractive distillation differs

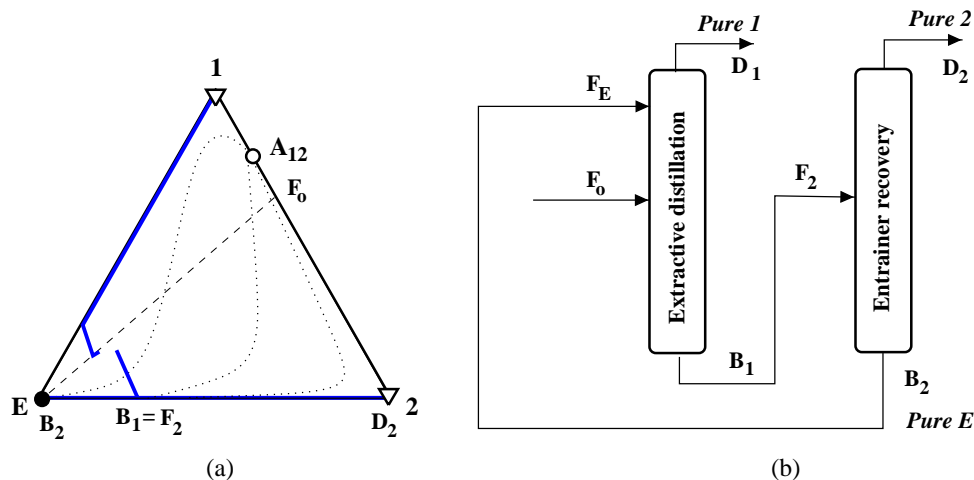


Figure 2.20: *Extractive distillation: (a) composition profile (bold line), material balance line (dashed) and distillation lines (dotted); (b) extractive distillation column sequence.*

distinctly from conventional homogeneous azeotropic distillation in the organization of the flows and the resulting material balance equations (operating line). The crucial element is the extractive section with countercurrent flow of volatile and non-volatile components. A greater entrainer flowrate generally yields better separation, but this increases the energy demand in both columns and increases the reboiler temperature in the extractive column (Smith, 1995).

In extractive distillation a saddle is obtained as a distillate product which is “against” the distillation lines (residue curves) (see the composition profile in Figure 2.20). This is the main characteristic of the extractive distillation process. Wahnschafft and Westerberg (1993), Knapp and Doherty (1994) and Bauer and Stichlmair (1995) presents extractive distillation composition profiles for the system of acetone, methanol and water (Class 1.0-1a), and geometric representations of the extractive distillation process are given in a series of papers by Doherty and coworkers (Levy and Doherty, 1986; Knapp and Doherty, 1990; Knapp and Doherty, 1994). The liquid composition profile along the column shown in Figure 2.20 turns off the binary edge between the distillate product (1) and the entrainer (E). The imbalance of mixing due to the entrainer feed  $F_E$  causes a shift in the composition profile and the profile moves across the distillation lines (or residue curves) in the extractive section.

For the mixture given in Figure 2.19, the minimum-boiling azeotrope is an unstable node in the whole composition triangle. The pure components 1 and 2 are both saddle points (but the component 1 is an unstable node of the binary edge between component 1 and the entrainer). The univolatility line of the azeotrope constituents, that is, the locus of points in the composition space where  $\alpha_{12} = 1$ , extends from the azeotrope  $A_{12}$  to the binary edge between component

1 and the entrainer. Thus, component 1 is recovered in the distillate since it is the most volatile component in the rectifying section (Laroche *et al.*, 1993). Component 2 is removed as bottom product together with the entrainer. Thus, the complete extractive distillation scheme requires a sequence of two columns, one extractive distillation column and one ordinary column (or stripper) to separate component 2 from the entrainer.

High reflux may be harmful in extractive distillation because it weakens the extractive effect (decreases the entrainer concentration in the extractive column section). Previous studies on continuous extractive distillation have shown that there is a maximum as well as a minimum reflux ratio to make the separation scheme feasible (Andersen *et al.*, 1995; Laroche *et al.*, 1993). Increased reflux ratio moves the distillate composition from the saddle (component 1) to the unstable node ( $A_{12}$ ) in Figure 2.19.

The same extractive distillation scheme can in principle be applied to the symmetrical system of separating a maximum-boiling azeotrope using a light entrainer (antipodal diagram Class 1.0-1a), and this process is referred to as *re-extractive distillation*. The light entrainer feed is here introduced below the original mixture feed point. However, this system is not as beneficial because the entrainer interactions predominantly occur in the liquid phase and with a volatile entrainer this effect is more difficult to obtain than in the conventional scheme.

According to Smith (1995), extractive distillation is more useful than heteroazeotropic distillation because the process does not depend on the formation of an azeotrope and thus a greater choice of mass separating agent is, in principle, possible. Although it is correct that it is easier to find suitable entrainers for extractive distillation, this is not because “the process does not depend on the formation of an azeotrope”. High selectivity is one of the most desirable features of an entrainer, and this is generally related to a high degree of nonideality (molecular interaction). Formation of an azeotrope is not necessarily a disadvantage for the extractive distillation scheme.

#### *Heteroextractive distillation*

If a new heteroazeotrope forms between the extractive entrainer and the component of the original mixture that is to be removed as distillate, then both heteroazeotropic and the extractive distillation can be combined into a single process as illustrated in Figure 2.21. The heteroazeotrope  $A_{2E}$  (saddle) is removed overhead and separated by condensation and decantation, while excess of the entrainer is removed in the bottom product together with the one of the original mixture component that it extracts (here: component 1). The extractive process works within one distillation line (residue curve) region (Cell II) of the complex diagram, and the distillation boundaries are crossed by the liquid-liquid phase splitting in the heterogeneous region (Wijesinghe, 1985). This is in fact a very attractive separation method because the entrainer is double-effective. Example mixtures of the type given in Figure 2.21 are methyl ethyl ketone (2-butanone) - water - cyclohexanone; isopropanol - water - isobutanol; acetone - methylene chloride ( $\text{CH}_2\text{Cl}_2$ ) - water; methanol - carbon tetrachloride ( $\text{CCl}_4$ ) - water. In the screening for entrainer such candidates are often ruled out, e.g. by the entrainer selection criteria given by Doherty and coworkers (1985; 1991; 1993) and Seader and Henley (1998). Thus, many of the entrainer selection criteria are too limiting, and one should not narrow the search for a new separation system by using conditions that apply for “old” processes, but rather see the possibilities and limitations that lie within each system in



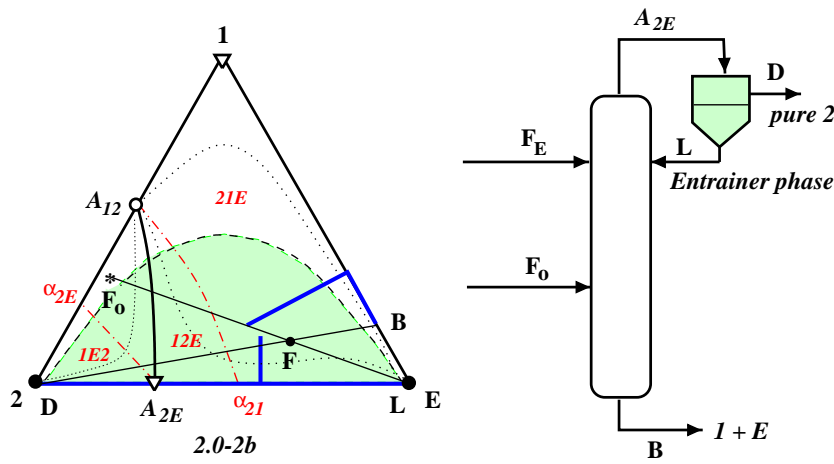


Figure 2.21: Heteroextractive distillation (Wijesinghe, 1985).

question.

Another interesting example, given by Petlyuk and Danilov (2000), is the separation of acetone and chloroform, which form a maximum-boiling homoazeotrope, by using water as an entrainer. Water is relatively high-boiling and selective to acetone. In addition, an immiscibility region and a binary heteroazeotrope  $A_{2E}$  and a ternary heteroazeotrope  $A_{12E}$  are formed as illustrated in Figure 2.22. Note that there is a change in volatility order of the components within the region

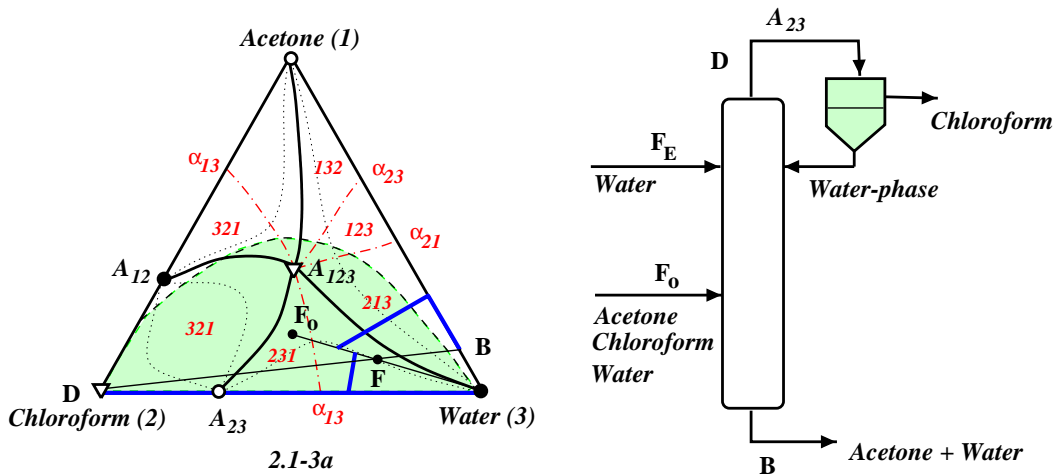


Figure 2.22: Heteroextractive distillation (Petlyuk and Danilov, 2000).

where the feed compositions are located. The  $\alpha_{13}$  univolatility line indicates this change. If the

summary feed  $F$  is located in the region with the 213 volatility order of the components, the azeotrope  $A_{23}$  is removed as distillate product (not the saddle azeotrope  $A_{123}$ ) and split into pure 2 and E by condensation and decantation.

In conclusion, one should be careful about limiting oneself when considering extractive distillation (“no distillation boundaries”) and also careful about using established selection criteria for entrainers.

## 2.4.6 Entrainer selection

The task of entrainer searching should be based on thermodynamic and physical insights (e.g. about the intermolecular forces and the VL(L)E diagram structure).

Ewell *et al.* (1944) studied the relationship between hydrogen bonding and azeotrope formation and classified entrainers into groups according to their molecular interactions. From this they developed guidelines to identify chemical classes suitable as entrainers for heteroazeotropic and extractive distillation. These guidelines were discussed by Berg (1969), who further developed a classification of organic and inorganic mixtures and used information about the molecular structure to point out promising entrainers for extractive and heteroazeotropic distillation. Berg (1969) states that successful entrainers for extractive distillation are highly hydrogen-bonded liquids (such as water, amino alcohols, amides, phenols alcohols and organic acids).

The effectiveness of the entrainer is based on its ability to modify the relative volatility of the original mixture. Various approaches for this evaluation are given, for example by Van Winkle (1967):

*Extractive distillation:* A promising entrainer forms a complex or hydrogen bond with one of the components  $i$  in the original mixture, resulting in a decrease in the vapor pressure of component  $i$  such that  $\alpha_{ij}$  decreases. If this reduces  $\alpha_{ij}$  to 0.8 (or  $\alpha_{ji}$  to 1.2 or greater), the separation is greatly enhanced.

*Heteroazeotropic distillation:* A promising entrainer “breaks” a complex formed between the components 1 and 2, or between 1 and 1, resulting in an increase in the vapor pressure of component 1 such that  $\alpha_{12}$  increases.

Van Winkle (1967) emphasizes that the whole process system must be considered in the selection of an effective entrainer and that the recovery process must be included in the evaluation. A candidate entrainer might have a very good selectivity, but it might be difficult to recover in the second column. Therefore, the final selection must be made based on an economic evaluation.

Molecular design of an entrainer may even be pursued (see for example Brignole *et al.* (1986) and Pretel *et al.* (1994)). Group contribution methods are used to synthesize entrainers with specific physical properties (Furtzer, 1994; Gmheling and Möllmann, 1998). Search for specific component properties in computerized data banks may be performed, where activity coefficients at infi-

nite dilution are helpful measures of the entrainer selectivity. Expert systems to identify candidate entrainers have been developed with heuristic rules implemented into knowledge databases.

## 2.5 Summary and conclusions

Separation of homogeneous azeotropic mixtures is a topic of great practical and industrial interest. Most liquid mixtures of organic components form nonideal systems. The presence of some specific groups, particularly polar groups (oxygen, nitrogen, chlorine and fluorine), often results in the formation of azeotropes. Binary homoazeotropes (at least the ones that are not pressure sensitive) are impossible to separate by ordinary distillation, but may be effectively separated by membrane-distillation hybrids or distillation methods where a third component is added to the system. Analysis of ternary VL(L)E diagrams is an efficient tool to predict feasible separations for entrainer-addition distillation processes. Simplest approaches are sufficient if used properly. We distinguish between three different entrainer-addition distillation methods depending on the properties of the entrainer and the organization of the column flows and the following conclusions can be made:

- Homogeneous azeotropic distillation (ordinary distillation of homoazeotropic mixtures)  
Only a few VLE diagram structures of the resulting ternary system of original mixture and entrainer are possible to separate by ordinary distillation (sequence of single-feed columns). The separation schemes are complex and may be very energy intensive, or may have multiplicities.
- Heteroazeotropic distillation (decanter-distillation hybrids involving heteroazeotropes)  
Several VLLE diagram structures that involves one or more heteroazeotropes are possible to separate by ordinary distillation combined with decantation. The separation schemes are fairly simple, but the range of feasible entrainers is rather limited.
- Extractive distillation  
Extractive distillation is the most general distillation method for separating homoazeotropic mixtures. The scheme is not sensitive to the type of original mixture as there is a broad range of feasible entrainers. The process is not limited to homogeneous entrainers, and heteroextractive distillation-decanter hybrids may be applied with success.

Insights into to the thermodynamic behavior of azeotropic mixtures is fundamental for the development of separation system involving azeotropic mixtures. This is an incentive to consider the powerful tool of graphical VLE representation in more detail.



## Chapter 3

# Azeotropic Phase Equilibrium Diagrams: A Survey

An analysis of the structural properties of vapor-liquid equilibrium (VLE) diagrams provides a fundamental understanding of the highly nonideal thermodynamic behavior of azeotropic mixtures.

In addition to a review of well-known fundamental work on the analysis of VLE diagrams, this survey comprises less known published results, especially from the Russian literature. Some new results are also presented for the first time.

### 3.1 Introduction

Distillation, where a liquid mixture is separated by successive evaporation and condensation, is the most important separation process in the chemical industry. The basis for the separation is that the vapor phase is richer in the more volatile component(s) than the liquid. This enrichment is determined by the vapor-liquid phase equilibrium. As a result, feasible separations in a distillation column and the operating parameters required for these separations depend on the vapor-liquid equilibrium of the mixture to be separated.

For ideal and nearly ideal mixtures the components of the given mixture can be ranked in order of their volatility, or, equivalently, in order of the pure components boiling points, and one can easily list all feasible separation sequences. In practice, we often have to deal with nonideal mixtures where the composition space is split into regions with different volatility ranking of the components, and the listing of feasible sequences is much more difficult. Furthermore, azeotropic behavior is often encountered where at some point(s) in the composition space the equilibrium vapor and liquid compositions are equal (for a given pressure and temperature). These points are

called azeotropes and mixtures with this phenomena are called azeotropic mixtures. The highly nonlinear vapor-liquid equilibrium behavior of azeotropic mixtures complicates the prediction of feasible separation sequences further, and an azeotrope itself cannot be separated by ordinary distillation since no enrichment of the vapor phase occurs at this point. Usually, special methods are required.

Azeotropic distillation is defined as distillation that involves components which form azeotropes. Generally, there are two cases of azeotropic distillation: (i) when the original mixture to be separated is an azeotropic mixture, and, (ii) when an azeotropic mixture is formed deliberately by adding one or more azeotrope-forming components to the original mixture. In the first case we have to find a way to separate the azeotropic mixture and obtain the desired product specifications and recovery. In the second case, in addition, we have to select an azeotrope-forming component (called entrainer) that is effective for the desired separation and easily recovered afterwards. In either case we should establish the options before analyzing them in detail. For this purpose we need a tool to qualitatively predict the feasible separations for multicomponent azeotropic mixtures. The tool is known as *thermodynamic topological analysis of distillation* (in Russian literature) or *residue curve (or distillation line) map analysis*. It provides an efficient way for preliminary analysis of nonideal distillation problems and presynthesis of separation sequences.

### Thermodynamic topological analysis

The thermodynamic topological analysis is based on the classical works of Schreinemakers (1901*b*; 1901*c*; 1902) and Ostwald (1902), where the relationship between the vapor-liquid equilibrium of a mixture and the behavior of open evaporation *residue curves* for ternary mixtures was established. Although open evaporation (a single vaporization step with no reflux) itself is not of much industrial interest in the 21st century, it nevertheless forms an important basis for the understanding of distillation (a sequence of partial vaporization steps with reflux). The findings by Schreinemakers did not receive recognition until the 1940s when Reinders and de Minjer (1940) and Ewell and Welch (1945) showed the possibility to use this approach to predict the behavior of batch distillation. These achievements stimulated subsequent investigations by Haase and Lang (1949; 1950*a*; 1950*b*; 1951) and Bushmakina and Kish (1957*a*; 1957) on the structure of phase equilibrium diagrams and its connection with batch distillation behavior. In 1958, Gurikov (1958) formulated the "Rule of azeotropy" and proposed a classification of ternary mixtures based on their thermodynamic topological structures (*residue curve map analysis*).

In the late 1960s, Zharov (1967; 1968*c*) gave a more rigorous mathematical foundation of the residue curve map analysis and expanded it to multicomponent mixtures. During the same period, Serafimov (1968*a*; 1968*d*) proposed to use structural information of VLE diagrams to predict feasible separations in continuous distillation. The results of Zharov and Serafimov initiated a large effort in Russia (USSR) on the development and application of qualitative analysis of multicomponent nonideal and azeotropic distillation. One reason for the large interest in this "pen-and-paper" approach in Russia in the 1960s and 70s was the fact that during these years the Russian chemical industry expanded whereas there was a shortage of computers and limited possibilities for numerical computation.

The contribution of Doherty and Perkins and co-workers (1978a; 1978b; 1979b; 1979a; 1985b; 1985a; 1985; 1985) formed the basis for a renewed interest in this subject also in the West. The reason for this renewed interest was the realization that, in spite of (or maybe because of) the great advances in vapor-liquid equilibrium calculations and simulations, there was a need for simpler tools to understand the fundamental limitations and possibilities in distillation of azeotropic mixtures. These tools are today well-established, and residue curve map analysis is included in the main recent encyclopedia in chemical engineering (Perry, 1997; Stichlmair, 1988; Doherty and Knapp, 1993). Four review papers have been published during the last few years (Pöllmann and Blass, 1994; Fien and Liu, 1994; Widagdo and Seider, 1996; Westerberg and Wahnschafft, 1996). Furthermore, the topic is included in recent textbooks (Biegler *et al.*, 1997; Seader and Henley, 1998; Stichlmair and Fair, 1998) as a fundamental part of chemical engineering.

Nevertheless, the field is still rather bewildering and we believe that many of the recent results have not been put into proper perspective and compared to earlier work, especially to work in the Russian literature. The main objective of this paper is therefore to present a broad survey of the field, which includes references also to papers that are less recognized in the English-language literature.

The theory of thermodynamic topological analysis (TTA) of distillation can be divided into two parts.

1. The first considers in detail the feasible structures of VLE diagrams (including their classification). The main concept is that there is a unique and relatively simple correspondence between the vapor-liquid equilibrium (VLE) characteristics of a given mixture and the path of equilibrium phase transformations such as residue curves and distillation lines.
2. The second part of the TTA is directed to the prediction of feasible separations in distillation, for which the main concepts are:
  - There is a unique correspondence between the state of a distillation column at extreme operating parameters (infinite flows or infinite stages) and the composition trajectories of simple phase transformations (e.g., residue curves). Consequently, these column states can be determined from specific VLE characteristics of the mixture to be separated depending on the feed composition of the mixture.
  - The state of a distillation column at real operating parameters can be qualitatively determined based on the column states at extreme operating parameters, that is, from the composition trajectories of the simple equilibrium phase transformations such as residue curve maps.
  - As a result, the product composition areas for all combinations of the operating parameters can be predicted qualitatively based on information about the simple phase transformation map (e.g., residue curve map) and, thus, the feasible separations and separation sequences can be determined.

Therefore, analysis of VLE diagrams is the starting point for the prediction of feasible separations by distillation. It allows us to determine the thermodynamic possibilities and limitations of the

separation caused by the nature of the mixture. After determining the feasible separations, we can synthesize the alternative separation sequences that should be subject to further investigation and comparison in order to choose the optimal one. Such an approach is called analysis-driven distillation synthesis (Westerberg and Wahnschafft, 1996). As a result of the analysis it may turn out that the mixture cannot be separated by conventional distillation. Then, special distillation methods may be employed. TTA (or residue curve map analysis) also provides a tool for evaluation of these separation techniques. In particular, TTA is very useful for the screening of entrainers for heteroazeotropic and extractive distillation.

## Comment on terminology

There are many alternative and even conflicting key terms in the distillation literature. Table 3.1 gives the correspondence between four central terms in English-language, Russian and German literature. Note in particular that in many Russian publications “distillation lines” means residue curves, “c-lines” means distillation lines and “node” means vector. One reason for this incompatible terminology is due to the historical fact that the term distillation was originally used to denote simple distillation (open evaporation, Rayleigh distillation). Schreinemakers (1901*b*) and succeeding researchers used the term “distillation lines” as a short term for simple distillation liquid composition trajectories, which was later termed *residue curves* by Doherty and Perkins (1978*a*). Today, the term distillation has become a common, simplified term for distillation with the use of reflux (rectification, fractional distillation). Stichlmair (1988) uses the term *distillation line* to denote the total reflux composition profile in an equilibrium staged distillation column. The term “node” is just a result of poor English language translation. In the present text we use the terms that are broadly accepted in English-language distillation publications. See section on Definitions of Terms for more detail.

Table 3.1: Correspondence between terms in English-, Russian- and German-language literature

Current terms commonly found in English-language literature (and in this paper)	Equivalent terms mainly found in Russian- and German-language literature	Example of reference where this term is used
equilibrium vector	tie-line node line mapping vector	Zharov and Serafimov (1975) Serafimov (1996) Widagdo and Seider (1996)
distillation line (continuous and discrete)	connecting line (c-line) chain of conjugated tie-lines tie-line curve equilibrium rectification line	Zharov (1968 <i>c</i> ) Zharov (1968 <i>c</i> ) Westerberg (1997) Pelkonen <i>et al.</i> (1997)
residue curve	distillation line of the residue residue curve distillation line	Schreinemakers (1901 <i>c</i> ) Ostwald (1902) Serafimov (1968 <i>b</i> )
distillate curve	distillation line of the vapor vapor line boil-off curve	Schreinemakers (1901 <i>b</i> ) Bushmakin and Kish (1957 <i>a</i> ) Fidkowski <i>et al.</i> (1993)



## Structure of the survey

This survey is devoted to the first part of thermodynamic topological analysis, that is, to the characteristics of vapor-liquid equilibrium diagrams. The thermodynamic basis of vapor-liquid equilibrium (VLE) and ways to graphically represent the VLE of a mixture are briefly given in Section 3.2. The various representations of the VLE for ternary mixtures are considered in detail in the subsequent sections: isotherm maps (Section 3.3); residue curve maps and evaporation distillate curve maps (Section 3.4); open condensation curve maps and distillation line maps (Section 3.5). These sections also include the structures of these maps and the relationship between the different representations. Some peculiarities of the simple equilibrium phase transformation maps for heterogeneous mixtures are considered in Section 3.6.

Section 3.7 is devoted to the classification of VLE diagrams for ternary mixtures and related issues such as completeness of classification, occurrence of the various structure classes in nature, and more. Determination of the VLE diagram structures based on incomplete information is discussed. In Section 3.8, unidistribution and univolatility line diagrams and their role in the determination of the geometry (pathway) of the residue curve and distillation line maps are considered. Finally, the overall conclusions are given in Section 3.9.

## Contributions

Fundamental theory on structural properties of VLE diagrams for azeotropic mixtures are reviewed. In addition, some new results and concepts are presented for the first time. In particular:

- A simple *rule on residue curve regions* is formulated: the composition space splits into the same number of residue curve regions as there are repeated nodes in the system. For example, if the residue curve system has two stable nodes and one unstable node, the number of nodes of the same type is two, and the residue curve map is split into two regions.
- The *relative location of the region boundaries* (separatrices) of residue curves, open condensation curves and distillation lines in the composition space are presented.
- The thermodynamical meaning of *distillation lines* are emphasized.
- Peculiarities of residue curves for heterogeneous mixtures are examined. Although the topology of the residue curve maps generally do not differ from homogeneous mixtures, and can be determined in a similar way from the shape of the boiling temperature surface, there are some peculiarities of the "inner" topology in heterogeneous mixtures.
- A table of *correspondence between the different classifications* of ternary VLE diagrams is given. The classifications by Gurikov (1958), Serafimov (1970*b*), Zharov and Serafimov (1975) and Matsuyama and Nishimura (1977) are included.
- The question of the *existence* of all the classified structures is evaluated. Although a structure may be thermodynamically and topologically feasible, its occurrence is determined by

the probability of certain combinations of molecular interactions. We present data on the reported *occurrence* of ternary mixtures, and reveal factors that limit the natural occurrence of mixtures with certain VLE diagram structures.

- The problem of *indeterminacy* in predicting ternary VLE diagram structures based on incomplete information (binary or experimental data only) is critically considered.
- Feasible patterns of the VLE functions for binary mixtures represented by the equilibrium line, distribution coefficients and relative volatility depending on the molecular interactions are presented.
- The structures of *unidistribution and univolatility line diagrams* for ternary mixtures of different classes and types, and the relation to the *shape* of simple equilibrium phase transformation trajectories such as residue curves and distillation lines, are considered in detail. We show that a combined diagram of these unitylines can successfully be used as a characteristic of the VLE. These maps are easy to generate and a lot of information can be retrieved from them.
- Rules on the *location of the inflection point curves* in the composition space are given.

## 3.2 Thermodynamic basis

The fundamental laws of thermodynamics and phase equilibrium is all that is needed to derive the results presented in this paper, and in this section we briefly review the thermodynamic basis. From thermodynamics, the compositions of liquid and vapor in phase equilibrium are determined by the vapor-liquid equilibrium (VLE) condition which may be expressed as:

$$\mathbf{y} = f(P, T, \mathbf{x}) \quad (3.1)$$

where  $\mathbf{x}$  and  $\mathbf{y}$  are the liquid and vapor compositions, and  $P$  and  $T$  are the system pressure and temperature, respectively.  $P$ ,  $T$  and  $\mathbf{x}$  are not independent at the equilibrium state since:

$$\sum_{i=1}^n y_i = 1 \quad (3.2)$$

For example,  $[T, \mathbf{y}]$  may be determined as a function of  $[P, \mathbf{x}]$ . Thus, at *isobaric* conditions we may use only the liquid composition  $\mathbf{x}$  as the independent variable, and we may write (“E-mapping”):

$$\mathbf{y} = E(\mathbf{x}), \quad T = T_{bp}(\mathbf{x}) = T_{dp}(\mathbf{y}) \quad (3.3)$$

where  $E$  is the equilibrium mapping function that assigns a composition in the liquid phase to the corresponding equilibrium vapor phase composition, and  $T_{bp}$  and  $T_{dp}$  are the mixture boiling

temperature (bubble-point) and condensation temperature (dew-point), respectively. Equivalently, we may write (“C-mapping”):

$$\mathbf{x} = C(\mathbf{y}), \quad T = T_{dp}(\mathbf{y}) = T_{bp}(\mathbf{x}) \quad (3.4)$$

where  $C = E^{-1}$  is the inverse equilibrium mapping function that assigns a composition in the vapor phase to the corresponding equilibrium liquid phase composition.

For any liquid composition  $\mathbf{x}$ , there is a point  $[T, \mathbf{x}]$  on the boiling temperature surface  $T_{bp}(\mathbf{x})$  and a corresponding point  $[T, \mathbf{y}]$  on the condensation temperature surface  $T_{dp}(\mathbf{y})$  that are connected by an equilibrium vector (also called a vapor-liquid tie-line). The projection of this equilibrium vector onto the composition space represents the *equilibrium mapping vector*  $\overrightarrow{\mathbf{x}\mathbf{y}}$ , that is, the graph of the function  $E : \mathbf{x} \rightarrow \mathbf{y}$ . In this sense, the condensation temperature surface  $T_{dp}(\mathbf{y})$  is simply an equilibrium  $E$ -mapping of the boiling temperature surface  $T_{bp}(\mathbf{x})$ . The two temperature surfaces merge at the points of pure components where  $x_i = y_i = 1$  for component  $i$  and  $x_j = y_j = 0$  for all other components  $j \neq i$ . According to Gibbs-Konovalov Law formulated in the 1880s (Prigogine and Defay, 1954; Tester and Modell, 1997), the existence of an extremum of the boiling temperature function  $T_{bp}(\mathbf{x})$  leads to an extremum of the condensation temperature function  $T_{dp}(\mathbf{y})$ . At the extremal points, the liquid and its equilibrium vapor compositions are equal and the temperature surfaces are in contact. The existence of such extrema is called *azeotropy*, and the corresponding compositions where  $\mathbf{y} = \mathbf{x}$  are called *azeotropes*. Mixtures that form azeotropes are called *azeotropic*, and mixtures that do not form azeotropes are called *zeotropic*.

The existence of azeotropes complicates the shape of the boiling and condensation temperature surfaces and the structure of the *vapor-liquid envelope* between them, and the equilibrium mapping functions. The envelope of the equilibrium temperature surfaces defines the feasible operating region in  $T - \mathbf{x}, \mathbf{y}$  space in which any real distillation process must operate. This motivates a more careful analysis of the VLE behavior. For the prediction of feasible separations upon distillation of azeotropic mixtures we need a qualitative characterization of the VLE, preferable a graphical representation.

### Graphical VLE representation

The possibility to graphically represent the VLE depends on the number of components in the mixture. In a mixture of  $n$  components, the composition space is  $(n-1)$ -dimensional because the sum of molefractions must be equal to unity. For binary mixtures the composition space is one-dimensional. Graphical representations of the VLE for the most common types of binary mixtures are presented in Figure 3.1. The left part of Figure 3.1 shows a combined graph of the boiling and condensation temperatures and the vapor-liquid equilibrium phase mapping, which gives a complete representation of the VLE. In addition, the right part gives the equilibrium phase mapping alone. Each of these diagrams uniquely characterizes the type of the mixture (zeotropic or azeotropic, minimum- or maximum-boiling etc.), and, what is more important, we do not need the exact trajectories of the functions to make this characterization. It is sufficient to know the

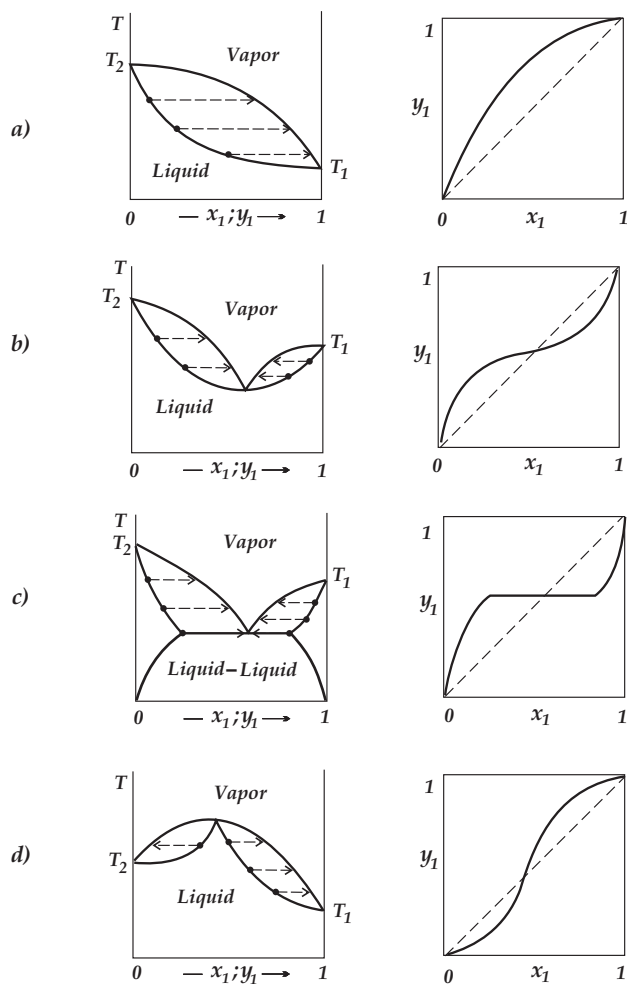


Figure 3.1: Graphical representations of the VLE for the most common types of binary mixtures at constant pressure: a) zeotropic; b) minimum-boiling homoazeotrope; c) minimum-boiling heteroazeotrope; d) maximum-boiling azeotrope. Left: boiling temperature  $T_{bp}$  and condensation temperature  $T_{dp}$  and the equilibrium mapping vectors in  $T - x, y$  space. Right:  $x - y$  relationship (equilibrium line).

boiling points of the pure components and azeotropes, if any, to determine the type of the mixture and to qualitatively predict the distillation behavior for various feed compositions of the mixture.

For ternary mixtures the composition space is a two-dimensional normalized space and its graphical representation is an equilateral or rectangular triangle. The VLE functions are surfaces in a three-dimensional prism. The complete representation of the VLE is the vapor-liquid envelope

of the boiling and condensation temperature surfaces, and the set of equilibrium vectors between them, as illustrated in Figure 3.2a. The equilibrium mapping function itself can be represented by pair of the surfaces  $y_i(x)$  and  $y_j(x)$  in the prism  $Y-X$ , as illustrated in Figure 3.2b. It is difficult

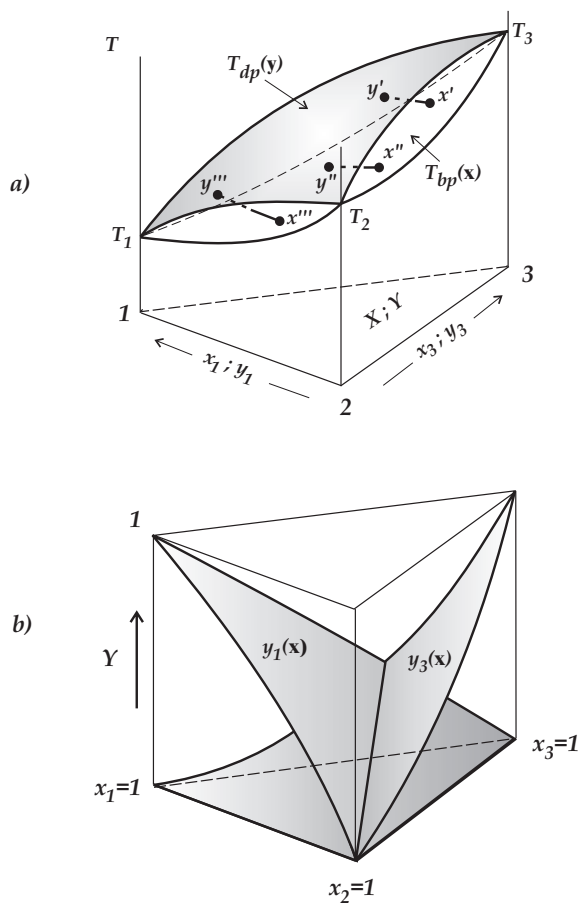


Figure 3.2: Graphical representation of the VLE for a ternary zeotropic mixture: a) boiling and condensation temperature surfaces and the connecting equilibrium vectors; b) equilibrium vector surfaces.

to interpret three-dimensional surfaces in a two-dimensional representation, thus other representations are preferred for ternary mixtures. The most straightforward approach is to use contour plots of the surfaces similar to topographic maps with isolines of constant values of the functions to be represented. Such isoline maps, specially isotherm map of the boiling temperature, play an important role in the qualitative analysis of VLE diagrams. Isotherm maps are considered in Section 3.3.

The dependence of the equilibrium vapor composition on the liquid composition given by the equilibrium  $E$ -mapping function can be graphically represented by a field of equilibrium vectors in the composition plane. Such vector fields usually appear rather chaotic (see, for example, the equilibrium vector fields for ternary mixtures in Gmehling's "Vapor-Liquid Equilibrium Data Collection"). They do not give a clear graphical representation of the VLE. In addition, this representation has the disadvantage of being discrete and requires a great number of (experimental) data to draw it.

An alternative method to graphically represent the VLE for a given mixture is by using *simple equilibrium phase transformations* such as open evaporation (simple distillation), open condensation and repeated equilibrium phase mapping. The liquid and vapor composition changes during these transformations can be represented by trajectories in the composition space. The pathway of these trajectories depends on the vapor-liquid equilibrium only, and in turn characterizes the VLE. This is the topic of Sections 3.4 and 3.5.

For multicomponent mixtures ( $n \geq 4$ ) the composition space is  $(n-1)$ -dimensional and its graphical image is a polyhedron (tetrahedron for  $n = 4$ , pentahedron for  $n = 5$  and so on). In the case of quaternary mixtures it is possible to graphically represent the VLE functions in a composition tetrahedron, but it may be complicated to interpret. If the number of components is more than four, graphical representation is difficult. However, a multicomponent mixture may be divided into ternary subsystems of components and pseudo-components. The ternary VLE sub-diagrams are evaluated as a whole. Alternatively, a multicomponent mixture may be represented by a pseudo-ternary or quaternary system of three or four of its key components. Obviously, VLE information may be used without graphical representation too.

In conclusion, most of the studies on the qualitative analysis of VLE are focused on ternary mixtures where graphical representations are readily visible and can be used for the prediction of distillation behavior.

### 3.3 Isotherm maps of ternary mixtures

Throughout this paper we assume constant pressure. Isotherms are contour lines of constant temperature (also called isotherm-isobars). Isotherm maps as a way to represent the system of VLE functions Equations (3.3) and (3.4) were first used by Schreinemakers (1901*b*). Isotherms of the boiling temperature surface  $T_{bp}(x)$  and the isotherms of the condensation temperature surface  $T_{dp}(y)$  were later called *liquid isotherms* and *vapor isotherms*, respectively, by Reinders and de Minjer (1940). The liquid compositions of a liquid isotherm are connected with the vapor compositions of the corresponding vapor isotherm (at the same temperature) by the equilibrium vectors in the composition space  $\overline{xy}$ , see Figure 3.3. Such a diagram is a complete graphical representation of the VLE system Equation (3.4). Schreinemakers (1901*c*) studied complete graphical representations of the VLE system Equation (3.3) for various combinations of a given binary azeotropic mixture with a third component that forms additional binary and ternary azeotropes. He also showed the analogy between an isobar map at constant temperature and the isotherm

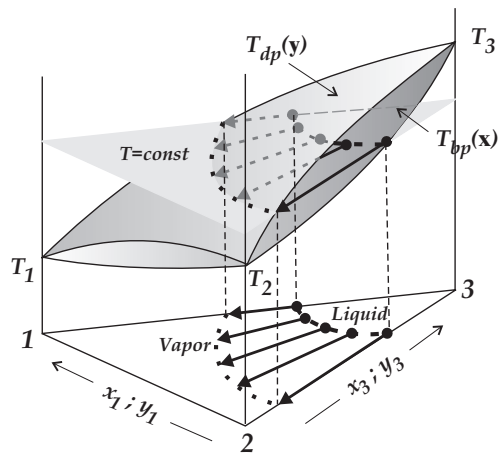


Figure 3.3: *Liquid and vapor isotherms and the equilibrium vectors that connects them for a ternary zeotropic mixture with pure component boiling points  $T_1$ ,  $T_2$  and  $T_3$  at constant pressure (Schreinemakers, 1901b).*

maps at constant pressure. Isotherm maps are presented in Figure 3.4 as they are given in the original publication by Schreinemakers (1901b). From this study, Schreinemakers established that:

1. Ternary mixtures may exhibit distinctly different isotherm maps depending on the existence of azeotropes, their type (binary or ternary, minimum-, maximum- or intermediate-boiling), their location, and the relative order of the boiling points of the pure components and azeotropes.
2. A binary azeotrope that is an extremal point of the binary mixture temperature functions, is not necessary a global temperature extreme for the ternary mixture as a whole, thus being a saddle point.
3. In the same way, a ternary azeotrope is not necessary a global temperature extreme for the ternary mixture, thus being a saddle point (minimax) of the temperature surface.

The examples of isotherm maps given in Figure 3.4 are only for purposes of illustration. In practice, it is difficult to draw such combined diagrams of liquid and vapor isotherms (at constant pressure) because an isotherm of one phase may be (and usually is) intersected by isotherms of the other phase at other temperatures. Equilibrium vector field diagrams are also confusing since the equilibrium vector projections in the composition space intersect each other. The more detailed diagram we want to draw, the less understandable it becomes. Isotherm maps, for example as a representation of the boiling temperature function, are more readable. But, with the exception of binary mixtures, it is difficult to immediately understand the distillation behavior of ternary

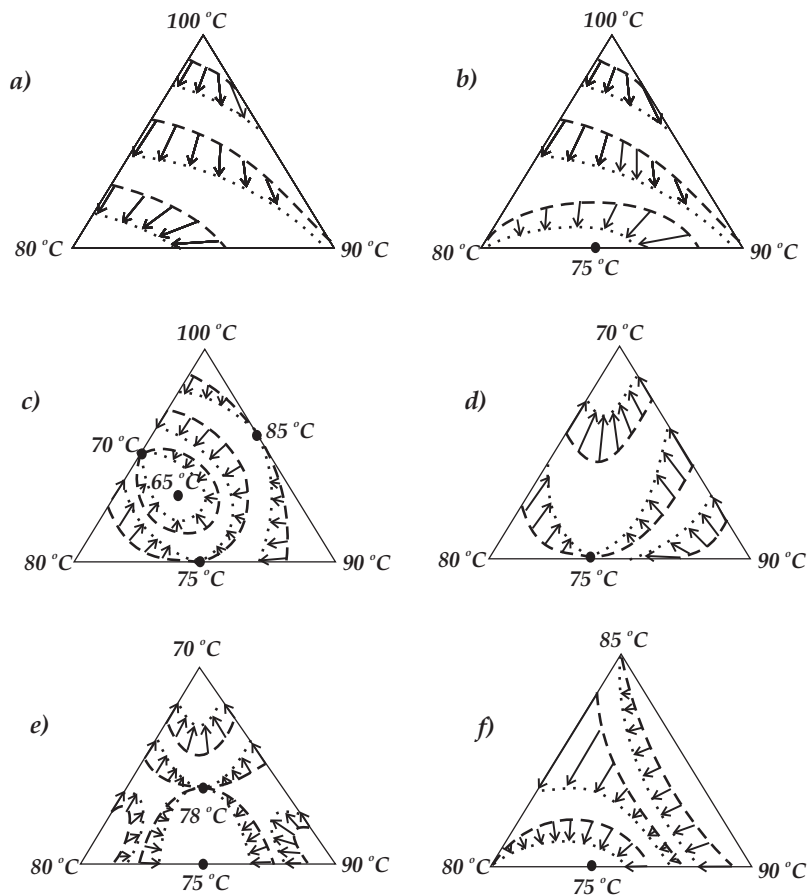


Figure 3.4: Liquid and vapor isotherms and equilibrium vectors in the composition space at constant system pressure: a,b,c,d) examples from Schreinemakers (1901b); e,f) additional examples.

mixtures from the liquid isotherm map without special knowledge. Schreinemakers demonstrated the severity of the problem, and it has taken the efforts of many investigators to find a proper way of characterizing vapor-liquid equilibrium diagrams.

The key to a qualitative characterization of the VLE lies with the analysis of *simple equilibrium phase transformation processes*, and above all of open evaporation (simple distillation) which is the topic of the next section.



## 3.4 Open evaporation

### 3.4.1 Residue curves

Open evaporation, also known as simple distillation or Rayleigh distillation, is batch distillation with one equilibrium stage where the vapor formed is continuously removed so that the vapor at any instant is in equilibrium with the still-pot liquid (residue). Schreinemakers (1901c) considered the instantaneous mass balance equation of this process:

$$d(Lx_i) = -y_i dV \Rightarrow Ldx_i = -dV(y_i - x_i) \quad i = 1, 2, 3 \quad (3.5)$$

where  $L$  [mol] is the amount of the residue liquid in the still-pot,  $dV$  [mol] is the amount vapor evaporated,  $x_i$  and  $y_i$  are the mole fractions of the component  $i$  in the still-pot liquid and in the vapor, respectively. Schreinemakers called the liquid composition trajectory of simple distillation a "distillation line". The present term used in English is *residue curve* (Doherty and Perkins, 1978a). Schreinemakers proposed for ternary mixtures to consider the ratio of still-pot liquid components:

$$\frac{dx_i}{dx_j} = \frac{(y_i - x_i)}{(y_j - x_j)} \quad (3.6)$$

Integrating Equation (3.6) from any initial composition  $x_0$  will generate a residue curve. It is evident from Equation (3.6) that the residue curve paths are governed by the VLE solely, that is, by the set of functions in system Equation (3.3), and, in turn, can characterize the VLE of any given mixture. We also see from Equation (3.6) that the equilibrium vector in the composition space  $\vec{x}\vec{y}$  is tangent to the line of still-pot liquid composition change at any point  $x$ .

Schreinemakers established that the interior of the composition space is filled in with residue curves. The points of components and azeotropes are the isolated residue curves, and the edges of the composition space between the singular points are residue curves too. He analyzed the relation between the position of the equilibrium vectors at the liquid isotherms and the path of the residue curves. This connection is presented in Figure 3.5. Based on this, he derived what in the Russian literature is referred to as Schreinemakers' rules:

1. a residue curve always moves along the boiling temperature surface in the direction of increasing temperature and cannot intersect twice with the same liquid isotherm;
2. residue curves cannot intersect each other.

The path of the residue curves can be determined from the isotherm map, but the intersection angle between the liquid isotherm and the residue curve does not depend on the shape of the isotherm but rather on the direction of the equilibrium vector at this point. Hence, the path of residue curves can only be *qualitatively* determined from the isotherm map. A residue curve map is a more legible representation of the VLE than isotherms because from this diagram we can immediately

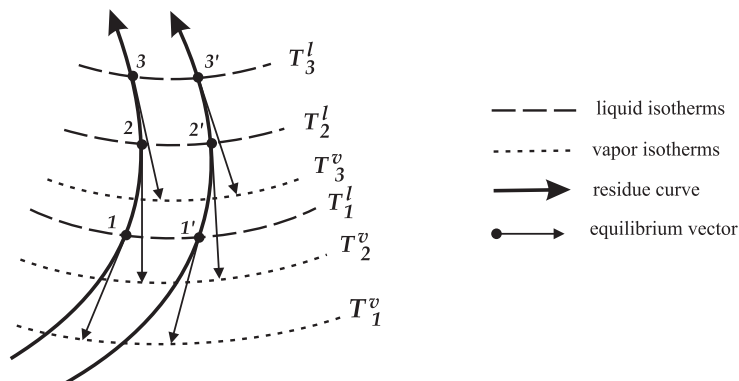


Figure 3.5: Relationship between the path of residue curves and the isotherms and equilibrium vectors in the composition space (Schreinemakers, 1901c).

see the behavior of the given mixture during the simple distillation process (open evaporation). Further, we can determine the change of the relative volatility order of the components in the mixture from the change of the tangent slope along the residue curves.

Residue curve maps that corresponds to the mixtures given in Figure 3.4 (isotherm maps) are presented in Figure 3.6. A point with minimum boiling temperature is an initial point of the residue curves. A point with maximum-boiling temperature is a terminal point of the residue curves. For zeotropic mixtures, Figure 3.6a, the residue curves have a hyperbolic path in the vicinity of singular points with intermediate boiling temperature. For azeotropic mixtures, the residue curves sometimes have a hyperbolic path in the vicinity of intermediate singular boiling points (Figure 3.6 b,f), and, in other cases, a singular point with intermediate boiling temperature is an initial or final point of the residue curves (Figure 3.6 c,d,e). Schreinemakers established that in some cases the residue curves are split into *residue curve regions* where the residue curves of each region have the same initial and final points (Figure 3.6 c,d,e). Schreinemakers established the existence of singular residue curves as boundaries of these regions. It has been shown (Schreinemakers, 1902) that, in general, against the opinion by Ostwald, the residue curve boundaries are curved.

Haase (1949) proved the validity of the Schreinemakers' rules for ternary mixtures analytically by solving both the residue curve equation and the phase equilibrium condition. The assumptions by Schreinemakers were confirmed experimentally by Reinders and De Minjer (1940a; 1940b; 1947a; 1947b; 1947c), Ewell and Welch (1945) and Bushmakina and Kish (1957a). In particular, Ewell and Welch was the first to report a ternary saddle azeotrope, the existence of which was predicted theoretically about 1900 by Ostwald and Schreinemakers.

In conclusion, Schreinemakers not only introduced the concept of residue curves, but revealed their main properties as well.

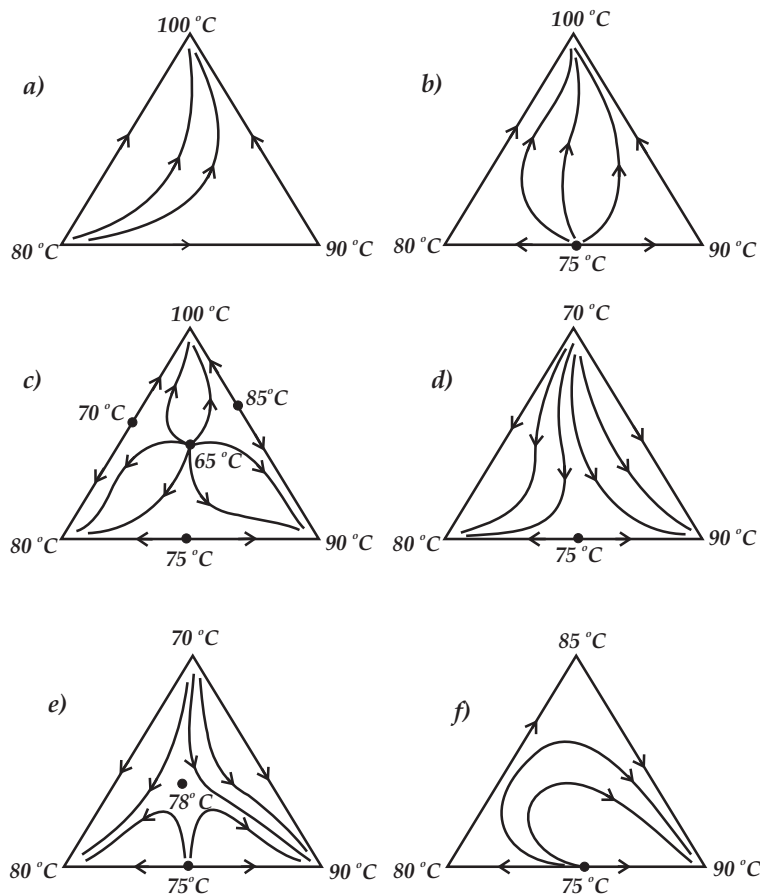


Figure 3.6: Residue curve maps for the mixtures whose isotherm maps are presented in Figure 3.4: a,b,c,d) examples from Schreinemakers (1901b); e,f) additional examples.

### 3.4.2 Properties of residue curves' singular points

Haase (1949) studied the behavior (paths) of the residue curves near the vertices of the composition triangle and the azeotropic points (i.e., near the residue curves' singular points). In particular, he found that a pure component vertex is an initial or a final point (node) of the residue curves if the liquid boiling temperature increases or decreases (near it) by the movement from the vertex along both adjoining edges. At other singular points (saddles), the residue curves have a hyperbolic shape in the vicinity of the vertex if the liquid boiling point temperature increases at the movement from the vertex along one of the edges and decreases at the movement along another edge. This observations are known in Russian literature as Haase's rule. In summary, the residue

curves originate and ends at nodes of the boiling temperature surface and have a hyperbolic path in the vicinity of their saddles.

Considering the feasible paths of isotherms and residue curves in the vicinity of nodes and saddles for homogeneous mixtures, Bushmakin and Kish (1957a) and Bushmakin and Molodenko (1957) established the correspondence between their trajectories. It was found that residue curves begin or end at a singular point (node) that is an isotherm point itself (“dot” isotherm), Figures 3.7a, b, c. Residue curves have a hyperbolic shape near the singular point if a “finite length isotherm”

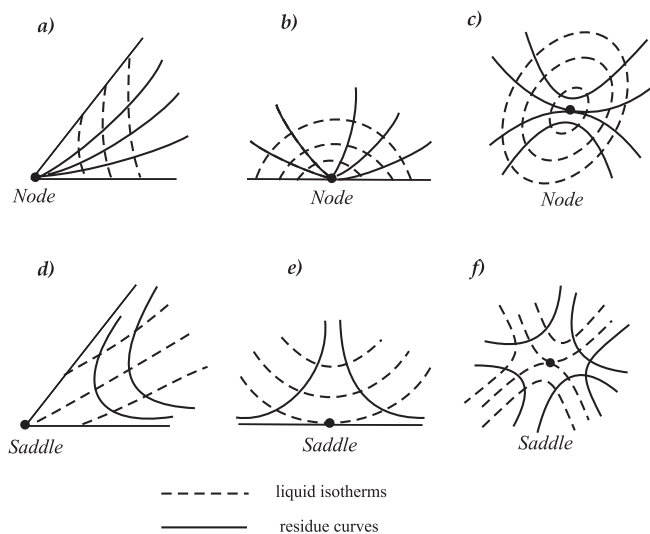


Figure 3.7: Patterns of isotherms and residue curves near singular points at constant pressure (Bushmakin and Molodenko 1957).

passes through this singular point (saddle), Figure 3.7d, e, f. If all the residue curves terminates in a singular point, then the point is a stable node. If all the residue curves extend from a singular point, then the point is an unstable node. If the residue curves both approach and depart a singular point, then the point is a saddle.

Gurikov (1958) proposed to use the qualitative theory of ordinary differential equations to analyze the behavior of residue curves, and in this context, a singular point that is an initial or a final point of the residue curves is a *node*, and a singular point in which the residue curves have a hyperbolic shape near it is a *saddle*. Analyzing the combined solution of Equation (3.6) and the thermodynamic stability criteria, Gurikov showed that the residue curve system for ternary mixtures does not have singular points of the type *focus* or *isola*.

Zharov (1967; 1968b; 1968a; 1969), Serafimov (1968a; 1968d; 1968b; 1968c; 1969a; 1969b; 1969c) and later Doherty and Perkins (1978a; 1978b) considered simple distillation (evaporation residue curves) for the general case of multicomponent mixtures given by the following set of

autonomous differential equations:

$$\frac{dx_i}{d\tau} = -(y_i - x_i) \quad i = 1, 2, \dots, n - 1 \quad (3.7)$$

Here  $\tau$  is a dimensionless time describing the relative loss of the liquid in the still-pot;  $d\tau = dV/L$ . Note that Zharov and Serafimov use opposite sign of the Equation (3.7) according to their definition of  $\tau$ , and thus the sign of the eigenvalues are opposite in their thermodynamic topological analyses. Fortunately, the results on the properties of the residue curves' singular points are independent of this choice of preserving the minus sign in Equation (3.7) or not. By solving Equation (3.7) together with the Van der Waals-Storonkin condition of the coexistence of phases (a generalization of Van der Waals' equation of two-component two-phase system and Clausius' equation for one-component system for the general case of multicomponent multiphase system), Zharov proved that the Schreinemakers' rules are valid also for multicomponent mixtures. The right-hand side of Equation (3.7) is equal to zero at the points of pure components and azeotropes, and the system has no other singular points. From the theory of differential equations it is known that the type of a singular point depends on the signs of the eigenvalues of Equation (3.7) in the vicinity of the singular point. From this, Zharov showed that the singular point of Equation (3.7) can only be a generalized node or a generalized saddle. The signs of the eigenvalues of Equation (3.7) can also be determined from the signs of the derivatives  $\delta T/\delta x_i$  in the vicinity of the singular point. The eigenvalue is negative (positive) if the liquid boiling point temperature decreases (increases) as we move from the singular point in the direction of the eigenvalue:

- If the temperature decreases in all directions (all eigenvalues are negative), the singular point is a stable node (*SN*).
- If the temperature increases in all directions (all eigenvalues are positive), the singular point is an unstable node (*UN*).
- If the temperature decreases in some directions and increases in other directions (eigenvalues of different signs), the singular point is a saddle (*S*).

Thus, the character of the behavior of the residue curves in the vicinity of a singular point uniquely depends on the shape of the boiling temperature surface near this point.

The ten possible types of singular points for *ternary mixtures* given by Zharov and Serafimov (1975) are presented in Figure 3.8. The arrows point in direction of increasing temperature, or equivalently, in the direction of increasing  $\tau$ . Similar diagrams are also presented by Matsuyama and Nishimura (1977) and by Doherty and Caldarola (1985). Whereas Figure 3.7 is determined from the direction of increasing temperature moving along the boiling temperature surface  $T_{bp}(x)$ , Figure 3.8 is determined based on stability properties of the singular points. For ternary mixtures, the type of singular points of the residue curves of any dimension (one-component, binary or ternary) is characterized by two eigenvalues. The singular point is a stable node if both eigenvalues are negative (Figure 3.8a, b, c left triangles SN). The singular point is an unstable node if both eigenvalues are positive (Figure 3.8a, b, c right triangles UN). If one of the eigenvalues is negative and the other is positive, the singular point is a saddle (Figure 3.8d, e, f).

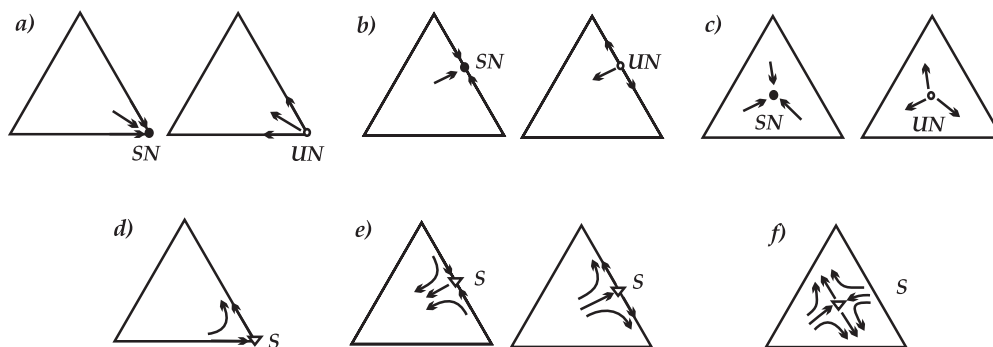


Figure 3.8: Types of singular points for ternary mixtures indicated by  $\bullet$  stable node (SN),  $\circ$  unstable node (UN), and  $\nabla$  saddle (S) (Zharov and Serafimov, 1975). Arrows point in the direction of increasing boiling temperature, and the letters (a, b, c, d, e, f) show the correspondence to Figure 3.7.

The twenty types of singular points for *quaternary mixtures* that are given in Zharov and Serafimov (1975) are presented in Figure 3.9. The sign of the topological indices are valid according to the sign of Equation (3.7) given in the present text. For quaternary mixtures, the type of the residue curves' singular points of any dimension (one-component, binary, ternary or quaternary) is characterized by three eigenvalues. The singular point is a stable node if all the three eigenvalues are negative (Figure 3.9a, e, k, q). The singular point is an unstable node if all three eigenvalues are positive (Figure 3.9b, f, l, r). The singular point is a saddle if one eigenvalue is positive and the other eigenvalues are negative (Figure 3.9c, g, i, m, o, s), or, if one eigenvalue is negative and the other eigenvalues are positive (Figure 3.9d, h, j, n, p, t). Only elementary singular points are presented in Figure 3.8 and 3.9.

In summary, the type of singular points (nodes and saddles) of the residue curves can be determined from the direction of increasing boiling temperature in the vicinity of these point.

### 3.4.3 Rule of azeotropy

The boiling temperature surface, in which simple distillation residue curves belong, is a continuous surface. It follows from topological theory that a combination of singular points of such surfaces corresponds to certain topological restrictions. Using Poincaré's theory of topological properties of continuous surfaces, Gurikov (1958) showed that for ternary simple distillation the combination of the singular points of different type always satisfies the rule:

$$2N_3 + N_2 + N_1 = 2S_3 + S_2 + 2 \quad (3.8)$$

where  $N_3(S_3)$  is the number of ternary nodes (saddles),  $N_2(S_2)$  is the number of binary nodes (saddles), and  $N_1$  is the number of pure component nodes. All thermodynamically and topo-

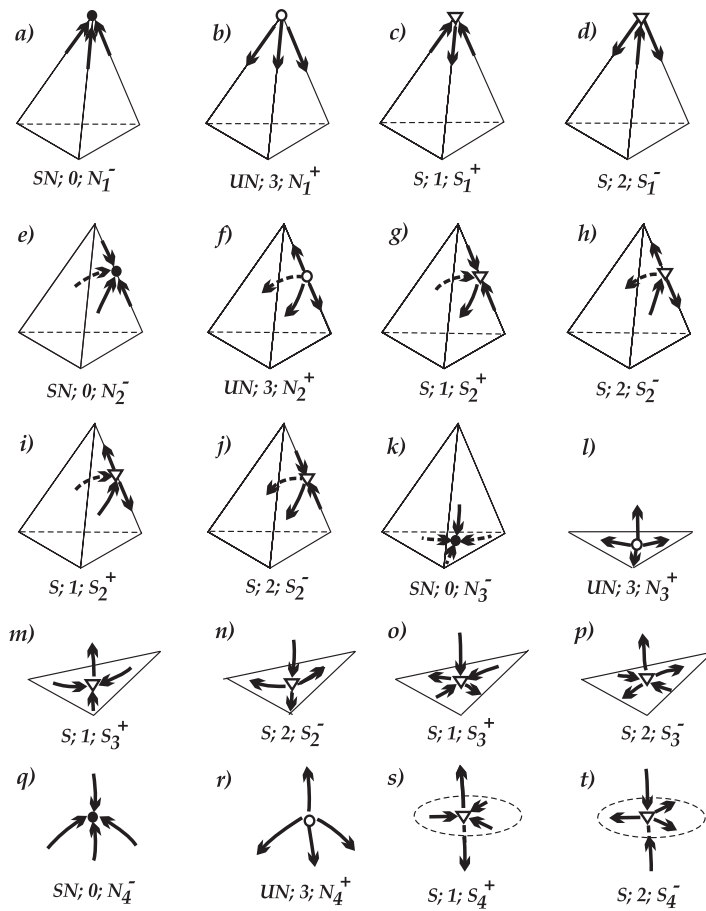


Figure 3.9: Types of singular points for quaternary mixtures indicated by • stable node SN, ○ unstable node UN, and ▽ saddle S, and their corresponding topological indices (Zharov and Serafimov 1975). Arrows point in the direction of increasing boiling temperature.

logically feasible combinations of the singular points of ternary residue curve maps must obey this "Rule of azeotropy". Zharov (1969a) extended this consideration to multicomponent mixtures. Using the concept of topological index (theorems by Kronecker and Hopff) he obtained the generalized rule of azeotropy for  $n$ -component mixtures:

$$\sum_{k=1}^n [2^k (N_k^+ + S_k^+ - N_k^- - S_k^-)] = 1 + (-1)^{n-1} \quad (3.9)$$

where  $N_k^+$  ( $N_k^-$ ) is the number of  $k$ -component nodes with positive (negative) index,  $S_k^+$  ( $S_k^-$ ) is the number of  $k$ -component saddles with positive (negative) index. The index of the singular

point can be determined from the signs of the eigenvalues of Equation (3.7). An index is positive (negative) if the number of negative eigenvalues is even (odd). Gurikov's Equation (3.8) is the specific case of Equation (3.9) for ternary mixtures. From the topological analysis of the singular points given in Section 3.4.2 we have for ternary mixtures that all nodes (stable or unstable, one-component, binary or ternary) have an index  $+1$  and all saddles have an index  $-1$ . The numbers of negative nodes and positive saddles are equal to zero. Thus, for *ternary mixtures* Equation (3.9) has the form:

$$8(N_3^+ - S_3^-) + 4(N_2^+ - S_2^-) + 2(N_1^+ - S_1^-) = 2 \quad (3.10)$$

Excluding all the indices and taking into account that  $S_1 = 3 - N_1$  we obtain Gurikov's rule of azeotropy given by Equation (3.8). For *quaternary mixtures*, the unstable and stable nodes have different indices, and the saddles can be positive or negative. Referring to Figure 3.9, where the different types of singular points are given for a quaternary mixture, we can determine the topological indices given in Table 3.2.

Table 3.2: *Topological indices for quaternary mixtures*

Case in Figure 3.9	Number of negative eigenvalues	Type of singular point	Topological index	Nomination
a, e, k, q	3	stable node	-1	$N_k^-$
b, f, l, r	0	unstable node	+1	$N_k^+$
c, g, i, m, o, s	2	saddle	+1	$S_k^+$
d, h, j, n, p, t	1	saddle	-1	$S_k^-$

Another approach to the analysis of topological restriction was independently performed by Serafimov (1968*d*; 1968*b*; 1968*c*; 1969*a*; 1969*b*; 1969*c*). The results of both authors were summarized in Serafimov *et al.* (1971) and Zharov and Serafimov (1975) and recently presented in Serafimov (1996).

In conclusion, the rule of azeotropy simply means that a definite combination of singular points of the various types must lead to a definite system of residue curves. It is used in the topological classification of VLE diagrams that we present in Section 3.7.

### 3.4.4 Structure of residue curve maps

Based on the rule of azeotropy and the postulate that residue curves must be closed (that is, originate and end in nodes), it has been found that if we know the type of all singular points (i.e., the direction of the residue curves near all points of pure components and azeotropes), then we can qualitatively construct the diagram of residue curves (Serafimov, 1968*d*; Zharov and Serafimov, 1975; Doherty, 1985). Some examples of qualitatively residue curve map construction are given in Figure 3.10 for various cases of azeotropy of a ternary mixture of component 1 (light), 2 (intermediate) and 3 (heavy), where the boiling points are  $T_1 < T_2 < T_3$ . We can see that in



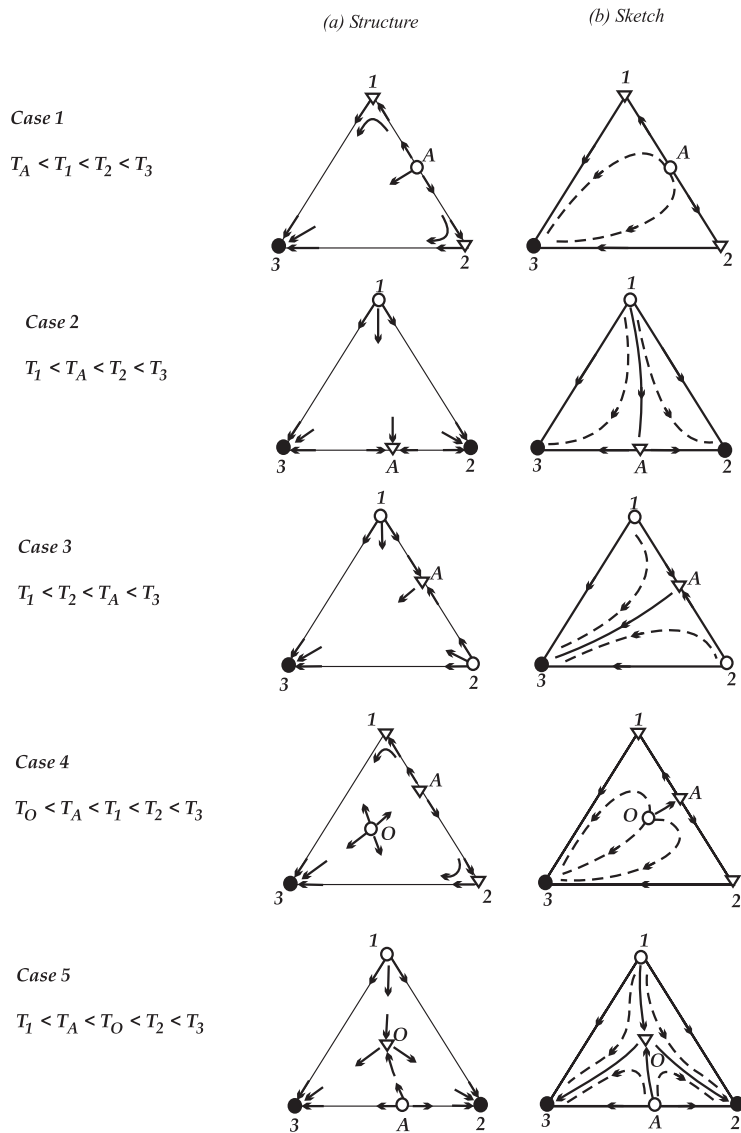


Figure 3.10: Examples of qualitative residue curve map construction: (a) directions of residue curves near the singular points; (b) sketch of the residue curve diagram.

some cases (Cases 2, 3 and 5) the composition triangle is split into several residue curve regions. Recall that Schreinemakers (1901c) defines a “simple distillation region” (residue curve region) as a set of residue curves with common initial and final points. The residue curve boundaries

are the singular residue curves that divide the composition space into these regions. Only saddle separatrices interior to the composition space can be residue curve boundaries.

Bushmakin and Molodenko (1957) and Doherty and Perkins (1978a) proposed to distinguish between *stable separatrices* (boundaries going from a saddle to a stable node), and *unstable separatrices* (boundaries going from an unstable node to a saddle). In Figure 3.10 we can see the unstable separatrices (Cases 2 and 4, separatrices 1O and AO in Case 5), and the stable separatrices (Case 3, separatrices O2 and O3 in Case 5). Bushmakin and Molodenko (1957) assumed (correctly) that the composition triangle is split into residue curve regions only when there is at least one saddle binary azeotrope, or, in other words, when there is at least one separatrix interior to the composition triangle (necessary condition). However, we can see by the example of Case 4 in Figure 3.10 where we only have one residue curve region in spite of the existence of an unstable separatrix, that the existence of a binary saddle (A) and its separatrix (OA) is not a sufficient condition for the splitting of the composition space into several residue curve regions. This may cause confusion (see, for example, Safrit (1996)), but the "contradiction" has a simple answer. Strictly speaking, the separatrix itself is a simple distillation region and the existence of the binary saddle leads to the splitting of the interior of the composition triangle into two "regions" with distinct final points: (1) the separatrix itself and (2) the set of the liquid compositions belonging to all other non-singular residue curves. Here, the separatrix is not a boundary because it does not correspond to the adopted definition of a boundary (it does not divide the family of the residue curves into different bundles).

Thus, a boundary is a separatrix but a separatrix is not necessarily a boundary. We can formulate the general rule:

- The composition space is split into several *residue curve regions* if there are several unstable or several stable nodes (necessary condition).
- The number of *residue curve regions* equals the total number of repeated nodes, that is, nodes of the same type (stable or unstable). For example, if we have three stable nodes and one unstable node the total number of repeated nodes is three and we have three residue curve regions. If we have two stable nodes and two unstable nodes the total number of repeated nodes is four and we have four residue curve regions.

Here, a residue curve region is defined as the set of residue curves with common initial and final points. Doherty and Perkins (1978a) proposed another definition of residue curve regions as the set of liquid compositions that belong to the residue curves with a common stable node. Thus, any unstable separatrix is a residue curve region boundary, and only unstable separatrices can be the boundaries of residue curve regions. We can see from Figure 3.10 that both statements are invalid. In Case 4 there is an unstable separatrix which is not a residue curve boundary. Furthermore, Case 3 has two residue curve regions separated by a stable separatrix boundary. The definitions were corrected by Doherty *et al.* (1985; 1993), but the error appeared again in Rev (1992) and in the review paper by Fien and Liu (1994).

It should be stressed that we cannot construct an exact map of residue curves for a given mixture without knowing the (exact) location and shape of the separatrices (in addition to knowing the

initial and terminal points), and the exact location and shape of ordinary residue curves. Thus, we hereafter distinguish between the *residue curve map*, *sketch of the residue curve map* and *structure of the residue curve map*. The first term means the exact representation of the residue curves and must be constructed by integration of the simple distillation residue curve Equation (3.7). The term "sketch" means the qualitative diagram of residue curves representing the sign of curvature (convex/concave) and the existence (or nonexistence) of inflection points (qualitatively), but not the exact location of the residue curves. This is the focus in Section 3.7.4. Finally, the term "structure of the residue curve map" is the simplest graphical representation that characterizes the VLE and simple distillation of a given mixture (Serafimov, 1968*d*). The structural diagram represent the topology of the residue curve map as given by the residue curves' singular points (nodes and saddles), the residue curves going along the edges of the composition triangle, and the saddles separatrices located interior to the composition space (Serafimov, 1968*d*), that is, only the the singular residue curves. For example, the dashed residue curves in Figure 3.10 are unnecessary for the characterization of the structure.

As mentioned earlier, using information about the shape of the boiling temperature surface near the singular points we can only determine the *structure* of the residue curve map. Since the residue curves follow the direction of increasing boiling temperature, the structure of the residue curve map is also the structure of the boiling temperature surface. Representing the VLE diagram structure by an oriented graph of the boiling temperature increase allows us to determine the structure of the diagrams for multicomponent mixtures. Algorithms for this were proposed by Vitman and Zharov (1971*b*; 1971*a*) and Babich (1972). These oriented graphs may be visualized for quaternary mixtures, but not readily if the number of components is more than four. Instead, the graphs can be represented in matrix form and the determination of the VLE diagram structure can be computerized. Algorithms for computer-aided determination of multicomponent VLE diagrams structures were developed by Petlyuk *et al.* (1975*b*; 1975*a*; 1977*a*; 1977*c*; 1977*b*; 1978), and are also given by Julka and Doherty (1993), Rooks *et al.* (1998) and Safrit and Westerberg (1997*a*) and others.

### 3.4.5 Separatrices of residue curves and flexure of the boiling temperature surface

A surface can be characterized by its topology. As just noted the topology of the residue curve diagram and the boiling temperature surface coincide. That is, their stable nodes (peaks), unstable nodes (pits) and saddle points are the same. Thus, it may appear that the stable separatrices of a residue curve diagram are coincident with the projections of the locus of the ridges in the boiling temperature surface onto the composition simplex, and the unstable separatrices with the valleys. This was claimed by Reinders and de Minjer (1940) based on the intuitive assumption that residue curves could not cross the ridges or valleys in the boiling temperature function  $T_{bp}(x)$ , since this would violate the Schreinemakers' rules. Opposed to this, Haase (1949) stated that the location of the flexures (ridges and valleys) in the boiling temperature surface cannot coincide with the boundaries of the simple distillation regions. Haase was right, however, this point was not immediately recognized.

Based on experiments, Bushmakina and Kish (1957a) argued that for the mixture methyl acetate-chloroform-methanol the boundaries of simple distillation regions run along the projections of the flexures in the boiling temperature surface on the plane of the composition triangle "within the limits of the experimental accuracy". However, they did not describe how they localized the flexures, nor did they give a quantitative comparison of the path of the boiling temperature surface flexures and the simple distillation region boundaries. It should be noted that Bushmakina and Kish did not vigorously claim the identity of the boundaries with the flexures in the boiling temperature surface in the general case, but wrote about the correspondence between them (Bushmakina and Molodenko, 1957). Nevertheless, these papers supported the hypothesis by Reinders and De Minjer resulting in its added confidence. Numerous attempts were subsequently made to prove the identity of the simple distillation boundaries with the flexures in the boiling temperature surface. The interest in this problem is understandable. Although a separatrix is the singular line of the residue curve family, its equation is not distinct from the equation of the ordinary residue curves. Under integration of Equation (3.7), the separatrix can be localized only as a line which arrives at  $\varepsilon$ -vicinity of a saddle at  $\tau \rightarrow \infty$ , or, starts from  $\varepsilon$ -vicinity of a saddle at  $\tau \rightarrow -\infty$ . In other words, the localization is only approximate. If the separatrix had the specific property that it coincides with the flexure of the boiling temperature function it could be exactly localized in a simple way. Various ways to determine the flexure (ridges and valleys) in the boiling temperature surface have been proposed:

- As the locus of extremal boiling temperatures when moving along straight lines parallel to the edges of the composition triangle (see, for example, Doherty and Perkins, 1978a);
- As the separatrix of the steepest gradient lines (Malenko, 1970; Kogan and Kafarov, 1977a; Kogan and Kafarov, 1977b; Van Dongen and Doherty, 1984);
- As the locus of liquid composition points with maximum isotherm curvature (Boyarinov *et al.*, 1974). Path of the largest gradient on the boiling point surface (Stichlmair and Fair, 1998);
- As the locus of liquid composition points where the equilibrium vector is co-linear with the temperature gradient (Sobolev *et al.* (1980)).

However, as it was demonstrated by Van Dongen and Doherty (1984) and Rev (1992), these flexures do not coincide with the separatrices of residue curves. This finally confirmed the conclusion made by Haase as early as 1949.

This conclusion is not surprising since the pathways of the residue curves do not only depend on the boiling temperature surface, but also on the direction of the equilibrium vectors between the phases. The direction of the equilibrium vectors are not necessarily the same as that of the temperature gradient.

Kiva and Serafimov (1973) showed that residue curves crossing the valley or ridges of the boiling temperature surface do not violate Schreinemaker's rules since the residue curve " [...] rises along the slope, intersects the fold [ridge] at an acute angle, and, [...] continues to rise, moving

along the opposite slope of the curved fold [ridge] to its highest point". Even when a residue curve crosses a ridge or valley, the residue temperature is continuously increasing. Similar considerations are given in more detail by Rev (1992).

In conclusion, although the *structure* of a residue curve map can be determined solely from the shape of the boiling temperature surface, the (exact) location of the residue curve separatrices cannot be determined from these data.

### 3.4.6 Structure of distillate curve maps

The vapor composition trajectory during open evaporation (simple distillation) can be represented graphically by the "vapor line" (Schreinemakers, 1901*c*), later named a *distillate curve* by Doherty and Perkins (1978*a*). Each distillate curve is connected to a residue curve and moves along the condensation temperature surface  $T_{bp}(\mathbf{y})$ . The distillate curves are going through the vapor ends of the equilibrium vectors that are tangent to the corresponding residue curve. The projection of the distillate curve in the composition space is always positioned on the convex side of the corresponding residue curve projection. The less the curvature of the residue curve, the less is the gap between it and the corresponding distillate curve. The vapor condensation temperature is equal to the liquid boiling temperature at any instant and increases monotonically during the open equilibrium evaporation process. The system of distillate curves has the same singular points as the system of residue curves, and the singular point type is the same as the type of the corresponding singular point of the residue curves (Haase, 1950*b*; Storonkin, 1967).

## 3.5 Other simple equilibrium phase transformations

### 3.5.1 Open condensation

Open condensation is another equilibrium phase process that solely depends on the VLE (no design or operating parameters) and can in turn characterize it. Open condensation, or simple condensation, is a hypothetical process where drops of condensate are continuously removed from a bulk of vapor in such a way that the composition of this liquid drop of condensate is in equilibrium with the still-pot vapor composition, at any instant. This process is symmetrical to the simple distillation process (Kiva and Serafimov, 1973*c*). It may appear that the *open condensation curves* are directed opposite to the simple distillation residue curves, but this is not correct. Only the structure is the same, but they do not coincide in general. It is evident from Figure 3.11, where simple distillation residue curves and open condensation curves going through points  $\mathbf{x}$  and  $\mathbf{y}$  of an arbitrary equilibrium vector are given. Nevertheless, open condensation and open evaporation (simple distillation) are symmetrical processes with isomorphous composition trajectory maps for antipodal VLE diagrams (diagrams with inverted signs of the nodes and opposite directed trajectories).

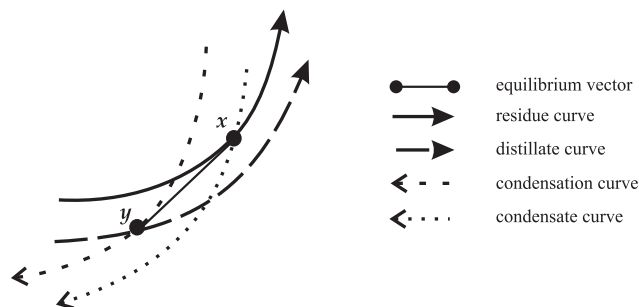


Figure 3.11: Vapor and liquid composition trajectories of open evaporation and open condensation going through the points  $x$  and  $y$  of an equilibrium vector in the composition space.

### 3.5.2 Repeated equilibrium phase mapping and distillation lines

Zharov (1968c; 1969b) proposed the use of repeated equilibrium  $E$ -mapping as a characterization of the VLE:

$$x_1 \xrightarrow{E^1} y_1; y_1 = x_2; x_2 \xrightarrow{E^2} y_2; \dots; x_N \xrightarrow{E^N} y_N \quad (3.11)$$

Zharov named the sequence  $E^N x_1$  a "chain of conjugated tie-lines [equilibrium vectors]", today often referred to as *tie-line curves* or *discrete distillation lines*. The repeated equilibrium phase mapping is illustrated in Figure 3.12. The chain describes the stepwise movement along both the boiling and condensation surfaces similar to the McCabe-Thiele approach for binary mixtures at total reflux. Starting with a given liquid composition  $x_1$ , the equilibrium relationship ( $E$ -mapping) determines the corresponding equilibrium vapor composition  $y_1$ . The vapor is totally condensed and, thus, the vapor and liquid compositions are equal at each step,  $y_N = x_{N+1}$ , which gives the initial point  $x_2$  of the next step and so forth. The VLE describes movement horizontally ( $T$  constant) in Figure 3.12. Projection of a sequence of equilibrium phase mappings onto the composition plane presents a discrete line. When there is a number of repeated mappings, the sequence strives to the component or azeotropic point that has a minimum boiling temperature. The sequence will follow the direction of decreasing boiling (condensation) temperature, that is, it has the same direction as the composition trajectories of open condensation. Choosing several different initial points  $x_1$ , we will obtain a set of equilibrium vector chains. With the proper choice of the initial points we obtain a map of the chains of conjugated equilibrium vectors in the composition space that characterizes the equilibrium mapping function  $E : x \rightarrow y$ . The set of these equilibrium vector chains is an organized selection from the equilibrium vector field. Zharov proposed to consider smooth "connecting lines" instead of the discrete chains of conjugated equilibrium vectors. The term connecting line ("c-line") means a smooth line going in such a way that the vapor-liquid equilibrium vector at an arbitrary point is a chord of this line. As result, any connecting line is a common arc of infinite equilibrium mappings as illustrated in Figure 3.13. Today, these lines are commonly named *distillation lines*. For homogeneous mixtures the distillation lines (connecting lines) cannot intersect each other (in contrast to the chains of

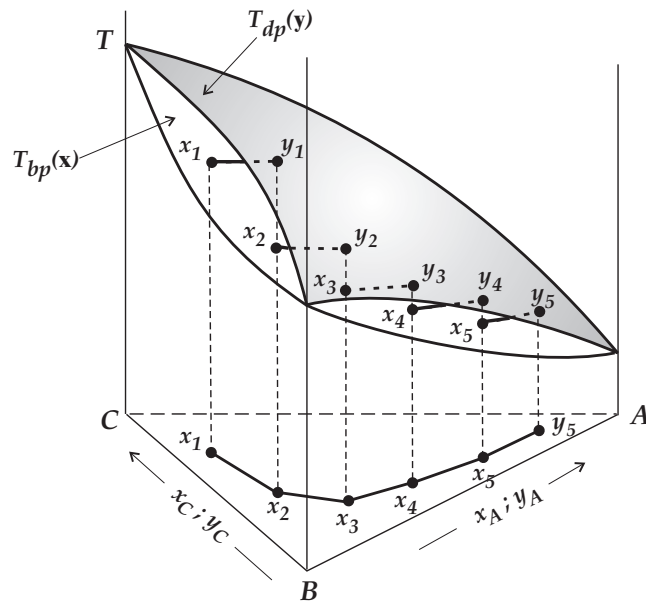


Figure 3.12: *Equilibrium distillation line (also named tie-line curve) is a chain of conjugated vapor-liquid equilibrium vectors in the composition space (a sequence of repeated equilibrium phase mapping).*

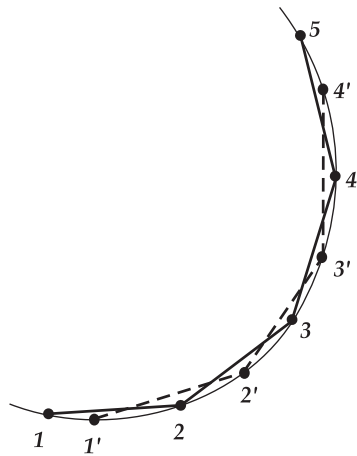


Figure 3.13: *Distillation line (connecting line) and tie-line curves (chains of conjugated vapor-liquid equilibrium vectors).*

conjugated vectors in the composition space as shown in Figure 3.13) and qualitative differential equation theory can be used for their analysis. Based on this analysis, Zharov showed that the properties of distillation lines near the pure component and azeotropic points are identical with those of the residue curves, but the signs of the eigenvalues and indices of the singular points are inverted according to their opposite direction (which is just a matter of definition). As a result, the structure of the distillation line map (and of the conjugated vector chain map too) can be determined from the shape of the boiling temperature surface in the same way as the structure of the (simple distillation) residue curve map.

Zharov (1968c) noted that the discrete distillation line coincides with the composition profile of an equilibrium staged distillation column at total reflux. Based on this coincidence, Stichlmair (1988; 1989) uses the name *distillation lines* for the connection lines of conjugated vapor-liquid equilibrium vectors. Wahnschafft *et al.* (1992) named the discrete chain of conjugated equilibrium vectors a *tie-line curve*. These terms are in common use in English-language literature, and we will consequently use them in the present text. Wahnschafft *et al.* (1992) and Widagdo and Seider (1996) define a tie-line curve and a distillation line as the liquid composition profile of a distillation column at total reflux. Wahnschafft *et al.* noted that these trajectories "*are in principle dependent of tray efficiency*". This is true with regard to a column composition profile. However, they concluded that tie-line curves and distillation lines cannot be uniquely defined in a thermodynamic sense. This is not true. Discrete distillation lines (tie-line curves) are defined uniquely from the VLE solely, regardless of its connection with the column composition profile. Tie-line curves are equivalent to residue curves as characteristics of the VLE in a thermodynamic sense. Stichlmair (1988) underlines that the (discrete) distillation lines give information about the lengths of the vapor-liquid equilibrium vectors which can characterize not only the qualitative course of distillation, but the distillation separability as well. The larger the distance between the points on the distillation line, the easier is the separation. Residue curves do not bring this information.

Discrete distillation lines (tie-line curves) are readily constructed for any given mixture by computation if the mathematical description of the VLE is available. This computation is quicker than the computation of residue curves. However, the exact construction of the distillation lines is more ambiguous because the equation of this line is not determined (not mathematically uniquely defined) and various algorithms of its construction, for example as given by Pöllmann *et al.* (1996), will not be simpler than the integration procedure for the construction of the residue curves. However, the determination of the *structure* of the distillation line maps does not differ from the residue curve map structures. Along with  $N$ -fold and infinity  $E$ -mappings, we can consider  $N$ -fold and infinite  $C$ -mappings, that is, the sequence  $C^N \mathbf{y}_1$ :

$$\mathbf{y}_1 \xrightarrow{C^1} \mathbf{x}_1; \mathbf{x}_1 = \mathbf{y}_2; \mathbf{y}_2 \xrightarrow{C^2} \mathbf{x}_2; \dots; \mathbf{y}_N \xrightarrow{C^N} \mathbf{x}_N \quad (3.12)$$

We name this chain of conjugated "vapor-to-liquid" vectors a *reverse* discrete distillation line (reverse tie-line curve). It is apparent that the chains of conjugated vectors  $\overrightarrow{\mathbf{y}\mathbf{x}}$  and their smooth connecting lines will follow the direction of increasing boiling (condensation) temperature. Thus, they have the same direction as residue curves of open evaporation. For homogeneous mixtures the reverse distillation lines are direct inversions of distillation lines. In other words, distillation



lines (discrete and continuous) are reversible.

Similar to residue curves, the system of distillation lines may split into distinct regions. A distillation line region is the set of compositions that belongs to the distillation lines with the same initial and final points. The structure of a distillation line map is isomorphous to the structure of the open condensation curve maps, or, symmetric to the structure of the residue curve map for any given mixture. Distillation line region boundaries are saddle separatrices of the distillation line system.

### 3.5.3 Relationship between residue curves, distillation lines and condensation curves

It is apparent from simple geometric considerations that a residue curve and a distillation line that go through an arbitrary liquid composition point do not coincide (see, for example, Wahnschafft *et al.* (1992); Figure 3 and Widagdo and Seider (1996); Figure 7). Fidkowski *et al.* (1993) write that "the difference between these types of curves are negligible unless stated otherwise". Wahnschafft *et al.* (1992) were more subtle writing "the difference between residue curves and distillation lines is normally not very significant". However, any general statements are not valid here because the difference between both types of lines depends on their curvature and the lengths of the equilibrium vectors. The residue curve is crossed by distillation lines and condensation lines at any of its points. Similarly, the distillation line is crossed by residue curves and condensation curves at any of its points. Figure 3.14 shows the bands of residue curves and condensation curves that intersects an arbitrary distillation line for a ternary zeotropic mixture. The difference between

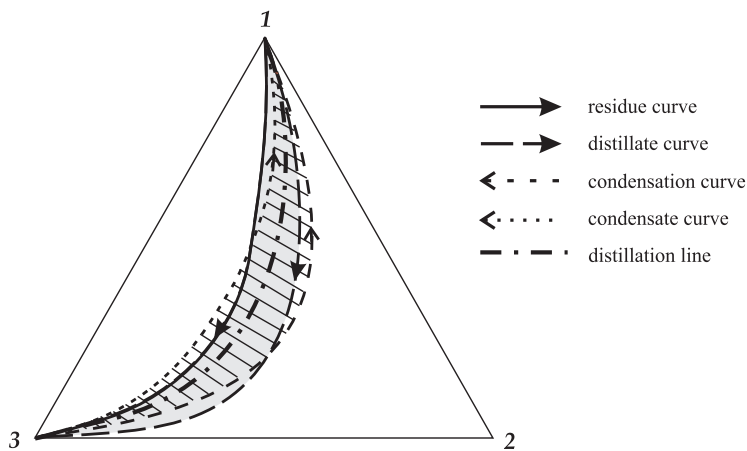


Figure 3.14: Bands of residue curves and condensation curves crossing an arbitrary distillation line for a ternary zeotropic mixture.

these ordinary residue curves and distillation lines raises a concern regarding the difference be-

tween residue curve boundaries and distillation line boundaries. It is apparent that maps of the different lines have similar topology for a given mixture, and that the separatrices of all systems of lines have the same set of singular points. But, the (exact) location of the separatrix does generally not coincide for the different line systems. The relationship between the composition trajectory separatrices of simple distillation, open condensation and repeated phase mapping are considered by Kiva and Serafimov (1975; 1976a) based on simple geometric considerations. The relationship between separatrices is shown in Figure 3.15. The relative location of boundaries of

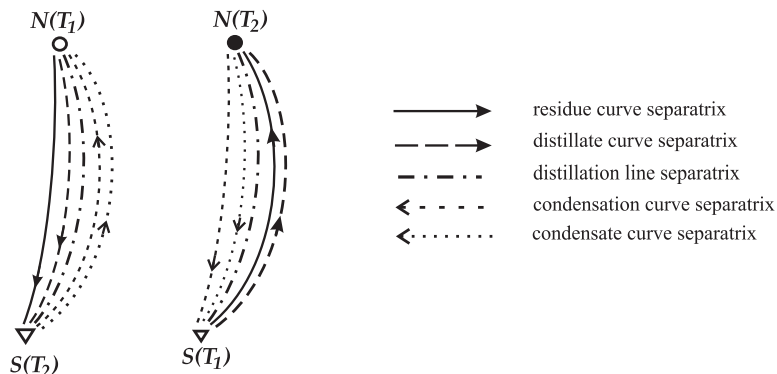


Figure 3.15: *Relative location of boundaries of different simple equilibrium phase transformations: • stable node, ◦ unstable node, and ∇ saddle.*

different simple phase transformations satisfies the following rules:

- a) If the residue curve separatrix goes from an unstable node to a saddle (unstable separatrix), then the separatrix of distillation lines lies on its convex side. The separatrix of the condensation curves lies on the convex side of the distillation line separatrix. The separatrix of the distillate curves is located between the separatrices of residue curves and distillation lines, and the separatrix of the condensate curves lies on the convex side of the separatrix of condensation curves ( see Figure 3.15 a).
- b) If the residue curve separatrix goes from a saddle to a stable node (stable separatrix), then the separatrix of the distillation lines lies on its concave side. The separatrix of the condensation curves lies on the concave side of the distillation line separatrix. The separatrix of the condensate curves is located between the separatrices of the distillation lines and the condensation lines. The separatrix of the distillate curves lies on the convex side of the residue curve separatrix (see Figure 3.15 b).

### 3.6 Heterogeneous mixtures

Heterogeneous mixtures include a composition region of two immiscible liquid phases as a result of molecular interaction (repulsion). Equilibrium between two liquid phases is considered in detail in textbooks and encyclopedia, for example Treybal (1963), Walas (1985), Müller (1988). An example of vapor and liquid isotherm map and the connection between by the vapor-liquid equilibrium vectors for a heterogeneous mixture is given in Figure 3.16. The compositions that

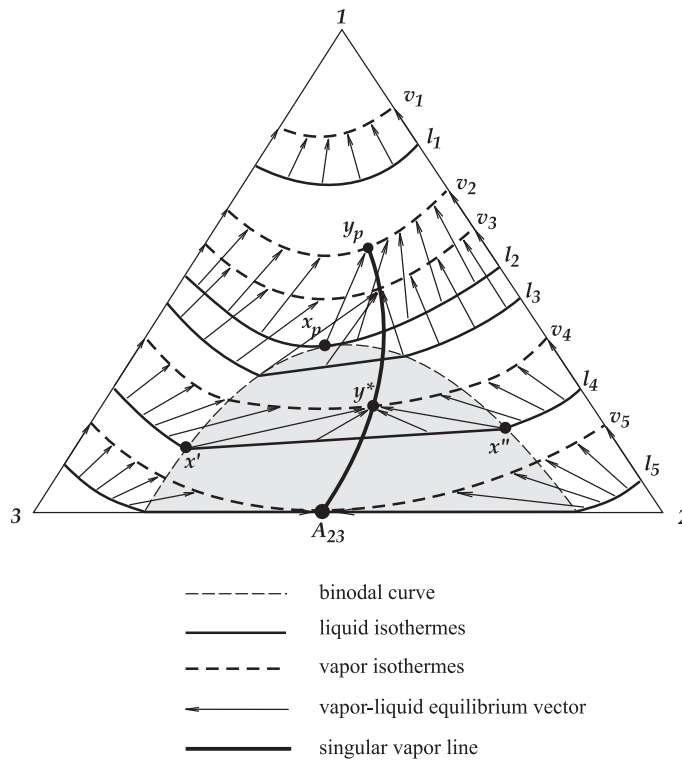


Figure 3.16: An example of liquid and vapor isotherm map for a heterogeneous mixture.

belong to one liquid-liquid tie-line  $\overrightarrow{x'x''}$  have the same boiling temperature and are split into the same set of the liquid phases  $x'$  and  $x''$  in equilibrium with each other and in equilibrium with the vapor composition  $y^*$ . The heterogeneous region is a flat fragment of the boiling temperature surface, and the liquid isotherms in this region coincide with the liquid-liquid tie-lines (Schreinemakers, 1901a). A *singular vapor line* corresponds to all phase complexes of the heterogeneous region (Haase, 1950a; Storonkin and Smirnova, 1963; Pham and Doherty, 1990b)

### 3.6.1 Simple phase transformations in heterogeneous mixtures

The specific features of vapor-liquid-liquid phase equilibria lead to peculiarities of the simple phase transformations for heterogeneous mixtures. It has been shown by Haase (1950*a*) that the Equation (3.6) of open evaporation residue curves for ternary mixtures can be applied to heterogeneous mixtures referring to the overall liquid composition. The tangents to the residue curves are the vapor-liquid equilibrium vectors in the homogeneous region. In the heterogeneous region, the tangents to the residue curves are the vapor-liquid equilibrium vectors in the *point of the overall liquid composition*. Storonkin and Smirnova (1963) proved that the residue curves move continuously in the direction of the increasing boiling temperature and cross the binodal curves without a gap or a fracture. Timofeev *et al.* (1970) proved that all the conclusions concerning the behavior of open evaporation residue curves are valid also for ternary and multicomponent heterogeneous mixtures.

The main feature that distinguishes heterogeneous mixtures from homogeneous mixtures is that a heterogeneous azeotrope (hereafter called a heteroazeotrope) is either an unstable node or a saddle. It cannot be a stable node since heteroazeotropes cannot be maximum-boiling azeotropes. This is easily explained by physical reasoning: heterogeneity (liquid-liquid phase splitting) and minimum-boiling azeotropes occurs when the different components of the mixture repel each other, whereas maximum-boiling azeotrope occurs when the components attract each other.

The relationship between isotherms and residue curves for ternary heterogeneous mixtures presented by Timofeev *et al.* (1970) is shown in Figure 3.17. Unlike homogeneous mixtures, the isotherm passing through the point of a heteroazeotrope is always an "isotherm of final longitude". Bushmakin's definition of the connection between an isotherm and the patterns of the residue curves (Section 3.4.2) should be reformulated as follows:

- (a) A heteroazeotropic point is a nodal point if the isotherm passing through this point is an "isolated" isotherm surrounded by the closed isotherms or by the isotherms which end at the edges of the composition triangle (see Figure 3.17c and d).
- (b) A heteroazeotropic point is a saddle point if the isotherm passing through this point is a closed isotherm or an isotherm which ends at the edges of the composition triangle (see Figure 3.17a and b).

Thus, the main relationship between the structure of the boiling temperature surface and the structure of the residue curve map applies to both homogeneous and heterogeneous mixtures. Pham and Doherty (1990*b*) arrived at the same conclusions. The topology of a residue curve map of a heterogeneous mixture does not differ from that of a homogeneous mixture with the same set of singular points. However, distillate curves do not satisfy the uniqueness condition in the whole composition space. For the part of a residue curve in the heterogeneous region, the corresponding distillate curve moves along the singular vapor line. As a result, the distillate curves partially coincide with each other and with the singular vapor line (Storonkin and Smirnova, 1963; Pham and Doherty, 1990*b*). This means that the behavior of the distillate curves will be somewhat different from that of the residue curves for the same mixture, namely:

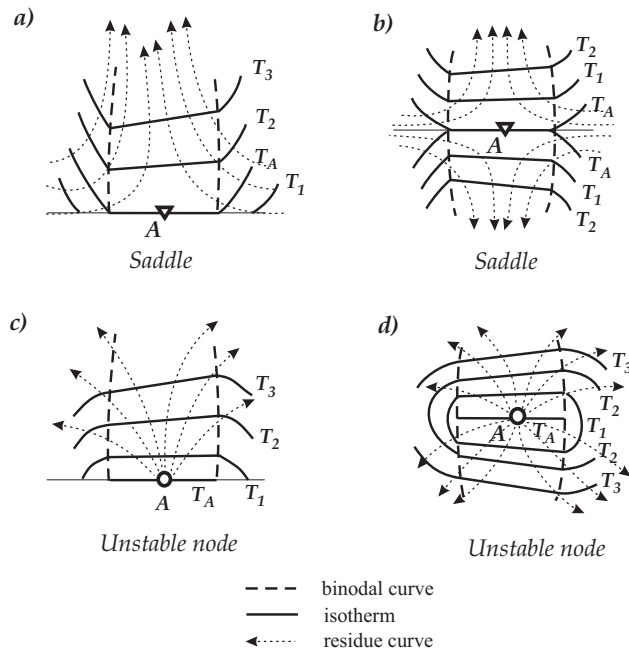


Figure 3.17: *Patterns of isotherms and residue curves near heterogeneous azeotropic points (Timofeev 1970).*

- (1) there is a singular line in addition to the pure component and azeotropic points;
- (2) if the composition space is split into residue curve regions and the boundary is related to the existence of the singular vapor line (this is not necessary), then the boundary of the distillate regions coincide partially or completely with the singular vapor line, and the coinciding part of both lines will be a manifold of contact for adjacent regions;
- (3) the system of distillate curves can include a nonelementary singular point in addition to the component and azeotropic points.

Nevertheless, the global structure of the distillate curve map (initial and final points and splitting into regions) will be identical to the residue curve map.

### 3.6.2 Examples of simple equilibrium phase transformation maps

As an example, let us consider a mixture of Serafimov's class 2.0-2b (Section 3.7.1). Three types of heterogeneity for this structure are presented in Figure 3.18. When the heterogeneous region includes both the unstable node  $A_{12}$  and the binary saddle  $A_{13}$ , the singular vapor line

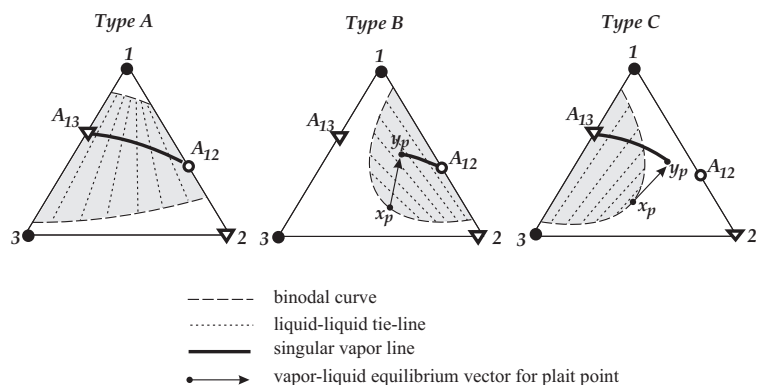


Figure 3.18: Three possible types of heterogeneity for a mixture with the boiling temperature structure of Serafimov's class 2.0-2b. The singular points are indicated by  $\bullet$  stable node,  $\circ$  unstable node, and  $\nabla$  saddle.

moves from the unstable node to the saddle inside the heterogeneous region (Type A). When the heterogeneous region only includes the unstable node  $A_{12}$ , the singular vapor line moves from the unstable node in the direction of increasing temperature and has the end point  $y_p$  inside the heterogeneous region (Type B). When the heterogeneous region only includes the saddle  $A_{13}$ , the singular vapor line moves from the saddle in the direction of decreasing temperature and has the end point  $y_p$  outside the heterogeneous region (Type C).

The structures of the residue curve maps for these cases are presented in Figure 3.19. In all the cases the residue curve maps have the same structure, though the shapes of the residue curves will differ from one another. In all cases the residue curve boundary is located at the concave side of the singular vapor line.

The structures of the distillate curve maps are presented in Figure 3.20. For the mixture of Type A all equilibrium vectors that extend from the residue curve separatrix terminate at the singular vapor line. Hence, the singular vapor line is a separatrix (region boundary) of the distillate curves.

For the mixture of Type B, the equilibrium vectors arrive at the singular vapor line for the part of the residue curve separatrix that is located in the heterogeneous region (that is, from the point  $A_{12}$  to the point of intersection of the separatrix with the binodal curve  $x_b$ ). Hence, the part of the singular vapor line from  $A_{12}$  to  $y_b$  will coincide with the boundary of the distillate regions, where point  $y_b$  is the end point of the equilibrium vector which is tangential to the separatrix of the residue curves at the point  $x_b$ .

For the mixture of Type C, the equilibrium vectors arrive at the singular vapor line for the part of the residue curve separatrix that is located in the heterogeneous region (that is, from the point  $A_{13}$  to the point of intersection of the separatrix with the binodal curve  $x_b$ ). Hence, the part of the singular vapor line from  $A_{13}$  to  $x_b$  will coincide with the boundary of the distillate regions, where point  $y_b$  is the end point of the equilibrium vector which is tangential to the separatrix of

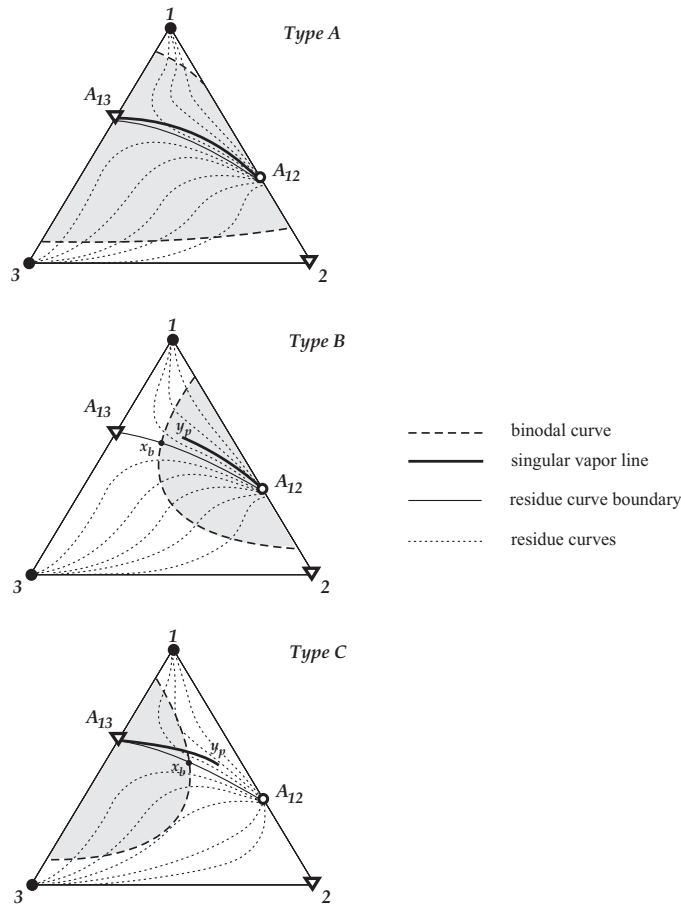


Figure 3.19: Residue curve maps for the three types of heterogeneity given in Figure 3.18.

the residue curves at the point  $x_b$ . For both diagrams of Types B and C, point  $y_b$  is a point of bifurcation of the singular vapor line and the separatrix of the distillate curves.

One can see that, unlike the residue curves, the behavior of distillate curves depends not only on the structure of the boiling temperature surface but on the location of the binodal curve as well. The peculiarities of the inner topology of the distillate curve maps include:

- (1) distillate curves may coincide with each other along the singular vapor line;
- (2) the coinciding part of singular vapor line and the distillate curve boundary is a manifold of contact for adjacent regions;
- (3) the system of distillate curves can include a nonelementary singular point in addition to the

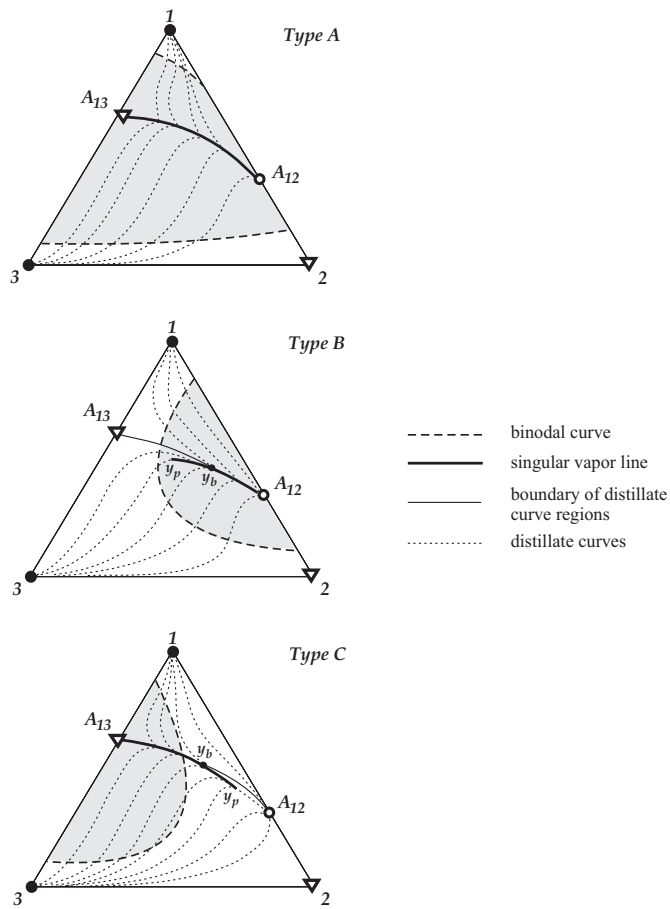


Figure 3.20: Distillate curve maps for the three types of heterogeneity given in Figure 3.18.

pure component and azeotropic points.

The global structure of the distillate curve map (initial and final points and splitting into regions) is similar to that of the residue curve map.

Analysis of the structure of the *distillation line map* and of the composition trajectory map for *open condensation* has not been made yet and it will be a subject of special investigation. We assume that the "inner" topology of these maps will be more complex than the topology of the residue curve map. Nevertheless, it is reasonably safe to suggest that the topology in general (that is, the initial and final points of the composition trajectories and the splitting into the regions) will depend on the shape of the boiling temperature surface in a similar way as of homogeneous mixtures.



## 3.7 Ternary VLE diagrams. Classification, occurrence and structure determination

### 3.7.1 Classifications of ternary VLE diagrams

From the previous discussions we conclude that the structure of simple phase transformations maps is determined, in general, by the shape of the boiling temperature surface for both homogeneous and heterogeneous mixtures. As a consequence, knowledge of the shape of the boiling temperature surface alone permits us to characterize, distinguish and classify any ternary mixture. Since the feasible structures must satisfy the rule of azeotropy (Section 3.4.3), this rule may be used to classify ternary VLE diagrams. This classification was first proposed by Gurikov (1958). Gurikov considers ternary mixtures with no more than one binary azeotrope for each binary pair of the components and no more than one ternary azeotrope (no biazeotropy), i.e.,  $N_3 + S_3 \leq 1$  and  $N_2 + S_2 \leq 3$ . He denotes the total number of binary azeotropes as being  $M$  where  $M = N_2 + S_2$ . Substitution into Equation (3.8) gives:

$$2S_3 + M + 2 = 2N_3 + 2N_2 + N_1 \quad (3.13)$$

Both  $M$  and  $N_1$  can take the values 0, 1, 2 or 3. From Equation (3.13) we see that the quantities  $M$  and  $N_1$  are bound to be of equal parity. If  $M$  is an even number (0 or 2), then  $N_1$  is also even. If  $M$  is an odd number (1 or 3), then  $N_1$  is also an odd number. Gurikov uses the quantity  $M$  as a classification parameter. Specifying the value of  $M$  he considers feasible variants of the structure of residue curve maps for each of the two corresponding values of  $N_1$ . A structure is considered feasible if it does not violate Schreinemakers' rules (Section 3.4.1) and the condition of closed sets of the residue curves (i.e. extending from and terminating in pure component and azeotropic singular points). From this analysis Gurikov revealed 22 feasible topological structures of residue curve maps (or boiling temperature surfaces).

Serafimov (1968*d*; 1970*b*) extended the work of Gurikov and used the total number of binary azeotropes  $M$  and the number of ternary azeotropes  $T$  as classification parameters. Serafimov's classification denotes a structure class by the symbol "M.T" where  $M$  can take the values 0, 1, 2 or 3 and  $T$  can take the values 0 or 1 (i.e. same assumption as Gurikov that the ternary mixture does not exhibit biazeotropy). These classes are further divided into types and subtypes denoted by a number and a letter. As a result of this detailed analysis, four more feasible topological structures, not found by Gurikov, were revealed. Thus Serafimov's classification includes 26 classes of feasible topological structures of VLE diagrams for ternary mixtures. The foundation of this work is also presented more recently (Serafimov, 1996).

Both the classifications of Gurikov and Serafimov consider *topological* structures and thus do not distinguish between antipodal (exact opposite) structures since they have the same topology. Thus, the above classifications include ternary mixtures with opposite signs of the singular points and opposite direction of the residue curves (antipodal diagrams). Serafimov's classification is presented graphically in Figure 3.21. The transition from one antipode to the other (e.g. changing from minimum- to maximum-boiling azeotropes) can be made by simply changing the signs of

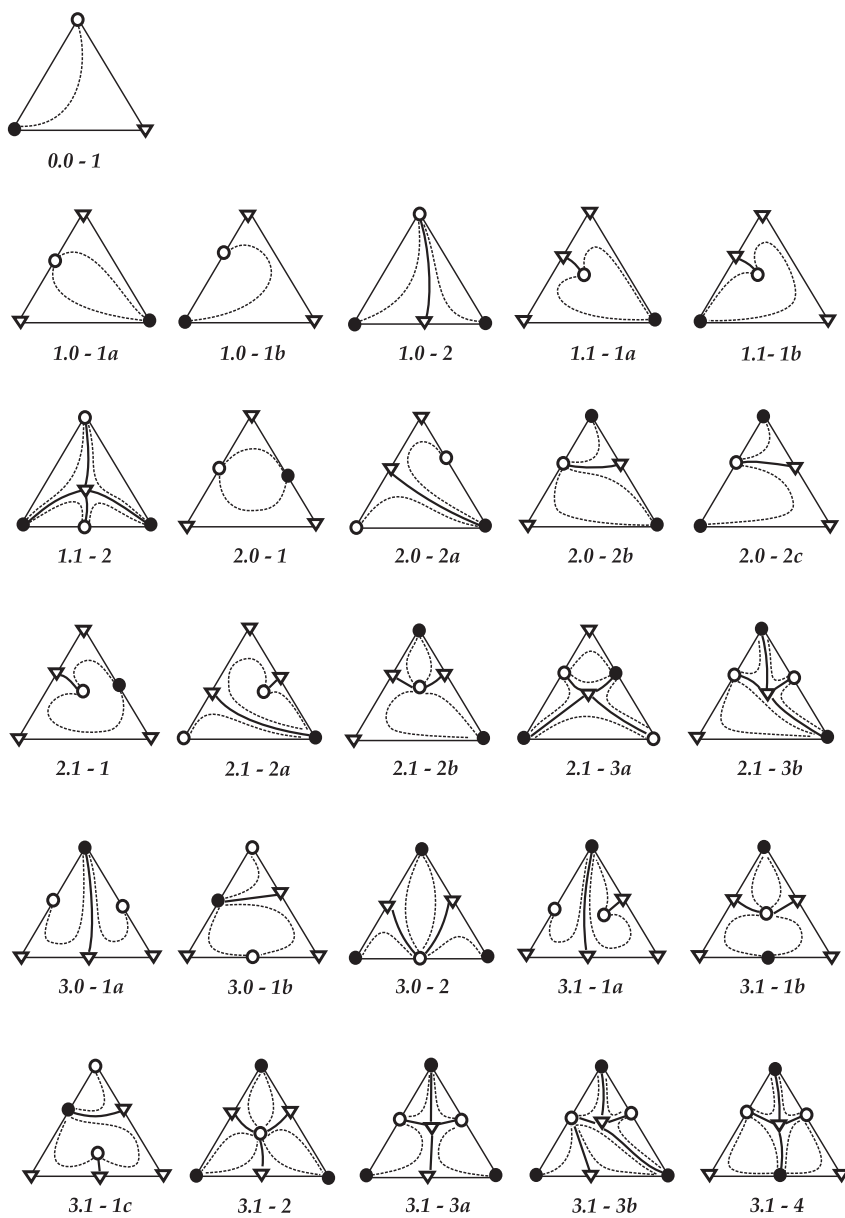


Figure 3.21: Feasible topological structures of VLE diagrams for ternary mixtures according to classification by Serafimov (1970b): ● - stable (unstable) node, ○ - unstable (stable) node, ▽ - saddle.

the nodes and inverting the direction of the arrows. As discussed in Sections 3.3 to 3.5, all the representations of the VLE (isotherm map, residue curve map, vector field of equilibrium vectors in the composition space) are related and are equally capable of classifying the mixtures. Feasible structures of residue curve maps, isotherm maps and vector fields for ternary mixtures are presented by Serafimov (1971; 1973).

The classification of ternary mixtures may be refined by distinguishing between antipodes inside each structure class, based on the reasoning that "*minimum- and maximum-boiling azeotropes have dissimilar physical nature and dissimilar behavior during distillation*" (Zharov and Serafimov, 1975). This refined classification includes a total of 49 types of feasible VLE diagrams (p. 96-98 in Zharov and Serafimov, 1975). An even more detailed classification is proposed by Matsuyama and Nishimura (1977). This classification is founded on the same principles, but the diagrams are further distinguished according to the relative location of the binary azeotropic points on the edges of the composition triangle. The components are ranked in the order of their boiling temperature ("light", "intermediate" and "heavy"). The classification includes 113 diagram classes of which 87 are presented graphically by Doherty and Calderola (1985). Nevertheless, among these 113 classes there are still only the 26 topologically distinct structures of Serafimov. Matsuyama and Nishimura's classes are denoted by three digits according to the existence and type of binary azeotropes at the edges 12, 23 and 13. The digits can take values 0 (no azeotrope), 1 (minimum-boiling azeotrope, unstable node), 2 (minimum-boiling azeotrope, saddle), 3 (maximum-boiling azeotrope, stable node) or 4 (maximum-boiling azeotrope, saddle). When a ternary azeotrope exists, a letter follows the three-digit classification code: m (minimum-boiling ternary azeotrope, unstable node), M (maximum-boiling ternary azeotrope, stable node) and S (intermediate-boiling ternary azeotrope, saddle).

In this connection we want to emphasize that the relative volatility of the components in an azeotropic mixture change within the composition space. The terms "light", "intermediate" and "heavy" component have little meaning in general for nonideal and azeotropic mixtures. This distinction made in Matsuyama and Nishimura's classification does not give any additional information. Actually, it is sometimes ambiguous, as some of Matsuyama and Nishimura's classes where a ternary saddle azeotrope is present have two or even three possible topological structures. For example, code 112-S can be either of Serafimov's topological class 3.1-3a or 3.1-3b depending on whether there is a saddle - saddle separatrix or not. This ambiguity was also pointed out by Foucher *et al.* (1991) who recommend an extension of the Matsuyama and Nishimura's classification code name in these cases. This issue is further discussed in Section 3.7.4.

The relationship between the different classifications is presented in Table 4.2 where the classes are ordered according to Serafimov's classification (1970*b*) with increasing number of azeotropes occurring in the ternary mixture. Hereafter we use Serafimov's (1970*b*) nomenclature for the topological classes and Zharov and Serafimov's (1975) nomenclature for the antipodal structure types (referred to as the ZS-type).

Table 3.3: Correspondence between different classifications of ternary VLE diagrams

Gurikov (1958) 22 classes	Serafimov (1970) 26 classes	ZS-type <sup>a</sup> 49 classes	Matsuyama & Nishimura (1977) 113 classes
1	0	1	000
4a	1.0-1a	3a	100
		7a	030
4b	1.0-1b	3b	001
		7b	003
3	1.0-2	4	020
		8	400
2a	1.1-1a	2a	200-m
		6a	040-M
2b	1.1-1b	2b	002-m
		6b	004-M
5	1.1-2	5	010-S
		9	300-S
9	2.0-1	15	031, 103, 130
8a	2.0-2a	17	023, 320
		18	401, 410
8c	2.0-2b	11a	102, 120, 021
		21a	043, 430, 403
8b	2.0-2c	11b	201, 210, 012
		21b	034, 304, 340
7	2.1-1	13	032-m, 230-m, 203-m
		14	041-M, 140-M, 104-M
-	2.1-2a	16a	420-m, 402-m
		16b	024-m, 420-M
6	2.1-2b	10	022-m, 220-m, 202-m
		20	044-M, 440-M, 404-M
10a	2.1-3a	19	013-S, 310-S, 301-S
10b	2.1-3b	12	011-S, 110-S, 101-S
		22	033-S, 330-S, 303-S
14a	3.0-1a	29	411
		33	323
14b	3.0-1b	28	123, 321, 132, 213, 312, 231
		34	413, 314, 431, 341, 134, 143
13	3.0-2	24	212, 122, 221
		37	434, 344, 443
-	3.1-1a	27b	421-m, 412-m
		32b	423-M, 324-M
12	3.1-1b	26	232-m, 223-m, 322-m
		31	414-M, 441-M, 144-M
-	3.1-1c	27a	142-M, 241-M, 124-M, 214-M, 421-M, 412-M
		32a	423-m, 324-m, 432-m, 342-m, 234-m, 243-m
11	3.1-2	23	222-m
		36	444-M
15	3.1-3a	25a	121-S, 112-S, 211-S
		38a	343-S, 334-S, 433-S
-	3.1-3b	25b	121-S, 112-S
		38b	343-S, 334-S, 433-S
16	3.1-4	30	131-S, 113-S, 311-S
		35	133-S, 313-S, 331-S

<sup>a</sup> ZS-type refers to the refined classification on antipodal structures by Zharov and Serafimov (1975)

### 3.7.2 Completeness of classifications

The classifications presented above do not include (by assumption) biazeotropic mixtures, i.e. mixtures where two binary azeotropes exist for one or more of the binary constituents or where there exists two ternary azeotropes. Kogan (1971) suggested that the rule of azeotropy is not valid for biazeotropic mixtures. However, this is not true, because the rule of azeotropy is a topological rule based on the combination of singular points of different types for continuous surfaces (without a gap), and its validity does not depend on the number of singular points of one element of the surface. This fact has been proved by Komarova *et al.* (1974) and by Matsuyama and Nishimura (1977), and is also discussed in Serafimov (1996). An example of a hypothetical biazeotropic mixture is given in Figure 3.22. The set of singular points in the mixture is  $S_3 = 1$ ,

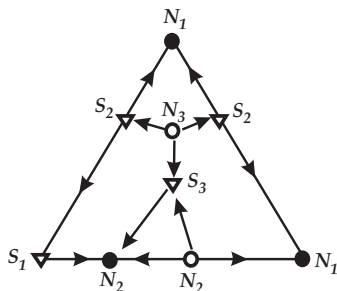


Figure 3.22: *The rule of azeotropy also applies to biazeotropic mixtures: Hypothetical mixture with two ternary azeotropes and two binary azeotropes for one of the binary pairs.*

$N_3 = 1$ ,  $N_2 = 2$ ,  $S_2 = 2$ ,  $S_1 = 1$  and  $N_1 = 2$ , which satisfies the rule of azeotropy.

The classifications do not take into account structures with nonelementary singular points. The existence of biazeotropy and nonelementary singular points of the residue curves is closely connected to tangential azeotropy. The structure of residue curve maps and the rule of azeotropy for such mixtures are considered in the papers by Serafimov (1971*b*; 1971*a*; 1971*c*; 1971*d*; 1974), Doherty and Perkins (1979*a*), Kushner *et al.* (1992) and Serafimov *et al.* (1996). It is beyond the scope of this survey to review these papers, though they touch upon interesting aspects. For example, structures with biazeotropic elements and nonelementary singular points are encountered in the transition from one topology to another with pressure (or temperature) change. The fact that the classifications do not include such transient structures, which usually exist over only very small pressure (temperature) intervals, does not limit their practical use.

### 3.7.3 Occurrence of predicted structures

Experimental VLE data indicates the natural occurrence of ternary mixtures for at least 16 of Serafimov's 26 topological classes, and 28 of the 49 antipodal types given by Zharov and Serafimov (1975). Serafimov (1968*d*) analyzed the occurrence of different types of VLE diagrams

among 418 reported data on azeotropic mixtures. Later, Reshetov made a similar study for 1609 ternary mixtures (in which 1365 are azeotropic) based on thermodynamic data published during the period from 1965 to 1988 (Reshetov, 1998). The occurrence of the various classes and types of ternary mixtures based on these data are presented in Table 4.1, and a graphical representation is given in Figure 3.23. using the mixture group number (No.) in Table 4.1. The structures

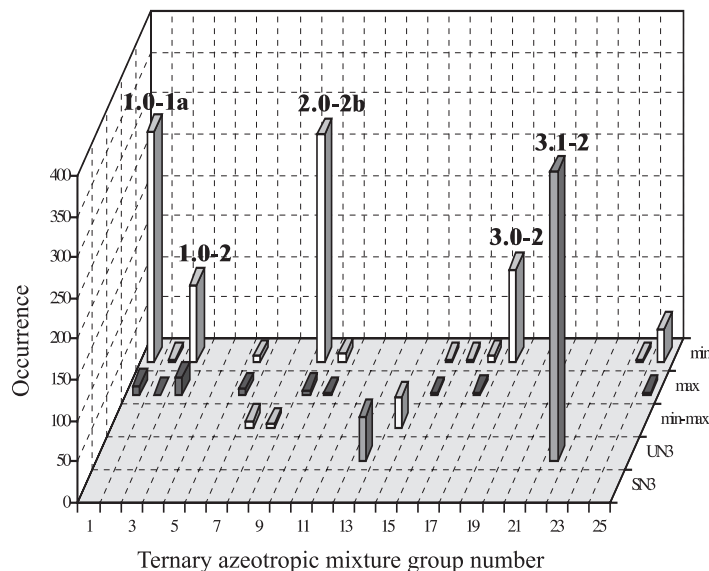


Figure 3.23: Occurrence of classes among published data for ternary mixtures (Reshetov's statistics 1965-1988).

are divided into groups including only or mostly minimum-boiling azeotropes ("min"), only or mostly maximum-boiling azeotropes ("max"), equal number of minimum- and maximum-boiling azeotropes ("min-max"), and minimum- and maximum-boiling ternary azeotropes ("UN3" and "SN3", respectively).

Obviously, the distribution reported in these studies does not necessarily reflect the real occurrence in nature. The azeotropic data selection is small and occasional. Moreover, the distribution can be distorted compared to the unknown "natural" distribution since the published components data are the results of a deliberate search for entrainers for specific industrial separation problems. Nevertheless, these data are interesting and can be used for some deductions.

Both statistics, from Serafimov (1968*d*) and Reshetov (1965-1988) show the same trend. Serafimov's class 3.1-2 with three minimum-boiling binary azeotrope and one minimum-boiling ternary azeotrope has the largest number of reported mixtures. About 26 % of the 1365 ternary azeotropic mixtures in the study by Reshetov, and 41 % of 418 mixtures in the study by Serafimov, are of this class. In the statistics by Reshetov, the second largest class (1.0-1a) has one minimum-boiling binary azeotrope, and the third largest class (2.0-2b) has two minimum-boiling binary azeotropes.

Table 3.4: Occurrence of classes of ternary VLE diagrams found in published mixture data

No.	Serafimov's Class	Occurrence Serafimov (until 1968)	ZS-type of Antipodal Structure	Set of Azeotropes	Occurrence Reshetov (1965-1988)
0	0	-	1	zeotropic	244
1	1.0-1a	13	3a 7a	min max	283 12
2	1.0-1b	2	3b 7b	min max	4 1
3	1.0-2	20	4 8	min max	95 21
4	1.1-1a	None	2a 6a	min + min A <sub>3</sub> max + max A <sub>3</sub>	None None
5	1.1-1b	None	2b 6b	min + min A <sub>3</sub> max + max A <sub>3</sub>	None None
6	1.1-2	7	5 9	min + S <sub>3</sub> max + S <sub>3</sub>	8 8
7	2.0-1	1	15	min + max	9
8	2.0-2a	None	17 18	min + max max + min	2 3
9	2.0-2b	77	11a 21a	min + min max + max	280 6
10	2.0-2c	2	11b 21b	min + min max + max	10 2
11	2.1-1	None	13 14	min + max + min A <sub>3</sub> min + max + max A <sub>3</sub>	None None
12	2.1-2a	None	16a 16b	min + max + min A <sub>3</sub> min + max + max A <sub>3</sub>	None None
13	2.1-2b	3	10 20	min + min + min A <sub>3</sub> max + max + max A <sub>3</sub>	55 None
14	2.1-3a	14	19	min + max + S <sub>3</sub>	37
15	2.1-3b	5	12 22	min + min + S <sub>3</sub> max + max + S <sub>3</sub>	2 1
16	3.0-1a	None	29 33	min + min + max max + max + min	None None
17	3.0-1b	None	28 34	min + min + max max + max + min	9 3
18	3.0-2	85	24 37	min + min + min max + max + max	114 None
19	3.1-1a	3	27b 32b	min + min + max + min A <sub>3</sub> max + max + min + max A <sub>3</sub>	None None
20	3.1-1b	None	26 31	min + min + max + min A <sub>3</sub> max + max + min + max A <sub>3</sub>	None None
21	3.1-1c	None	27a 32a	min + min + max + max A <sub>3</sub> max + max + min + min A <sub>3</sub>	None None
22	3.1-2	171	23 36	min + min + min + min A <sub>3</sub> max + max + max + max A <sub>3</sub>	355 None
23	3.1-3a	None	25a 38a	min + min + min + S <sub>3</sub> max + max + max + S <sub>3</sub>	None None
24	3.1-3b	None	25b 38b	min + min + min + S <sub>3</sub> max + max + max + S <sub>3</sub>	None None
25	3.1-4	15	30 35	min + min + max + S <sub>3</sub> max + max + min + S <sub>3</sub>	41 4

min - minimum-boiling binary azeotrope, max - maximum-boiling binary azeotrope

A<sub>3</sub> - ternary node azeotrope, S<sub>3</sub> - ternary saddle azeotrope

Baburina *et al.* (1983; 1988) claimed that some types of the VLE diagrams are thermodynamically inconsistent, namely Serafimov's classes 1.0-1a, 1.0-1b, 2.1-1, 3.0-1a, 2.0-2a, 3.0-1a, 3.0-1b, 3.1-3a and 3.1-3b. Thus, according to Baburina, the number of feasible classes of topological VLE diagram structures is only 15 rather than 26. This statement was based on the reasoning that: (a) mixtures of these classes were not reported in Serafimov's statistics (Serafimov, 1968*d*); (b) these diagrams cannot be described by the Wilson activity coefficient equation; (c) theoretical analysis by the authors confirms the inconsistency of these diagrams. All these arguments appear to be incorrect: (a) real mixtures representing the classes 1.0-1a, 1.0-1b, 2.0-2a, and 3.0-1b are found as shown in the statistics given above; (b) Zhvanetskij *et al.* (1993) demonstrated that all the 26 classes of VLE diagrams can be simulated by the Wilson activity coefficient equation; (c) it has been shown that the theoretical analysis by Baburina *et al.* is not valid (Reshetov *et al.*, 1990; Zhvanetskij *et al.*, 1993). Later, accepting Baburina's claims, Pöllmann and Blass (1994) and Pöllmann *et al.* (1996) proposed to reduce the number of ternary VLE diagrams to consider only "physically meaningful" structures. The list of "physically meaningful" structures in Pöllmann and Blass (1994) includes 19 structures of Serafimov's classes 0, 1.0-1a, 1.0-1b, 1.0-2, 1.1-2, 2.0-1, 2.0-2a, 2.0-2b, 2.0-2c, 2.1-2b, 2.1-3a, 2.1-3b, 3.0-1a, 3.-1b, 3.0-2, 3.1-1b, 3.1-2, 3.1-3a, 3.1-4.

However, in our opinion, it is impossible in principle to state that some classes of ternary mixtures cannot exist in nature or are "physically meaningless" because all the structures predicted by the rule of azeotropy are thermodynamically and topologically consistent by definition. We can only discuss the *probability* of the existence of some types of the VLE diagram structure. It is well-known that binary maximum-boiling azeotropes are less abundant than minimum-boiling azeotropes. According to Lecat (1949) the ratio of the minimum-boiling versus maximum-boiling azeotropes that occur in nature is about 9 to 1, and the statistics of Reshetov confirms this approximate rule, see Figure 3.24. In particular, no ternary mixture with three binary maximum-boiling azeotropes has been found among the selection of 1365 mixtures, and no ternary maximum-boiling azeotrope has been found. As a result, even for the topological structures where existence is beyond question, the occurrence of antipodes with maximum-boiling azeotropes is much less common than that of antipodes with minimum-boiling azeotropes, see Table 3.5.

Table 3.5: Occurrence of antipodes of the most common topological classes of ternary VLE diagrams

Serafimov's Class	Reshetov's Statistics (1965-1988)	
	min. azeotrope(s)	max. azeotrope(s)
1.0-1a	283	12
1.0-2	95	21
2.0-2b	280	6
2.1-2b	55	None

We propose to consider some conditions that limit the natural occurrence of certain VLE diagram structures. First, we find for maximum-boiling azeotropes:



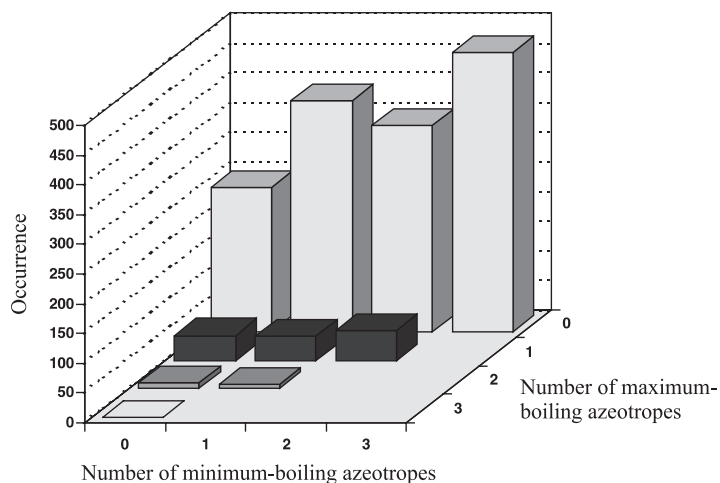


Figure 3.24: Occurrence of various combination of binary azeotropes in ternary mixtures.

**1A** low probability of three binary maximum-boiling azeotropes occurring in a ternary mixture

**1B** low probability of the occurrence of a ternary maximum-boiling azeotrope.

Second, the following structures require unlikely molecular interactions:

**2A** low probability that there is a saddle separatrix that is not a boundary of the residue curve region

**2B** low probability that there is a ternary node in a mixture with binary azeotropes of different signs

**2C** low probability that there is a ternary saddle in a mixture with binary azeotropes of the same sign.

Based on these assumptions, we can reveal the structures that are expected to be rare. These “improbable” structures are presented in Table 3.6. The table includes two structures that are on the list of “physically meaningful” structures given by Pöllmann and Blass (classes 3.1-1b and 3.1-3a). None of the structures in Table 3.6 are reported to occur in real mixtures according to the statistics presented in the previous section. Low probability does not mean that these structures do not exist, but Table 3.6 can be used as an Ockham’s Razor in analysis of VLE and azeotropic distillation. It is conceivable that some of these structures occur in nature but only as tangential azeotropes (i.e., the singular points responsible for these structures are close to an edge of the composition triangle to such an extent that they have not been detected experimentally or through modeling). For practical purposes the existence of such singular points can be neglected in such

Table 3.6: *Improbable types of topological classes of ternary VLE diagrams*

Serafimov's Class	ZS <sup>a</sup> -type	Matsuyama and Nishimura's Class	Probability	Limiting Factors
1.1-1a	2a 6a	200-m 040-M	low improbable	2A 2A + 1B
1.1-1b	2b 6b	020-m 004-M	low improbable	2A 2A + 1B
2.1-1	13 14	032-m, 230-m, 203-m 041-M, 140-M, 104-M	low improbable	2B 2B + 1B
2.1-2a	16a 16b	420-m, 402-m 024-m, 420-M	low improbable	2A 2A + 1B
2.1-2b	20	044-M, 440-M, 404-M	improbable	1B
3.1-1a	27b 32b	421-m, 412-m 423-M, 324-M	low improbable	2A + 2B 2A + 2B + 1B
3.1-1b	26 31	232-m, 223-m, 322-m 414-M, 441-M, 144-M	low improbable	2B 2B + 1B
3.1-1c	27a 32a	142-M, 241-M, 124-M, 214-M, 421-M, 412-M 423-m, 324-m, 423-m, 342-m, 234-m, 243-m	improbable low	2A + 2B 2A + 2B + 1B
3.1-2	36	444-M	improbable	1A + 1B
3.1-3a	25a 38a	121-S, 112-S, 211-S 343-S, 334-S, 433-S	low very low	2C 2C + 1A
3.1-3b	25b 38b	121-S, 112-S 343-S, 334-S, 433-S	low very low	2C 2C + 1A

<sup>a</sup> ZS-type refers to the refined classification on antipodal structures by Zharov and Serafimov (1975)

cases. The mixtures in the collection by Reshetov are ranked in the order of decreasing occurrence in Table 3.7. Most common VLE diagram structures are given in Group A. Group B structures are also common, and Group C can be considered as rare structures.

### 3.7.4 Determination of the structure

The question of whether it is possible to determine the VLE diagram structure of a mixture solely from the boiling temperatures of the pure components and azeotropes has been discussed since the first publications in this field. It was claimed by Gurikov (1958) and later confirmed by Serafimov (1968*a*), and Zharov and Serafimov (1975) that, in general, pure component and azeotropic boiling temperature data only are *not* sufficient to construct the diagram uniquely and that additional information about the *direction* of increasing boiling temperature near some singular points is needed. It has been proposed using ebulliometric measurements to obtain this additional information experimentally (Serafimov, 1968*a*; Zharov and Serafimov, 1975). Obviously, a mathematical description of the VLE may be used for this purpose too.

Table 3.7: Identified structures of ternary VLE diagrams among real mixtures according to Reshetov's statistics (1965 to 1988)

	No.	Structure of Ternary VLE Diagram			Occur %
		Serafimov's Class	ZS <sup>a</sup> -type	Matsuyama & Nishimura's Class	
Group A > 5 %	1	3.1-2	23	222-m	26.0
	2	1.0-1a	3a, 7a	100, 030	21.6
	3	2.0-2b	11a, 21a	102, 120, 021, 043, 430, 403	21.0
	4	1.0-2	4, 8	020, 400	8.5
	5	3.0-2	24	212, 122, 221	8.4
Group B 1 - 5 %	6	2.1-2b	10	022-m, 220-m, 202-m	4.0
	7	3.1-4	30, 35	131-S, 113-S, 311-S, 133-S, 313-S, 331-S	3.3
	8	2.1-3a	19	013-S, 310-S, 301-S	2.7
	9	1.1-2	5, 9	010-S, 300-S	1.2
Group C < 1 %	10	2.0-2c	11b, 21b	201, 210, 012, 034, 304, 340	0.9
	11	3.0-1b	28	123, 321, 132, 213, 312, 231	0.88
	12	2.0-1	15	031, 103, 130	0.66
	13, 14	2.0-2a	17, 18	023, 320, 401, 410	0.36
	13, 14	1.0-1b	3b, 7b	001, 003	0.36
	15	2.1-3b	12, 22	011-S, 110-S, 101-S, 033-S330-S, 303-S	0.22

<sup>a</sup> ZS-type refers to the refined classification on antipodal structures by Zharov and Serafimov (1975)

Doherty (1985) stated that the residue curve maps can be uniquely and explicitly determined from the components and azeotropes boiling points only. This concept is used by Bernot (1990), Foucher *et al.* (1991) and Peterson and Partin (1997). However, this assumption is not theoretically founded and is not valid in general. On the other hand, as noted by Foucher *et al.* (1991) and as we show below, in most cases the simple ranking of singular points (components and azeotropes) in order of increasing boiling points is sufficient to construct the structure of the residue curve map. In specific cases we have indeterminacy (Foucher *et al.*, 1991), but this is really a result of the lack of data required for a unique solution. The cases where different structures of VLE diagrams correspond to the same order of the boiling temperatures of the singular points are presented in Figures 3.25 and 3.26.

In Cases 1 and 2 the indeterminacy occurs for one topological class (antipodes). Case 1 is described by Foucher *et al.* (1991). For all the cases in Figure 3.25 the real structure of the given mixture can be easily determined experimentally. Depending on the direction of the increasing temperature b or c near the singular point in the triangle given in column a) the mixture has a structure as given in column b) or c). A more complex situation presented in Figure 3.26 is also described by Foucher *et al.* (1991) and named "global" indeterminacy. The real structure cannot be identified from additional investigation of the boiling temperature surface, and computing the actual residue curve map is required. Fortunately, this type of structure has low probability (no mixtures reported yet, see Table 3.6).

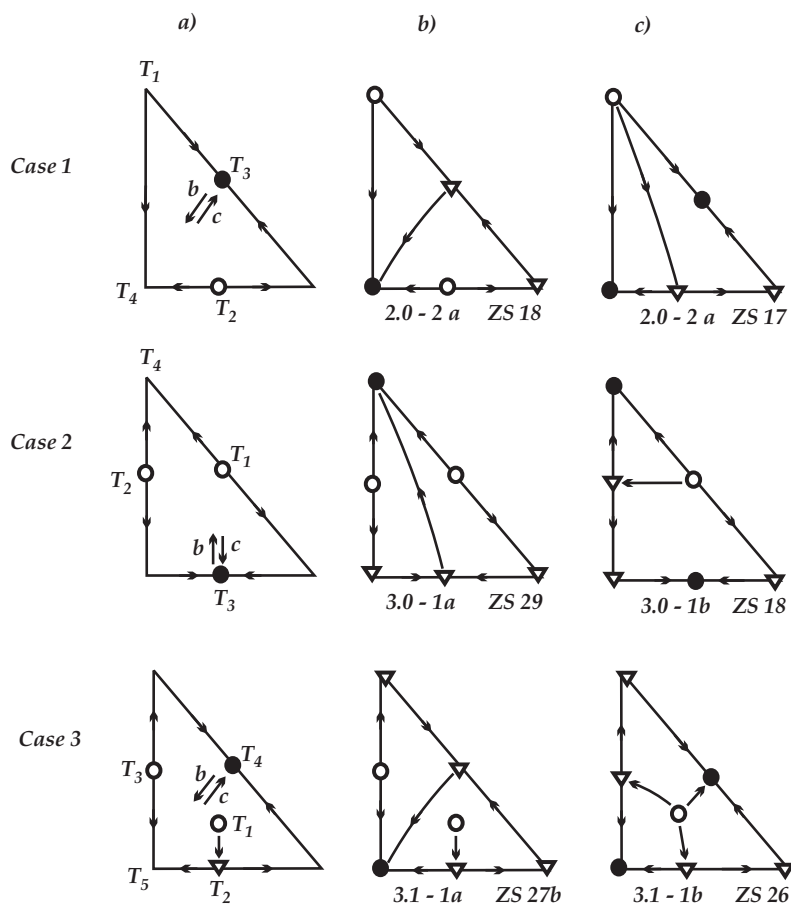


Figure 3.25: Indeterminacy of the residue curve map structure for a ternary mixture with the given order of the components and azeotropic temperature points: a) the given set of temperature ordered singular points; b,c) feasible structure alternatives.

There are some cases where identification of the structure of VLE diagram can be made with a high degree of probability from the data on the components and binary azeotropes. These cases are presented in Table 3.8. In all other cases, binary data are not sufficient for the precise identification of the structure. By way of example let us consider the mixtures with two and three binary minimum-boiling azeotropes where we know all singular points at the edges of triangle (Figure 3.27 a, cases 1 and 2). Three feasible structures are shown in Figure 3.27 (b, c, d for each case). All feasible alternatives are likely to occur and it is very risky to assign a structure to the given mixture based on information about the singular points at the edges of triangle only.

This is also pointed out by Westerberg (1997): *Generally, we cannot construct a unique diagram if*

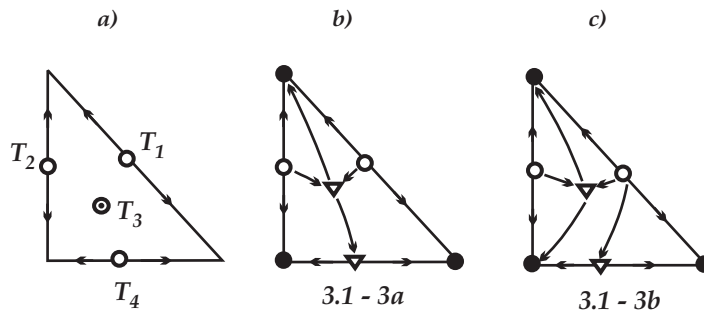


Figure 3.26: “Global” indeterminacy of the residue curve map structure for a given ranking of the components and azeotropic points (according to Foucher, 1991): a) the given ranking of the singular points; b,c) feasible structure alternatives.

Table 3.8: Window of prediction of ternary VLE diagram structures from binary data only

Singular points on the edges 12-23-13 (Matsuyama’s nomination)	Structure Alternatives				Most probable structure		
	Serafimov’s Class	ZS-type	Serafimov’s Class	ZS-type	Serafimov’s class	ZS-type	Comment
100	1.0-1a	3a	1.1-1a	2a	1.0-1a	3a	most probable
030	1.0-1a	7a	1.1-1a	6a	1.0-1a	7a	almost certain
001	1.0-1b	3b	1.1-1b	2b	1.0-1b	3b	most probable
003	1.0-1b	7b	1.1-1b	6b	1.0-1b	7b	almost certain
103 ( or 130, or 031)	2.0-1	15	2.1-1	13	2.0-1	15	most probable
			2.1-1	14			

we only know the existence of the azeotropes and their boiling point temperatures. If we know the temperature and also the nature of all the pure component and azeotrope points (type of saddle, stable node, unstable node), then we can sketch a unique diagram.

It has been stated by Matsuyama and Nishimura (1977), Yamakita *et al.* (1983) and Foucher *et al.* (1991) that the rule of azeotropy can be used to check the consistency of azeotropic data. It is appropriate to emphasize that this only applies to the consistency of the experimentally determined ternary azeotropic points. Furthermore, only when the boiling temperature of this point lies between the temperatures of the singular point of a separatrix or a line between an unstable node and a stable node, can an erroneous ternary azeotrope be singled out and excluded. If the experimentally determined singular point has a boiling point temperature outside these intervals it cannot be excluded on the basis of the rule of azeotropy. This is demonstrated in Figure 3.28.

The issues concerning the identification of the VLE diagram structure on the basis of incomplete

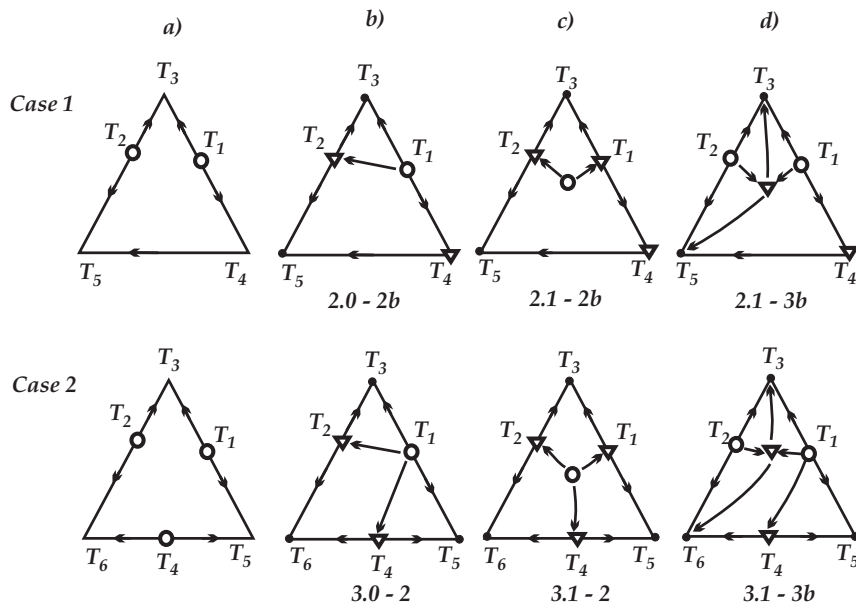


Figure 3.27: Feasible alternatives of the residue curve map structure for the given ranking of the singular points at the edges of the composition triangle: a) the given set of ranking of the components and azeotropic points at the edges of the composition triangle; b) structure without ternary azeotrope; c) structure with a ternary unstable node azeotrope; d) structure with a ternary saddle azeotrope.

information (and indeterminacy and inconsistency of such identification) were of great significance before the mathematical modeling of VLE became widely applicable. Today we can obtain an appropriate mathematical description of the ternary VLE, find all singular points and construct the diagram of residue curves or distillation lines based on data for the binary constituents. It is also possible to predict the binary parameters from the characteristics of the pure components (e.g., by means of the group contribution models). VLE diagrams obtained by modeling are determined and consistent by definition (but they do not necessarily represent the behavior of the real mixtures properly). The real issue today is the accuracy of the model description. The description of a ternary mixture can be wrong even with reliable binary data because the ternary azeotrope can be found (or not found) mistakenly by the model. For example, modeling the VLE for the mixture of n-butanol, n-butyl acetate and water by means of the Wilson and NRTL activity coefficient equations may give different topological structures of the diagrams depending on the binary parameters sets that were chosen, see Figure 3.29. The parameters for the model can be readily corrected if experimental data on the ternary azeotrope are available. However, topological or thermodynamic considerations do not help to select the correct model in such a situation if only binary data are available.

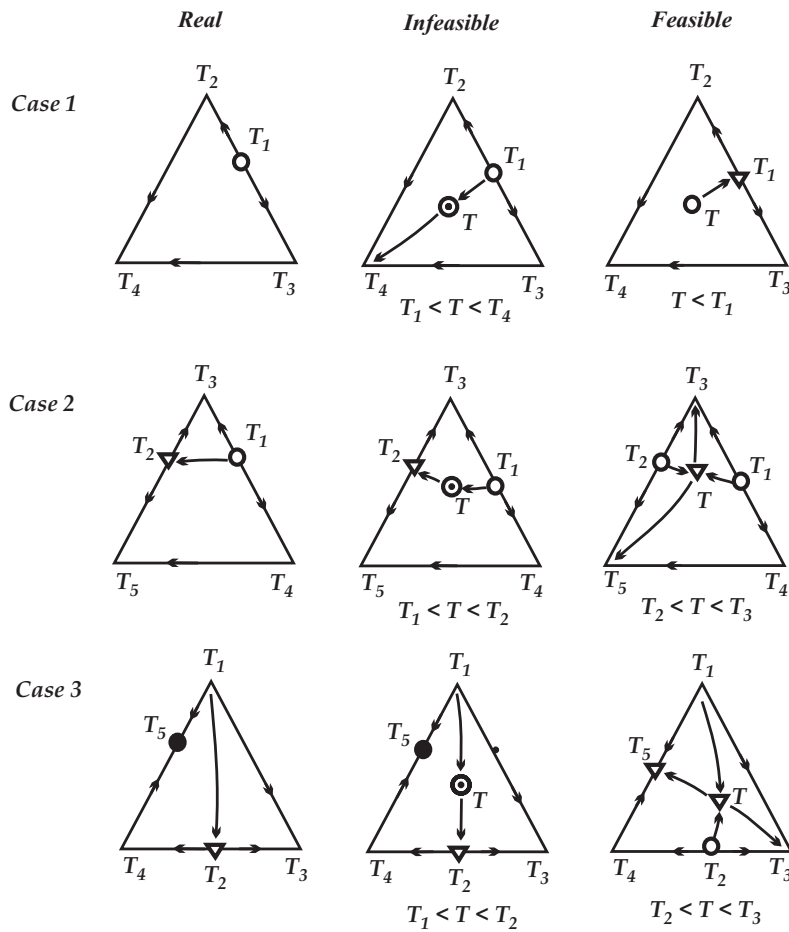


Figure 3.28: Consistency test based on the rule of azeotropy may fail to detect an erroneous experimentally determined ternary azeotrope ( $\odot$ ): a) real structure; b) infeasible structure (existence of the false ternary azeotrope is excluded); c) feasible structure (existence of the false ternary azeotrope obeys the rule of azeotropy and cannot be excluded).

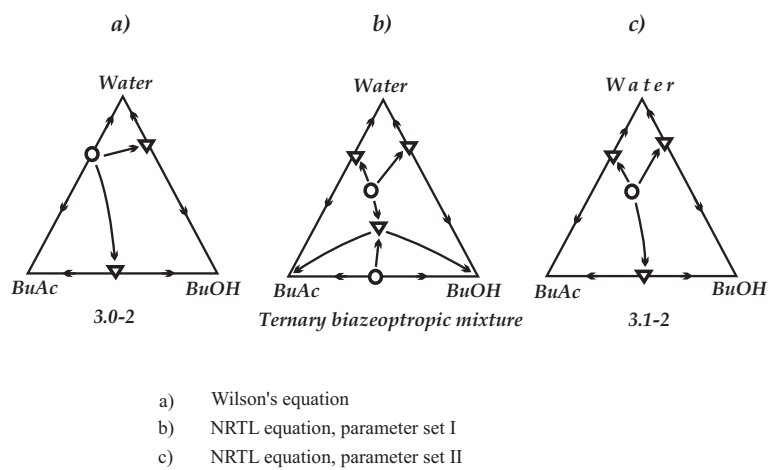


Figure 3.29: Prediction of the VLE diagram structure for the mixture butanol-butyl acetate - water based on thermodynamic models.



## 3.8 Unidistribution and univolatility lines

### 3.8.1 Distribution coefficient and relative volatility

The distribution coefficient and relative volatility are well-known characteristics of the vapor-liquid equilibrium. The distribution coefficient  $K_i$  is defined by:

$$K_i = y_i/x_i \quad (3.14)$$

As the name implies,  $K_i$  characterizes the distribution of component  $i$  between the vapor and liquid phases in equilibrium. The vapor is enriched with component  $i$  if  $K_i > 1$  and is impoverished with component  $i$  for  $K_i < 1$  compared to the liquid. The ratio of the distribution coefficients of components  $i$  and  $j$  gives the relative volatility of these components, usually denoted by  $\alpha_{ij}$ :

$$\alpha_{ij} = \frac{K_i}{K_j} = \frac{y_i/x_i}{y_j/x_j} \quad (3.15)$$

The relative volatility characterizes the ability of component  $i$  to transfer (evaporate) into the vapor phase compared to the ability of component  $j$ . Component  $i$  is more volatile than component  $j$  if  $\alpha_{ij} > 1$ , and less volatile if  $\alpha_{ij} < 1$ . For ideal and nearly ideal mixtures, the relative volatilities for all pair of components are nearly constant in the whole composition space. The situation is different for nonideal and in particular azeotropic mixtures where the composition dependence can be complex. The qualitative characteristics of the distribution coefficient and relative volatility functions are also considered in a general form by the "pen-and-paper" approach that is typical for the thermodynamic topological analysis.

Serafimov (1970a) considered the behavior of these functions for binary mixtures. Based on Serafimov's approach and the paper by Kushner *et al.* (1992) we present the feasible patterns of the distribution coefficient functions  $K_i(x)$  and  $K_j(x)$  for *binary mixtures* according to the feasible paths of the equilibrium line  $y(x)$  in Figure 3.30. The distribution coefficients of the azeotrope-forming components are equal to unity in the points of the pure components and the azeotrope. One of these distribution coefficient functions has an extremum when the equilibrium line ( $y - x$  relationship) has an inflection point, and both distribution coefficient functions have extrema when there is an azeotrope in the mixture. The relative volatility function  $\alpha_{ij}(x)$  intersect the line  $\alpha = 1$  at the azeotrope points(s). The transitions from one type of diagram to another is caused by the change of the molecular interactions of the components resulting in positive or negative deviations from ideality given by Raoult's law. The particular deviation from Raoult's law is determined by the balance between the physiochemical forces between identical and different components in the mixture, and we can make the following qualitative distinction for binary mixtures of component 1 and 2:

*Positive deviation:* The components 1 and 2 do not like each other. The attraction between identical molecules is stronger than between different molecules, which may cause a minimum-boiling azeotrope.

*Negative deviation:* The components 1 and 2 like each other. The attraction between identical molecules is the strongest, which may cause a maximum-boiling azeotrope.

In conclusion, the composition dependence of the distribution coefficients are qualitative and quantitative characteristics of the VLE for the given mixture. The patterns of these functions determines not only the class of binary mixture (zeotropic, minimum- or maximum-boiling azeotrope, or biazeotropic), but the individual behavior of the given mixture as well, as will be shown in the following section.

### 3.8.2 Univolatility and unidistribution line diagrams

The composition dependence of the distribution coefficients of a ternary mixture of components 1, 2 and 3 can be represented by three surfaces  $K_1(x)$ ,  $K_2(x)$  and  $K_3(x)$ . Serafimov (1970a) proposed to consider the system of *unidistribution lines* in the composition space where the distribution coefficient of the given component  $i$  equals unity  $K_i(x) = 1$ .

The dynamic system of open evaporation residue curves Equation (3.7) can be represented as:

$$\frac{dx_i}{d\tau} = x_i (1 - K_i) \quad i = 1, \dots, n - 1 \quad (3.16)$$

The singular points of this system are related to the unidistribution lines, because:

- (a) in the point of pure component  $i$        $K_i = 1, x_j = 0, x_h = 0$
- (b) in the point of binary azeotrope  $A_{ij}$        $K_i = K_j = 1, x_h = 0$
- (c) in the point of ternary azeotrope  $A_{ijh}$        $K_i = K_j = K_h = 1$

Thus, the existence of a binary azeotrope gives rise to two unidistribution lines ( $K_i = 1$  and  $K_j = 1$ ), and the existence of a ternary azeotrope gives rise to three unidistribution lines ( $K_i = 1, K_j = 1, K_h = 1$ ). The point of pure component  $i$  may (or may not) give rise to an unidistribution line of component  $i$ . Serafimov (1970b; 1970a; 1973) showed that a given residue curve map corresponds to given feasible diagrams of unidistribution lines.

In a similar way, the relative volatility function can be represented by *isovolatility lines*, that is, contour lines in the composition plane of the three surfaces  $\alpha_{ij}(x)$  for all pairs of the components. It is difficult to interpret all three isovolatility lines ( $\alpha_{ij}, \alpha_{ih}, \alpha_{jh}$ ) in the same diagram. Serafimov *et al.* (1972) propose to use the system of *univolatility lines* where  $\alpha_{ij} = 1$ . However, isovolatility lines for other values than unity are useful to evaluate the influence of a component  $h$  on the relative volatility of the other two components  $ij$  given by  $\alpha_{ij}^h$ , in the search for an entrainer for extractive distillation (Laroche *et al.*, 1993; Wahnschafft and Westerberg, 1993).

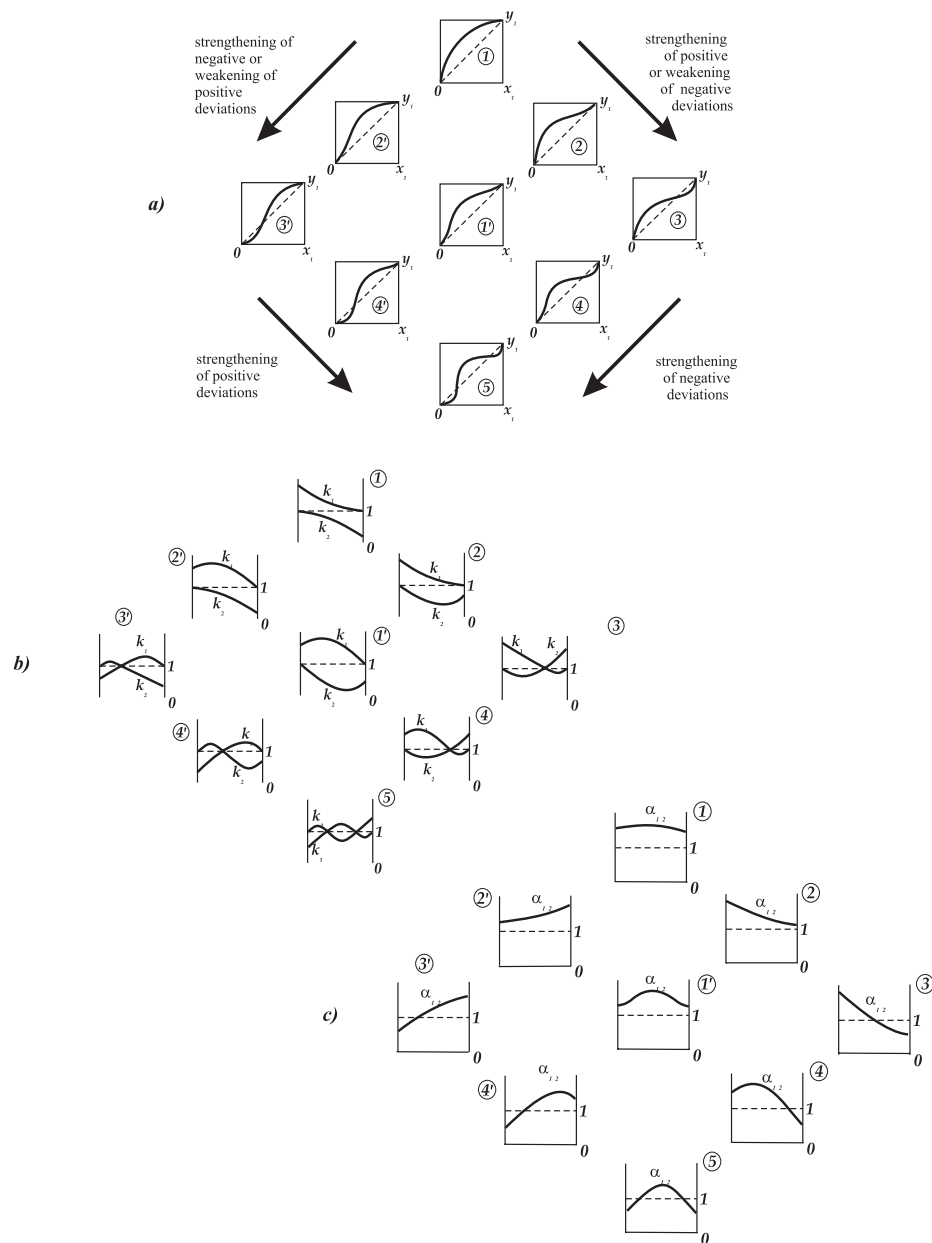


Figure 3.30: Feasible patterns of the VLE functions for binary mixtures of components 1 and 2: a) equilibrium line  $y(x)$ ; b) distribution coefficients  $K_i(x)$  and  $K_j(x)$ ; c) relative volatility  $\alpha_{ij}(x)$ .

We use the term *univolatility lines* to distinguish between the lines where  $\alpha_{ij} = 1$  from other isovolatility lines where  $\alpha_{ij} \neq 1$ . It is evident that the point of a binary azeotrope  $Az_{ij}$  gives rise to an  $\alpha_{ij}$ -univolatility line and that the point of a ternary azeotrope gives rise to the three univolatility lines ( $\alpha_{ij} = 1$ ,  $\alpha_{ih} = 1$ , and  $\alpha_{jh} = 1$ ). Serafimov *et al.* (1972) showed that in addition there are univolatility lines which are not connected with the azeotropic points, and that such lines can occur even in zeotropic mixtures.

Analysis of feasible diagrams of unidistribution and univolatility lines is given by Serafimov (1970*b*; 1970*a*; 1972). The main aim of this work was to consider feasible structures of the residue curve maps in more detail, and in fact exactly this approach helps to construct more refined classification of ternary diagrams. Later, the diagrams of unidistribution lines were used as a main tool for analysis of tangential azeotropy and biazeotropy (Serafimov, 1971*b*; Serafimov, 1971*a*; Serafimov, 1971*c*; Serafimov, 1971*d*; Kushner *et al.*, 1992; Serafimov *et al.*, 1996). The diagrams of univolatility lines were used for the same purpose by Zhvanetskij and Reshetov *et al.* (Zhvanetskij *et al.*, 1988; Zhvanetskij *et al.*, 1989; Zhvanetskij *et al.*, 1993; Reshetov *et al.*, 1990; Sluchenkov *et al.*, 1990). In addition, Zhvanetskij *et al.* (1988) noted that univolatility lines split the composition triangle into regions of certain order of volatility of components which they named “regions of  $K$ -ranking”, or, “ $K$ -ordered regions”. The feasible structures of the diagrams of unidistribution and univolatility lines given by Serafimov are considered in Section 3.8.3 for the purpose of sketching the simple phase transformation trajectories such as residue curves and distillation lines.

The unidistribution ( $K_i = 1$ ) and univolatility ( $\alpha_{ij} = 1$ ) lines play the role as “road signs” for the pathway of the simple phase transformation composition trajectories (such as residue curves and distillation lines) Kiva and Serafimov (1973):

1. Along the unidistribution line ( $K_i = 1$ ) all equilibrium vectors in the composition space  $\vec{x}\vec{y}$  are parallel to the edge  $jh$  of the composition triangle (see Figure 3.31).
2. Along the univolatility line ( $\alpha_{ij} = 1$ ) at a point  $x$ , the equilibrium vector  $\vec{x}\vec{y}$  lies at the secant going from the vertex  $H$  through this point (see Figure 3.32).
3. At the intersection of a residue curve with the unidistribution line ( $K_i = 1$ ) there is an extrema of the composition  $x_i$  ( $dx_i/d\tau = 0$ ) (see Figure 3.31).
4. If there are no univolatility lines, there are no inflection points of the simple phase transformation trajectories (see Figure 3.31).
5. The univolatility line  $\alpha_{ij}$  gives rise to an inflection point on the residue curves (and the other simple phase transformation trajectories) if there is no  $K_i$ - or  $K_j$ -unidistribution lines along the residue curve between the univolatility line in question and the stable or unstable nodes of the residue curves. This rule is illustrated in Figure 3.32 for a zeotropic mixture of components 1-2-3 with two univolatility lines ( $\alpha_{12} = 1$  and  $\alpha_{23} = 1$ ). It can be seen that there is no unidistribution line between the unstable node (1) and the  $\alpha_{23}$ -univolatility line, and there is an inflection point on the residue curves between the unstable node and

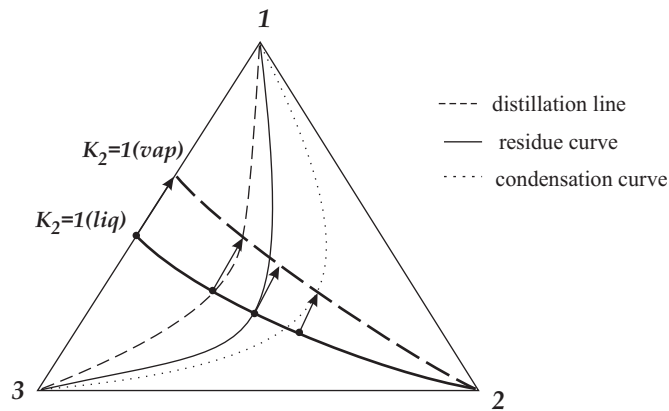


Figure 3.31: The lines of simple phase transformation trajectories have extremal compositions along the unidistribution ( $K$ ) lines (shown for zeotropic mixture).

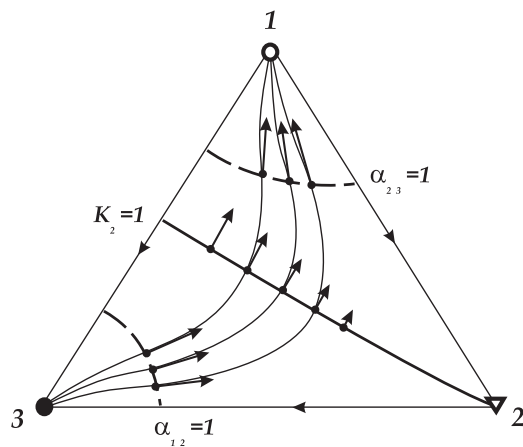


Figure 3.32: Residue curve map with two inflection points on the residue curves for a zeotropic mixture with two univolatility lines. The mixture is of Serafimov's class 0.0-1 with two-sided arc-wise univolatility lines.

the univolatility line. In a similar way, there is no unidistribution line between the  $\alpha_{12}$ -univolatility line and the stable node (3), and there is an inflection point of the residue curves between this univolatility line and the stable node too. However, there is a  $K_2$ -unidistribution line between the  $\alpha_{23}$ -univolatility line and the  $\alpha_{12}$ -univolatility line, and there are no inflection points between univolatility lines.

6. The inflection points for all lines on the residue curve bundle intersecting the univolatility line are positioned at the "inflection line" (i.e., locus of inflection points). The rule of interposition of the inflection lines for various simple phase transformations can be determined from the simple geometric considerations. This rule is illustrated for an example mixture in Figure 3.33.

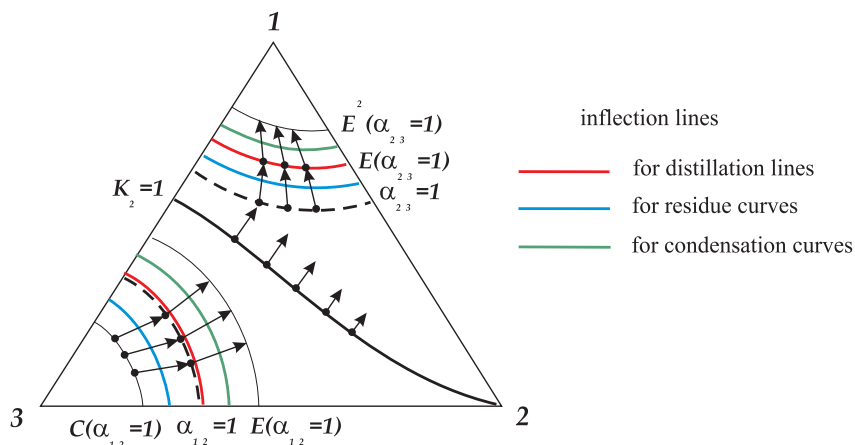


Figure 3.33: *Interposition of the inflection lines for various simple phase transformations relative to the position of the univolatility lines and their equilibrium vectors.*

7. The inflection line of the distillation lines coincides with the univolatility line if the inflection exists between the univolatility line and the maximum-boiling node. The inflection line of the distillation lines coincides with the  $E$ -mapping of the univolatility line if the inflection exists between the univolatility line and the minimum-boiling node. The inflection line of the residue curves is shifted from the inflection line of the distillation lines in the direction of the residue curves movement (the shift is less than one equilibrium vector). The inflection line of the condensation curves is shifted from the inflection line of the distillation lines in the direction of the condensation curves movement (the shift is less than one equilibrium vector). In addition, the inflection points occur if the line of the simple phase transformation intersects the unidistribution lines of the same index (component(s)) or the same univolatility lines twice in succession. Examples of these situations are given in Figure 3.34 and 3.35.

For the mixture represented in Figure 3.35 some of the distillation lines have two inflection points (between the minimum-boiling node 1 and the  $\alpha_{23}$ -univolatility line, and between two intersections of the  $\alpha_{23}$ -univolatility line).

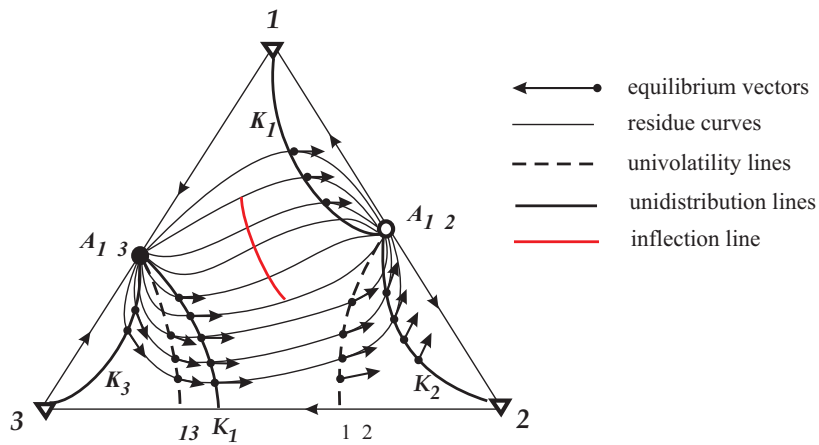


Figure 3.34: Existence of inflection points between two unidistribution lines of the same index ( $K_1$ ). The mixture is of Serafimov's class 2.0-1.

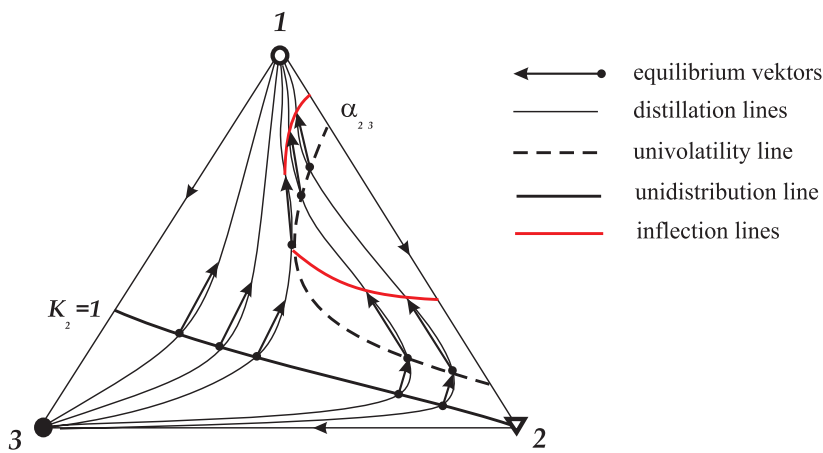


Figure 3.35: Appearance of inflection points between two intersections of the same univolatility line. The mixture is of Serafimov's class 0 with single-sided arc-wise univolatility line.

Figure 3.36 illustrates how, on the basis of unidistribution and univolatility lines, we can make a complete sketch of the residue curve map.

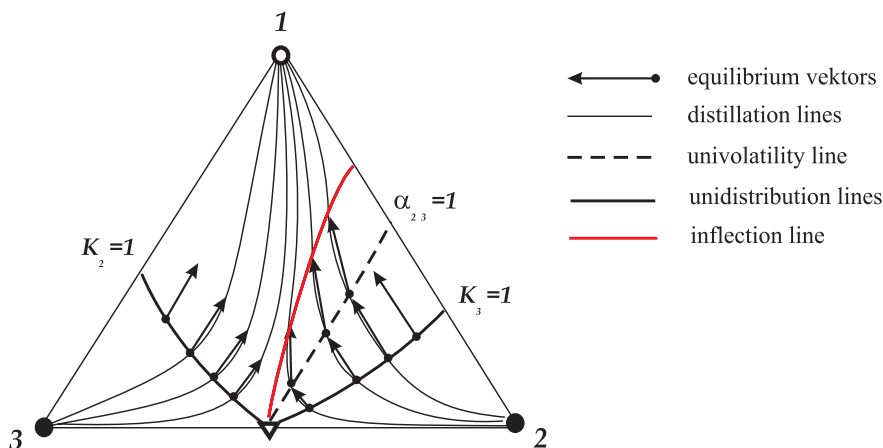


Figure 3.36: Sketch of the distillation line map for a mixture of Serafimov's Class 1.0-2.

The splitting of the composition space into regions of volatility ranking (K-ranking) is shown in Figure 3.37 for the examples presented in Figure 3.32 and 3.34-3.36. The regions are determined by the combination of three digits corresponding to the number of components, and the order of the digits corresponds to the order of decreasing volatility, e.g. 123, means that 1 is the most volatile and 3 the least.

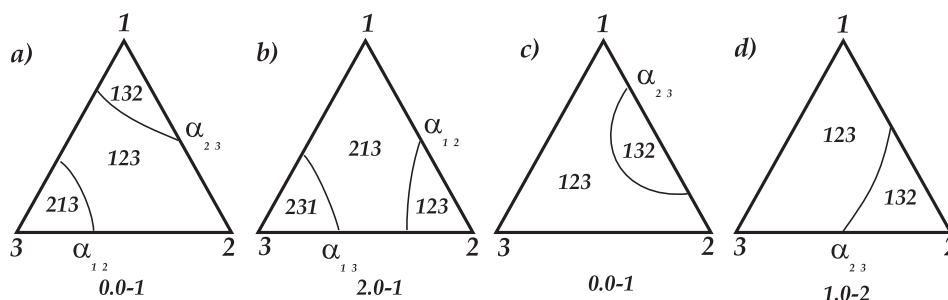


Figure 3.37: Examples of how the composition space is split into regions of K-ranking (according to Zhvanetskij et al., 1988): (a) mixture given in Figure 3.32; (b) mixture given in Figure 3.34; (c) mixture given in Figure 3.35; (d) mixture given in Figure 3.36

The diagrams in Figure 3.37 clearly illustrate that the order of volatilities of the components cannot coincide with their boiling point temperatures in the whole composition space even for zeotropic mixtures if the diagram includes univolatility lines. The combined diagram of unidis-



tribution and univolatility lines permits us to construct quantitatively the sketch of the map of the simple phase transformations. It not only characterizes the topology of the maps but their geometry as well. The unidistribution and univolatility lines can be readily determined numerically (by simulation) based on a VLE model of the given mixture (see for example Bogdanov and Kiva (1977)) and their computation is much easier than computation of the residue curves or (especially) the distillation lines.

### 3.8.3 Structure of unidistribution and univolatility line diagrams

The unidistribution and univolatility lines can be easily located quantitatively by computation of the VLE for the given mixture (see, for example, Bogdanov and Kiva (1977)), and diagrams for the most common structures of ternary VLE diagrams according to Reshetov's statistics as given in Table 3.7, Section 3.7.3, are presented in Figure 3.38.

The theory for finding such feasible structures of unidistribution line diagrams was developed by Serafimov (1970b; 1970a) and presented in Serafimov *et al.* (1973). Feasible structures of univolatility line diagrams were considered by Serafimov *et al.* (1972).

To understand the ideas better, let each binary composition diagram present a side of the unfolded triangle formed by the three components in ternary mixtures as shown in Figure 3.39. Various combinations of binary constituents and shapes of the  $K_i(x)$  surfaces lead to various structures of the ternary diagrams.

#### *Example 1. Zeotropic mixture 1-2-3*

- a) Let us assume that all three binary constituents are mixtures of Type 1. Unfolding the prism, we draw the curves  $K_i(x)$  at the edges of the prism and determine the values  $K_{i(j)}^\infty$  (infinite dilution of  $i$  in  $j$ ) at the edges of the prism (Figure 3.39). Here:

$$\begin{aligned} (K_1 = 1) &> K_{2(1)}^\infty &> K_{3(1)}^\infty \\ K_{1(2)}^\infty &> (K_2 = 1) &> K_{3(2)}^\infty \\ K_{1(3)}^\infty &> K_{2(3)}^\infty &> (K_3 = 1) \end{aligned}$$

Assuming that the functions  $K_{i(jh)}^\infty$  are monotonous, we construct their feasible trajectories at the edges of the prism. We can see that line  $K_{2(13)}^\infty$  intersects line  $K = 1$  and there are only two points with the value  $K_2 = 1$  at the edges of the triangle. These points are connected by the  $K_2$ -unidistribution line. There are no univolatility lines and, consequently, there are no inflection points at the residue curves or distillation lines. A sketch of the diagram is made based on the location of unidistribution line. This cell of residue curves (distillation lines) is C-shaped.

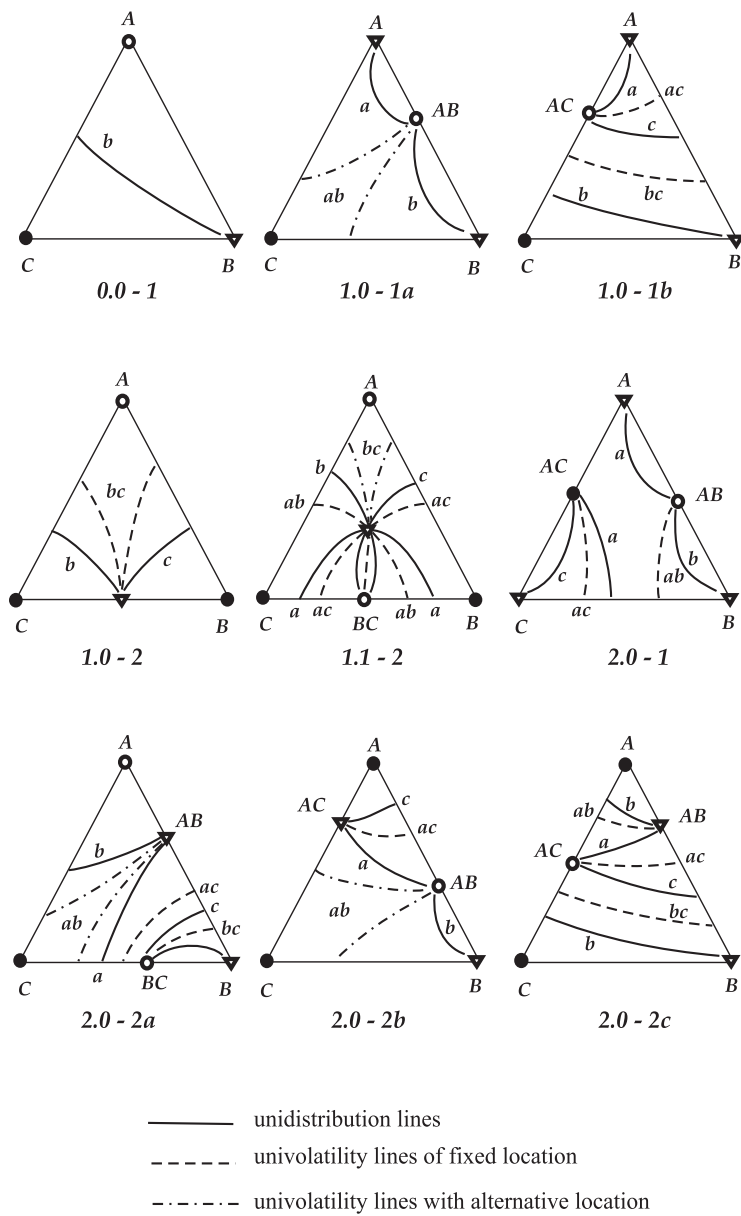


Figure 3.38: Unidistribution and univolatility line diagrams for the most probable classes of ternary mixtures according to Reshetov's statistics.

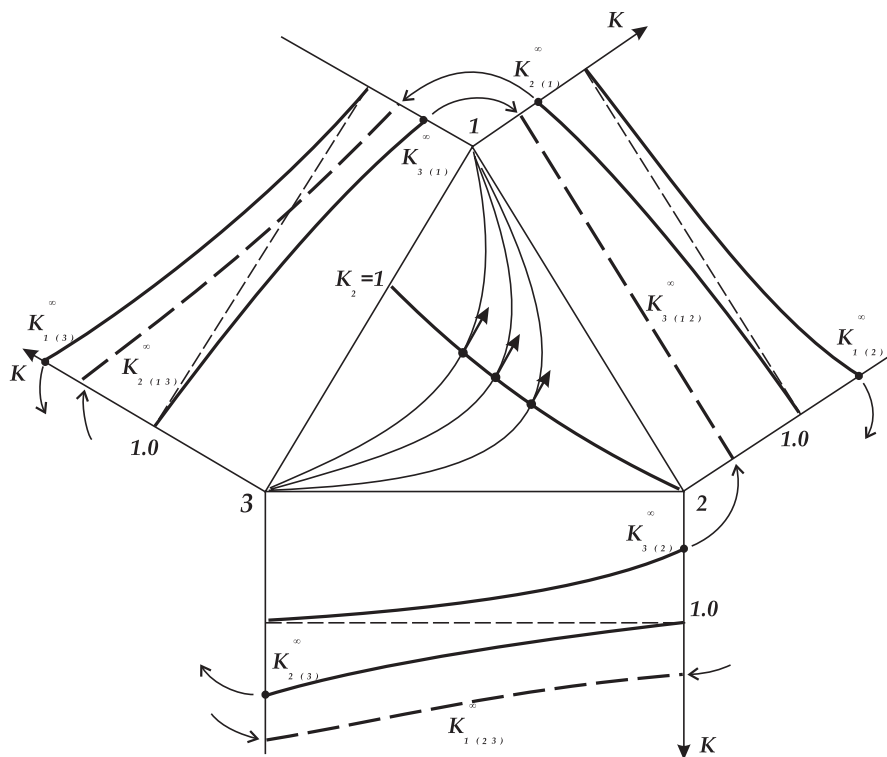


Figure 3.39: The construction of the ternary VLE diagram for a zeotropic mixture 1-2-3 where all the binary constituents are mixtures of Type 1 (C-shaped residue curves).

- b) Let us assume that the binary mixture 1-3 is the mixture of Type 2', i.e. it becomes more negative or less positive than the mixture 2-3 (Figure 3.40).

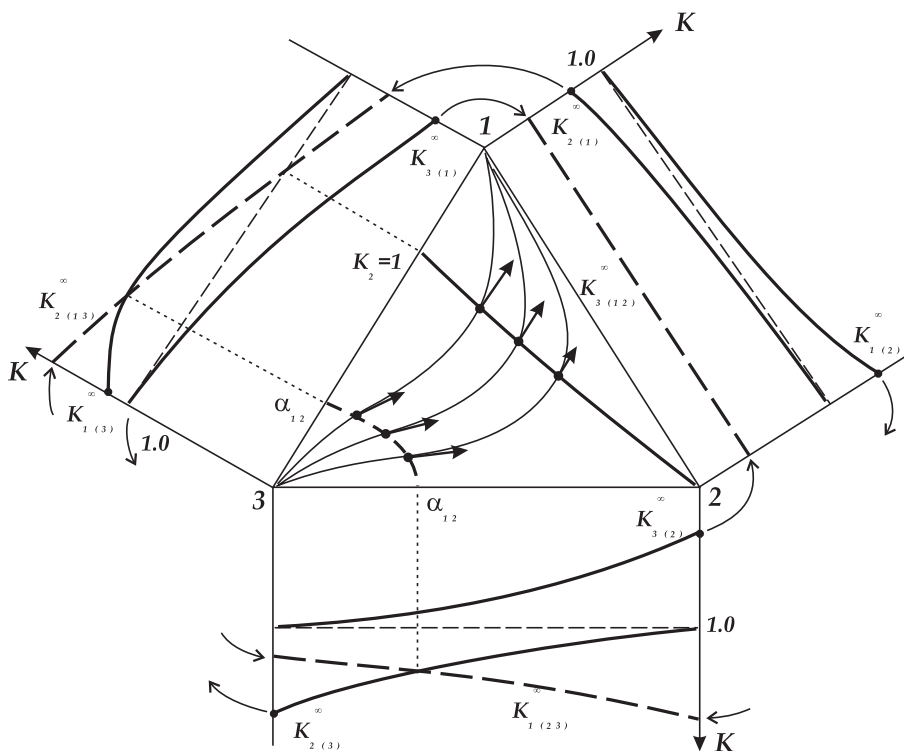


Figure 3.40: Univolatility and unidistribution line diagram and phase portrait of the residue curve map for a zeotropic mixture 1-2-3 where the binary constituents 1-3 are a mixture of Type 2' (S-shaped residue curves).

Then there is  $K_{2(3)}^\infty > K_{1(3)}^\infty > (K_3 = 1)$ , and there are points of intersection of the lines  $K_1(x)$  and  $K_2(x)$  at the edges 13 and 23. As a result, the  $\alpha_{12}$ -univolatility line connects edges 13 and 23 of the composition triangle (Figure 3.40), and there is not a unidistribution line between this line and the stable node of residue curves. This univolatility line gives rise to inflection points of residue curves and distillation lines. A sketch of the diagram is determined based on the position of unidistribution and univolatility lines. This cell of residue curves (distillation lines) is S-shaped.

- c) Let the binary mixture 1-3 be a mixture of Type 2, i.e. it becomes more positive than the mixture 12. In the similar way we find that there is an  $\alpha_{23}$ -univolatility line connecting edges 12 and 13 and no unidistribution lines between it and the unstable node of the residue curves (Figure 3.41). This univolatility line gives rise to inflection points of residue curves and distillation lines. A sketch of the diagram is determined basing on the position of

unidistribution and univolatility lines. This cell of residue curves (distillation lines) is S-shaped too but with opposite sign of the curvature.

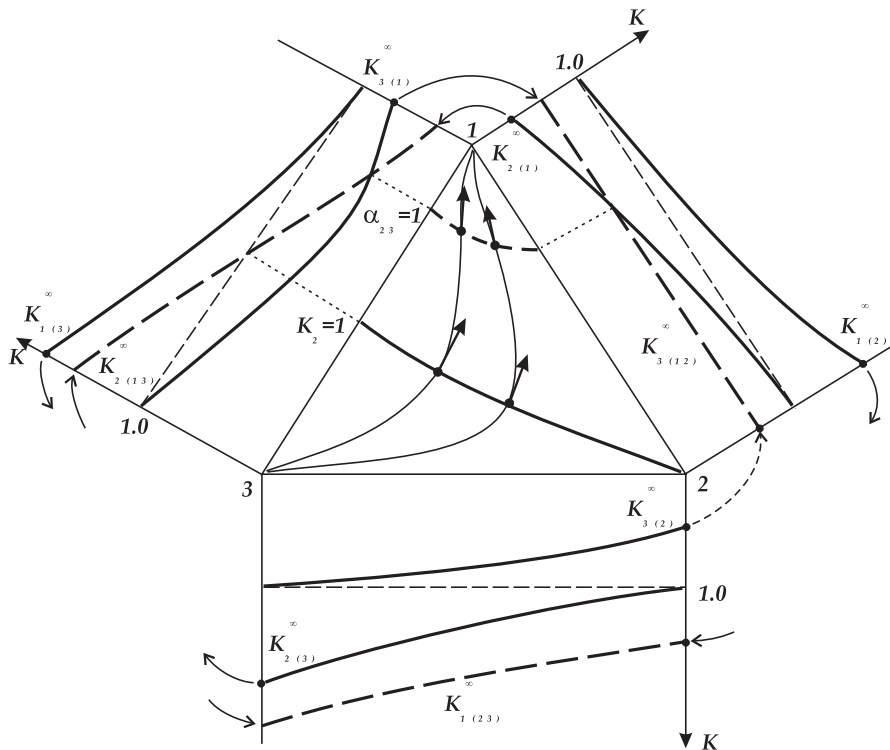


Figure 3.41: Unidistribution and univolatility line diagram and the sketch of residue curves for a zeotropic mixture 1-2-3 where the binary constituents 1-3 are a mixture of Type 2 (S-shaped residue curves).

- d) Let the binary mixture 1-3 be a mixture of Type 1', i.e., it has a mixed deviation from ideal mixtures. The diagram of unidistribution and univolatility lines and the sketch of the RC (DL) map here is given above in Figure 3.32. In this case there are both an  $\alpha_{1,2}$ -univolatility line connecting edges 13 and 23 and an  $\alpha_{2,3}$ -univolatility line connecting edges 12 and 13. Any line of the simple phase transformations has two inflection points, and the lines are  $\Omega$ -shaped.
- e) Let the binary mixture 1-2 be a mixture of Type 1'. The diagram of unidistribution and univolatility lines and the sketch of the RC (DL) map here is given above in Figure 3.35. Here, there is the  $\alpha_{2,3}$ -univolatility line as an arc at edge 12 of the composition triangle. A part of the residue curves or distillation lines intersects this univolatility line twice in succession. Each of these lines of a bunch will have two inflection points (one point between the inter-

section points and other between the univolatility line and the Apex 1. These lines have a specific  $\Omega$ -shape and other lines are  $C$ -shaped.

It can be seen from these examples that the single unidistribution line going from the saddle point is an inherent characteristic of zeotropic mixtures (Serafimov's Class 0). Univolatility lines can optionally exist if the mixture is nonideal, and there is a diversity of the diagrams of univolatility lines caused by various combinations of the deviation from ideality in the binary constituents.

Detailed analysis of all feasible variants of the univolatility lines for ternary zeotropic mixtures was made later by Zhvanetskij et al., 1988, and 33 variants of these diagrams were revealed. Though the occurrence of most of these types is questioned, all these types are possible theoretically.

**Example 2. Mixture 1-2-3 with minimum-boiling azeotrope  $A_{12}$  (Serafimov's Class 1.0-1a)**

a) The mixture 1-2 in this ternary mixture must be the mixture of Type 3. Let both mixtures 2-3 and 1-3 be mixtures of Type 1. The diagram of unidistribution and univolatility lines and the sketch of the RC (DL) map are presented in Figure 3.42 a. The -univolatility line goes from the point of azeotrope to the edge 13. The lines of the simple phase transformations have inflection points between the univolatility line and Apex 3. A part of the lines in this cell are  $C$ -shaped, and the other lines are  $S$ -shaped.

b) Let the mixture 13 be a mixture of Type 2', i.e., it is more negative (or less positive) than mixture 2-3. Here the -univolatility line goes from the point of azeotrope to edge 23. The lines of the simple phase transformations have another sign of curvature (Figure 3.42 b).

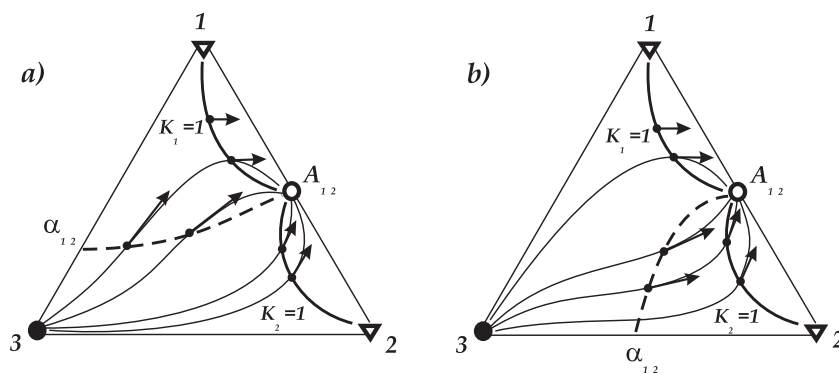


Figure 3.42: Unidistribution and univolatility line diagram and the sketch of residue curves for a mixture 1-2-3 with a minimum-boiling azeotrope  $A_{12}$  for various types of the binary constituents: a) both mixtures 1-3 and 2-3 are mixtures of Type 1; b) mixture 1-3 is a mixture of Type 2.

Let us consider now various trajectories of the functions  $K_i(x)$  at edge  $K-1-2$  of the prism. In the case where mixtures 1-3 and 2-3 are the mixtures of Type 1, the only intersection of  $K$ -lines

corresponds to the point of binary azeotrope, and it leads to the structure presented in Figure 3.42 a. Other cases are presented in Figure 3.43.

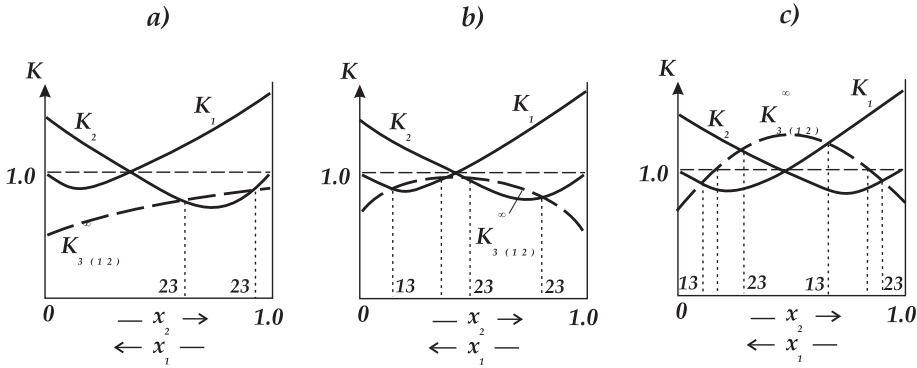


Figure 3.43: Distribution coefficient trajectories  $K_i(x)$  at the edge  $K-1-2$  for a mixture 1-2-3 with minimum-boiling azeotrope 1-2: a) Mixture 2-3 is a mixture of Type 2; b) both mixtures 2-3 and 1-3 are the mixtures of Type 2; c) additional positive deviations at the ternary mixture.

In Case (a), the mixture 2-3 becomes more positive (Type 2), and the line  $K_{3(12)}^\infty$  intersects twice in succession with the line  $K_2(12)$ . It leads to the appearance of two points  $\alpha_{12} = 1$  at edge 1-2. The lines of the simple phase transformation have two inflection points when they intersect twice in succession with the  $\alpha_{23}$ -univolatility line and there is a local deformation of the residue curves or distillation lines. The corresponding diagram is presented in Figure 3.44a.

In Case (b), both mixtures 1-3 and 2-3 are mixtures of Type 2 (more positive). Line  $K_{3(12)}^\infty$  intersects twice in succession with the line  $K_2(12)$ , and intersects twice in succession with the line  $K_1(12)$ . It leads to the appearance of two points  $\alpha_{12} = 1$  and  $\alpha_{13} = 1$  two points at the edge 1-2. The lines of simple phase transformation have two inflection points where they intersect these arc-wise univolatility lines, and the map has two local deformations (Figure 3.44 b).

Both these diagrams are diagrams of Serafimov's Class 1.0-1a but they have more complex geometry in the simple phase transformation lines than the mixtures represented in Figure 3.42, corresponding to a more complex diagram of univolatility lines.

It can be seen that the inherent characteristic of the diagram of Class 1.0-1a is just existence of two unidistribution lines going from the azeotrope point to tops 1 and 2 and the  $\alpha_{12}$ -univolatility line going between them to one of sides 13 or 23. The movement of the  $\alpha_{12}$ -univolatility line and the existence of other univolatility lines are the specific characteristics of the given mixture.

Let us consider the situation where both mixtures 13 and 23 are mixtures of Type 2, but the positive deviations in the ternary mixture are so strong that line  $K_{3(12)}^\infty$  has a maximum with the value  $K > 1$  (Figure 3.43 c). Here we have in addition two points at edge 12. This changes the diagram of unidistribution and univolatility lines totally and, consequently, changes the RC (DL) map (Figure 3.44 c). We can see that strengthening of positive deviations leads to appearance of

ternary minimum-boiling azeotrope, and this diagram is a diagram of another class (Serafimov's Class 1.1-1a).

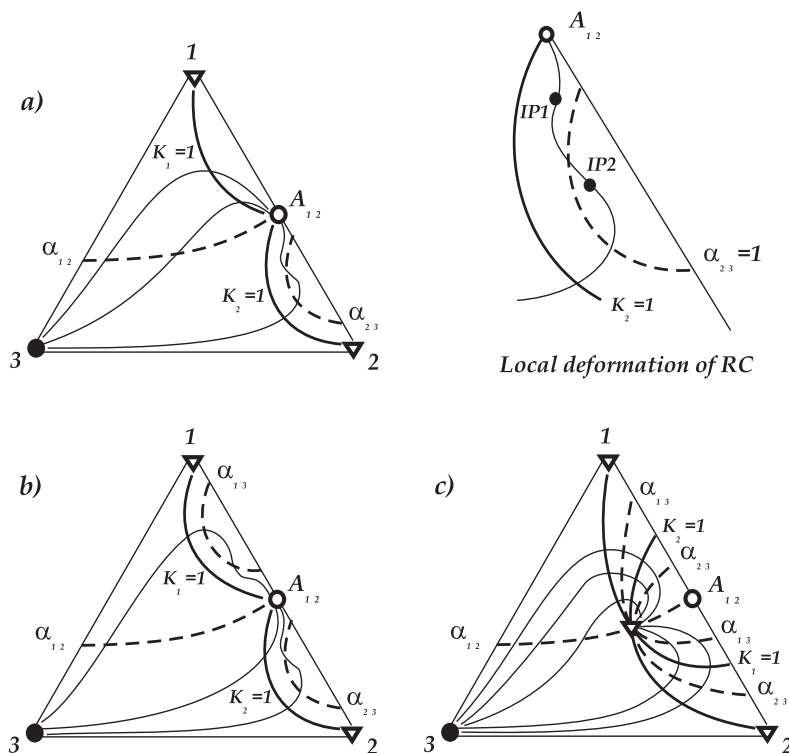


Figure 3.44: Unidistribution and univolatility line diagram and the sketch of the residue curve (distillation line) map for the cases presented in Figure 3.42.

**Example 3. Mixture 1-2-3 with the minimum-boiling azeotrope 13 (Serafimov's Class 1.0-1b)**

a) The mixture 1-3 in this ternary mixture must be a mixture of Type 3. Let the mixtures 1-2 and 2-3 be mixtures of Type 1. The diagram of unidistribution and univolatility lines and the sketch of the RC (DL) map are presented in Figure 3.45.

This diagram includes two univolatility lines, one which ( $\alpha_{23}$ -univolatility line) is not connected with an azeotrope. Both univolatility lines are blocked from each side by the corresponding unidistribution lines, and its existence does not lead to the inflection points of the lines of simple phase transformations. These lines are U-shaped. This structure is a diagram of Serafimov's Class 1.0-1b. This set of unidistribution and univolatility lines is an inherent characteristic of the diagrams of this class. The feasible variations of the diagram of this class are presented in Figure 3.46 where additional univolatility lines exist, optionally depending on the combination of the binary constituents.



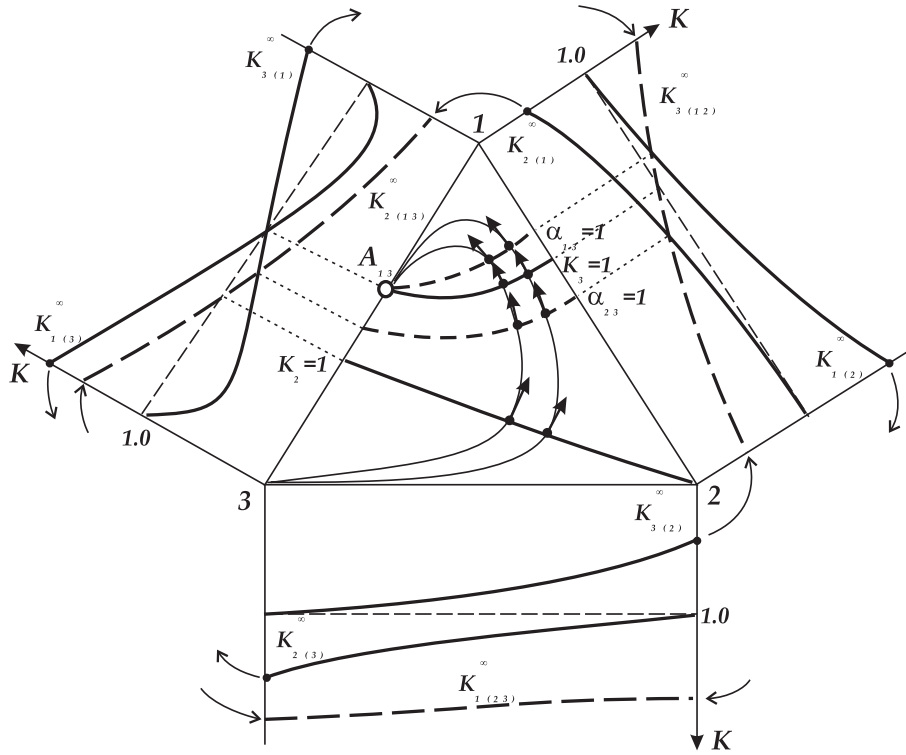


Figure 3.45: Unidistribution and univolatility line diagram and the sketch of the residue curve map for the mixture of Class 1.0-1b (U-shaped residue curves).

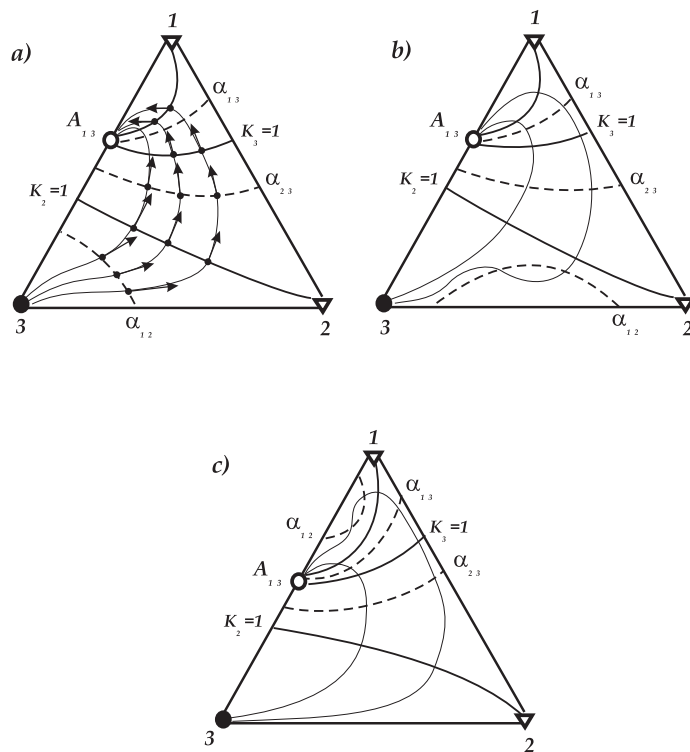


Figure 3.46: Types of the diagrams of unidistribution and univolatility lines and of the sketch of residue curve map for mixture of Class 1.0-1b: a) mixture 13 is the Type 4 mixture; b) mixture 23 is the Type 1' mixture; c) mixture 12 is the Type 2 mixture.

We can see that optional (additional) univolatility lines lead to the local deformation of the lines of the simple phase transformations. They change the geometry of the diagram, but do not change the topological structure.

**Example 4. Mixture 1-2-3 with minimum-boiling azeotrope 12 and maximum-boiling azeotrope 23 (Serafimov's Class 2.0-1)**

Let mixture 12 be a mixture of Type 3, mixture 13 be a mixture of Type 3', and mixture 23 be a mixture of Type 1. The diagram of unidistribution and univolatility lines and the sketch of residue curves (distillation lines) was presented in Figure 3.34. The univolatility lines are blocked from both sides by the corresponding unidistribution lines and do not give rise to any inflection points. However, part of the lines of simple phase transformations intersect the unidistribution line of the same index ( $K_1$ ) twice in succession, and it leads to the existence of inflection points for these lines. Some feasible variations of this diagram at the different combinations of the binary

constituents are presented in Figure 3.47. Any or both of the additional univolatility lines at side 1-2 can appear when mixture 23 is Type 2' mixture (Figure 3.47 a, b). Case (c) can appear when mixture 23 is Type 2 mixture, and the case (d) can appear when the mixture 23 is Type 2 mixture and the mixture 13 is Type 4' mixture.

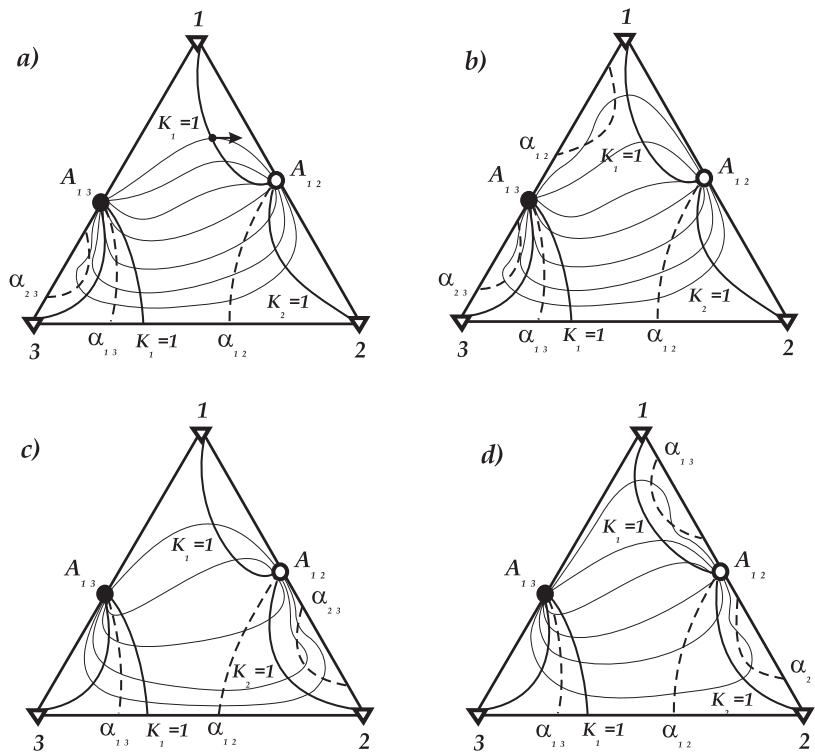


Figure 3.47: Types of the diagram of unidistribution and univolatility lines and of the sketch of the residue curve map for a mixture of Class 2.0-1.

The additional univolatility lines lead to the local deformation of the residue curves or distillation lines. However, we can see that the set of the unidistribution and univolatility lines of the "basic" diagram (Figure 3.34) is an inherent characteristic of this class of the topological structures (Serafimov's Class 2.0-1).

**Example 5. Mixtures with three minimum-boiling binary azeotropes.**

Let us consider the diagrams of unidistribution and univolatility lines and the sketches of the residue curves (distillation lines) for the ternary mixture 1-2-3 with minimum-boiling azeotrope in any binary constituent. The diagrams are presented in Figures 3.48 - 3.50 assuming that in all cases we have the same functions  $K_i(i,j)$ . We can see that the different types of behavior of the curves  $K_{i(jh)}^\infty$  lead to different diagrams of unidistribution and univolatility lines and also to a

different topological class of the residue curve (distillation line) map. It is interesting to note that the simplest behavior of the curves  $K_{i(jh)}^\infty$  leads to the appearance of ternary minimum-boiling azeotrope (Class 3.1-2, Figure 3.48, and this type of mixture is the most common. More complex behavior of the curves  $K_{i(jh)}^\infty$  leads to the appearance of the diagram of Serafimov's Class 3.0-2 (Figure 3.49), and the mixtures of this class occur more rarely. The most complex behavior of the curves  $K_{i(jh)}^\infty$  leads to the appearance of a ternary saddle azeotrope (Class 3.1-3b, Figure 3.50), and the occurrence of such mixtures is almost negligible.

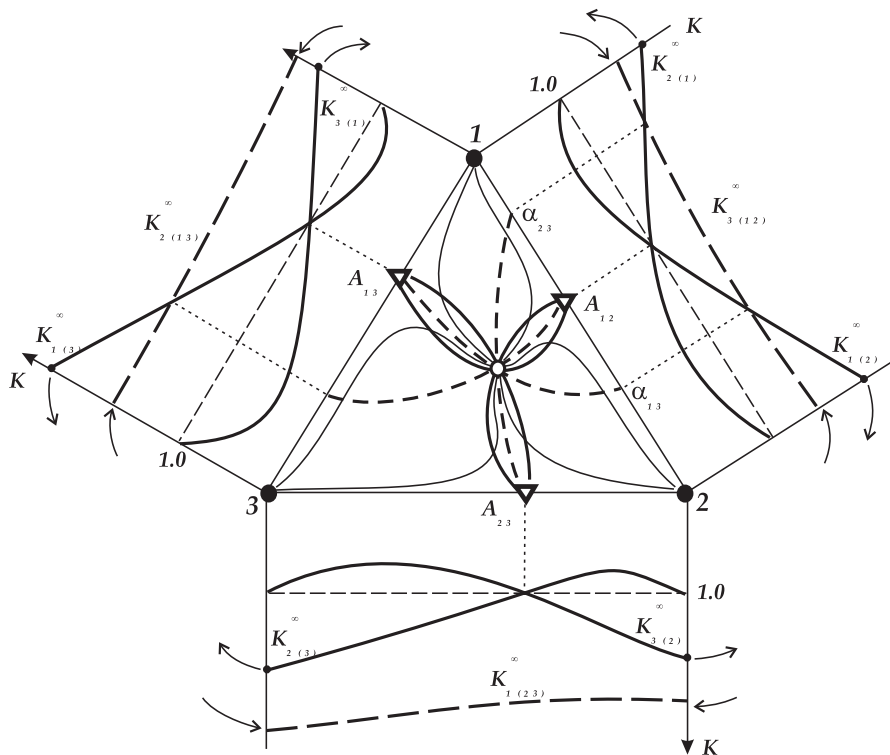


Figure 3.48: Unidistribution and univolatility line diagram and sketch of the residue curve map for a mixture of Class 3.1-2.

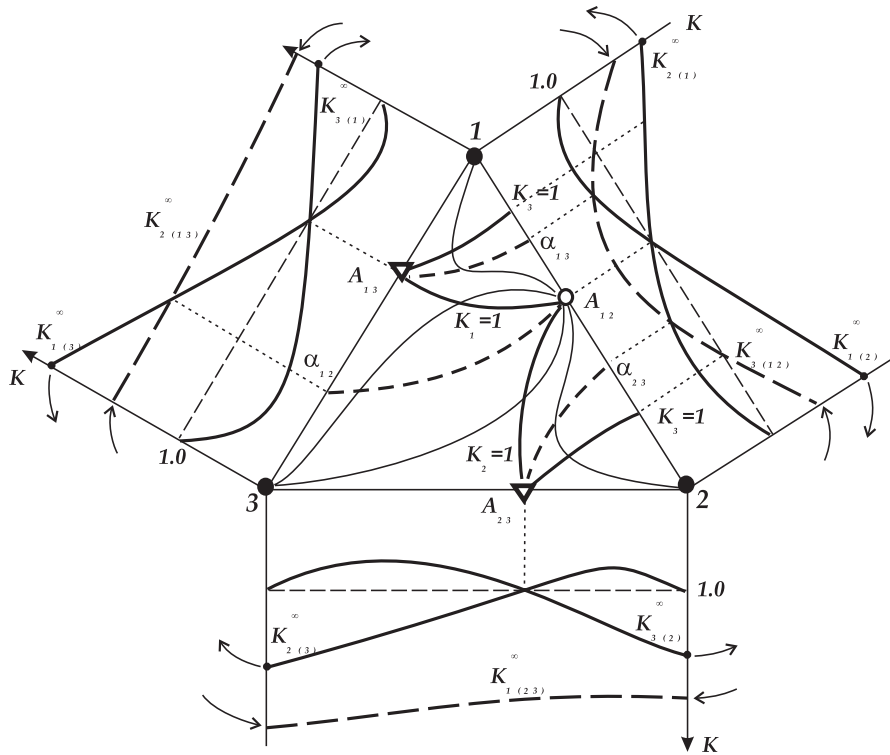


Figure 3.49: Unidistribution and univolatility line diagram and sketch of the simple phase transformation line map for a mixture of Class 3.0-2.

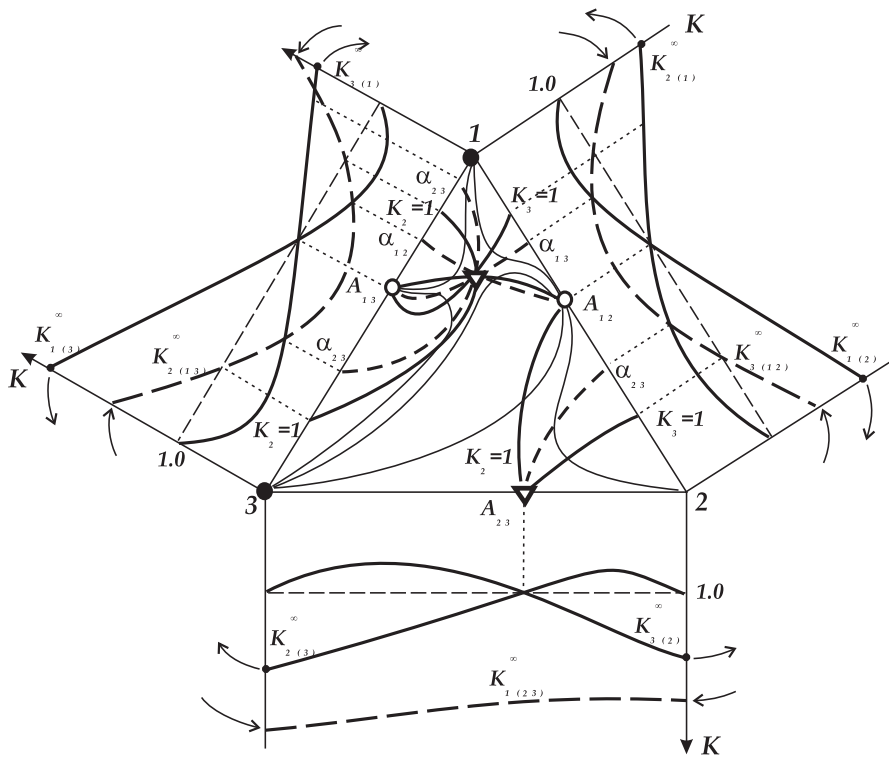


Figure 3.50: Unidistribution and univolatility line diagram and sketch of the simple phase transformation line map for a mixture of Class 3.1-3b.

**In summary:** We see from the above examples that a combined diagram of unidistribution and univolatility lines can characterize the VLE for any given mixture and permits the construction of the sketch of the residue curves and distillation lines maps without any computation. An overview of the unidistribution and univolatility line diagrams for the most probable classes of ternary mixtures is presented in Figure 3.38, where only the intrinsic univolatility lines are given.

## 3.9 Conclusions

The main conclusions that can be reached from the literature on qualitative analysis of the VLE diagrams and the additional investigations presented in this survey are:

Vapor-liquid equilibrium can be characterized by various means; first and foremost by simple phase transformation maps, among which open evaporation residue curve maps and distillation line maps have received broad acceptance. Note that distillation lines (discrete and continuous) have a well-defined thermodynamical meaning. These lines are rigorously defined by the VLE and, in turn, characterize it, as well as the residue curves.

The VLE can also be qualitatively characterized by unidistribution line diagrams and univolatility line diagrams. Univolatility line diagrams give additional information about the regions of the composition space with different volatility order of the components. The combined diagram of unidistribution and univolatility lines characterizes the shape (geometry) of the trajectories of simple phase transformations.

We recommend that a distinction is made between the *topological structure* of simple phase transformation maps (i.e., the set of singular points and the splitting into regions of the simple phase transformation trajectories), the *sketch* of the map (i.e., the qualitative pattern of the trajectories with representation of their shape), and the *exact map* of the simple phase transformation trajectories (residue curves or distillation lines).

The structures of VLE diagrams of azeotropic mixtures are limited by rigorous topological constraints. The structures for ternary mixtures without biazeotropy are classified into 26 possible topological structures. All types of the classified diagrams are topologically and thermodynamically feasible, but their occurrence in nature is determined by the probability of certain combinations of molecular interactions. Data on the natural occurrence of various mixture classes permit us to exclude rare or improbable diagrams from consideration in the investigation of the correlation between VLE diagram structures and feasible separations upon distillation.

Usually the (topological) structure of the VLE diagram for a given mixture can be uniquely determined based solely on information of the existence and boiling point temperature of all singular points (pure components and azeotropes). It should be noted however, that there are some cases of indeterminate diagram structure.

The (topological) structure of the VLE diagram identifies the class of a given mixture, but not its specific characteristic like the shape of the singular and ordinary simple phase transformation trajectories.

A sketch of the simple phase transformation map (residue curve or distillation line map), including the specific features of a given mixture (i.e., the shape of the trajectories), can be determined from the localization of the unidistribution and univolatility lines. These lines give complete information about the curvature (path) of singular and ordinary trajectories of the simple phase transformation.

Generating an exact map including the localization of simple phase transformation trajectory boundaries (separatrices) requires numerical calculation. Often, only the boundaries are located by appropriate simulation rather than by generating a complete trajectory map.

It is reasonable to use the combined diagram of unidistribution and univolatility lines as a representative qualitative characteristic of the VLE.

## Definitions of Terms

This section contains an alphabetic listing with definitions of central terms as they are used in this text. In addition, Table 3.1 in the introductory pages gives an overview (quick reference) of the different terms used for key concepts in the azeotropic distillation literature and may be helpful in particular when reading Russian publications that are translated into English.

**Antipode** - exact opposite, but topological equivalent structure.

**Azeotrope** - mixture whose equilibrium vapor and liquid compositions are equal at the given system temperature and pressure. Mathematically: a singularity in the VLE manifold that does not correspond to a pure component.

**Azeotropic distillation** - distillation that involves azeotropic mixtures. Note that this is a much broader definition than traditionally used in the distillation literature where the term is frequently used as an abbreviation of heteroazeotropic distillation.

**Azeotropic mixture** - mixture that forms one or several azeotrope(s).

**Biazeotropic mixture** - mixture that forms two binary azeotropes for a binary pair or two ternary azeotropes.

**Composition space** - for an  $n$ -component mixture the composition space contains all the  $n$ -dimensional vectors of  $\mathcal{R}^n$  where the elements sum to unity.

**Composition trajectory** - the steady state or instantaneous composition profile of a distillation column, or the trajectory of composition change during batch distillation.

**Condensate curve** - open condensation liquid composition trajectory.

**Condensation curve** - open condensation vapor composition trajectory.

**Conjugate** - an element of a mathematical group that is equal to a given element of the group multiplied on the right by another element and on the left by the inverse of the latter element. [*Britannica*]

**Distillate curve** - composition trajectory of the vapor during open evaporation.



**Distillation** - the process of separating a liquid mixture by successive evaporation and condensation.

**Distillation boundary** - locus of compositions that cannot be crossed by the given distillation process. The existence and location of such boundaries depend critically on the type of distillation in question. Distillation boundaries are thermodynamic barriers for multicomponent distillations in the same way that azeotropes are barriers to binary distillation. They split the composition space into distillation regions.

**Distillation line** - the set of points  $x$  for which the vapor composition in equilibrium  $y$  also lies on the same line in the composition space (Zharov and Serafimov, 1975). A discrete distillation line is drawn as a piecewise linear curve through a sequence of conjugated vapor-liquid equilibrium vectors in the composition space. Continuous distillation lines interpolate the same sequence of equilibrium points and are not mathematically unique.

**Distillation line map** - diagram that shows distillation lines for different initial conditions for a given mixture in the composition space.

**Distillation region** - a subspace of the composition space defined by a family of distillation trajectories that join a stable and unstable node.

**Distribution coefficient** - ratio of mole fractions in vapor and liquid phase for the given species. Commonly referred to as vapor-liquid equilibrium ratio or K-value.

**Entrainer** - material (liquid component) that acts as a mass separating agent.

**Equilibrium vector** - composition vector between two phases in equilibrium, also named *tie-line*.

**Equilibrium staged distillation** - staged distillation column where vapor-liquid equilibrium is assumed between the phases on all trays.

**Heteroazeotrope** - azeotrope where the vapor phase coexists with two liquid phases.

**Heterogeneous mixture** - mixture with more than one liquid phase.

**Homoazeotrope** - azeotrope where the vapor phase coexists with one liquid phase.

**Homogeneous mixture** - mixture with a single liquid (and vapor) phase.

**Ideal mixture** - mixture that obeys Raoult's law (or Henry's law), i.e., the activity coefficients for all components of the liquid are equal to unity. Ideal mixtures are a special case of zeotropic mixtures.

**Inflection point** - root of the second order derivative of a given function, point of change of function curvature.

**Inflection point curve** - locus of inflection points.

**Injective** - being a one-to-one mathematical function.

**Isodistribution line** - locus of points in the composition space where the distribution coefficient for a particular component is constant.

**Isomorphic** - being of identical or similar form, shape, or structure. Antipodal topological VLE diagrams are isomorphous.

**Isotherm** - locus of points in the composition space where the temperature for a given mixture at vapor-liquid equilibrium is constant. Liquid isotherms are lines of constant value of the boiling temperature and vapor isotherms are lines of constant value of the condensation temperature.

**Isotherm map** - diagram that shows isotherms for a given mixture in the composition space. Contour plot of one or both of the vapor-liquid equilibrium temperature surfaces for a given mixture.

**Isovolatility line** - locus of points in the composition space where the relative volatility of a pair of components is constant.

**K-value** - see distribution coefficient.

**Mapping** - to assign (as a set or element) in a mathematical correspondence.

**Mapping function** - function that gives the mathematical correspondence between two sets of elements.

**Monoazeotropic mixture** - mixture that forms only one azeotrope at each element of the composition simplex (only one binary azeotrope for each binary pair in an azeotropic mixture).

**Node** (*mathematically*) - critical point with all paths either approaching (stable) or departing (unstable).

**Nonideal mixture** - mixture that exhibits deviations from Raoult's law (or Henry's law). Non-ideal mixtures may be zeotropic or azeotropic.

**Ockham's Razor** - principle stated by English philosopher William of Ockham (1285-1347/49) that the simplest of competing theories should be preferred to the more complex, and that entities are not to be multiplied beyond necessity.

**Open condensation** - condensation of a vapor phase where the liquid formed is removed continuously.

**Open distillation** - distillation with input and/or output mass streams.

**Open evaporation** - evaporation of a liquid phase where the vapor formed is removed continuously. Also referred to as simple distillation or Rayleigh distillation.

**Open evaporation distillate curve** - see distillate curve.

**Relative volatility** - the ratio of distribution coefficients for pair of components in a mixture.

**Residue curve** - composition trajectory of the residue liquid in the still during open equilibrium evaporation. Sometimes referred to as “distillation line” in Russian and old German-language literature.

**Residue curve map** - diagram that shows residue curves for different initial still compositions for a given mixture in the composition space.

**Residue curve region** - set of liquid compositions in the composition space that belong to a family of residue curves with common initial and final points.

**Saddle** (*mathematically*) - singular point with finitely many paths both approaching and departing. Only separatrix extends or terminate in the saddle point. All other paths have a hyperbolic course in the vicinity of the singular point.

**Separatrix** - locus of bifurcation points of differential equations, i.e., points at which an infinitesimal perturbation causes at least one of the integration endpoints to change. A separatrix may be stable or unstable dependent on whether solutions in its vicinity approach or depart as the value of the independent (integration) parameter goes to infinity.

**Simple distillation** - see open evaporation.

**Simple distillation region** - see residue curve region.

**Simple distillation residue curve** - see residue curve.

**Simple equilibrium phase transformation** - process where the composition of one phase changes according to its phases equilibrium and where the other phase is continuously removed. Open evaporation and open condensation are such processes.

**Simplex** - spatial configuration of  $(n-1)$  dimensions determined by  $n$  points in a space of dimension equal to or greater than  $(n-1)$ . A triangle together with its interior determined by its three vertices is a two-dimensional simplex in the plane.

**Singular point** - root to the first order derivative of a function. The singular points of the residue curve Equations (3.7) are given by the solution of  $x = y = 0$ . Azeotropes and pure components are singular points of Equations (3.7).

**Tie-line** - see equilibrium vector.

**Tie-line curve** - sequence of conjugated vapor-liquid equilibrium vectors (tie-lines) in the composition space. Here referred to as a *discrete distillation line*, see distillation line.

**Topology** - a branch of mathematics concerned with those properties of geometric configurations (as point sets) which are unaltered by elastic deformations (as a stretching or a twisting).

**TTA** - thermodynamic topological analysis.

**Unidistribution line** - locus of points in the composition space where the distribution coefficient of the given component equals unity. At each point along the unidistribution line of component  $i$ , the equilibrium vector in the composition space has a direction normal to the component  $i$  vertex of the composition simplex.

**Unity lines** - collective term for unidistribution and univolatility lines.

**Univolatility line** - locus of points in the composition space where the relative volatility of pair of components equals unity. In ternary systems, a univolatility line of the components  $i$  and  $j$  is the locus where the equilibrium vectors in the composition space point directly at the third component  $h$  vertex.

**VLE** - vapor-liquid equilibrium.

**VLE manifold** - union of all possible vapor-liquid equilibrium pairs in a mixture.

**VLE diagram** - graphical presentation of the vapor-liquid equilibrium functions of a mixture like isotherm maps, residue curve maps and distillation lines maps.

**Zeotropic mixture** - mixture that does not form azeotropes. A mixture may be zeotropic, but still nonideal.

## Chapter 4

# On the Topology of Ternary VLE Diagrams: Elementary Cells

The classification of ternary vapor-liquid equilibrium (VLE) diagrams is a key to simple azeotropic distillation analysis. We find that all ternary mixtures so far reported occurring in nature can be qualitatively represented by a combination of only four elementary cells. This greatly reduces the number of VLE diagram structures that need to be analyzed in order to reveal the qualitative characteristics of any ternary azeotropic mixture.

### 4.1 Introduction

Ternary vapor-liquid equilibrium (VLE) diagrams provide a graphical tool to predict qualitatively the feasible separations for multicomponent azeotropic mixtures before detailed simulation or experimental study of their distillation. The various graphical representations of the VLE (residue curve and distillation line maps, isotherm map, equilibrium vector field) are closely related and are equally capable of characterizing the mixture. In this paper, we consider *residue curves* (Schreinemakers, 1901c; Ostwald, 1902; Zharov, 1967; Serafimov, 1968a; Doherty and Perkins, 1978a), and the topological classification of ternary mixtures into 26 diagrams by Serafimov (1970b). Our considerations apply equally well to *distillation lines* (Zharov, 1968c; Stichlmair, 1988). We refer to the review of Widagdo and Seider (1996) and to the literature mentioned for a detailed description of these tools and their application to distillation column profiles. Our contribution is to propose a set of elementary topological cells which are constituents of all feasible ternary VLE diagrams. We show that the until now reported ternary diagram classes include only four of these elementary cells.

## 4.2 Classification of ternary VLE diagrams

The number of feasible VLE diagram structures is limited by topological and thermodynamical constraints. A complete classification of these feasible structures for ternary mixtures was given by Serafimov (1970*b*) and Serafimov *et al.* (1971; 1973), and is more recently presented by Serafimov (1996). Serafimov's classification results in the 26 classes of ternary VLE diagrams presented in Figure 4.1. The classification is based on the simplifying and common assumption that there exists no more than one binary azeotrope for each binary pair and no more than one ternary azeotrope. The classification of Serafimov considers topological structures and thus does not distinguish between antipodal diagrams (switching of minimum- and maximum-boiling azeotropes) since they have the same topology. Transition from one antipode to the other can be made by simply changing the sign of the nodes and inverting the direction of the arrows of increasing boiling temperature.

Gurikov (1958) was the first to derive the rule of azeotropy and propose a thermodynamic topological classification of ternary mixtures. However, his classification was incomplete, and Serafimov (1968*d*) revealed four additional feasible structures and established the 26 topological classes presented in Figure 4.1. Later, Serafimov's classification of ternary mixtures was refined by distinguishing between antipodes inside each structure class, based on the reasoning that "*minimum- and maximum-boiling azeotropes have dissimilar physical nature and dissimilar behavior during distillation*" (Zharov and Serafimov, 1975). This refined classification includes a total of 49 types of ternary VLE diagrams. An even more detailed classification is proposed by Matsuyama and Nishimura (1977) who also rank the components in the order of their boiling temperatures ("light", "intermediate" and "heavy"). This classification includes 113 diagram classes of which 87 are presented graphically by Doherty and Caldarola (1985). Nevertheless, among these 113 classes there are only the 26 topologically distinct structures of Serafimov. Actually, the classification of Matsuyama and Nishimura adds some ambiguity as some of their classes with a ternary saddle azeotrope have two or three possible topological structures. For example, their classification code 112-S can be either of Serafimov's class 3.1-3a or 3.1-3b depending on whether there exists a saddle - saddle separatrix or not. This is also pointed out by Foucher *et al.* (1991) who recommend an extension of the Matsuyama and Nishimura's classification code name in these cases.

In this paper, we use Serafimov's (1970*b*) classification of the topological classes and Zharov and Serafimov's (1975) refinement of the antipodal structure types (referred to as the ZS-type). The relationships between the classifications of Gurikov (1958), Serafimov (1970*b*), Zharov and Serafimov (1975) and Matsuyama and Nishimura (1977) are presented in Table 4.2. The table is useful when relating publications where the different classifications are used.

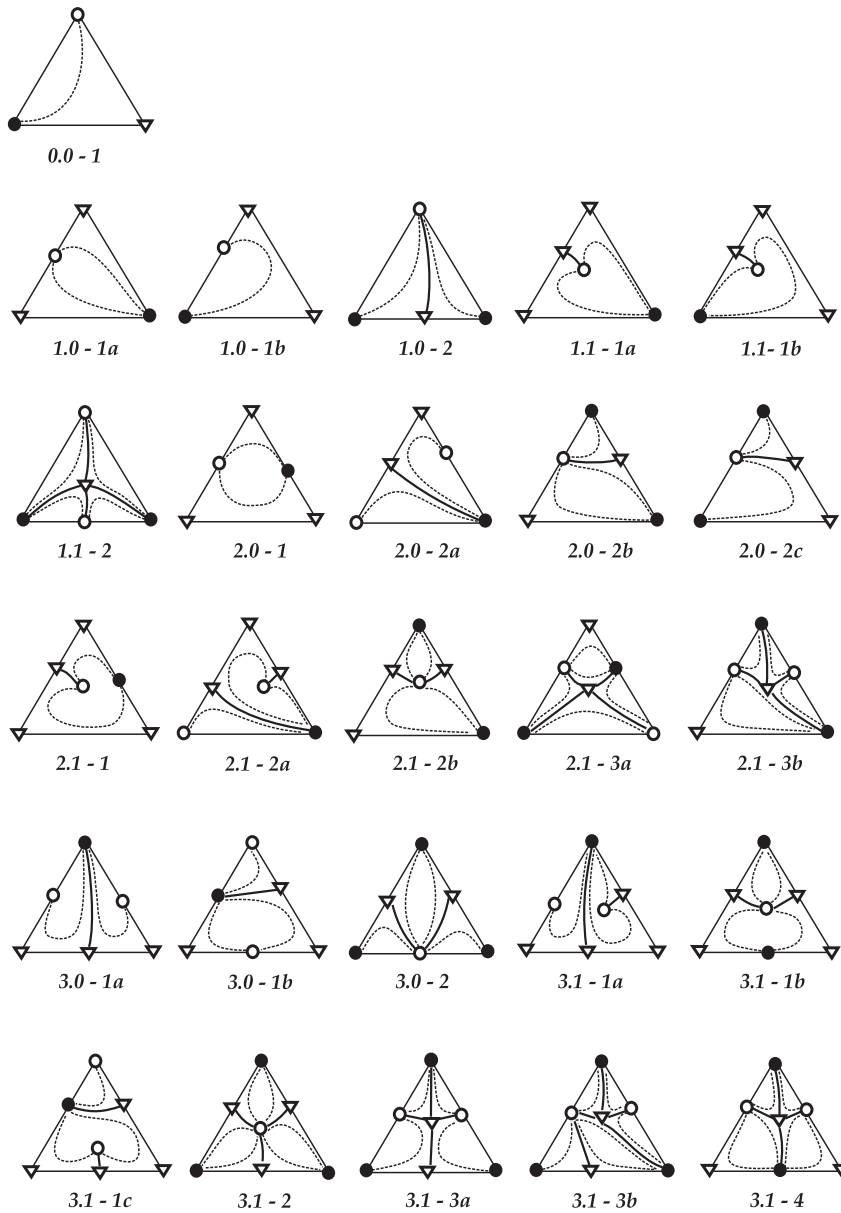


Figure 4.1: Classification of ternary mixtures' thermodynamic topological structure by Serafimov (1970b). Structural characteristics of residue curves (or distillation lines) shown by dashed lines with the singular points indicated by ● stable (unstable) node, ○ unstable (stable) node, and ∇ saddle, and the region boundaries given by bold lines.

### 4.3 Elementary cells

There is a great diversity of VLE diagrams for ternary mixtures caused by the variety in physical properties of the components and their molecular interaction. As mentioned, if we consider only topological differences there are 26 distinct types as presented in Figure 4.1. Furthermore, there is a far greater diversity in possible shapes (geometry) of the simple phase transformation trajectories such as residue curves and distillation lines. It is possible to reduce this complexity to a combination of a few topological building blocks (“elementary cells”) and some basic internal structures (shapes of the simple phase transformation trajectories). We use residue curves to represent the simple phase transformation trajectories in this paper.

We find that among Serafimov’s 26 topological classes there are eight elementary topological cells (denoted I, II, III, IV, II’, III’, IV’ and V) that constitute all the ternary diagrams, where a cell is defined as one residue curve region taken with its boundaries (that is, a subspace of the composition space constrained by residue curve boundaries, if any, and the composition simplex). From these eight elementary cells we may construct all the 26 diagrams as shown in Figure 4.2. Each cell has one unstable and one stable node and some set of saddle points. There are four “primary” diagrams where the composition triangle consists of a single cell (one residue curve region; Serafimov’s class 0.0-1, 1.0-1a, 1.0-1b and 2.0-1), and these elementary cells (denoted I, II, III, IV) are also the only so far reported for naturally occurring mixtures. Cells II’, III’ and IV’ are modifications of the primary cells II, III and IV, respectively (with internal nodes), for which there are no reported physical mixtures. Cell V only occurs as an element in Serafimov’s class 3.1-1b, and also for this class there is so far no physical mixture reported.

The four primary diagrams and the corresponding elementary cells I, II, III, IV are shown in Figure 4.3. Each elementary cell is characterized by a certain set and order of the singular points (nodes and saddles) along the contour of its border (that is, by its topology). Accordingly we can name them as given in Figure 4.3.

There is an important difference between an elementary cell of the “primary” diagrams (one residue curve region) and an elementary cell incorporated into more complex diagrams. If an elementary cell is a primary diagram, the saddle point is a pure component point. The borders of the cell are the edges of the composition triangle (linear). The (stable and unstable) nodes are pure component points or points of binary azeotropes. If an elementary cell is a constituent of a complex diagram, at least one of its saddles is a binary or a ternary azeotrope, and, therefore, at least one of the borders of the cell is a residue curve boundary (curved) showed by the solid thick lines in Figure 4.2. One of the nodes can be a point of a ternary azeotrope. In general, the composition space is broken into several residue curve regions (cells) if there are more than one unstable node or more than one stable node.

Despite these differences, a single elementary cell and an elementary cell incorporated into a complex diagram are topological equivalent. Note, however, that inside similar topological cells there may be various shapes of the residue curves (simple phase transformation trajectories).



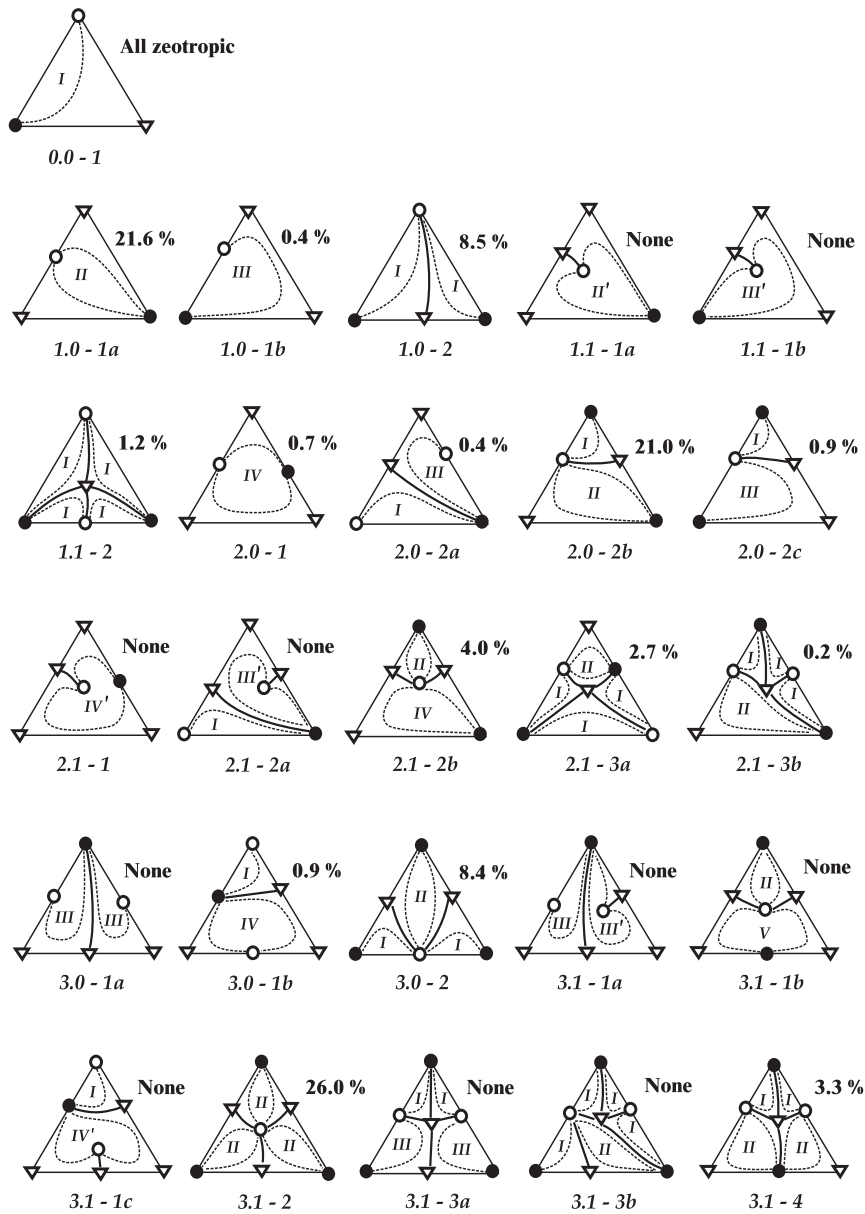


Figure 4.2: Elementary cells (I, II, III, IV, II', III', IV' and V) within Serafimov's 26 topological classes. Physical occurrence (%) of azeotropic mixtures reported in the literature according to Reshetov's statistics (based on data from 1965 to 1988).

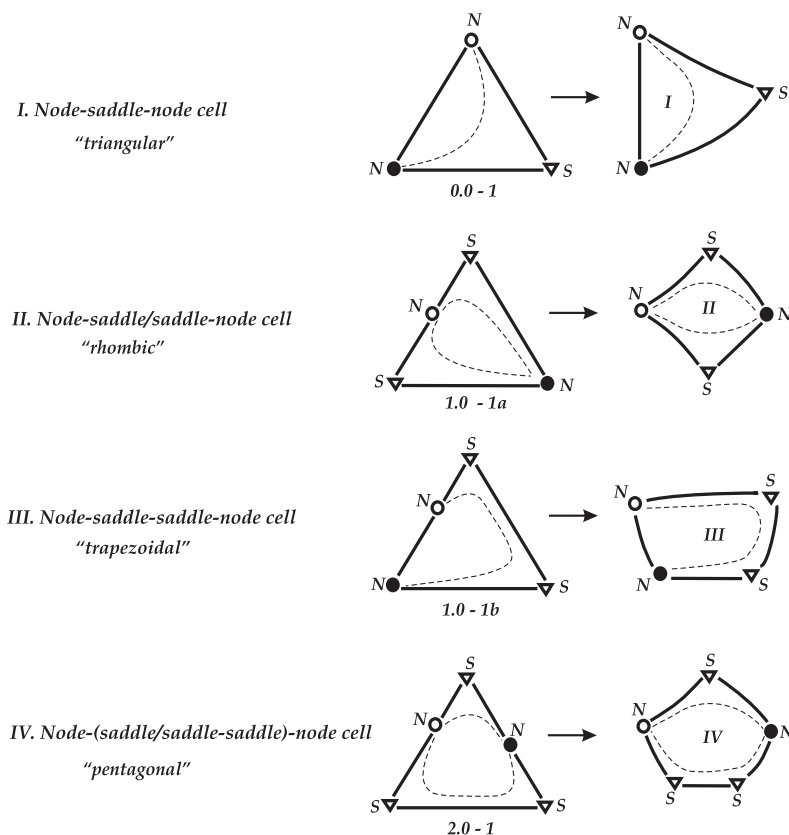


Figure 4.3: Generalization of the four elementary topological cells I, II, III, IV from the diagrams with one residue curve region. Each cell is characterized by the set and order of the nodes ( $N$ ) and saddles ( $S$ ) along the contour of its border. The singular points are also indicated by  $\bullet$  stable (unstable) node,  $\circ$  unstable (stable) node,  $\nabla$  saddle. The dashed lines indicate the qualitative paths of the residue curves.

## 4.4 Occurrence in nature

Even though all the classified diagrams in Figure 4.2 are topologically and thermodynamically feasible, their occurrence in nature is limited by the probability of certain combinations of molecular interactions. In this section we present data on the occurrence of the different classes among the mixtures reported in the literature. This permits us to exclude rare or improbable diagram classes from consideration.

Serafimov (1968*d*) analyzed the occurrence of different types of VLE diagrams among 418 reported (experimental) data on ternary azeotropic mixtures. Reshetov (1998) made a similar study

for 1609 ternary mixtures (in which 1365 are azeotropic) based on thermodynamic data that were published during the period from 1965 to 1988. To the best of our knowledge we have not found any other publications that address this issue. The occurrence of the various classes as reported by Serafimov and Reshetov are given in Table 4.1. (Reshetov's statistics are also presented in Figure 4.2). Note that Reshetov (1998) found that the three mixtures reported for class 3.1-1a in the statistics by Serafimov (1968*d*) actually was of another structure class. From Reshetov's data we see that only 16 of Serafimov's 26 classes are reported to occur in nature. If we also differentiate between minimum- and maximum-boiling azeotropes (ZS-type), then we find that 27 of the 48 classes are reported. The distribution reported in these studies does not necessarily reflect the real occurrence in nature. The azeotropic data selection is small and occasional. Moreover, the distribution can be distorted compared to the unknown natural distribution since the published components data are results of deliberate search for entrainers for specific industrial separation problems. Nevertheless, these data are interesting and can be used for some deductions:

- Serafimov's class 3.1-2 with three minimum-boiling binary azeotropes and one minimum-boiling ternary azeotrope has the largest number of reported mixtures. About 26 % of the 1365 ternary azeotropic mixtures in the study by Reshetov are of this class.
- Elementary cells I and II covers more than 90 % of all the reported ternary azeotropic mixtures. The three most common structures are Serafimov's class 1.0-1a (21.6 %), 2.0-2b (21.0 %) and 3.1-2 (26.0 %). Among these three classes only cells I and II occur.
- Ternary azeotropes are common in nature. About 40 % (37.9 %) of the reported ternary mixtures have a ternary azeotrope. These are Serafimov's class 1.1-2, 2.1-2b, 2.1-3a, 2.1-3b, 3.1-2 and 3.1-4.

For each of the reported classes, one may find a great number of (similar) mixtures in nature. However, for those classes with no reported mixtures, and with a structure that requires a set of molecular interactions that are unlikely, we expect that few if any real mixtures will be found. The experimental data for ternary azeotropic mixtures used for the above statistics is rather limited. However, the experimental data for binary azeotropic pairs is considerably more extensive. For example, Gmehling *et al.* (1994) has compiled data for 18 800 binary systems (involving about 1 700 components). From this we can estimate the behavior of a large number of ternary mixtures combinations from a VLE model, but to our knowledge no systematic effort has yet been done.

It is well-known that binary maximum-boiling azeotropes are less abundant than minimum-boiling azeotropes. According to Lecat (1949) the ratio of minimum-boiling versus maximum-boiling azeotropes that occurs in nature is about 9 to 1. The statistics of Reshetov confirm this heuristic rule. Thus, the more maximum-boiling binary azeotropes that are included in the ternary mixture, the less is the probability of its occurrence. This is clearly demonstrated in Table 4.1. In particular, no ternary mixture with three binary maximum-boiling azeotropes has been found among Reshetov's selection of 1365 mixtures, and no ternary maximum-boiling azeotrope has been found. As a result, even for the topological structures where the existence is beyond question, the occurrence of antipodes with maximum-boiling azeotropes is much less than that of antipodes with minimum-boiling azeotropes.

Table 4.1: Occurrence of ternary VLE diagram structures found in published mixture data

Serafimov's class	Occurrence Serafimov (until 1968)	ZS-type	Set of azeotropes <sup>a</sup>	Occurrence Reshetov (1965-1988)
0.0-1	-	1	zeotropic	244
1.0-1a	13	3a	min	283
1.0-1b	2	7a	max	12
1.0-2	20	3b	min	4
		7b	max	1
		4	min	95
		8	max	21
1.1-1a	None	2a	min + min Az <sub>3</sub>	None
1.1-1b	None	6a	max + max Az <sub>3</sub>	None
1.1-2	7	2b	min + min Az <sub>3</sub>	None
		6b	max + max Az <sub>3</sub>	None
		5	min + S <sub>3</sub>	8
		9	max + S <sub>3</sub>	8
2.0-1	1	15	min + max	9
2.0-2a	None	17	min + max	2
2.0-2b	77	18	max + min	3
2.0-2c	2	11a	min + min	280
		21a	max + max	6
		11b	min + min	10
		21b	max + max	2
2.1-1	None	13	min + max + min Az <sub>3</sub>	None
2.1-2a	None	14	min + max + max Az <sub>3</sub>	None
2.1-2b	3	16a	min + max + min Az <sub>3</sub>	None
		16b	min + max + max Az <sub>3</sub>	None
		10	min + min + min Az <sub>3</sub>	55
		20	max + max + max Az <sub>3</sub>	None
2.1-3a	14	19	min + max + S <sub>3</sub>	37
2.1-3b	5	12	min + min + S <sub>3</sub>	2
		22	max + max + S <sub>3</sub>	1
3.0-1a	None	29	min + min + max	None
3.0-1b	None	33	max + max + min	None
		28	min + min + max	9
		34	max + max + min	3
3.0-2	85	24	min + min + min	114
		37	max + max + max	None
3.1-1a	3	27b	min + min + max + min Az <sub>3</sub>	None
3.1-1b	None	32b	max + max + min + max Az <sub>3</sub>	None
3.1-1c	None	26	min + min + max + min Az <sub>3</sub>	None
		31	max + max + min + max Az <sub>3</sub>	None
		27a	min + min + max + max Az <sub>3</sub>	None
		32a	max + max + min + min Az <sub>3</sub>	None
3.1-2	171	23	min + min + min + min Az <sub>3</sub>	355
		36	max + max + max + max Az <sub>3</sub>	None
3.1-3a	None	25a	min + min + min + S <sub>3</sub>	None
3.1-3b	None	38a	max + max + max + S <sub>3</sub>	None
		25b	min + min + min + S <sub>3</sub>	None
		38b	max + max + max + S <sub>3</sub>	None
3.1-4	15	30	min + min + max + S <sub>3</sub>	41
		35	max + max + min + S <sub>3</sub>	4

<sup>a</sup> min - minimum boiling binary azeotrope; max - maximum boiling binary azeotrope; Az<sub>3</sub> - ternary node azeotrope; S<sub>3</sub> - ternary saddle azeotrope.

Pöllmann and Blass (1994) propose to reduce the number of ternary VLE diagrams by considering only "physically meaningful" structures. Their list includes 19 of Serafimov's 26 classes, excluding 1.1-1a, 1.1-1b, 2.1-1, 2.1-2a, 3.1-1a, 3.1-1c, and 3.1-3b. However, it is impossible in principle to state that some classes of ternary mixtures cannot exist in nature or are "physically meaningless", because all the structures in Figure 4.2 are thermodynamically and topologically feasible. We can only discuss the *probability* of the existence of some types of the VLE diagram structures.

## 4.5 Use of elementary cells

The concept of elementary topological cells is a simplification which primarily is made to reduce the number of structures of ternary VLE diagrams. It is useful for preliminary analysis of azeotropic distillation (presynthesis). Based on the knowledge of the distillation behavior of azeotropic mixtures of the primary diagrams elementary cells in Figure 4.3, or combinations of these, we also have information about what behavior to expect from other more complex mixtures. It is important to recognize that each real mixture has its own specific thermodynamic characteristics and should therefore be analyzed in detail in a later step of the separation synthesis.

The concept of elementary cells is even more important when using the classification of Matsuyama and Nishimura with its 113 classes (less surveyable).

### 4.5.1 The album

One goal underlying the classification of ternary mixtures is to have a complete album of possible VLE diagram structures with their corresponding scheme of separation by distillation. But this is not established knowledge. Prediction of feasible distillation product compositions for even some of the simplest diagram structures is still under development. Furthermore, methods or separation schemes to separate all classes of (ternary) azeotropic mixtures are not established. One reason is that there are many possible structures with deformation of the simple phase transformation paths due to regions with different volatility order within the composition space, making this an almost impossible task. Instead, we propose to consider selected VLE diagrams and specific mixtures of these diagrams in detail:

1. Zeotropic mixture, ideal and nonideal with univolatility line(s)  
(Serafimov's class 0.0-1: cell I);
2. Mixture with one separatrix (one binary azeotrope)  
(Serafimov's class 1.0-2: combination of two cell I's);
3. Mixture without separatrix, but with one binary azeotrope  
(Serafimov's class 1.0-1b: cell III);

4. Mixture without separatrix, but with two binary azeotropes nodes  
(Serafimov's class 2.0-1: cell IV).

An illustration of a ternary mixture with one binary saddle azeotrope (Class 1.0-2) consisting of two elementary cell I's is given in Figure 4.4. The left cell has "C-shaped" residue curves,

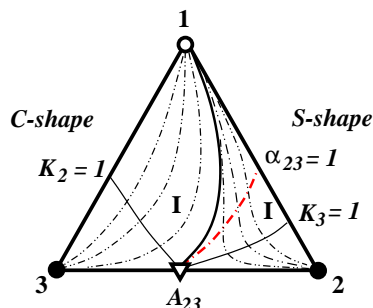


Figure 4.4: Ternary azeotropic mixture with one binary saddle azeotrope (Class 1.0-2 consisting of two Cell I's). Residue curves; undistribution (solid) and univolatility (dash-dotted) lines are given.

and the right cell has "S-shaped" residue curves (inflection) caused by the univolatility line  $\alpha_{23}$ . Although both cells are of type I, this difference in shape may have a large effect on the actual separation process. For details on the internal structure ("shape") of ternary VLE diagrams, the reader is referred to Chapter 3 and Reshetov *et al.* (1999).

## 4.5.2 Multiple steady states

As an example of the use of elementary cells we may consider the possibility for multiple steady states in (homogeneous) azeotropic distillation. Such multiplicities may lead to problems in column operation and control, as well as problems in column design and simulation. When two or more multiple steady states exists for the same inputs it is possible that, for some disturbance, the column profile jumps from the desirable (in terms of product specifications) to an undesirable steady state. However, such catastrophic jumps may be avoided by proper control of the column, and the separation schemes for such mixtures may well be feasible and economical. The possibility of multiple steady states at infinite efficiency of the distillation (infinite reflux, infinite theoretical equilibrium trays, and  $D/F$  from 0 to 1) was first noted by Balashov *et al.* (1970). They considered a mixture of Serafimov's class 1.0-1b (primary diagram of elementary cell III with U-shaped residue curves) with a binary maximum-boiling azeotrope (ZS-type 7b), and found that for these mixtures it is feasible to have multiple products for the same value of the parameter  $D/F$ . Later, Petlyuk and Avet'yan (1971) analyzed this issue in more detail (including bifurcation analysis). This analysis is also included in the textbook by Petlyuk and Serafimov (1983), where Petlyuk writes "the existence of more than one saddle along a distillation line for sharp

(infinite reflux, infinite column) separation going from an unstable node to a stable node leads to multiplicity of the separation products for the same feed composition and the same value of parameter  $D/F$ ". The geometrical considerations given by Petlyuk and coworkers are also found in Serafimov *et al.* (1971). This is a sufficient, but not a necessary condition for multiplicity of the mixture. Bekiaris *et al.* (1993) give a similar condition, roughly that the *existence of two or more neighboring saddles* may lead to output multiplicity. Bekiaris *et al.* (1993) also identifies other structural characteristics that may induce multiple steady states, such as highly curved distillation boundaries ("pseudosaddles"), as for the mixture of acetone-chloroform-methanol.

The elementary cells that may lead to output multiplicity are III, III', IV and IV'. From this we can predict the *possibility* of multiple steady states (sufficient condition) for any given mixture that is caused by these structural characteristics. From Figure 4.2 we see that 14 of the 26 diagrams include these elementary cells (1.0-1b, 1.1-1a, 1.1-1b, 2.0-1, 2.0-2a, 2.0-2c, 2.1-1, 2.1-2a, 2.1-2b, 3.0-1b, 3.1-1a, 3.1-1b, 3.1-1c, 3.1-3a). From the statistics by Reshetov we find that about 7 % of the reported VLE diagram structures include these cells. Serafimov's class 2.1-2b, which includes cell IV, is relatively common (4 %), and this class may give multiplicities for feeds in the region with U-shaped residue curves.

The significance of multiplicities for column operation have been studied by Morari and coworkers (Laroche *et al.*, 1992a; Laroche *et al.*, 1992b; Bekiaris *et al.*, 1993; Bekiaris and Morari, 1996; Güttinger and Morari, 1996; Güttinger and Morari, 1997). Mixtures with one binary minimum-boiling azeotrope of Serafimov's class 1.0-1b (primary diagram of cell III with U-shaped residue curves) has been the focus, in particular the mixture of acetone - heptane - benzene. However, from the occurrence statistics we see that Serafimov's class 1.0-1b is not very common.

Bekiaris and Morari (1996) found multiple steady states for the mixture ethanol - ethyl propanoate - toluene (Serafimov's class 2.0-2a, ZS-type 18, which includes cells I and III) for a specific feed region. The specific feed region corresponds exactly to elementary cell III.

## 4.6 Pseudo-component subsystem

An idea related to the concept of elementary cells is the concept of pseudo-components. This approach is known to many engineers working with azeotropic distillation. Vogelpohl (1999) proposes to analyze real azeotropic mixtures as subsystems approximated by zeotropic mixtures where each azeotrope is represented by a pseudo-component. A residue curve region with  $k$  singular points (pure component and azeotropes) is thus represented as a  $k$ -component zeotropic mixture by assuming constant relative volatilities between the real components and the pseudo-components (azeotropes). *Ideal distillation lines* are calculated for each subsystem. However, this strong simplification has major pitfalls. The ideal distillation lines (or residue curves) diverge from the real (exact) ones as azeotropic mixtures necessarily have univolatility lines that deform the simple phase transformation trajectories and cause S-,  $\Omega$ -, and even more complex shapes (internal structures) of the distillation lines (residue curves). For example, a ternary azeotropic mixture of Serafimov's class 1.0-2 (Figure 4.4) may be considered to be a quaternary system with

the binary saddle azeotrope as an intermediate boiling pseudo-component. From this, for both of the cells I in the diagram, C-shaped ideal distillation lines are calculated. However, this is not true for the real mixture. Furthermore, the approach results in straight line distillation boundaries which in general are curved (Schreinemakers, 1902).

We argue that when only the *qualitative* shape of the curves are needed, one can sketch the residue curve map (by hand) rather than calculate the exact, but incorrect, ideal subsystems map based on the constant relative volatility assumption. For example, we know that for mixtures of Serafimov's class 1.0-2 (Figure 4.4) with one binary azeotrope saddle and a separatrix that splits the composition space into two cells I, one of these cells must have a univolatility line extending from the azeotrope and to one of the binary edges resulting in an inflection point of the residue curves (S-shape).

Vogelpohl (1999) emphasizes that his main point is not to approximate the distillation lines of real mixtures by the distillation lines of ideal systems, but to show that the distillation behavior of real (zeotropic and azeotropic) mixtures is not fundamentally different from the distillation behavior of ideal systems, and that, therefore, the large body of knowledge developed from the theory of multicomponent distillation may be applied to better understand the distillation of real multicomponent mixtures. This is in line with the idea behind elementary cells presented in this paper.

## 4.7 Conclusion

The concept of elementary topological cells of ternary VLE diagrams is a key to a simple and surveyable azeotropic distillation analysis. Any real ternary mixture can be qualitatively represented by a combination of only four elementary cells. This greatly reduces the number of VLE diagram structures that need to be analyzed in order to reveal the qualitative characteristics of any ternary azeotropic mixture.

## Acknowledgments

Dr. S.A. Reshetov at the Karpov Institute of Physical Chemistry in Moscow is gratefully acknowledged for providing the statistics on the occurrence of Serafimov's classes for reported ternary azeotropic mixtures.



Table 4.2: Relationship between different classifications of ternary VLE diagrams

	Gurikov (1958)	Serafimov (1970)	ZS-type <sup>a</sup>	Matsuyama & Nishimura (1977)
Zeotropic	1	0.0-1	1	000
One binary azeotrope	4a	1.0-1a	3a 7a	100 030
	4b	1.0-1b	3b 7b	001 003
	3	1.0-2	4 8	020 400
One binary and one ternary azeotrope	2a	1.1-1a	2a 6a	200-m 040-M
	2b	1.1-1b	2b 6b	002-m 004-M
	5	1.1-2	5 9	010-S 300-S
Two binary azeotropes	9	2.0-1	15	031, 103, 130
	8a	2.0-2a	17 18	023, 320 401, 410
	8c	2.0-2b	11a 21a	102, 120, 021 043, 430, 403
	8b	2.0-2c	11b 21b	201, 210, 012 034, 304, 340
Two binary and one ternary azeotrope	7	2.1-1	13 14	032-m, 230-m, 203-m 041-M, 140-M, 104-M
	-	2.1-2a	16a 16b	420-m, 402-m 024-m, 420-M
	6	2.1-2b	10 20	022-m, 220-m, 202-m 044-M, 440-M, 404-M
	10a	2.1-3a	19	013-S, 310-S, 301-S
	10b	2.1-3b	12 22	011-S, 110-S, 101-S 033-S, 330-S, 303-S
Three binary azeotropes	14a	3.0-1a	29 33	411 323
	14b	3.0-1b	28 34	123, 321, 132, 213, 312, 231 413, 314, 431, 341, 134, 143
	13	3.0-2	24 37	212, 122, 221 434, 344, 443
Three binary and one ternary azeotrope	-	3.1-1a	27b 32b	421-m, 412-m 423-M, 324-M
	12	3.1-1b	26 31	232-m, 223-m, 322-m 414-M, 441-M, 144-M
	-	3.1-1c	27a 32a	142-M, 241-M, 124-M, 214-M, 421-M, 412-M 423-m, 324-m, 432-m, 342-m, 234-m, 243-m
	11	3.1-2	23 36	222-m 444-M
	15	3.1-3a	25a 38a	121-S, 112-S, 211-S 343-S, 334-S, 433-S
	-	3.1-3b	25b 38b	121-S, 112-S 343-S, 334-S, 433-S
	16	3.1-4	30 35	131-S, 113-S, 311-S 133-S, 313-S, 331-S

<sup>a</sup> ZS-type refers to the refined classification of the 49 antipodal structures by Zharov and Serafimov (1975), p. 96-98



## **Part II**

# **Studies on Batch Distillation Operation**



## Chapter 5

# Holdup Effect in Residue Curve Map Prediction of Batch Distillation Products

*Originally presented at Process Design and Control Center Meeting  
at the University of Massachusetts, U.S.A., June 1996*

In this study we examine the effect of tray holdup on the composition dynamics in batch distillation of ternary azeotropic mixtures. In general, for separations with small amounts of one of the volatile components, there is an upper limit on the amount of holdup in the column section in order to get pure products. For azeotropic mixtures this can happen even for feeds with large amounts of each component, for example, when one component is present in a small amount relative to a distillation boundary. Prediction of the sequence of product cuts using residue curve map analysis must be used with care for such separations.

### 5.1 Introduction

In batch distillation of nonideal and azeotropic mixtures, the order of product fractions may vary depending on the feed composition. Residue curve maps may be used to predict distillate product sequences in batch distillation. The approach is well described in the classical work by Reinders and DeMinjer (1940; 1947c), Ewell and Welch (1945) and Bushmakina and Kish (1957b). The basic principle for the product prediction is that when an invariant component (i.e. pure component or azeotrope) is distilled from a mixture in a conventional batch distillation column, then the

composition of the remaining liquid (reboiler residue) moves rectilinearly in the opposite direction from the invariant components. From this, it is possible to predict the sequence of constant boiling vapor distillates which appears overhead, directly from the residue curve map without solving any equation.

The use of residue curve maps for synthesis and design of batch distillation has been further explored in a number of more recent papers (Van Dongen and Doherty, 1985*a*; Bernot *et al.*, 1990; Bernot *et al.*, 1991; Ahmad and Barton, 1994; Ahmad and Barton, 1996; Ahmad, 1997; Ahmad *et al.*, 1998; Safrit, 1996; Safrit and Westerberg, 1997*a*; Safrit and Westerberg, 1997*c*). We refer to the literature mentioned for a detailed description of the application of residue curve map analysis to batch distillation.

In design studies of batch distillation, holdup on the trays is usually neglected, resulting in the simple material balance:

$$\frac{d(H_B x_B)}{dt} = -D y_D \quad (5.1)$$

where  $x_B$  is the liquid composition in the reboiler and  $y_D$  is the vapor composition in the distillate. Here

$$\frac{dH_B}{dt} = -D \quad (5.2)$$

and by introducing the dimensionless time  $\xi$ , describing the relative loss of the liquid in the reboiler, we get:

$$\frac{dx_B}{d\xi} = x_B - y_D \quad (5.3)$$

Equation (5.3) tells us that the distillate and reboiler compositions lie on a straight line that is tangent to the change of the reboiler composition (i.e., the batch distillation reboiler composition trajectory). The equation differs from the (open evaporation) residue curve equation in that  $y_D$  is not in equilibrium with  $x_B$  ( $y_D$  will be in equilibrium with the liquid in the condenser with composition  $x_D$ ).

In conventional batch distillation with a high reflux and a large number of equilibrium trays, it is possible to divide the composition diagram into *batch distillation regions* defined as the set of compositions that leads to the same set of product cuts (Ewell and Welch, 1945). For any initial feed composition taken in a given region, leads to the same set of distillate cuts. The batch distillation regions are similar to the residue curve regions, but are further subdivided by straight “material balance” line boundaries (dashed lines in Figure 5.3). Ewell and Welch (1945) differentiate between these straight line boundaries and the curved boundaries (separatrices) by the fact that the straight lines *cannot* be crossed during batch distillation. The batch distillation composition trajectories may “cross” a residue curve boundary as this is not a boundary for high reflux batch distillation.

There are two limiting conditions:

$R = 0$ : batch distillation reboiler composition trajectory coincides with the residue curve.

$R = \infty$ : batch distillation reboiler composition trajectory coincides with the *distillation line*.

The distillation line boundary is located from the concave side of the curved residue curve boundary in Figure 5.3 (see Chapter 3, Section 3.5.3).

Bernot (1990) used residue curve analysis to predict the product distribution in batch distillation using a simple dynamic model of the batch column with no holdup on the trays or in the condenser, i.e. based on constant molar overflow (CMO) and quasi steady state (QSS) assumptions. However, there is always some holdup in a real column, and models of batch distillation which ignore column holdup, such as Equation (5.3), may in some cases lead to significant errors (Robinson, 1970). The overall material balance including column holdup may be written:

$$\frac{d}{dt}(H_B x_B) + \sum_j \frac{d}{dt}(H_j x_j) = -D y_D \quad (5.4)$$

The amount of column holdup  $\sum H_j$  varies with the column design (diameter, trays, packing material etc.). A typical value of the total liquid holdup is about 5-10 % of the *total column volume* for staged columns (Skogestad, 1992) and 2-4 % for packed columns. In our simulations the amount of holdup was varied to see the effect on the distillate composition path (product sequence). We considered the following column holdups as a percentage of the *initial feed charge*: 2.1 % (low), 4.1 % (normal) and 10.5 % (high). According to King (1980) one can employ the quasi steady state (QSS) Equation (5.3) for batch distillation when the column holdup is less than 5 % of the charge to the reboiler (still).

Referring to the early work of Pigford and Rose (during the 1940-50s), Perry and Chilton (1973) summarize the following two compensating effects of column holdup in batch distillation:

1. During startup, the reboiler composition is depleted in the more volatile component while the column holdup is established. Thus, the separation becomes more difficult and the distillate composition is less "pure" than would be expected from neglecting column holdup.
2. Column holdup presents an inertia effect, which slows the composition dynamics and usually improves the separation.

Later, several authors have studied the column (liquid) holdup in batch distillation (e.g. Sørensen (1994) and Mujtaba and Macchietto (1998)). The main conclusion is that the column holdup has a large impact on the separation efficiency for difficult separations, and for separations with a small amount of the light component in the initial feed (for regular batch distillation).

Our objective is to study the effect of column holdup in residue curve map prediction of batch distillation products and off-cuts. We will show that the distillate product sequence may differ from that found from an analysis neglecting holdup.

## 5.2 Model and data

A conventional batch distillation column is shown in Figure 5.1.

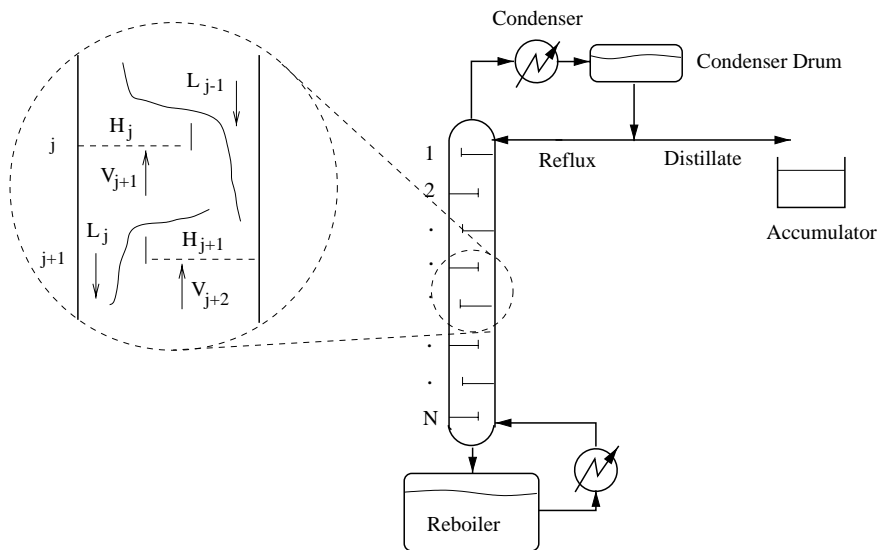


Figure 5.1: *Holdup on the trays in a conventional batch distillation column.*

The assumptions and mathematical model equations are the same as used for the simulations presented in Chapter 7 (Appendix 7A) assuming constant molar stage holdup:

$$\frac{H_j}{dt} = 0 \quad (5.5)$$

This assumption is partly justified by the fact that the dominant composition dynamics are much slower than the flow dynamics and nearly unaffected by the flow dynamics (Skogestad, 1992), and it may therefore be used to get good estimates of the dominant response.

We introduce a dimensionless “warped time” (Van Dongen and Doherty, 1985a):

$$d\xi = \frac{D}{H_B} dt \quad (5.6)$$

where  $D$  represents the distillate flowrate (denoted  $L_D$  in Appendix 7A) and  $H_B$  is the instantaneous liquid holdup in the reboiler.



The thermodynamical data for the azeotropic mixture acetone - methanol - chloroform are given in Table 5.3 (Appendix 5A) and the corresponding residue curve map is shown in Figure 5.2.

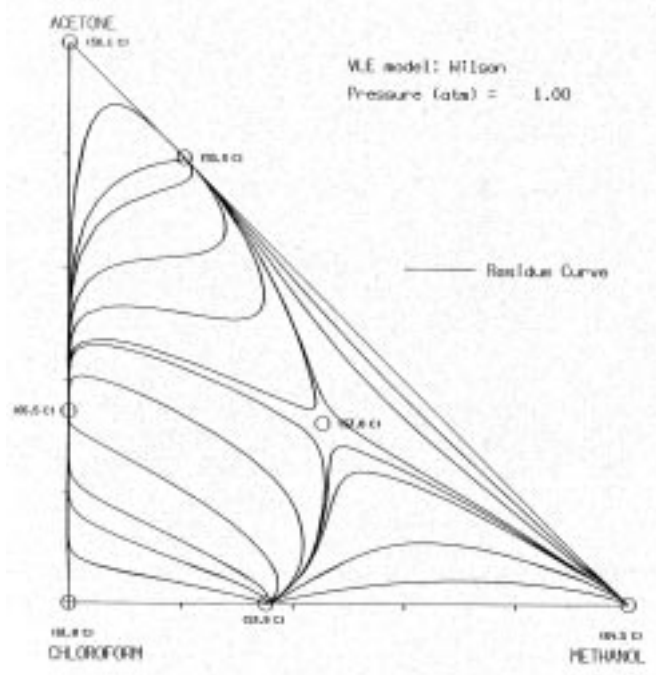


Figure 5.2: Residue curve map for the mixture acetone (1) - methanol (2) - chloroform (3) at atmospheric pressure (Serafimov's class 3.1-4). The pure components and azeotropes are indicated by open circles (from Mayflower [presently: HYSYS Conceptual Design Application<sup>TM</sup>]).

This is a mixture of Serafimov's class 3.1-4 where the composition space consists of four residue curve regions. This mixture system was considered by Ewell and Welch (1945) who stated that it "illustrates the effect of binary maximum and minimum azeotropes on batch distillation".

The residue curve map in Figure 5.2 is split into six *batch distillation regions* (Bernot *et al.*, 1990) as illustrated in Figure 5.3.

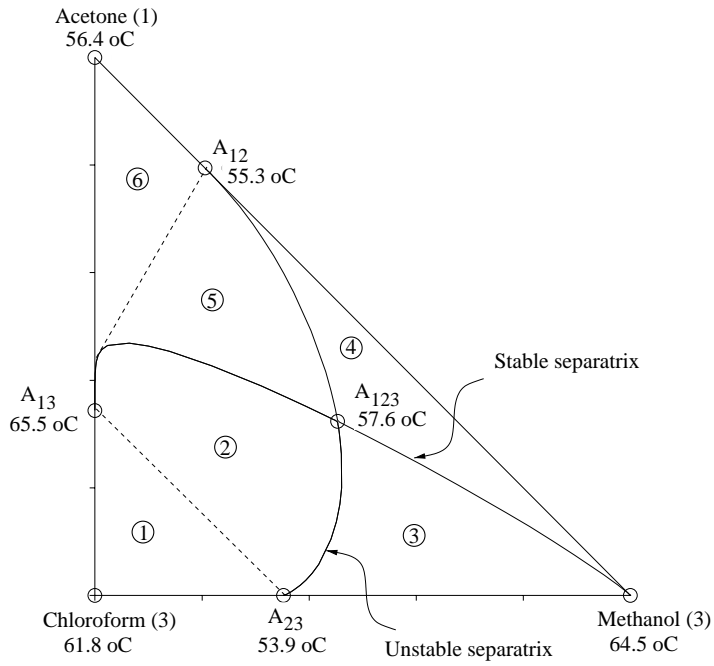


Figure 5.3: Predicted batch distillation regions for the residue curve map in Figure 5.2.

## 5.3 Results and discussion

In batch distillation of an azeotropic mixture several kinds of cuts can be obtained. We define the “azeotropic cuts” as those containing an azeotrope and the “pure component cuts” as those producing a (nearly) pure component.

We here focus on feeds located in the batch distillation region 5 in Figure 5.3 ( $x_{F0} = [0.3, 0.4, 0.3]$ ), which from a residue curve map analysis gives a counterintuitive distillate sequence due to the highly curved boundary of this region referred to as “distillation anomaly” (Van Dongen and Doherty, 1985*b*; Bernot *et al.*, 1990):

1. Azeotropic cut  $A_{12}$  ( $T_{bp} = 53.3^\circ C$ )
2. Azeotropic cut  $A_{123}$  ( $T_{bp} = 57.6^\circ C$ )
3. Azeotropic cut  $A_{12}$  ( $T_{bp} = 53.3^\circ C$ )
4. Pure component 1 (acetone) cut ( $T_{bp} = 56.4^\circ C$ )
5. Azeotropic cut  $A_{13}$  ( $T_{bp} = 65.5^\circ C$ )

The “anomaly” is seen from the fact that the distillate temperature decreases as we go from cut  $A_{123}$  ( $57.6^\circ C$ ) and back to cut  $A_{12}$  ( $53.3^\circ C$ ). It is caused by the highly curved residue curve boundary between batch distillation regions 2 and 5 (see Figure 5.3).

Note that this set of “product cuts” is mostly of theoretical interest as it is unlikely that one would want to obtain four “unpure” azeotropic products in real operation. Nevertheless, our question is whether introducing holdup on the trays will alter this sequence of cuts predicted by the residue curve map analysis. We consider three cases of total liquid holdup in the column section as a percentage of the initial feed charge to the reboiler: 2.1 % (low), 4.1 % (normal) and 10.5 % (high).

The column specifications used in the simulations for the limiting conditions of high reflux and large number of trays are given in Table 5.1.

Table 5.1: Column data for the limiting conditions of high reflux and large number of trays.

Total no. of trays	$N = 40$ (excl. reboiler)
Reflux ratio	$R = L/D = 200$
Initial reboiler holdup	$H_{B0} = 10.000$ kmol
Condenser holdup	$H_D$ specified in Table 5.2
Tray holdup	$H_j$ specified in Table 5.2
Boilup, vapor flow (constant)	$V_B = 5.0$ kmol/h

The resulting distillate and reboiler composition trajectories are shown in Figures 5.4 - 5.6. The corresponding product sequences are summarized in Table 5.2.

Table 5.2: Results of batch distillation with column holdup given as a percentage of the initial feed charge to the reboiler.

	Holdup <sup>a</sup>	Sequence of product cuts
Case 1: 2.1 % (low)	$H_j = H_D = 0.005$ kmol	1. Azeotropic cut $A_{12}$ 2. Azeotropic cut $A_{123}$ 3. Azeotropic cut $A_{12}$ 4. "Pure" acetone cut 5. Azeotropic cut $A_{13}$
Case 2: 4.1 % (normal)	$H_j = H_D = 0.01$ kmol	1. Azeotropic cut $A_{12}$ 2. Azeotropic cut $A_{123}$ 3. Azeotropic cut $A_{12}$ 4. Azeotropic cut $A_{13}$
Case 3: 10.5 % (high)	$H_j = H_D = 0.025$ kmol	1. Azeotropic cut $A_{12}$ 2. Azeotropic cut $A_{123}$ 3. Azeotropic cut $A_{12}$ 4. Azeotropic cut $A_{13}$

<sup>a</sup>Holdup on each stage and in the condenser

We see that the expected sequence of distillate products is obtained when the holdup is low, but that the pure acetone product cut disappears when the holdup is medium and large. We also note that the composition trajectories "cross" the residue curve boundary (stable separatrix), but not the distillation line boundary (not shown).

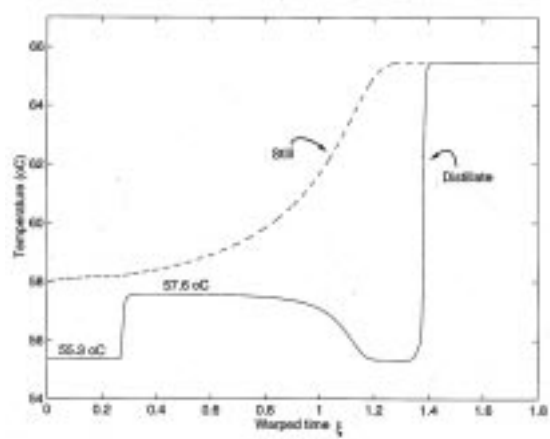
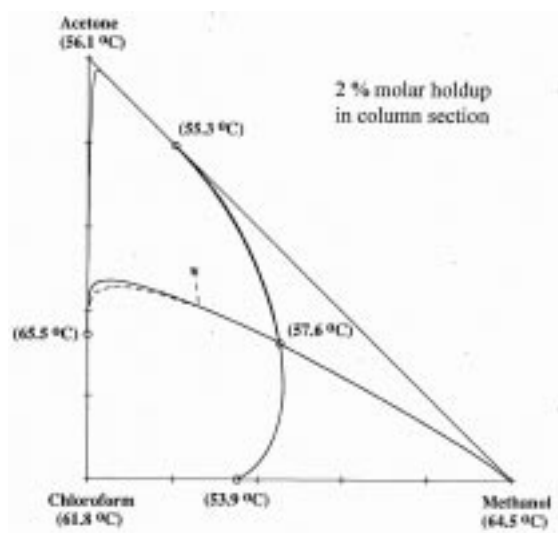


Figure 5.4: Distillate composition trajectory (solid curve) and reboiler composition trajectory (dashed line) with corresponding temperature change with time for 2.1 % holdup (Case 1).

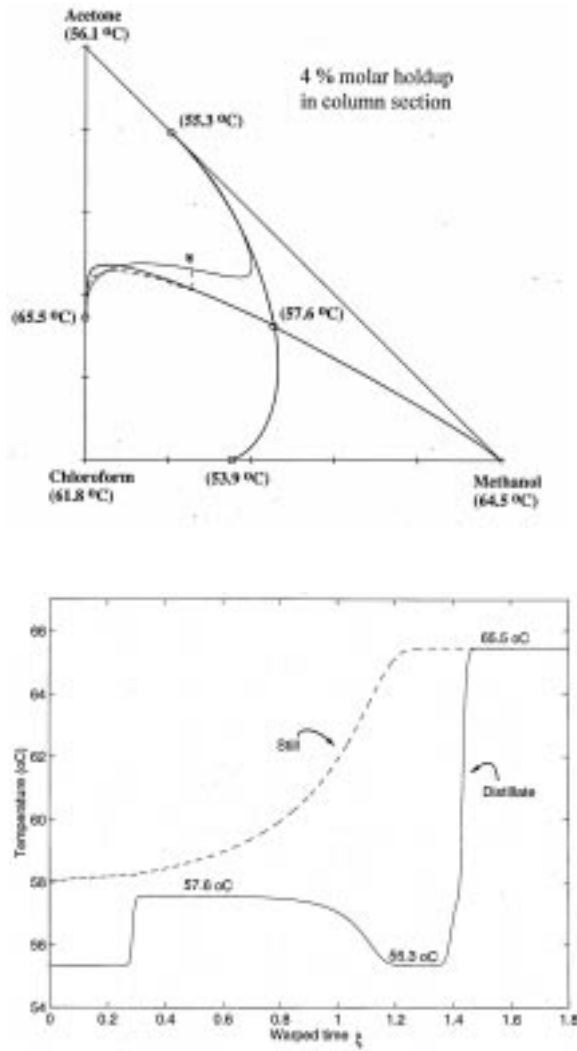


Figure 5.5: Distillate composition trajectory (solid curve) and reboiler composition trajectory (dashed line) with corresponding temperature change with time for 4.1 % holdup (Case 2).

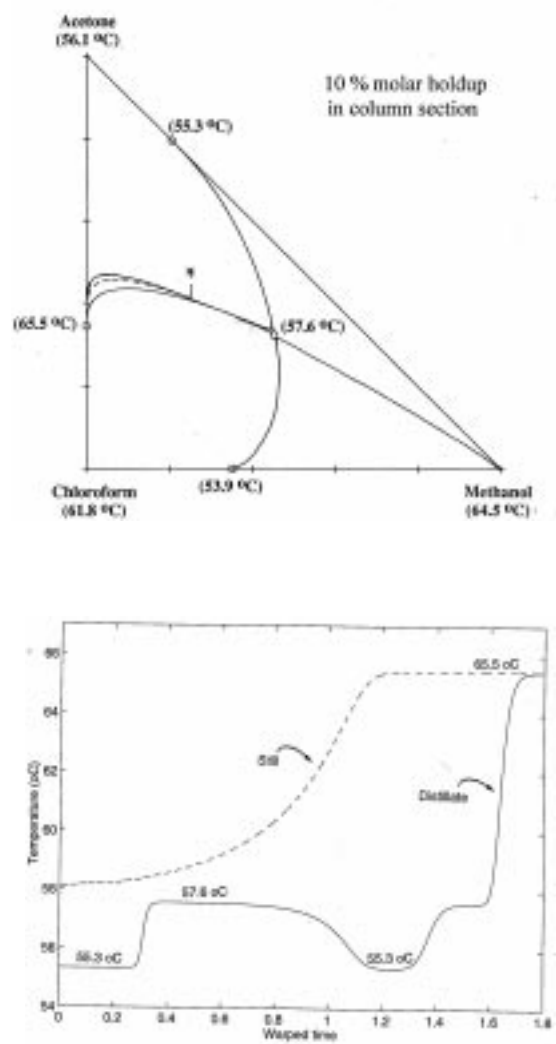


Figure 5.6: Distillate composition trajectory (solid curve) and reboiler composition trajectory (dashed line) with corresponding temperature change with time for 10.5 % holdup (Case 3).

## 5.4 Conclusion

We conclude that we can use analysis based on residue curve maps for the prediction of the sequence of products and off-cuts in batch distillation of azeotropic mixtures, but in special cases column holdup can have significant impact on the product purities and cuts and this simple approach must be used with care.



## Appendix 5A

Table 5.3: *Thermodynamic data for the mixture acetone-water-chloroform (from Mayflower [presently: HYSYS Conceptual Design Application<sup>TM</sup>]).*

Parameters for the Antoine Equation				
Component	A	B	C	$V_i \left[\frac{m^3}{mol}\right]$
1) Methanol	23.49989	3643.3136	-33.434	40.73
2) Acetone	21.3099	2801.53	-42.875	74.04
3) Chloroform	20.865	2696.900	-46.160	80.67
Binary Interaction Parameters for the Wilson Equation				
	$A_{11} = 0$	$A_{21} = -161.8813$	$A_{31} = -351.1964$	
	$A_{12} = 583.1054$	$A_{22} = 0$	$A_{32} = -484.3856$	
	$A_{13} = 1760.6741$	$A_{23} = 28.8819$	$A_{33} = 0$	



## Chapter 6

# Batch Distillation Columns and Operating Modes: Comparison

In addition to a brief introduction and overview of batch distillation columns and operating modes, this chapter includes a comparison of the time (energy) consumption of two equilibrium batch distillation operations; that is, the cyclic column and the closed middle vessel column for separating ternary ideal mixtures.

### 6.1 Introduction

Although batch distillation generally is less energy efficient than continuous distillation, it has received increased attention during the last few years along with the expansion in the pharmaceutical and fine- and specialty chemical industries. One reason is that batch distillation offers the possibility of separating multicomponent mixtures into high purity products using a single column. Second, batch columns are flexible and robust to variations in feed composition and specifications. Furthermore, batch distillation can be used for liquids with contaminants (such as solids and tars or resins), and the batch equipment can be cleaned or sterilized between the batch operations (Rousseau, 1987).

Nevertheless, the choice between continuous and batch distillation operation depends primarily on the amount of feed to be processed. Other aspects include the complexity of the mixture (multicomponent, low relative volatilities or nonideal, feed composition), and whether flexible multi-purpose facility is required. Usually, continuous distillation is chosen for large throughputs (above 5000 tons per year) and batch distillation is chosen for low throughputs (less than 500 tons per year) and in batch production and multi-purpose plants. 5000 tons per year corresponds to a daily processes batch of 20 tons (in 250 days) or 100 tons per week. Batch stills up to 40

000 liters capacity are quite common according to Drew (Schweitzer, 1997). For batch times exceeding about 12 hours, time losses due to startup and shutdown are not severe.

Batch distillation is generally more expensive than its continuous counterparts in terms of costs per unit of product (Rousseau, 1987). However, for multicomponent mixtures with a large number of components it may be less expensive to use batch distillation since only one column is required for any number of products. A single batch column can separate a  $n$ -component mixture whereas  $(n-1)$  continuous distillation columns would be required.

Batch distillation is also preferred when there are special operational conditions that makes continuous operation difficult, for example, processes that requires very long residence times, materials that are difficult to pump and processes where the equipment needs frequent cleaning.

## 6.2 Batch distillation column configurations

There are many possible configurations for batch distillation columns. The simplest example is evaporation (without reflux), often called Rayleigh distillation. Of more practical importance is batch distillation *with reflux* as described in the following.

### 6.2.1 Regular and inverted columns

In the regular batch column (also called the *batch rectifier*) illustrated in Figure 6.1a, the feed vessel is located at the bottom of a rectifying column and product fractions are sequentially removed overhead as distillate. In the inverted column (also called the *batch stripper*) illustrated in Figure 6.1b, the feed vessel is located at the top of a stripping column and the product fractions are sequentially removed in the bottom. For more detail about batch distillation in general we refer to, for example, Diwekar (1995) and Perry (1997).

### 6.2.2 Middle vessel and multivessel columns

The combination of the regular and inverted batch columns connected by an intermediate vessel (holdup tank), later named the *middle vessel column*, was proposed by Robinson and Gilliland (1950) and is illustrated in Figure 6.1c. There are two principally different applications for the middle vessel batch distillation column: (1) binary mixtures separation, and (2) ternary or multicomponent mixtures separation. In both cases, the mixture is usually charged to the middle vessel initially, but it may also be distributed along the column or charged to the reboiler. For the first application, the binary separation is performed simultaneously in the rectifying and stripping sections. The light component is removed as a distillate product and the other component as a bottoms product. The amount in the middle vessel decreases steadily during the distillation run. This closely resembles continuous distillation. In the second application, which is the focus in this thesis, the intermediate component(s) may be accumulated in the middle vessel whereas light

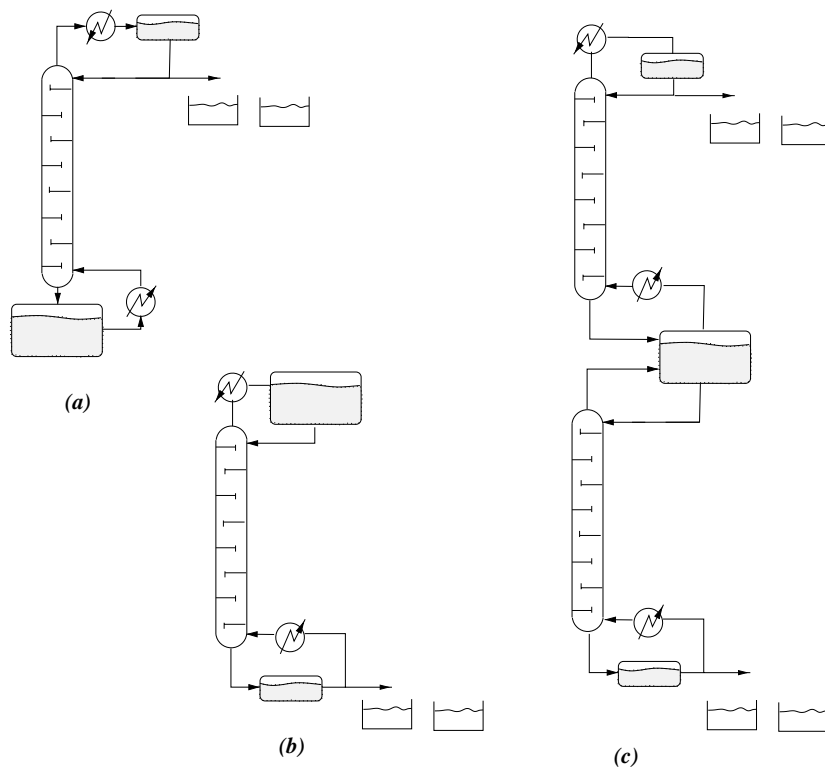


Figure 6.1: Batch distillation columns: (a) regular batch column; (b) inverted batch column; (c) middle vessel column.

and heavy products are collected at the column ends. The middle vessel batch distillation column can also be operated as a batch rectifier or as a batch stripper depending on the operating parameters. The generalized configuration with several intermediate vessels and column sections is the *multivessel batch column* proposed by (Hasebe *et al.*, 1995).

The idea of using the middle vessel batch distillation column for separating ternary mixtures is not new. In the textbook by Robinson and Gilliland (1950), this combined operation of a batch rectifier and a batch stripper is mentioned for accumulating an intermediate component in an intermediate vessel while removing light and heavy impurities. Bortolini and Guarise (1970) described the middle vessel column for separation of binary ideal mixtures where the composition in the middle vessel was approximately constant removing products from both the top and the bottom (i.e., open operation). The operation stops when the middle vessel is empty. This mode of operation is found to be optimal in some cases (Davidyan *et al.*, 1994; Meski and Morari, 1995).

In 1976, Devyatikh and Churbanov [as referenced by Davidyan *et al.* (1994)] described separation of *ternary mixtures* by the middle vessel batch distillation column.

In a series of papers, Davidyan, Kiva and Platonov (1991*b*; 1991*a*; 1992*b*; 1992*a*; 1993) presented the use of batch distillation columns with a middle vessel for separating binary and ternary mixtures. Based on this work, Davidyan *et al.* (1994) presented an analytical analysis of the dynamic behavior of the middle vessel batch distillation column for separating multicomponent mixtures. The authors point out several advantages and new opportunities for the middle vessel configuration as compared to conventional batch distillation column designs (Davidyan *et al.*, 1994):

- *A binary mixture can be separated into pure components under finite reboil and reflux ratio and, in some cases, faster than using conventional types of batch distillation columns.*
- *For ternary separation one can always choose parameters, like reflux and reboil ratios, such that the composition in the middle vessel tends to either one of the three components [e.g. the intermediate-boiling component for ideal mixtures].*
- *A multicomponent mixture can be separated into heavy, intermediate and light fractions simultaneously, so one can remove light and heavy impurities from the mixture.*

Meski and Morari (1995) analyzed the behavior of the middle vessel configuration for binary and ternary mixtures at total reflux and minimum reflux conditions. They confirm the previous results by Hasebe *et al.* (1992) that the middle vessel batch distillation column always perform better than the conventional batch distillation design. They also conclude that it is optimal to operate the column under constant reflux- and reboil ratios in the case of binary separation, keeping the composition in the middle vessel constant at the initial feed composition with gradual decreasing holdup of the middle vessel. Barolo and Guarise *et al.* (1996*a*; 1996*b*; 1996) address issues on design and operation of the middle vessel batch distillation column for separating ternary mixtures, partly based on experience from operating a continuous distillation pilot plant in a batch mode.

In the multivessel column (also called multieffect column by Hasebe *et al.* (1995)) several batch distillation columns are coupled by vapor and liquid streams with vessels (holdup tanks) between, but with only one reboiler and one condenser. One objective is to minimize the energy consumption, and this is analogous to integrated (multieffect) continuous columns like the Petlyuk column. The Petlyuk column configuration is a fully thermally coupled distillation column arrangement where two or more columns are linked together through vapor and liquid streams without reboilers or condensers between the columns or simply one column with a dividing wall inside one column shell. Such complex column arrangements are shown to offer large potential savings in energy compared with sequences of simple columns for multicomponent continuous distillation separation systems.

Several authors have presented comparative studies of conventional batch distillation columns and the middle vessel batch configuration. Hasebe *et al.* (1992) compared the performance of

the middle vessel batch distillation column with conventional batch distillation for separating ideal ternary mixtures. The middle vessel batch distillation column was shown to have the best separation performance. The idea of using a middle vessel was later extended to a multivessel batch column configuration with total reflux operation for separating more than three components (Hasebe *et al.*, 1995). They claim that the multivessel batch distillation column is potentially more energy efficient than the corresponding sequence of continuous distillation columns for mixtures with more than five components. However, their comparison was rather unfair since there was no energy integration for the continuous columns. Hasebe *et al.* (1997) gave optimization results on optimal vessel holdup policy in the closed multivessel column for ideal mixtures in terms of minimum batch time. They proposed to charge the feed to the reboiler and gradually increase the holdups of the other vessels up to pre-calculated (optimized) values and then run in total reflux mode until the desired product purities are reached in each vessel.

Skogestad *et al.* (1997) proposed a simple feedback control strategy for operation of the closed multivessel batch distillation column where the reflux flow out of each vessel is manipulated to control the temperature at some location in the column section below. This indirectly adjust the vessel holdups and there is no need for level control. The feasibility of this strategy was demonstrated by simulations for an ideal quaternary mixture separated in a column with four vessels, and later experimental verification was given for the zeotropic mixture of methanol, ethanol, n-propanol and n-butanol (Wittgens and Skogestad, 1997). Up to 50 % reduction in energy consumption was found separating a quaternary mixture using the closed multivessel column compared to conventional batch distillation Wittgens and Skogestad (1998). Furlonge *et al.* (1999) studied optimal (open) operation of the multivessel batch distillation column for quaternary ideal mixtures and also found up to 50 % time savings compared with conventional batch distillation.

## 6.3 Operating policies

Determining the best way of running a batch distillation column is important in order to improve the efficiency of energy consumption and the product quality, to reduce production time and to reduce waste cuts. Sørensen (1997) found that time savings of up to 70 % can be made by using alternative operating procedures.

Batch distillation is usually operated with production cycles consisting of charging, heat-up, equilibration, product draw-off, slop cut (off-cut removal), product draw-off, cool-down, dumping and cleanup. The size of the off-cuts (if any) depends on the sharpness of separation between the products. The sharpness of separation depends on holdup, relative volatility, reflux and number of plates or amount of packing. Intermediate cuts are often recycled.

In this study we consider unconventional batch distillation operations and columns such as the middle vessel column and extractive batch distillation. Thus, we need to define some basics for the various ways of operating such columns.

### 6.3.1 Open operation (conventional)

There are various modes of operation of the different batch distillation columns. The conventional operating policies for regular batch distillation columns are:

1. Constant reflux ratio (variable distillate composition)
2. Constant distillate composition (variable reflux ratio)
3. Optimal reflux ratio (usually variable reflux ratio)

The constant distillate composition policy (2) is usually implemented using feedback control with either reflux flow or distillate flow as the manipulated variable. The reflux ratio policies (1 and 3) are open loop operations, that is, predefined values are used without feed back from the process.

#### *Constant reflux with varying distillate composition*

With the constant reflux ratio policy, the reflux ratio is maintained constant throughout the batch. It is the simplest policy to implement, but less efficient than the other variable reflux ratio policies.

If a batch distillation is to be run at constant reflux, then it follows that the distillate product composition must change with time.

#### *Constant distillate composition with variable reflux*

With the constant distillate composition policy, the product is usually withdrawn at the maximum possible rate consistent with there being sufficient reflux to maintain the product composition at the desired value. As the batch progresses, the composition of the product tends to deteriorate and the reflux ratio is increased gradually by reducing the product withdrawal rate, until the desired composition can no longer be maintained. At this point the product is diverted to another receiver and an intermediate cut (off-cut) is withdrawn usually at a constant high reflux ratio.

This procedure is repeated until all the product fractions have been removed. If the next batch contains the same mixture components, the off-cuts are usually returned to the still together with fresh charge.

### 6.3.2 Closed operation

The total reflux operation (no product withdrawal) is normally used during startup equilibration, but it may be a mode of operation as well. Total reflux operation is used to get the best possible separation, without regarding the length of time required for the revaporization of the reflux.



This operating mode is particularly useful when separating close boiling mixtures since it obviates the necessity for keeping a close watch on the temperature and adjusting the reflux ratio accordingly (Pratt, 1967). The temperature feedback approach of Skogestad *et al.* (1997) for the multivessel column may also be successfully used for the closed operation of conventional (two-vessel) distillation.

### 6.3.3 Cyclic operation

In cyclic operation (e.g. Sørensen and coworkers (1994; 1997; 1999)) there is a series of closed operations with product withdrawal between each. Sørensen and Skogestad (1994) and Sørensen and Prenzler (1997) studied the optimal operation of the cyclic policy and compared it to conventional operating policies. The cyclic policy was found to be favorable for difficult separations where small amounts of light product is to be recovered. More than 30 % reduction of the batch time were found.

### 6.3.4 Semicontinuous operation

The middle vessel batch column operation where the feed is charged to the middle vessel which is gradually emptied during operation, closely resembles continuous distillation. Sometimes, the middle vessel column is operated with re-charging of the middle vessel during operation and a more appropriate term for this operating mode may be semicontinuous operation because the feed mixture is continuously supplied during parts of the batch operation.

Obviously, if the middle vessel does not have entering streams the operation is continuous (within the time frame of emptying the feed vessel).

## 6.4 Comparison of cyclic and closed middle vessel columns

It is widely assumed that multieffect column configurations like the Petlyuk column in continuous distillation and the multivessel column in batch distillation are most suited when the ideal ternary mixture feed is rich in the intermediate-boiling component and when the product specifications and relative volatilities are uniform (see for example Lestak and Collins (1997)). In this study we examine the validity of this statement.

Hasebe *et al.* (1992) compared conventional batch distillation with open middle vessel batch column for removal of light and heavy impurities from a ternary mixture feed rich in intermediate-boiling component. They concluded that the middle vessel column is “effectively used when the heavy impurity is easy to remove compared with the light impurity“.

In this study, we compare the batch time for the cyclic column and the closed middle vessel column for separating ternary ideal mixtures, illustrated in Figure 6.2. The effects of mixture

volatilities, feed composition and feed charge location are investigated. Both columns are operated with indirect level control.

The underlying assumption is that there are economical benefits of minimizing the batch time, either because this frees the equipment for other separations, or, because the energy consumption (given constant heat input) is reduced. To minimize batch time the column is therefore operated at maximum boilup (reboiler capacity). Thus, in this study the vapor flow is constant and equal in all column sections. The ratio of the vapor flow relative to the total initial charge ( $V/H_{F0}$ ) is a measure on how many times the feed charge is reboiled. In this study this is once per hour, i.e.  $V/H_{F0} = 1$  hr.

The larger the value of the relative volatility between a pair of components in a mixture  $\alpha_{ij}$ , the easier it is to separate component  $i$  from component  $j$ . We have investigated theoretical ternary mixtures of components 1-2-3 where the relative volatilities are set constant and equal for each binary pair. Three values of the relative volatilities are considered: 1.2 (low), 2.0 (medium) and 5.3 (high).

The theoretical minimum batch time is given for the limiting case of infinite column sections, which in this study is approximated by a very large number of equilibrium stages (with negligible holdups). The operation is terminated when the compositions of the liquid in all the vessels satisfy the specifications for the final products, that is, 99.0 mol % purity.

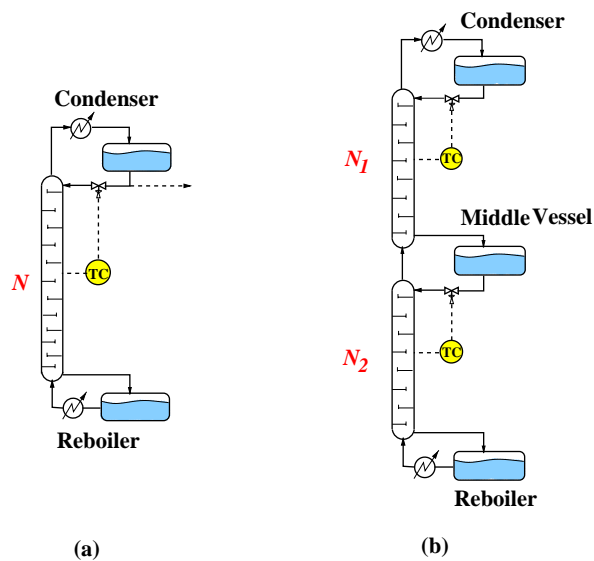


Figure 6.2: Closed batch distillation column alternatives for ternary mixtures separation: (a) cyclic column (sequential separation); (b) closed middle vessel column (simultaneous separation).

### 6.4.1 Results

The resulting time consumption and separation performance of the cyclic two-vessel column (indirect split) for various initial feed compositions are given in Table 6.1. The corresponding time consumption of the closed middle vessel column with difference feed charge locations (reboiler, middle vessel, distributed according to the given feed composition, equally distributed in the vessels) are given in Table 6.2, and the corresponding separation performances are given in Table 6.3. In most cases the middle vessel column is better than cyclic operation.

Ideally, we should have compared the middle vessel column with the best of the cyclic column sequences (indirect or direct split). Furthermore, a measure such as the *degree of difficulty of separation* proposed by Christensen and Jørgensen (1987) would have been better than relative volatility to characterize the batch distillation column separations task. Nevertheless, the results show an interesting tendency and the conclusions give a guideline for further investigations.

- Time savings with the middle vessel column compared to cyclic operation are more significant for difficult separations (low  $\alpha$ ) for which savings up to about 50 % were obtained.
- Time savings with the middle vessel column:
  - Difficult separation ( $\alpha = 1.2$ ): up to about 50 %
  - Medium difficult separation ( $\alpha = 2.0$ ): up to about 40 %  
(saving varied from negative, that is more time consumption, to 46.5 %)
  - Easy separation ( $\alpha = 5.3$ ): up to about 10 %
- Largest savings were found for the following feed compositions:
  - Difficult separation ( $\alpha = 1.2$ ): low in intermediate component
  - Medium difficult separation ( $\alpha = 2.0$ ): low in intermediate component
  - Easy separation ( $\alpha = 5.3$ ): rich in heavy component, but no pronounced difference
- For difficult separations (low relative volatility), the middle vessel column is always better than the direct split in the cyclic column, however the time savings are not very large for feeds rich in light component.
- For medium difficult separations (intermediate relative volatility), the benefits of the middle vessel column are low for feeds rich in light component and feeds low in heavy component, but there is a large time saving for feeds rich in heavy component.
- For easy separations (high relative volatility), the middle vessel column has no pronounced benefit, except large time savings for feeds rich in heavy component.
- Least savings was found for feed compositions rich in intermediate.

The location of the initial feed charge affects the time consumption:

- For difficult separations (low relative volatility), the best location depends on the feed composition, but the difference between the best and the worst cases is not very large (about 5-10 %). The reason that the location of the feed charge is not important to the batch time, is that the initial period becomes small relative to the total batch time for low  $\alpha$  mixtures (that is, the impact of this “initial distribution” effect becomes less significant).
- For medium difficult separations (intermediate relative volatility), the best location was dependent on the feed composition. For an equimolar feed, feed charged to the reboiler showed the best performance (minimum time). Interestingly, charging the feed to the intermediate vessel was worst in all cases of feed composition.
- For easy separations (high relative volatility), we found large time saving for feed charged to the reboiler instead of to the middle vessel (in average 32.5 %).

## 6.4.2 Discussion

Meski *et al.* (1998) compared the middle vessel batch distillation column (open operation) with the regular and inverted batch columns for binary and ternary ideal mixtures. They considered both the direct and indirect split, and combinations of both in these columns and found that for ternary mixtures:

- The middle vessel column was best for feeds low in intermediate component.
- The batch time increases sharply as the product specification of the intermediate component become tighter (that is, it is time consuming to obtain high purity intermediate component in the middle vessel column).
- The middle vessel column was better than the direct split in the regular batch column for feeds low in the intermediate component;
- The regular and conventional columns were best for feeds rich intermediate component.

Our results on the cyclic and closed operation confirm and refine these findings, which contradicts the results found by Hasebe *et al.* (1992).

Meski *et al.* (1998) conclude by proposing heuristic rules, similar to continuous distillation separation sequencing, like “remove the most plentiful component first” and “easy separation first”.

Sørensen (1994) found for binary ideal mixtures that the cyclic operating policy is favorable for difficult separations (with small amounts recovered) and feeds low in light component. Further, Sørensen (1994) found that that feed low in light component is best separated in the inverted column. This result was also confirmed by Meski *et al.* (1998). For ternary mixtures, Meski *et al.* (1998) found as mentioned above that regular batch distillation (direct sequence) was best for

feeds rich in light component and low in heavy, and that the inverted column (indirect sequence) was best for feeds rich in heavy component and low in light component.

For difficult separations with low relative volatility, the actual time to achieve the (high purity) product specifications is closer to the time to reach steady state (“equilibrium time”) than for easy separations (Sørensen and Skogestad, 1996). This further favors closed operation for mixtures with low relative volatilities.

Our results also confirms the time savings found by Wittgens and Skogestad (1998) and Furlonge *et al.* (1999) for ideal quaternary mixtures.

Note that the conclusions made in this study only hold if the number of stages in each column section is sufficient for the separations. If the mixtures to be separated requires more stages than the column actually have, the cyclic two-vessel column is better than closed three-vessel column. In general, the closed multivessel column is only meaningful if number of stages is sufficient for the purity specifications. The effect of liquid column holdup was not included in our study, but Mujtaba and Macchietto (1998) found that the minimum batch time for conventional binary batch distillation (regular columns) increased from a few percent up to 15-20 % depending on the difficulty of separation. The effect was larger for easier separations.

In practice, the time consumption for the cyclic two-vessel column will be even higher because of the time used to discharge the condenser vessel between the cycles. In addition, distillation columns are usually operated with a safety margin, that is, the actual product compositions are higher than the specifications to cope with process upsets and other problems (Humphrey and Seibert, 1992). Thus, the cyclic column will in practice consume extra time since each cycle of the process will be operated longer than the final time reported in this study. This added time consumption will be less for the closed three-vessel column since the separation is done in one operation (that is, one only needs to run the process once). This is an additional advantage in terms of time (energy) consumption for the multivessel column.

### 6.4.3 Comparison with integrated continuous distillation

Table 6.4 gives the minimum energy requirement for ordinary continuous distillation (direct and indirect sequence) and Petlyuk column (minimum boilup with infinite number of equilibrium stages, sharp split analytical expressions) (Halvorsen and Skogestad, 1999). The energy consumption  $V_{\min}/F$  for continuous distillation can be compared directly with  $\tau V/H_{F0}$  for batch distillation as it in both cases represents the number of times the feed needs to be reboiled. In our case  $V/H_{F0} = 1 \text{ hr}^{-1}$  which means that the time consumption  $\tau$  [hr] for batch distillation (*batch time*) can be compared directly with  $V_{\min}/F$ . As expected, the energy consumption in continuous Petlyuk distillation ( $V_{\min}/F$  in Table 6.4) is significantly lower than for middle vessel batch distillation (minimum batch time in Table 6.2). We find that  $V_{\min}/F$  is less than  $0.4\tau$  in most cases. Moreover, interestingly, we note that there are similar trends for the Petlyuk column and the middle vessel column: they perform best for difficult separations (low  $\alpha$ ) and for feeds low in the intermediate-boiling component (but for high  $\alpha$  they are best for feeds rich in the heavy

component).

However, there is an important difference between batch and continuous distillation in terms of the operation time/energy consumption: increased purity above a certain limit does not cost energy in continuous columns (“high purity best in continuous”), but for batch operation an increase in purity always cost in an increase in operating time (= energy consumption).

#### **6.4.4 Conclusion**

The closed middle vessel column requires less operating time to obtain the same product purity and recovery than the conventional batch column operated in two closed cycles (indirect split). The time savings are largest for low relative volatilities (difficult separations) were up to 50 % time savings where obtained.

Table 6.1: Time consumption and separation performance in cyclic two-vessel batch distillation column for various constant relative volatilities and initial feed compositions <sup>a</sup>

<b>Low relative volatility mixture</b>		Time [hr]			Impurities %
$\alpha_{12} = \alpha_{23} = 1.2$		total	cycle 1	cycle 2	in B/D <sub>2</sub> /D <sub>1</sub>
Feed 0	equimolar	22.79	13.15	9.64	1.0/1.0/0.0
Feed 1	rich in light component	16.21	13.41	2.80	1.0/0.2/0.0
Feed 2	rich in intermediate component	41.82	11.44	30.38	0.0/1.0/0.0
Feed 3	rich in heavy component	26.30	11.70	14.60	0.4/1.0/0.0
Feed 4	low in light component	23.89	10.87	13.02	1.0/1.0/0.0
Feed 5	low in intermediate component	20.20	11.48	8.72	0.6/1.0/0.1
Feed 6	low in heavy component	32.57	14.16	18.41	0.0/1.0/0.0
Average (for all given feed compositions)		26.25			
<b>Medium relative volatility mixture</b>		Time [hr]			Impurities %
$\alpha_{12} = \alpha_{23} = 2.0$		total	cycle 1	cycle 2	in B/D <sub>2</sub> /D <sub>1</sub>
Feed 0	equimolar	4.91	2.71	2.20	1.0/1.0/0.0
Feed 1	rich in light component	3.13	2.47	0.66	1.0/1.0/0.0
Feed 2	rich in intermediate component	4.60	2.33	2.27	1.0/1.0/0.0
Feed 3	rich in heavy component	9.15	1.92	7.23	0.0/1.0/0.0
Feed 4	low in light component	5.04	2.08	2.96	1.0/1.0/0.0
Feed 5	low in intermediate component	7.05	2.34	4.17	0.0/1.0/0.0
Feed 6	low in heavy component	4.65	3.13	1.52	1.0/1.0/0.0
Average (for all given feed compositions)		5.50			
<b>High relative volatility mixture</b>		Time [hr]			Impurities %
$\alpha_{12} = \alpha_{23} = 5.3$		total	cycle 1	cycle 2	in B/D <sub>2</sub> /D <sub>1</sub>
Feed 0	equimolar	1.75	0.90	0.85	1.0/1.0/0.0
Feed 1	rich in light component	2.41	1.69	0.72	0.0/1.0/0.0
Feed 2	rich in intermediate component	2.28	0.60	1.68	1.0/1.0/0.0
Feed 3	rich in heavy component	2.13	0.37	1.76	0.0/1.0/0.0
Feed 4	low in light component	1.66	0.50	1.16	1.0/1.0/0.0
Feed 5	low in intermediate component	1.12	1.03	1.09	0.0/1.0/0.0
Feed 6	low in heavy component	2.14	1.17	0.97	1.0/1.0/0.0
Average (for all given feed compositions)		1.93			

<sup>a</sup> Feed 1: [0.80 0.10 0.10], Feed 2: [0.10 0.80 0.10], Feed 3: [0.10 0.10 0.80], Feed 4: [0.10 0.45 0.45], Feed 5: [0.45 0.10 0.45], Feed 6: [0.45 0.45 0.10]

Table 6.2: Time consumption in closed middle vessel batch distillation column for various constant relative volatilities, initial feed charge locations and initial feed compositions <sup>a</sup>

<b>Low relative volatility mixture</b> $\alpha_{12} = \alpha_{23} = 1.2$		Time consumption [hr] with feed charge in			
		reboiler	middle vessel	according to feed	equally distributed
Feed 0	equimolar	12.63	13.24	13.22	13.22
Feed 1	rich in light component	14.25	14.28	13.25	13.41
Feed 2	rich in intermediate component	16.85	16.21	16.34	16.65
Feed 3	rich in heavy component	11.12	11.79	11.12	11.25
Feed 4	low in light component	13.31	15.32	14.07	14.69
Feed 5	low in intermediate component	8.23	8.13	7.27	7.27
Feed 6	low in heavy component	15.81	15.60	14.07	14.75
Average	(for all given feed compositions)	13.17	13.52	12.76	13.03
<b>Medium relative volatility mixture</b> $\alpha_{12} = \alpha_{23} = 2.0$		Time consumption [hr] with feed charge in			
		reboiler	middle vessel	according to feed	equally distributed
Feed 0	equimolar	3.23	4.31	4.05	4.05
Feed 1	rich in light component	2.90	2.96	4.45	3.48
Feed 2	rich in intermediate component	3.39	5.37	5.32	5.04
Feed 3	rich in heavy component	2.33	2.48	2.28	1.95
Feed 4	low in light component	3.09	4.86	4.49	4.61
Feed 5	low in intermediate component	2.19	2.36	2.27	2.48
Feed 6	low in heavy component	4.72	5.22	4.44	4.71
Feed 7	rich in light, low in intermediate	2.30	2.98	3.74	2.59
Feed 8	rich in light, low in heavy	4.23	4.47	4.67	3.92
Feed 9	rich in heavy, low in intermediate	2.28	2.26	1.96	2.13
Feed 10	rich in heavy, low in light	3.06	3.95	3.15	3.66
Feed 11	rich in intermediate, low in light	2.91	5.44	5.30	5.19
Feed 12	rich in intermediate, low in heavy	4.74	5.64	5.28	5.19
Average	(for all given feed compositions)	3.18	4.02	3.95	3.77
<b>High relative volatility mixture</b> $\alpha_{12} = \alpha_{23} = 5.3$		Time consumption [hr] with feed charge in			
		reboiler	middle vessel	according to feed	equally distributed
Feed 0	equimolar	1.92	2.61	2.45	2.45
Feed 1	rich in light component	2.13	2.12	2.90	2.08
Feed 2	rich in intermediate component	1.82	3.29	2.90	2.90
Feed 3	rich in heavy component	0.69	2.01	0.70	1.39
Feed 4	low in light component	1.29	2.88	2.64	2.68
Feed 5	low in intermediate component	1.42	1.51	1.96	1.73
Feed 6	low in heavy component	2.63	3.21	2.70	2.89
Average	(for all given feed compositions)	1.70	2.52	2.32	2.30

<sup>a</sup> Feed 1: [0.80 0.10 0.10], Feed 2: [0.10 0.80 0.10], Feed 3: [0.10 0.10 0.80], Feed 4: [0.10 0.45 0.45],  
 Feed 5: [0.45 0.10 0.45], Feed 6: [0.45 0.45 0.10], Feed 7: [0.60 0.10 0.30], Feed 8: [0.60 0.30 0.10],  
 Feed 9: [0.30 0.10 0.60], Feed 10: [0.10 0.30 0.60], Feed 11: [0.10 0.60 0.30], Feed 12: [0.30 0.60 0.10]



Table 6.3: Separation performance of closed middle vessel batch distillation column corresponding to results in Table 6.2 <sup>a</sup>

<b>Low relative volatility mixture</b> $\alpha_{12} = \alpha_{23} = 1.2$		Impurities % in B/M/D with feed charge in			
		reboiler	middle vessel	according to feed	equally distributed
Feed 0	equimolar	0.1/1.0/0.0	0.0/1.0/0.0	0.0/1.0/0.0	0.0/1.0/0.0
Feed 1	rich in light component	0.0/0.0/1.0	0.0/0.0/1.0	0.0/0.2/1.0	0.0/0.1/1.0
Feed 2	rich in intermediate component	0.0/1.0/0.0	0.0/1.0/0.0	0.0/1.0/0.0	0.0/1.0/0.0
Feed 3	rich in heavy component	1.0/0.1/0.0	1.0/0.0/0.0	1.0/0.1/0.0	1.0/0.1/0.0
Feed 4	low in light component	1.0/0.2/0.0	0.0/1.0/0.0	0.1/1.0/0.0	0.0/1.0/0.0
Feed 5	low in intermediate component	1.0/0.4/0.4	0.5/0.0/1.0	0.4/1.0/0.6	0.2/1.0/0.3
Feed 6	low in heavy component	0.0/1.0/0.0	0.0/1.0/0.0	0.0/1.0/0.3	0.0/1.0/0.1
<b>Medium relative volatility mixture</b> $\alpha_{12} = \alpha_{23} = 2.0$		Impurities % in B/M/D with feed charge in			
		reboiler	middle vessel	according to feed	equally distributed
Feed 0	equimolar	0.2/1.0/0.0	0.0/1.0/0.0	0.0/1.0/0.1	0.0/1.0/0.1
Feed 1	rich in light component	0.0/1.0/0.0	0.0/1.0/0.0	0.0/0.4/1.0	0.0/0.4/1.0
Feed 2	rich in intermediate component	0.0/1.0/0.0	0.0/1.0/0.0	0.0/1.0/0.0	0.0/1.0/0.0
Feed 3	rich in heavy component	1.0/0.0/0.0	0.0/1.0/0.0	1.0/0.0/0.0	0.6/1.0/0.0
Feed 4	low in light component	1.0/0.4/0.0	0.0/1.0/0.0	0.0/1.0/0.0	0.0/1.0/0.0
Feed 5	low in intermediate component	1.0/0.4/0.0	0.0/1.0/0.0	0.0/0.9/1.0	0.0/1.0/0.9
Feed 6	low in heavy component	0.0/1.0/0.0	0.0/1.0/0.0	0.0/1.0/0.4	0.0/1.0/0.2
Feed 7	rich in light, low in intermediate	0.4/1.0/0.0	0.0/0.7/1.0	0.0/0.7/1.0	0.0/1.0/0.0
Feed 8	rich in light, low in heavy	0.0/1.0/0.0	0.0/1.0/0.0	0.0/0.2/1.0	0.0/1.0/0.8
Feed 9	rich in heavy, low in intermediate	1.0/0.1/0.0	0.0/1.0/0.0	1.0/1.0/0.5	0.3/1.0/0.5
Feed 10	rich in heavy, low in light	1.0/0.1/0.0	0.0/1.0/0.0	0.4/1.0/0.0	0.1/1.0/0.0
Feed 11	rich in intermediate, low in light	1.0/0.9/0.0	0.0/1.0/0.0	0.0/1.0/0.0	0.0/1.0/0.0
Feed 12	rich in intermediate, low in heavy	0.0/1.0/0.0	0.0/1.0/0.0	0.0/1.0/0.0	0.0/1.0/0.0
<b>High relative volatility mixture</b> $\alpha_{12} = \alpha_{23} = 5.3$		Impurities % in B/M/D with feed charge in			
		reboiler	middle vessel	according to feed	equally distributed
Feed 0	equimolar	0.0/1.0/0.0	0.0/1.0/0.0	0.0/1.0/0.1	0.0/1.0/0.1
Feed 1	rich in light component	0.0/1.0/0.0	0.0/1.0/0.0	0.0/0.5/1.0	0.0/0.5/1.0
Feed 2	rich in intermediate component	1.0/0.3/0.0	0.0/1.0/0.0	0.0/1.0/0.0	1.0/0.1/0.0
Feed 3	rich in heavy component	1.0/0.1/0.0	0.0/0.1/0.0	0.8/1.0/0.0	0.0/1.0/0.0
Feed 4	low in light component	1.0/0.3/0.0	0.0/1.0/0.0	0.0/1.0/0.0	0.0/1.0/0.0
Feed 5	low in intermediate component	0.0/1.0/0.0	0.0/1.0/0.0	0.0/1.0/0.9	0.0/1.0/0.9
Feed 6	low in heavy component	0.0/1.0/0.0	0.0/1.0/0.0	0.0/1.0/0.3	0.0/1.0/0.1

<sup>a</sup> Feed 1: [0.80 0.10 0.10], Feed 2: [0.10 0.80 0.10], Feed 3: [0.10 0.10 0.80], Feed 4: [0.10 0.45 0.45],  
 Feed 5: [0.45 0.10 0.45], Feed 6: [0.45 0.45 0.10], Feed 7: [0.60 0.10 0.30], Feed 8: [0.60 0.30 0.10],  
 Feed 9: [0.30 0.10 0.60], Feed 10: [0.10 0.30 0.60], Feed 11: [0.10 0.60 0.30], Feed 12: [0.30 0.60 0.10]

Table 6.4: Minimum energy in continuous and Petlyuk distillation columns for various constant relative volatilities and initial feed compositions<sup>a</sup>. Minimum boilup with infinite stages columns.

<b>Low relative volatility mixture</b>		$V_{\min}/F$			
$\alpha_{12} = \alpha_{23} = 1.2$		Direct	Indirect	Petlyuk	Savings
		sequence	sequence	column	%
Feed 0	equimolar	7.87	7.83	4.49	42.6
Feed 1	rich in light component	6.45	8.00	5.35	17.1
Feed 2	rich in intermediate component	10.11	10.11	5.61	44.5
Feed 3	rich in heavy component	7.31	5.68	4.68	17.6
Feed 4	low in light component	8.74	7.93	5.18	34.7
Feed 5	low in intermediate component	6.49	6.38	3.64	42.9
Feed 6	low in heavy component	8.30	9.08	5.10	38.6
Average	(for all given feed compositions)	7.90	7.86	4.86	34.0
<b>Medium relative volatility mixture</b>		$V_{\min}/F$			
$\alpha_{12} = \alpha_{23} = 2.0$		Direct	Indirect	Petlyuk	Savings
		sequence	sequence	column	%
Feed 0	equimolar	2.07	2.03	1.37	32.8
Feed 1	rich in light component	2.01	2.21	1.71	15.0
Feed 2	rich in intermediate component	2.73	2.73	1.83	33.0
Feed 3	rich in heavy component	1.52	1.24	1.04	16.1
Feed 4	low in light component	2.13	2.00	1.45	27.5
Feed 5	low in intermediate component	1.70	1.60	1.05	34.4
Feed 6	low in heavy component	2.37	2.47	1.57	33.6
Feed 7	rich in light, low in intermediate	1.82	1.85	1.32	27.4
Feed 8	rich in light, low in heavy	2.21	2.36	1.51	31.6
Feed 9	rich in heavy, low in intermediate	1.60	1.40	1.00	28.6
Feed 10	rich in heavy, low in light	1.86	1.68	1.28	23.8
Feed 11	rich in intermediate, low in light	2.39	2.32	1.62	30.2
Feed 12	rich in intermediate, low in heavy	2.52	2.58	1.68	33.3
Average	(for all given feed compositions)	2.07	2.04	1.42	28.3
<b>High relative volatility mixture</b>		$V_{\min}/F$			
$\alpha_{12} = \alpha_{23} = 5.3$		Direct	Indirect	Petlyuk	Savings
		sequence	sequence	column	%
Feed 0	equimolar	0.98	0.96	0.81	16.1
Feed 1	rich in light component	1.16	1.17	1.01	12.7
Feed 2	rich in intermediate component	1.32	1.32	1.11	15.9
Feed 3	rich in heavy component	0.48	0.41	0.36	11.3
Feed 4	low in light component	0.90	0.88	0.75	14.6
Feed 5	low in intermediate component	0.81	0.76	0.63	16.9
Feed 6	low in heavy component	1.24	1.25	1.04	16.4
Average	(for all given feed compositions)	0.98	0.96	0.82	14.8

<sup>a</sup>Feed 1: [0.80 0.10 0.10], Feed 2: [0.10 0.80 0.10], Feed 3: [0.10 0.10 0.80], Feed 4: [0.10 0.45 0.45],  
 Feed 5: [0.45 0.10 0.45], Feed 6: [0.45 0.45 0.10], Feed 7: [0.60 0.10 0.30], Feed 8: [0.60 0.30 0.10],  
 Feed 9: [0.30 0.10 0.60], Feed 10: [0.10 0.30 0.60], Feed 11: [0.10 0.60 0.30], Feed 12: [0.30 0.60 0.10]

## Chapter 7

# Closed Multivessel Batch Distillation of Ternary Azeotropic Mixtures

*Presented at ESCAPE-9, Budapest, May 31-June 2, 1999*

In this paper we consider the separation of ternary homogeneous azeotropic mixtures using two kinds of closed batch distillation column operations: (i) cyclic operation (with two vessels) where the products are separated in a sequence of closed operations; and (ii) closed middle vessel batch distillation (with three vessels) where all three components or azeotropes are separated simultaneously. VLE diagram information, such as distillation lines and isotherms, can be used directly to analyze the final steady state in both cases and we illustrate its use for operation and control considerations. An indirect level control strategy is implemented that eliminates the need for pre-calculating the vessel holdups and makes the closed operating policy flexible and simple to implement in practice.

### 7.1 Introduction

The operation and control of batch distillation, including other new configurations such as inverted and multivessel columns, have received a lot of attention lately. However, most of the studies have been for relatively ideal mixtures. The aim of this paper is to extend this to azeotropic mixtures. Our main tool is the (graphical) VLE diagram analysis which has been extensively used for continuous azeotropic distillation.

Conventional operation of multicomponent batch distillation columns requires timely switching between products and off-cuts and often a variable reflux ratio policy to ensure the wanted product purities. This may require a lot of attention from the operators and a complicated control system. Closed operation of multivessel batch distillation columns with the simple indirect level control strategy proposed by Skogestad *et al.* (1997) eliminates these difficulties and the products are separated in an energy efficient, stand-alone operation.

By closed multivessel batch distillation we mean a “total reflux” operation where the products are accumulated in vessels along the column (including the reboiler and condenser vessel). There are no input or output streams, but the internal liquid reflux flows may vary during the operation causing accumulation or depletion of mass in the vessels. Thus, *closed system* is a more correct term than “total reflux” since we generally only achieve total reflux as time approaches infinity, i.e., at steady state. We use the term *multivessel* column as a generalized configuration of all batch distillation columns. In this context the regular batch distillation operation (also called the batch rectifier), where the feed is charged to the reboiler and the products are withdrawn as distillate during operation, is a *two-vessel* column. Correspondingly, open operation of the inverted batch distillation column (batch stripper) and the middle vessel batch column (a combined system of a batch rectifier and a batch stripper where distillate and bottoms products are withdrawn from the column ends) are both two-vessel columns. However, the middle vessel column where the products are accumulated in the condenser, middle vessel and reboiler is a *three-vessel* column.

#### *Relation to previous work*

Simple total reflux operation until equilibrium followed by total distillate draw-off has been used in laboratory batch distillation for a long time (see for example Perry and Chilton (1963)). A repeated sequence of such total reflux operations is called the *cyclic operating policy* and is used for separation of multicomponent mixtures (Perry and Chilton, 1973). Treybal (1970) and Bortolini and Guarise (1970) independently investigated closed total reflux operation of the conventional batch distillation column with a condenser vessel (i.e., a two-vessel column) for separation of ideal binary mixtures. In both studies, total liquid reflux with pre-fixed condenser vessel holdup was suggested. This requires exact knowledge of the initial feed composition and charge to the column in order to pre-calculate the vessel holdups so that the wanted product purities are achieved at steady state. Kiva *et al.* (1988) extended this idea to separation of multicomponent and azeotropic mixtures in the two-vessel batch distillation column operated in a sequence of total reflux operations where the accumulated condenser (or reboiler) vessel product is discharged between each closed operation, i.e., the cyclic operating policy. In addition to general analytical considerations, experimental results on the ternary azeotropic mixture of acetone, isopropanol and water were reported. Sørensen and Skogestad (1994) and Sørensen (1999) found that the cyclic operating policy for separation of multicomponent mixtures in the two-vessel column requires significantly less batch time for some ideal mixtures as compared to the conventional open operating strategies. Closed operation of the middle vessel configuration for separation of ternary mixtures (i.e., a three-vessel column) was proposed by Bortolini and Guarise (1970). A further generalization is the multivessel column for separation of multicomponent mixtures suggested by Hasebe *et al.* (1995) which they call “multieffect batch distillation system”. In this configura-

tion it is possible to separate a multicomponent mixture simultaneously in one closed operation. Skogestad *et al.* (1997) proposed a novel feedback control strategy for closed multivessel batch distillation columns (described in Chapter 6). The feasibility of this strategy was demonstrated by simulations for an ideal quaternary mixture separated in a column with four vessels, and later experimental verification was given for the zeotropic mixture of methanol, ethanol, n-propanol and n-butanol (Wittgens and Skogestad, 1997).

In this study we extend some of the above considerations to azeotropic mixtures. Note that closed multivessel batch distillation does not offer a method of azeotropic mixtures separation, but only a simple way to operate the batch distillation process for multicomponent mixtures in general. However, new aspects on the operation and control of the closed multivessel batch distillation column are introduced when azeotropes are involved.

## 7.2 Columns and operating modes for ternary separation

There are basically two column alternatives for separation of ternary mixtures in the closed multivessel batch distillation scheme. One is the cyclic operation of the regular (two-vessel) batch distillation column shown in Figure 7.1 (referred to as the *cyclic column* or *cyclic operation* in the following), where the products are separated one at the time in a sequence of closed operations. Three alternative splits of an ideal ternary mixture may be performed: the direct split 1/23; the in-

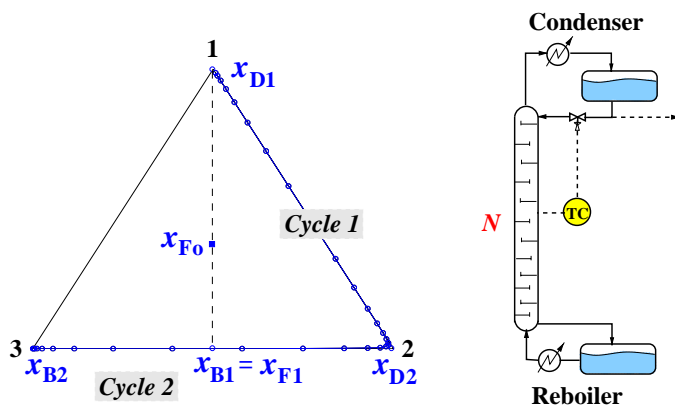


Figure 7.1: Cyclic two-vessel batch distillation of ternary zeotropic mixture. Sequential separation of all three components (direct sharp split illustrated). Steady state composition profiles (solid line with open circles along the edges of the composition triangle) and material balance line (dashed).

direct split 12/3; and the distributed split 12/23 where each vessel product must be re-processed in order to achieve all three components as pure products. In this study, we only consider the direct

(not necessarily sharp) split illustrated in Figure 7.1. The distillate product in the condenser after the first cycle (with composition  $x_{D1}$ ) is discharged from the condenser vessel. The second cycle is then mainly a binary split between the remaining components into a second distillate product (with composition  $x_{D2}$ ) and a bottom product (with composition  $x_{B2}$ ) in the reboiler. Column holdup may require the removal of an off-cut fraction between the cycles in order to achieve the desired product purities.

There are at least two advantages with the cyclic column compared to the regular open batch distillation operation where the products are continuously withdrawn overhead, one at a time. First, the closed operation is simpler since there is a definite distinction between the product change-overs (i.e., the condenser is discharged by on/off distillate withdrawal) and it is easier to assure the product qualities. Second, the “total reflux at steady state” operation utilizes the maximum attainable separation in the column (at least for ideal and nearly ideal mixtures) and is especially advantageous for high purity distillations.

The other closed multivessel column alternative for ternary mixtures separation is the closed middle vessel (three-vessel) column shown in Figure 7.2 (referred to as *middle vessel column* in the following), where all three components (or azeotropes) are separated simultaneously during one

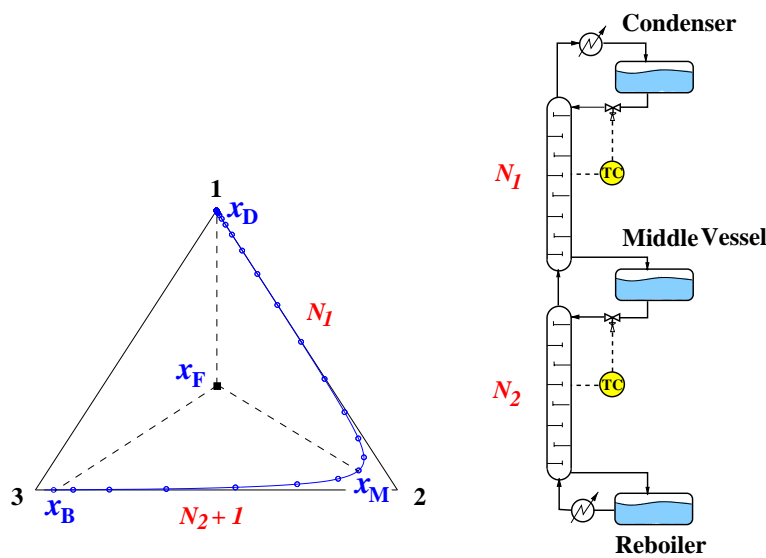


Figure 7.2: Closed middle vessel (three-vessel) batch distillation of ternary azeotropic mixture. Simultaneous separation of all three components. Steady state composition profile (solid line with open circles) and material balance lines (dashed).

closed operation. The three vessel products (with compositions  $x_D$ ,  $x_M$  and  $x_B$ ) are discharged from the vessels at the end of the batch operation. The main advantage of the closed vessel config-

uration is the simplicity of operation since no product change-overs are required during operation. In addition, it may imply energy savings as compared to both the regular open batch column and the cyclic column due to the multieffect (mass and heat integrated) nature of the process. Further, there is no need to remove an off-cut fraction as may be the case in the cyclic column for separating ternary mixtures. However, saddles (component 2 in Figure 7.2) are difficult to obtain as pure products and a large number of equilibrium stages may be required to obtain the product specifications of such intermediate fractions.

Some loss of products due to column holdup is unavoidable in batch distillation in general. To avoid that liquid holdup in the column sections contaminates the vessel products after the distillation is completed, there must be a shut-off valve on the liquid reflux into each vessel. This applies to both cyclic and closed middle column operation.

### 7.3 VLE diagrams and steady state composition profiles

There are various ways to graphically represent the VLE behavior of a mixture and its relationship to the distillation process. McCabe-Thiele diagrams for binary systems are probably the most known graphical tool. For ternary and multicomponent mixtures, residue curve maps and distillation line maps are two closely related VLE representations that are commonly used, particularly in nonideal and azeotropic distillation analysis. A distillation line is defined as a connection line through a sequence of equilibrium mapping vectors in the composition space (Zharov, 1968c; Stichlmair, 1988) and corresponds to the liquid (or vapor) composition profile at total reflux for equilibrium staged columns. The closely related residue curves (Schreinemakers, 1901c; Ostwald, 1902; Zharov, 1967; Serafimov, 1968a; Doherty and Perkins, 1978a) coincide exactly with total reflux packed distillation column profiles when all resistance to mass transfer is in the vapor phase (Serafimov *et al.*, 1973; Pöllmann and Blass, 1994). This makes distillation line maps and residue curve maps particularly suited to identify feasible products at the limiting operating condition of total reflux. In the closed operating regime, the correspondence between the VLE diagram and the steady state of the closed multivessel batch distillation column is simple and straightforward:

*The steady state vessel product compositions of a closed multivessel batch distillation column are connected by a distillation line with the given number of equilibrium trays. In addition the material balances must be satisfied.*

For the closed middle vessel (three-vessel) batch distillation column shown in Figure 7.2, the steady state material balances become (in the case of zero or negligible column holdup):

$$H_F = H_D + H_M + H_B \quad (7.1)$$

$$H_F \mathbf{x}_F = H_D \mathbf{x}_D^* + H_M \mathbf{x}_M^* + H_B \mathbf{x}_B^* \quad (7.2)$$

which gives

$$H_M(\mathbf{x}_F - \mathbf{x}_M^*) = H_D(\mathbf{x}_D^* - \mathbf{x}_F) + H_B(\mathbf{x}_B^* - \mathbf{x}_F) \quad (7.3)$$

The same equations applies to the steady state of each cycle in the cyclic conventional (two-vessel) column shown in Figure 7.1 by simply setting the middle vessel holdup  $H_M$  equal to zero. From Equation (7.3) we see that the feed composition is a linear combination of the vessel products. The vessel holdups must obey the so-called lever rule. The material balance is visualized by straight dashed lines in Figure 7.1 and 7.2 that connect the vessel products with the feed composition. The steady state compositions in the condenser, middle vessel and reboiler ( $x_D^*$ ,  $x_M^*$  and  $x_B^*$ , respectively) must lie on the same distillation line given by the vapor-liquid equilibrium mapping:

$$x_D^* = E^{N_1} x_M^* = E^{N_1+N_2+1} x_B^* \quad (7.4)$$

where  $E$  is the equilibrium mapping function (see Chapter 3). Consequently, distillation lines may be used to (graphically or analytically) determine the number of equilibrium trays needed for a given separation to convert  $x_D^*$  to  $x_B^*$  (or vice versa) given as the multiple of the vapor-liquid equilibrium phase mappings (Kiva *et al.*, 1988) in the same fashion as Fenske's equation. Thus, in this study the distillation line map analysis is not only a qualitative tool but also a quantitative tool. Note that if  $x_D^* = x_{Az}$  is specified, the number of equilibrium trays required is infinite,  $N_{min} = \infty$ . The number of equilibrium trays determines the achievable separation in the column and the steady state vessel holdups determines the purity of the product fractions (Kiva *et al.*, 1988).

In summary, the feasible region of vessel compositions in the middle vessel column are enclosed by the feed distillation line and the borders of the current feed distillation region and by the material balance triangle connecting the unstable node, the stable node and one of the saddles of the current feed distillation region. In the cyclic column, the material balance line that represents the total reflux steady state separation performed in each cycle is a chord of the distillation line joining the unstable node and the stable node of the current feed distillation region.

## 7.4 Mixtures studied

Ternary mixtures of elementary cells I and II are considered, represented by the mixtures given in Figure 7.3 and 7.4. In addition, a mixture with a distillation line boundary (separatrix) that consists of two cell I's is considered, represented by the mixture given in Figure 7.5. The elementary cell concept is described in Chapter 4.

The simplest example of Cell I is Serafimov's class 0.0-1. A mixture that represent this class is the zeotropic system of methanol, ethanol and 1-propanol shown in Figure 7.3. Note that the distillation lines in Figure 7.3 are drawn as smooth curves (spline interpolation) through the chains of conjugated equilibrium vectors according to the definition by Stichlmair (1988). For the other example mixtures presented in this paper, the distillation lines are drawn with solid straight tie-lines between each point of conjugation. Liquid isotherms (dotted lines) are contour plots of the boiling temperature surface.

The simplest example of Cell II is Serafimov's class 1.0-1a with one binary azeotrope and where



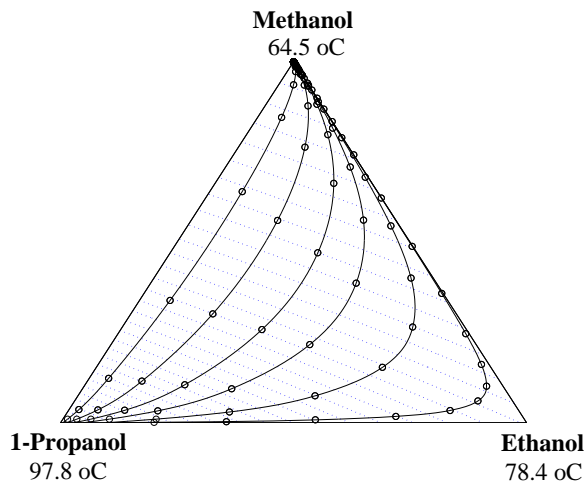


Figure 7.3: Zeotropic mixture of elementary cell I (Serafimov's class 0.0-1): Distillation lines and liquid isotherms for the ternary zeotropic mixture of methanol, ethanol and 1-propanol at atmospheric pressure.

the azeotrope-forming components are both saddle points. A mixture that represent this class is acetone, methanol and water shown in Figure 7.4.

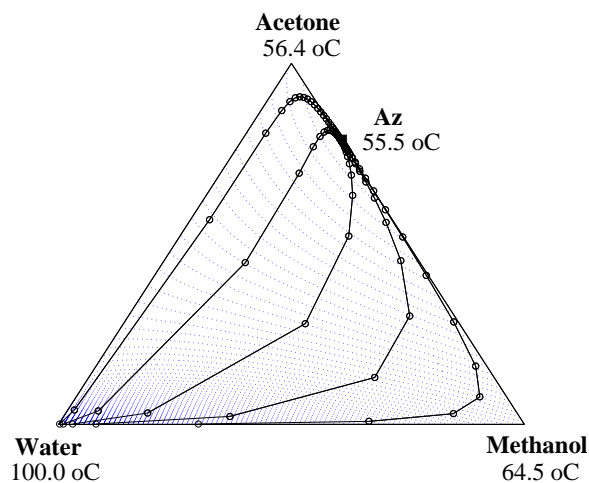


Figure 7.4: Azeotropic mixture of elementary cell II (Serafimov's class 1.0-1a): Distillation lines and liquid isotherms for the ternary azeotropic mixture of acetone, methanol and water at atmospheric pressure.

A mixture with a distillation line boundary that consists of two cell I's (Serafimov's class 1.0-2) is acetone, chloroform and benzene shown in Figure 7.5. The distillation line boundary splits the

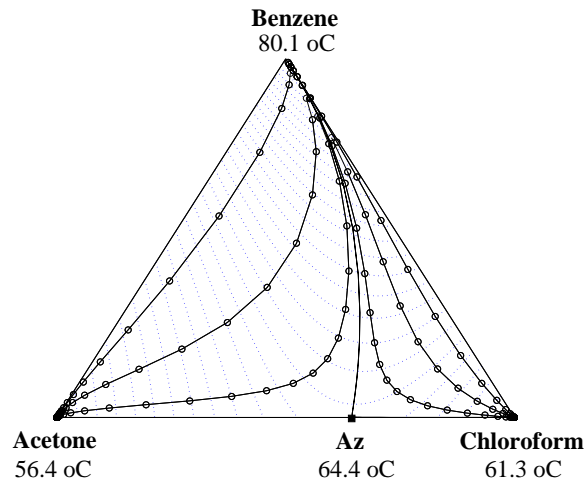


Figure 7.5: Azeotropic mixture with distillation line boundary (Serafimov's class 1.0-2): Distillation lines and liquid isotherms for the ternary azeotropic mixture of acetone, chloroform and benzene at atmospheric pressure. The distillation line boundary splits the composition space into two elementary cell I's.

VLE diagram into two separate distillation regions (two cell I's), both with S-shaped distillation lines for this particular mixture. Kiva *et al.* (1988) studied the mixture acetone - isopropanol - water, which is of the same structure Class 1.0-2 ("antipodal" diagram).

The qualitative results and conclusions apply in general to any system of these types and classes. It is important to note, however, that every mixture has its own specific features and that the concept of elementary topological cells (Chapter 4) is a strongly simplified description and only a way to reduce the complexity and extent of azeotropic mixtures analysis.

## 7.5 Mathematical model

The mathematical model of the closed multivessel batch distillation columns used in the dynamic simulations presented in this paper is described in Appendix A7. The model is based on the following simplifying assumptions: equilibrium stages, negligible vapor holdup, constant molar liquid holdups on all trays (i.e., neglecting liquid dynamics), constant molar vapor flow (i.e., simplified energy balance), constant pressure, total condenser and ideal behavior in the vapor phase. We implemented the indirect level control strategy proposed by Skogestad *et al.* (1997) where the liquid reflux flowrates out of each vessel are adjusted based on temperature feedback

control from the column section below

$$L = L_0 + K_c (T_{j,m} - T_{j,sp}) \quad (7.5)$$

where  $L_0$  is the bias term,  $K_c$  is the proportional gain,  $T_{j,m}$  is the measured temperature at some tray  $j$  in the column section below the actual vessel and  $T_{j,sp}$  is the temperature set-point. Note that there is no explicit level control, rather the holdup in each vessel is adjusted indirectly to meet the temperature specifications. As an initial choice of the proportional gain we used

$$K_c = \frac{V}{|\Delta T_{bp}|} \quad (7.6)$$

where  $V$  is the nominal vapor flow (in this study kept constant) and  $\Delta T_{bp}$  is the boiling point difference between the two main components (or azeotropes) being separated in that section. The controller bias was set equal to the vapor flow  $L_0 = V$  so that total reflux was achieved at steady state. This eliminates the need for using integral action to avoid steady state offset. In practical implementation of the indirect level control strategy, a PI-controller would be used since there are no direct measurement of the vapor flowrate in the column (Wittgens and Skogestad, 1998). The temperature measurement was taken on the middle tray in the column section since this temperature is more sensitive to composition changes than it is in, for example, the vessel or top tray that are dominated by the product component boiling point. For simplicity, the temperature set-point to the controller was set as the average boiling temperature of the two main components (or azeotropes) being separated in the given section (i.e., assuming 50-50 mole percent of the components on the middle tray in the column section). Alternatively, they can be obtained by steady state calculations to get a desired separation, or they may be optimized as a function of time. Other controller parameters such as the controller gain and the localization of the tray temperature measurement may also be optimized.

The dynamic models were implemented in the equation-oriented software package SpeedUp (1993), with user-written code for the nonideal thermodynamic VLE relationships. Thermodynamic data for the various example mixtures presented in this study are given in Table 7.19 (Appendix A7).

## 7.6 Simulation results

In addition to some dynamic column composition profiles, we present the steady state values and composition profiles which would be achieved in the closed multivessel columns under consideration if we were to let the batch time approach infinity. Of course, in practice we want the batch time to be as short as possible to minimize energy consumption and processing time and we would terminate the batch operation when the product specifications are met or the improvement in purity is small. Nevertheless, the steady state values are interesting since they give the achievable separation for a given case and have a simple connection to the VLE diagram of the mixture given by the distillation lines.

The column specifications and initial conditions for the simulations of the cyclic and middle vessel columns are given in Table 7.1.

Table 7.1: Columns data and initial conditions

Cyclic two-vessel batch distillation column	
Total no. of trays	15 (excl. reboiler)
Total initial charge	$H_{F0} = 5.385$ kmol
Initial condenser holdup	$H_{D0} = 0.035$ kmol
Initial reboiler holdup	$H_{B0} = 5.300$ kmol
Tray holdups (constant)	$H_j = 1/300$ kmol
Vapor flow (constant)	$V = 5$ kmol/h
Closed middle vessel batch distillation column	
Total no. of trays	30 (excl. reboiler)
No. of trays per section	$N_1 = 15, N_2 = 15$
Total initial charge	$H_{F0} = 5.385$ kmol
Initial condenser holdup	$H_{D0} = 0.035$ kmol
Initial middle vessel holdup	$H_{M0} = 5.000$ kmol
Initial reboiler holdup	$H_{B0} = 0.250$ kmol
Tray holdups (constant)	$H_j = 1/300$ kmol
Vapor flow (constant)	$V = 5$ kmol/h

In this study, the vapor flow (boilup) in the column sections is kept constant. The achievable separation is not dependent on the boilup, but the operating time to reach steady state is. Generally, batch distillation columns are usually operated at maximum boilup (reboiler capacity) to achieve maximum throughput (productivity) and minimize the batch time. The ratio of the vapor flow relative to the total initial charge ( $V/H_{F0}$ ) is a measure on how many times the feed charge is reboiled (this study: about once per hour) and is the same in both the cyclic column and the middle vessel column as given in Table 7.1. All simulations are at atmospheric pressure. Initial column compositions are equal to that of the feed mixture in all the simulations presented in this paper. Mostly equimolar feeds are studied and none of the mixture components are present in small proportions in the initial feed (relatively to the total column holdup). The influence of column holdup is not significant in this study. The liquid holdup in the column sections is less than 1 % of the total initial charge (e.g., about 2 % of the total charge is distributed on the trays in the middle vessel column). The temperature measurements for the indirect level controllers are on tray 8 in each column section (trays numbered from the top and down) in both the cyclic conventional column and the closed middle vessel column shown in Figures 7.1 and 7.2.

The desired product quality is at least 95 mole % in all the vessels. However, the number of column trays used in the simulations are set larger than the minimum number of equilibrium trays required in order to achieve the product specification. This is done to avoid the situation where the number of equilibrium trays in the columns limit the achievable separation (according to the given product specification) since we did not want to study the effect of limiting number of trays

in this paper. The recovery of component  $i$  in an arbitrary vessel is given by the equation

$$\eta_i = \frac{H \cdot x_i}{H_{F0} \cdot x_{F0,i}} \cdot 100\% \quad (7.7)$$

For the simulation results presented in the Figures given next, the steady state column composition profiles are given by solid lines with open circles for each equilibrium tray. The temperature set-points are in general set to the mean value of pair of the desired products boiling points and are visualized by the corresponding liquid isotherms as dotted lines.

### 7.6.1 Results on ternary zeotropic mixture (Cell I)

In this section we consider separation of the ternary zeotropic mixture of methanol, ethanol and 1-propanol which is given as an example mixture of elementary cell I (Serafimov's class 0.0-1) in Figure 7.3. The initial feed composition and controller parameters for both the cyclic conventional (two-vessel) and closed middle vessel (three-vessel) column are given in Table 7.2 where the parameter number indicates the Cycles 1 and 2, or, column section 1 and 2, respectively. The temperature set-points are the mean values of pair of the pure component boiling points.

Table 7.2: *Initial feed composition and controller parameters for methanol, ethanol and 1-propanol*

$x_{F0} = [1/3, 1/3, 1/3]$
$K_{c,1} = 0.36 \text{ kmol/h}^\circ\text{C}, T_{sp,1} = 71.5^\circ\text{C}$
$K_{c,2} = 0.26 \text{ kmol/h}^\circ\text{C}, T_{sp,2} = 88.1^\circ\text{C}$

For the middle vessel column, the equimolar feed was mainly charged to the middle vessel initially as given in Table 7.1. The dynamic development of the composition profile along with the resulting steady state composition profile are given in Figure 7.6. The steady state values of the vessel holdups and compositions and the product recovery are given in Table 7.3. For ternary zeotropic mixtures the whole composition space is encapsulated by the material balance triangle and is a feasible product region. The composition in the middle vessel was slowly changed by the gradual depletion of methanol and 1-propanol. High purity of methanol in the condenser and 1-propanol in the reboiler were achieved rapidly. The steady state values of the purities and vessel holdups are independent of the initial feed charge distribution. However, if the initial feed was mainly charged to the reboiler instead of to the middle vessel, for example, the dynamic development of the column composition profile would differ. This has an impact on the time to reach steady state in the column (i.e., approach to equilibrium) which is not an issue we address in this study. The effect of initial feed charge distribution on the time consumption of closed middle vessel batch distillation of ternary ideal mixtures is evaluated in Chapter 6 where the operation is terminated when a given product specification is reached in all three vessels (not until steady state as in this study).

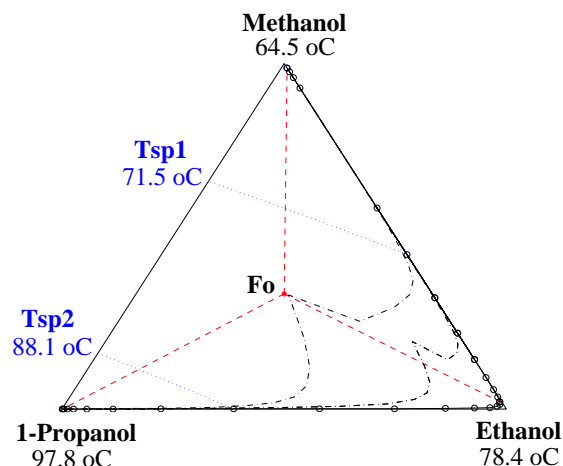
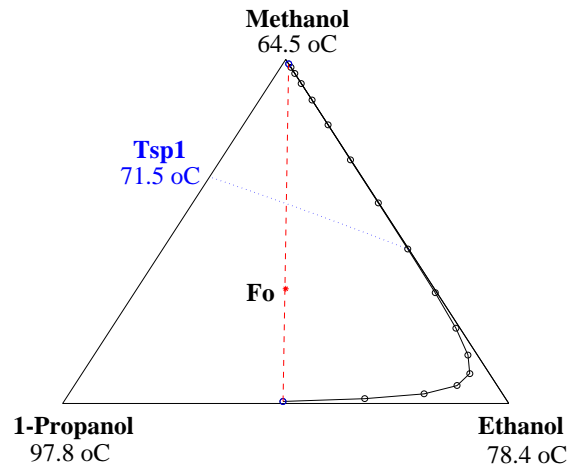


Figure 7.6: Middle vessel column composition profiles for an equimolar feed of methanol, ethanol and 1-propanol: Instantaneous profiles at 6 minutes and 2 hours (dash-dotted lines) and steady state profile (solid line with open circles along the edges of the composition triangle).

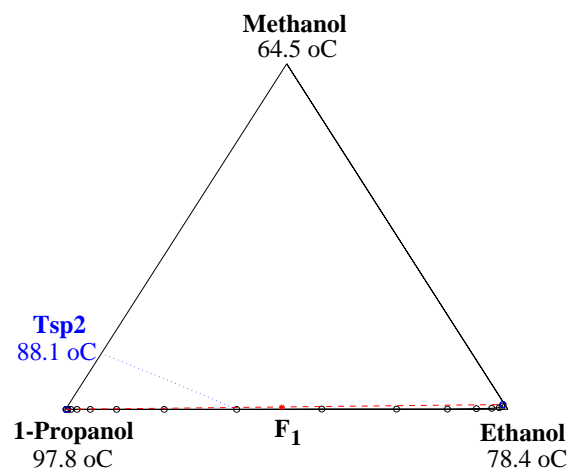
Table 7.3: Steady state data for closed middle vessel batch distillation of methanol, ethanol and 1-propanol illustrated in Figure 7.6.

	Condenser	Middle	Reboiler
Holdup [kmol]	1.757	1.765	1.763
$x_{Methanol}$	<b>0.987</b>	0.021	0.000
$x_{Ethanol}$	0.013	<b>0.975</b>	0.001
$x_{1-Propanol}$	0.000	0.004	<b>0.999</b>
Recovery %	<b>96.6</b>	<b>95.9</b>	<b>98.1</b>

For the cyclic column, the equimolar feed was mainly charged to the reboiler initially as given in Table 7.1. The resulting steady state composition profiles for each cycle are given in Figure 7.7. The corresponding steady state values of the vessel holdups and compositions and the product recovery are given in Table 7.4. After the first cycle, the condenser product was removed by emptying the condenser. Some residue of the first product component (methanol) still remains in the condenser and in the column section and this will contaminate the products of the second cycle. Therefore, an off-cut fraction was removed between the two cycles. This was done by closed operation with indirect level control where an off-cut fraction equal to the total column holdup in the condenser was accumulated in the condenser using the same controller parameters as for the second cycle. There are several (other) ways to remove the column holdup off-cut between the cycles. In practice, one would probably “blow-off” an off-cut fraction (i.e., open operation with no reflux) at the same time as the condenser vessel product of the first cycle is



(a) Cycle 1



(b) Cycle 2

Figure 7.7: Cyclic operation steady state column composition profiles for an equimolar initial feed of methanol, ethanol and 1-propanol (Cycle 1:  $x_{Fo} = [1/3, 1/3, 1/3]$ , Cycle 2:  $x_{F_1} = [0.006, 0.486, 0.508]$ ).

discharged into a product tank. It is also possible to simply drain the liquid in the column through an outlet between the cycles, but then the column profile must be rebuilt for the second cycle (i.e., a second start-up step in the cyclic conventional batch distillation operating procedure).

The feed of the second cycle ( $F_1$  in Figure 7.7b) is the composition in the reboiler residue. In addition, the liquid holdup in the column and condenser vessel should be included but the contribution to the overall feed composition is small due to the small column holdup in this study.

Table 7.4: Steady state data for cyclic batch distillation of methanol, ethanol and 1-propanol illustrated in Figure 7.7.

	Cycle 1		Cycle 2	
	Condenser	Off-Cut	Condenser	Reboiler
Holdup [kmol]	1.773	0.050	1.753	1.763
$x_{Methanol}$	<b>0.987</b>	0.501	0.014	0.000
$x_{Ethanol}$	0.013	0.498	<b>0.982</b>	0.001
$x_{1-Propanol}$	0.000	0.001	0.004	<b>0.999</b>
Recovery %	<b>97.3</b>	-	<b>95.9</b>	<b>98.1</b>

Both column alternatives show about the same separation performance for this specific simulation example. The cyclic column gives a slightly higher recovery of the first condenser product (methanol) and a higher purity but the same recovery of the second condenser product (ethanol) as compared to the middle vessel column. That is, a high purity saddle product (ethanol) is easier to obtain in the cyclic column. Furthermore, the removal of an off-cut fraction between the cycles (containing both methanol and ethanol) does not result in less recovery of the products.

In conclusion, for zeotropic mixtures separation, there seems to be not additional benefits of the closed middle vessel column (for the given number of equilibrium stages) compared to the cyclic operation of the regular batch column in terms of feasibility and separation performance. By “additional” we here mean in addition to the energy or time savings and ease of operation which were discussed in Chapter 6.

Our analysis and simulation results confirm that the assumption of constant relative volatility used in the study by Wittgens and Skogestad (1997) for the mixture methanol, ethanol and 1-propanol is acceptable and that the simple temperature set-points selection described in Section 7.5 (average boiling temperature of pair of the components) is satisfactory.



### 7.6.2 Results on ternary azeotropic mixture (Cell II)

In this section we consider the ternary azeotropic mixture of acetone, methanol and water which is given as an example mixture of elementary cell II (Serafimov's class 1.0-1a) in Figure 7.4. For mixtures of this class the composition space (or cell) is divided into two feed regions with different sets of possible steady state vessel products. This is illustrated by a straight line going from the azeotrope point to the zeotropic component vertex (water) in Figure 7.8 (that is, the secant between the opposite directed nodes in Cell II). Four different cases of initial feed composition and controller parameters for both the cyclic and the middle vessel column simulations are given in Table 7.5 where the parameter number indicates Cycle 1 and 2, or, section 1 and 2, respectively.

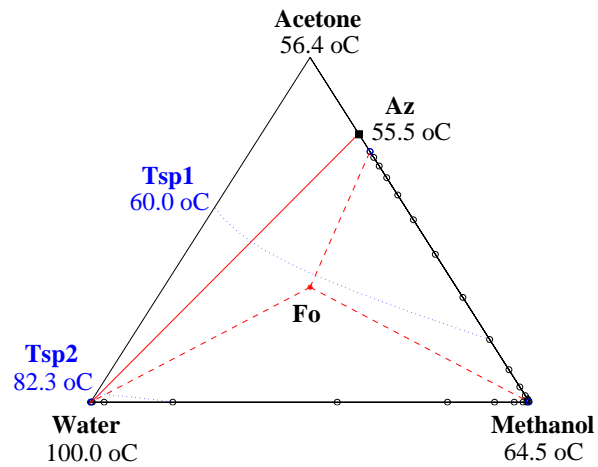
Table 7.5: Initial feed composition and controller parameters for acetone, methanol and water

Case 1:	$x_{F0} = [1/3, 1/3, 1/3]$ $K_{c,1} = 0.56 \text{ kmol/h}^\circ\text{C}, T_{sp,1} = 60.0^\circ\text{C}$ $K_{c,2} = 0.14 \text{ kmol/h}^\circ\text{C}, T_{sp,2} = 82.3^\circ\text{C}$
Case 1':	$x_{F0} = [0.6, 0.1, 0.3]$ $K_{c,1} = 0.56 \text{ kmol/h}^\circ\text{C}, T_{sp,1} = 60.0^\circ\text{C}$ $K_{c,2} = 0.14 \text{ kmol/h}^\circ\text{C}, T_{sp,2} = 82.3^\circ\text{C}$
Case 2:	$x_{F0} = [0.6, 0.1, 0.3]$ $K_{c,1} = 0.56 \text{ kmol/h}^\circ\text{C}, T_{sp,1} = 56.0^\circ\text{C}$ $K_{c,2} = 0.11 \text{ kmol/h}^\circ\text{C}, T_{sp,2} = 78.2^\circ\text{C}$
Case 3:	$x_{F0} = [1/3, 1/3, 1/3]$ $K_{c,1} = 0.56 \text{ kmol/h}^\circ\text{C}, T_{sp,1} = 56.0^\circ\text{C}$ $K_{c,2} = 0.11 \text{ kmol/h}^\circ\text{C}, T_{sp,2} = 78.2^\circ\text{C}$
Case 4:	$x_{F0} = [0.6, 0.1, 0.3]$ $K_{c,1} = 0.56 \text{ kmol/h}^\circ\text{C}, T_{sp,1} = 55.8^\circ\text{C}$ $K_{c,2} = 0.11 \text{ kmol/h}^\circ\text{C}, T_{sp,2} = 75.0^\circ\text{C}$

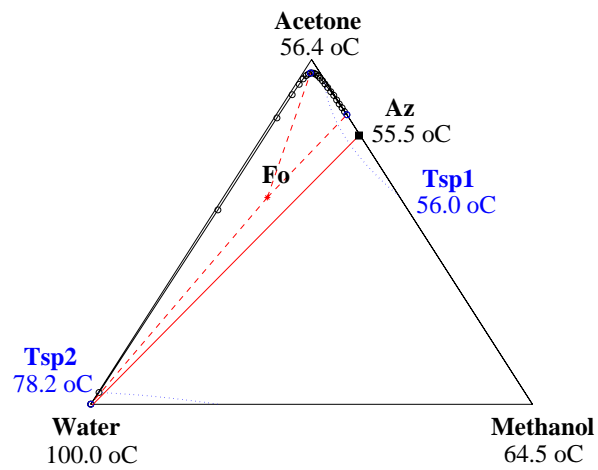
The steady state composition profiles along the middle vessel column are given for an initial feed in both feed regions in Figure 7.8 (Cases 1 and 2). The corresponding steady state values of the vessel holdups and compositions and the product recovery are given in Tables 7.8 and 7.7.

Table 7.6: Steady state data for closed middle vessel batch distillation of acetone, methanol and water (Case 1) illustrated in Figure 7.8a.

	Condenser	Middle	Reboiler
Holdup [kmol]	2.448	1.072	1.765
$x_{Acetone}$	<b>0.727</b>	0.001	0.000
$x_{Methanol}$	<b>0.273</b>	<b>0.998</b>	0.000
$x_{Water}$	0.000	0.001	<b>1.000</b>
Recovery %	<b>az</b>	<b>59.6</b>	<b>98.3</b>



(a) Lower feed region (Case 1)



(b) Upper feed region (Case 2)

Figure 7.8: Middle vessel column steady state composition profiles for two different locations of the feed composition of acetone, methanol and water (Case 1 and Case 2).

Table 7.7: Steady state data for closed middle vessel batch distillation of acetone, methanol and water (Case 2) illustrated in Figure 7.8b.

	Condenser	Middle	Reboiler
Holdup [kmol]	3.295	0.415	1.575
$x_{Acetone}$	<b>0.840</b>	<b>0.961</b>	0.000
$x_{Methanol}$	<b>0.160</b>	0.017	0.000
$x_{Water}$	0.000	0.022	<b>1.000</b>
Recovery %	<b>az</b>	<b>22.2</b>	<b>87.7</b>

If the feed is shifted from the lower feed region (Case 1) to the upper feed region without changing the temperature set-points (Case 1') there exists no steady state as illustrated in Figure 7.9. The indirect level controllers attempt to achieve products outside the material balance triangle of this feed region and the middle vessel runs empty. By simply changing the temperature set-points to

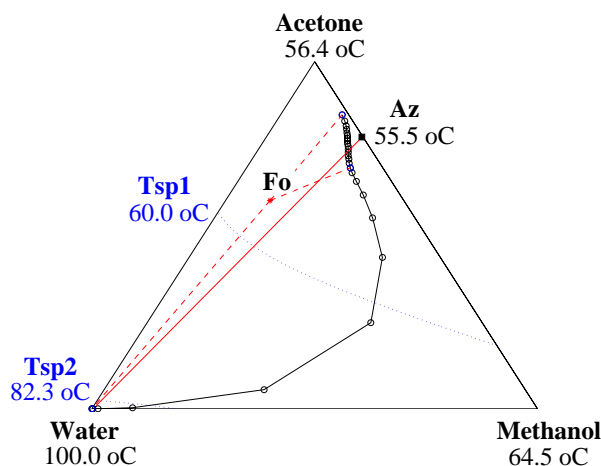


Figure 7.9: Infeasible temperature-set points for the middle vessel column with feed in the upper feed region (unsteady state composition profile at 1 hour and 50 minutes). The middle vessel runs empty (Case 1').

the mean boiling-point values of pair of the feasible products for this feed region (i.e., azeotrope, acetone and water for the upper feed region, Case 2), we achieve the steady state composition profile given in Figure 7.8b. Note that these temperature set-points (Case 2) are feasible for feeds in the lower feed region since the temperature specifications are feasible for this feed region as well (Case 3). The resulting steady state composition profile is given in Figure 7.10. In this manner, robust values of the temperature set-points may be chosen by inspection of the isotherms of the VLE diagram (isotherm map) if one expect variations in the feed composition of a mixture of this type (cell II). If the feed composition lies directly on the secant that divides the two feed regions, the middle vessel column performs a “binary” separation between the azeotrope and the

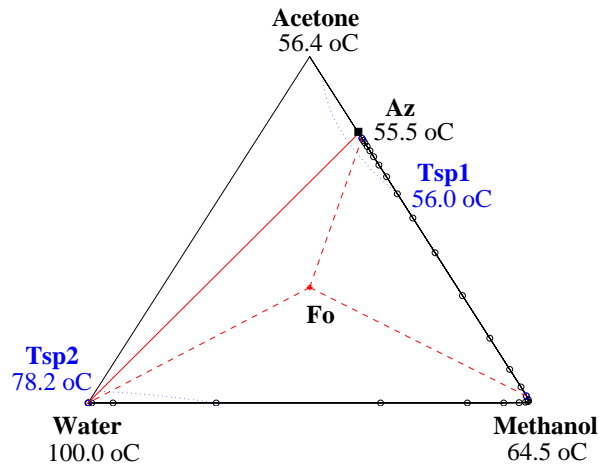


Figure 7.10: Middle vessel column steady state composition profile for an equimolar feed of acetone, methanol and water (Case 3).

water and we achieve zero holdup in the middle vessel. Each feed region of the composition triangle may be interpreted as a local Cell I, one with C-shaped distillation lines and the other with S-shaped distillation lines for this particular mixture.

Table 7.8: Steady state data for closed middle vessel batch distillation of acetone, methanol and water (Case 3) illustrated in Figure 7.10.

	Condenser	Middle	Reboiler
Holdup [kmol]	2.285	1.234	1.766
$x_{Acetone}$	<b>0.764</b>	0.020	0.000
$x_{Methanol}$	<b>0.236</b>	<b>0.979</b>	0.000
$x_{Water}$	0.000	0.001	<b>1.000</b>
Recovery %	<b>az</b>	<b>67.3</b>	<b>98.4</b>

For feeds located in the lower feed region, the temperature set-points in Case 3 result in a better separation performance (higher recovery but less purity of methanol) as compared to the temperature set-points in Case 1 because the distribution of the given number of equilibrium stages for each separation in the column sections is more favorable (split Az-methanol and split methanol-water). For feed located in the upper feed region, the separation is improved as compared to Case 2 by changing to the temperature set-points given in Case 4 for the same reasons. The steady state composition profile for Case 4 is given in Figure 7.11 and the corresponding steady state values of the vessel holdups and compositions and the product recovery are given in Table 7.9. Even this small change in the temperature set-points results in higher recoveries of both acetone and

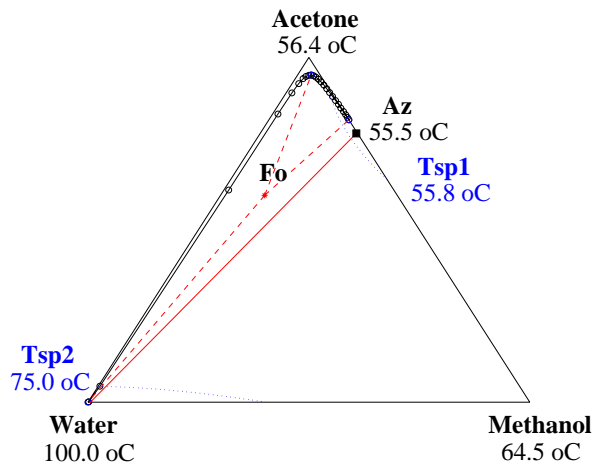


Figure 7.11: Middle vessel column steady state composition profile for an equimolar feed of acetone, methanol and water (Case 4).

water (as compared to Case 2). This demonstrates the importance of the proper choice of temperature set-points for the indirect level control strategy to obtain a specified separation (purity and recovery). The sensitivity is less if the number of equilibrium trays is significantly larger than the minimum number of trays required for the separation. For nonideal and azeotropic mixtures of Cell I and II (S-shape) it is not recommended to set the temperature set-points as the average boiling-point temperature of pair of the products for the given feed region.

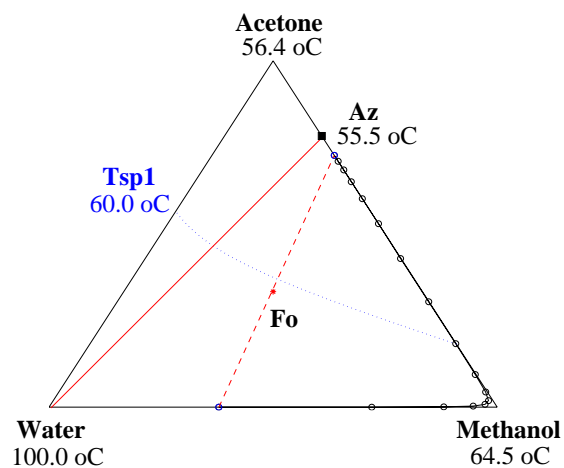
Table 7.9: Steady state data for closed middle vessel batch distillation of acetone, methanol and water (Case 4) illustrated in Figure 7.11.

	Condenser	Middle	Reboiler
Holdup [kmol]	2.788	0.930	1.567
$x_{Acetone}$	<b>0.819</b>	<b>0.949</b>	0.000
$x_{Methanol}$	<b>0.181</b>	0.031	0.000
$x_{Water}$	0.000	0.020	<b>1.000</b>
Recovery %	<b>az</b>	<b>27.3</b>	<b>97.0</b>

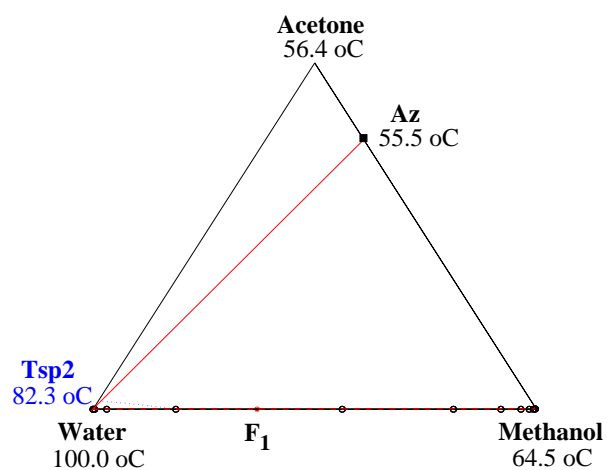
The steady state composition profiles for each cycle in the cyclic column for Case 1, 2, 3 and 4 in Table 7.5 are given in Figure 7.12, 7.13, 7.14 and 7.15. The corresponding steady state values for the vessel holdups and compositions and the product recovery are given in Tables 7.10, 7.11, 7.12 and 7.13. For feed in the lower feed region, the temperature set-points in Case 3 are better than the temperature set-points in Case 1 for the cyclic batch distillation process (higher recovery of methanol). For feed in the upper feed region, the temperature set-points in Case 4 is better than the temperature set-points in Case 2 (significant higher recovery of acetone). This is due to the

same reasoning as given for the middle vessel column, that is, these set-points result in a more favorable distribution of the equilibrium stages for the separations in each column section.

In conclusion, comparing the middle vessel and cyclic columns, we see that both columns show about the same separation performance in the lower feed region (Case 1 and 3). The distillation behavior in the lower feed region is similar to the methanol, ethanol, 1-propanol mixture (Cell I) discussed in the previous section. In the upper feed region (Case 2), the recovery of acetone and water are somewhat higher in the cyclic conventional (two-vessel) column as compared to the closed middle (three-vessel) vessel column.



(a) Cycle 1



(b) Cycle 2

Figure 7.12: Cyclic operation steady state composition profiles for an equimolar initial feed of acetone, methanol and water (Case 1:  $x_{F_o} = [1/3, 1/3, 1/3]$ ,  $x_{F_1} = [0.000, 0.370, 0.630]$ ).

Table 7.10: Steady state data for cyclic batch distillation of acetone, methanol and water (Case 1) illustrated in Figure 7.12.

	Cycle 1		Cycle 2	
	Condenser	Off-Cut	Condenser	Reboiler
Holdup [kmol]	2.448	0.050	1.075	1.765
$x_{Acetone}$	<b>0.727</b>	0.306	0.001	0.000
$x_{Methanol}$	<b>0.273</b>	0.694	<b>0.997</b>	0.000
$x_{Water}$	0.000	0.000	0.001	<b>1.000</b>
Recovery %	<b>az</b>	-	<b>59.7</b>	<b>98.3</b>

Table 7.11: Steady state data for cyclic batch distillation of acetone, methanol and water (Case 2) illustrated in Figure 7.13.

	Cycle 1		Cycle 2	
	Condenser	Off-Cut	Condenser	Reboiler
Holdup [kmol]	2.754	0.050	0.967	1.568
$x_{Acetone}$	<b>0.832</b>	0.897	<b>0.907</b>	0.000
$x_{Methanol}$	<b>0.167</b>	0.093	0.077	0.000
$x_{Water}$	0.001	0.010	0.016	<b>1.000</b>
Recovery %	<b>az</b>	-	<b>27.1</b>	<b>97.1</b>

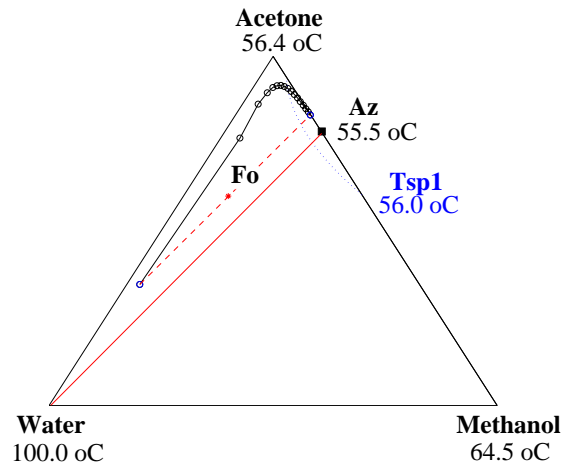
Table 7.12: Steady state data for cyclic batch distillation of acetone, methanol and water (Case 3) illustrated in Figure 7.14.

	Cycle 1		Cycle 2	
	Condenser	Off-Cut	Condenser	Reboiler
Holdup [kmol]	2.309	0.050	1.213	1.766
$x_{Acetone}$	<b>0.764</b>	0.495	0.006	0.000
$x_{Methanol}$	<b>0.236</b>	0.505	<b>0.993</b>	0.000
$x_{Water}$	0.000	0.000	0.001	<b>1.000</b>
Recovery %	<b>az</b>	-	<b>67.1</b>	<b>98.4</b>

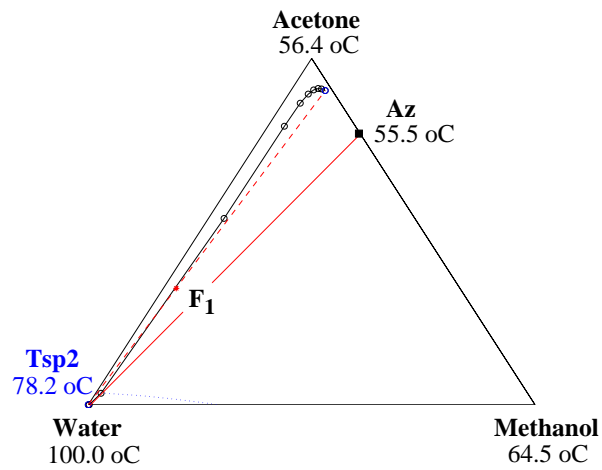
Table 7.13: Steady state data for cyclic batch distillation of acetone, methanol and water (Case 4) illustrated in Figure 7.15.

	Cycle 1		Cycle 2	
	Condenser	Off-Cut	Condenser	Reboiler
Holdup [kmol]	1.825	0.050	1.904	1.560
$x_{Acetone}$	<b>0.814</b>	0.869	<b>0.886</b>	0.000
$x_{Methanol}$	<b>0.186</b>	0.124	0.101	0.000
$x_{Water}$	0.000	0.007	0.014	<b>1.000</b>
Recovery %	<b>az</b>	-	<b>52.2</b>	<b>96.6</b>



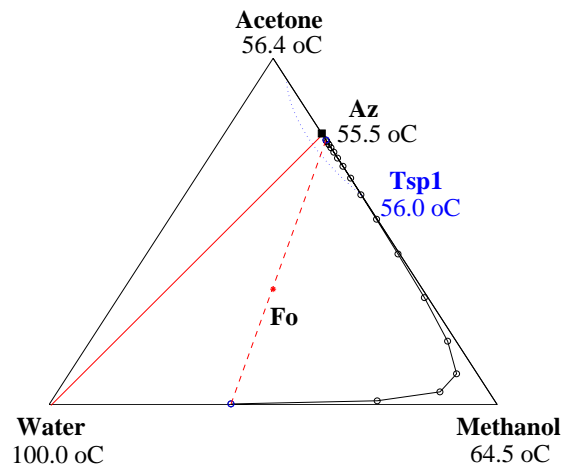


(a) Cycle 1

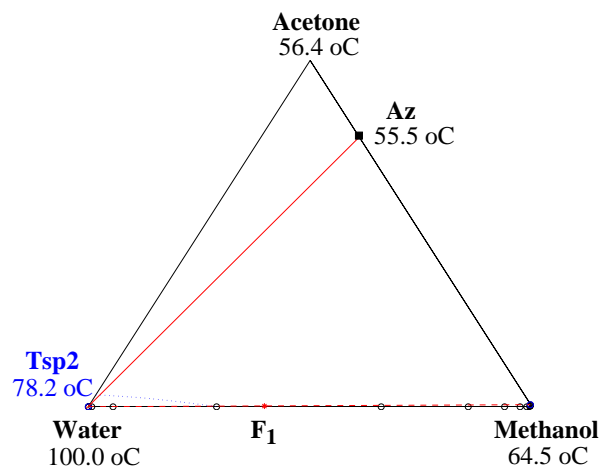


(b) Cycle 2

Figure 7.13: Cyclic operation steady state composition profiles for an upper feed region initial feed of acetone, methanol and water (Case 2:  $x_{F_0} = [0.6, 0.1, 0.3]$ ,  $x_{F_1} = [0.336, 0.029, 0.635]$ ).

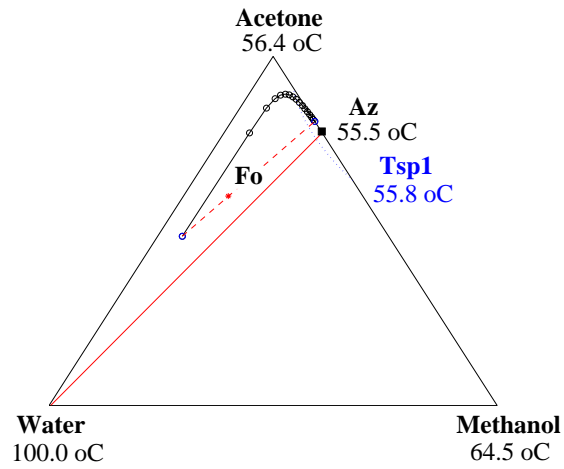


(a) Cycle 1

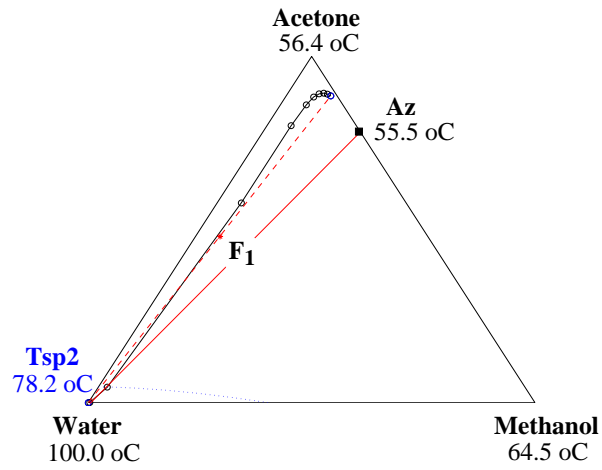


(b) Cycle 2

Figure 7.14: Cyclic operation steady state composition profiles for an equimolar initial feed of acetone, methanol and water (Case 3:  $x_{F_0} = [1/3, 1/3, 1/3]$ ,  $x_{F_1} = [0.002, 0.396, 0.602]$ ).



(a) Cycle 1



(b) Cycle 2

Figure 7.15: Cyclic operation steady state composition profiles for an upper feed region initial feed of acetone, methanol and water (Case 4:  $x_{F_0} = [0.6, 0.1, 0.3]$ ,  $x_{F_1} = [0.480, 0.055, 0.465]$ ).

### 7.6.3 Results on ternary azeotropic mixture with one distillation boundary

In this section we consider the ternary azeotropic mixture of acetone, chloroform and benzene which is given as an example mixture where a distillation line boundary splits the VLE diagram into two elementary cell I's (Serafimov's class 1.0-2) shown in Figure 7.5. This example is interesting because it clearly demonstrates an important difference between the closed middle vessel column separation and the cyclic column separation in terms of separation feasibility (feasible vessel products). Three different cases of initial feed composition and controller parameters for both the cyclic column and the middle vessel column were considered and the results are given in Table 7.14. The parameter number indicates Cycle 1 and 2, or, column section 1 and 2, respectively.

Table 7.14: Initial feed composition and controller parameters for acetone, chloroform and benzene

Case 1:	$x_{F0} = [1/3, 1/3, 1/3]$
	$K_{c,1} = 0.63 \text{ kmol/h}^\circ\text{C}, T_{sp,1} = 60.4^\circ\text{C}$
	$K_{c,2} = 0.32 \text{ kmol/h}^\circ\text{C}, T_{sp,2} = 72.3^\circ\text{C}$
Case 2:	$x_{F0} = [0.15, 0.05, 0.80]$
	$K_{c,1} = 0.63 \text{ kmol/h}^\circ\text{C}, T_{sp,1} = 60.4^\circ\text{C}$
	$K_{c,2} = 0.32 \text{ kmol/h}^\circ\text{C}, T_{sp,2} = 72.3^\circ\text{C}$

The steady state composition profile in the middle vessel column for Case 1 and 2 is given in Figure 7.16 and 7.17. The corresponding steady state values for the vessel holdups and compositions and the product recovery are given in Table 7.15 and 7.16.

In the closed middle vessel column the three vessel products are bounded within one distillation line region (cell) and it is not possible to cross a distillation line boundary. The distillation behavior of this class of mixture within one cell of the composition triangle is similar to the behavior of other mixtures of elementary cell I, as for example the mixture of methanol, ethanol, 1-propanol considered in the previous section. The azeotrope forms a saddle of the cell I and acts like a "pseudo-component". The purity of the vessel products for the same given temperature set-points is independent of the initial feed composition within one distillation line region (cell). This confirms the flexibility of the indirect level control strategy based on temperature feedback control as stated by Skogestad *et al.* (1997).

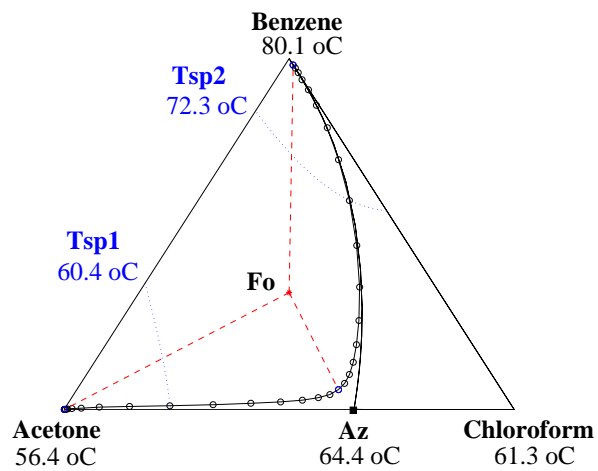


Figure 7.16: Middle vessel column steady state composition profile for an equimolar feed of acetone, chloroform and benzene (Case 1).

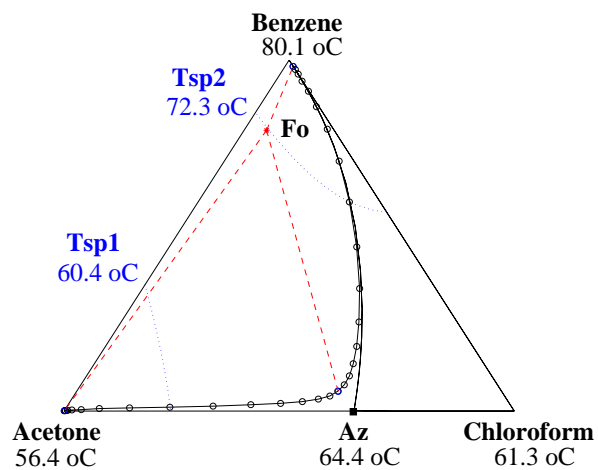


Figure 7.17: Middle vessel column steady state composition profile for a benzene-rich feed of acetone, chloroform and benzene (Case 2).

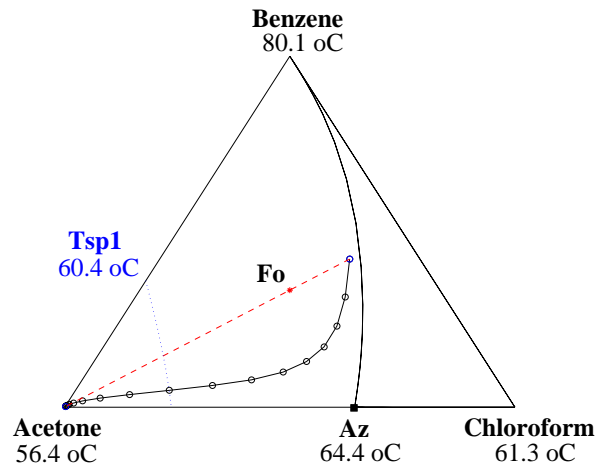
Table 7.15: Steady state data for closed middle vessel batch distillation of acetone, chloroform and benzene (Case 1) illustrated in Figure 7.16.

	Condenser	Middle	Reboiler
Holdup [kmol]	1.670	2.990	1.625
$x_{Acetone}$	<b>0.999</b>	<b>0.362</b>	0.000
$x_{Chloroform}$	0.0005	<b>0.581</b>	0.018
$x_{Benzene}$	0.0005	0.057	<b>0.982</b>
Recovery %	<b>92.9</b>	<b>az</b>	<b>88.9</b>

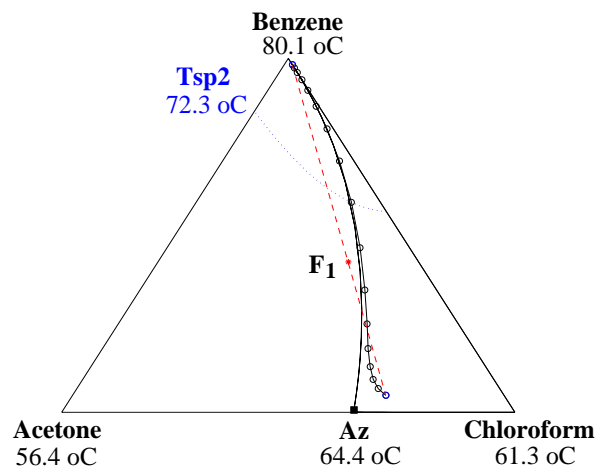
Table 7.16: Steady state data for closed middle vessel batch distillation of acetone, chloroform and benzene (Case 2) illustrated in Figure 7.17.

	Condenser	Middle	Reboiler
Holdup [kmol]	0.665	0.279	4.341
$x_{Acetone}$	<b>0.999</b>	<b>0.363</b>	0.000
$x_{Chloroform}$	0.0005	<b>0.581</b>	0.018
$x_{Benzene}$	0.0005	0.056	<b>0.982</b>
Recovery %	<b>82.2</b>	<b>az</b>	<b>99.0</b>

The steady state composition profile for each cycle in the cyclic column for Case 1 and 2 are given in Figure 7.18 and 7.19. The corresponding steady state values for the vessel holdups and compositions and the product recovery are given in Table 7.17 and 7.18. In both cases, the first condenser product (acetone) is discharged after the first cycle and an off-cut fraction equal to the column holdup is taken out between the cycles.



(a) Cycle 1



(b) Cycle 2

Figure 7.18: Cyclic operation steady state composition profiles for an equimolar initial feed of acetone, chloroform and benzene (Case 1:  $x_{F_0} = [1/3, 1/3, 1/3]$ ,  $x_{F_1} = [0.425, 0.420, 0.155]$ ).

Table 7.17: Steady state data for cyclic batch distillation of acetone, chloroform and benzene (Case 1) illustrated in Figure 7.18.

	Cycle 1		Cycle 2	
	Condenser	Off-Cut	Condenser	Reboiler
Holdup [kmol]	1.102	0.050	2.514	1.672
$x_{Acetone}$	<b>0.997</b>	0.734	<b>0.261</b>	0.000
$x_{Chloroform}$	0.000	0.235	<b>0.690</b>	0.018
$x_{Benzene}$	0.002	0.032	0.048	<b>0.982</b>
Recovery %	<b>61.0</b>	-	<b>az</b>	<b>91.5</b>

For the benzene-rich initial feed (Case 2) given in Figure 7.19, the first cycle bottoms product, which becomes the (reboiler) feed of the second cycle, lies on the binary edge of the composition triangle between chloroform and benzene. Thus, the second cycle of the cyclic conventional batch distillation process achieves chloroform as condenser product even if the initial feed to the process lies in the other distillation line region (cell). Note however that only small amounts of this second condenser product are recovered since the column feed of the second cycle mainly contains benzene. This is of theoretical interest only and included to illustrate the principal difference between the cyclic conventional batch distillation process and the closed middle vessel distillation in terms of feasible vessel products.

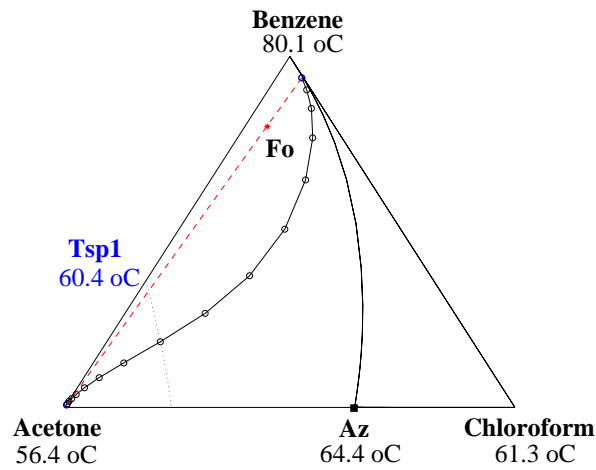
Comparing the separation in the closed middle vessel column with the separation in the cyclic column, we see that for Case 1 the middle vessel column has better performance since it achieves a higher acetone recovery even though less benzene recovery. Both columns achieves the azeotrope (saddle) as the intermediate product fraction. For Case 2, however, the separation in the cyclic column is much better since it achieves a higher acetone recovery, the same benzene recovery and, in addition, some chloroform is recovered (no azeotrope fraction).

Table 7.18: Steady state data for cyclic batch distillation of acetone, chloroform and benzene (Case 2) illustrated in Figure 7.19.

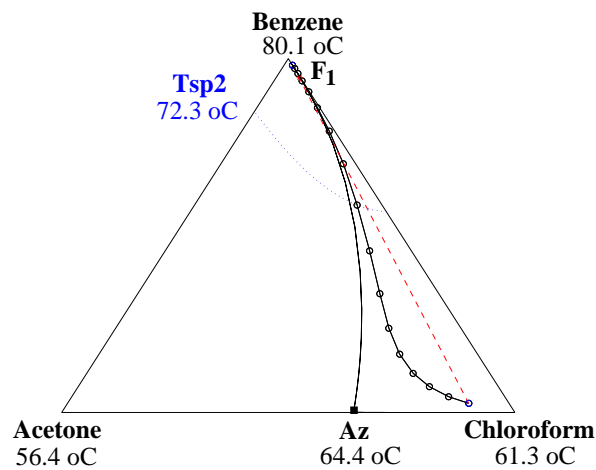
	Cycle 1		Cycle 2	
	Condenser	Off-Cut	Condenser	Reboiler
Holdup [kmol]	0.768	0.050	0.170	4.349
$x_{Acetone}$	<b>0.992</b>	0.589	0.089	0.000
$x_{Chloroform}$	0.000	0.340	<b>0.884</b>	0.019
$x_{Benzene}$	0.007	0.071	0.026	<b>0.981</b>
Recovery %	<b>93.9</b>	-	<b>55.8</b>	<b>99.0</b>

In the cyclic column only pair of the vessel products are bounded within one distillation line region and the column may operate in two different distillation line regions (cells) dependent on the column feed composition for each cycle. Due to the curved distillation line boundary of this particular mixture, the cyclic operation is able to cross the distillation line boundary and





(a) Cycle 1



(b) Cycle 2

Figure 7.19: Cyclic operation steady state composition profiles for a benzene-rich initial feed of acetone, chloroform and benzene (Case 2:  $x_{F_o} = [0.15, 0.05, 0.80]$ ,  $x_{F_1} = [0.946, 0.052, 0.002]$ ).

separate the mixture into its pure components. When the feed lies within a certain region of the composition space (i.e., in the area between the convex side of the distillation line boundary and the straight line going from the benzene node to the azeotrope saddle), the material balance line may cross the curved distillation line boundary as shown in Figure 7.18 (b). This is known from

continuous azeotropic distillation and may be utilized in separating azeotropic mixtures of this class into its pure components if the distillation line boundary is sufficiently curved (see Chapter 2). The indirect split of the cyclic column (i.e., where the benzene is the first reboiler product and discharged between the cycles) would not yield this “crossing” of the distillation line boundary.

## 7.7 Discussion and suggestions for further research

- *Heteroazeotropic closed multivessel column:* It would be interesting to consider heteroazeotropic distillation-decanter hybrids in the closed multivessel batch column. For example, a process where a heteroazeotropic mixture of Serafimov’s class 1.0-1b is separated in a two-vessel batch column where the upper vessel is a decanter. A mixture system that might be suitable for this scheme is the close-boiling zeotropic mixture acetic acid and water using ethyl acetate or butyl acetate as entrainer. The process is illustrated in Figure 7.20. During the closed operation there would then be a gradual accumulation of the water-

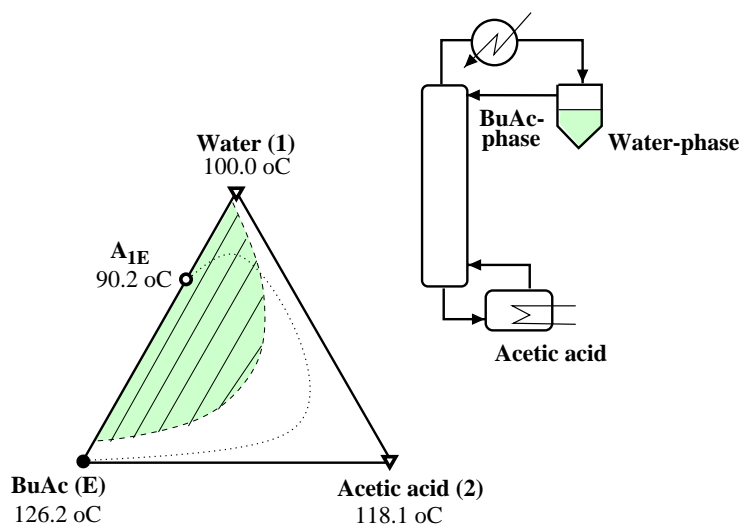


Figure 7.20: *Heteroazeotropic distillation-decanter hybrid in the closed two-vessel batch column for the ternary mixture acetic acid - water - butyl acetate with one binary heteroazeotrope (Class 1.0-1b).*

phase in the decanter (water product vessel), and the ethyl acetate phase could be recycled in the column until (nearly) steady state. Acetic acid would be obtained in the bottom reboiler vessel. This may be a promising alternative to the continuous process for small-scale industries.

- *Multiple steady states*: An issue that might be interesting to look more carefully into is the possibility of multiplicities in the closed middle vessel column.
  - For a given “purity” specification of the azeotrope product fraction (marked by a half-circle around the azeotropic point in Figure 7.21), there may be a certain region in the composition space where the same set of temperature set-points and feed composition yield different product sets (i.e., output multiplicity).

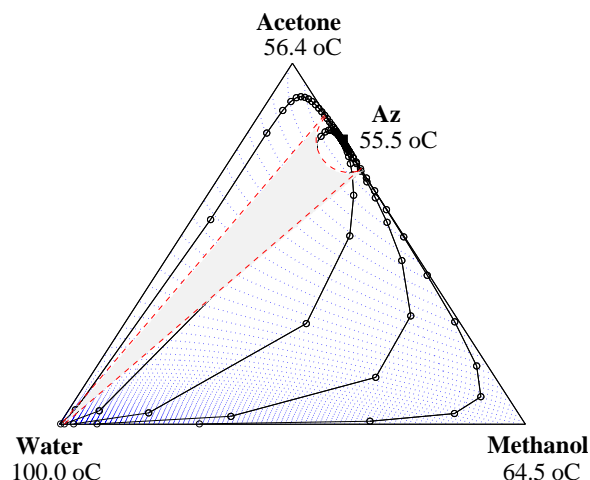


Figure 7.21: *Multiplicity for a certain feed region (gray area) is an open question. Azeotropic mixture of elementary cell II (Serafimov’s class 1.0-1a): Distillation lines (solid lines with open circles) and liquid isotherms (dotted) for the ternary azeotropic mixture of acetone, methanol and water at atmospheric pressure.*

- Analysis (and simulation study) of mixtures of the elementary cells III (U-shape) and IV (S/C and U-shape), see Chapter 4, in terms of batch columns operation in general and multiplicities in particular are also issues that should be addresses.
- *Extension to open operation*: There are many azeotropic distillation schemes that may be performed in the (open) middle vessel batch column. Recently, Warter and Stichlmair (2000) studied the scheme with recycle of (saddle) azeotrope to cross curved boundaries in the open (finite reflux) middle vessel batch distillation column. Cheong and Barton (1999a; 1999b; 1999c) gave extensive details on the geometric interpretation of the middle vessel column for distillation of ternary azeotropic mixtures in line with the work by Davidyan and Kiva and coworkers (see Chapter 6 and the reference list). They show that the middle vessel column (open operation) have the same possibilities and limitations as ordinary continuous distillation for azeotropic mixtures (e.g. crossing of curved distillation line boundaries at finite reflux described in Chapter 2).

## 7.8 Conclusion

For the closed operating policy considered in this paper including cyclic operations and middle vessel column, the feasibility analysis based on distillation lines applies directly to the steady state (as time approaches infinity) composition profile. The steady state compositions in the vessels are connected by a distillation line and must satisfy the material balance. Azeotropic mixtures of Class 1.0-1a (Cell II) and Class 1.0-2 (two Cell I's) cannot be separated in a single closed operation. However, cyclic batch distillation may in some cases be used to achieve products in two different distillation regions.

The indirect level control strategy based on single temperature feedback control loops eliminates the need for pre-calculated vessel holdups and makes both the closed and cyclic operating policies flexible and simple to implement in practice. The main differences between zeotropic and azeotropic mixtures is that for zeotropic mixtures one set of temperature set-points gives the same product sets for any feed composition whereas for azeotropic mixtures different temperature set-points are required for various feed compositions. Thus, if the mixture to be separated is azeotropic, the proper choice of temperature set-points is crucial in order to obtain the desired set of steady state vessel products. Isotherms maps may advantageously be used as a graphical tool in determination of the temperature set-points for the indirect level control strategy.

## Appendix 7A

The dynamic model of the closed multivessel batch distillation column (with two and three vessels) used in the simulations presented in this paper is based on the following assumptions:

- Staged distillation column sections (trays numbered from the top to the bottom)
- Perfect mixing and VLE on all trays and in all vessels
- Negligible vapor holdup
- Constant molar liquid holdups on all trays (i.e., neglecting liquid dynamics)
- Constant molar vapor flows (i.e., simplified energy balance)
- Constant pressure
- Total condenser
- Ideal behavior in the vapor phase

Note that the vapor flow does not pass through the intermediate vessels in our model of the multivessel column. Thus, the total number of equilibrium trays the closed middle vessel column shown in Figure 7.2 is  $N_1 + N_2 + 1$  (inclusive the reboiler).

### Material balances over

total condenser:

$$\frac{dH_D}{dt} = V_1 - L'_D, \quad (7.8)$$

$$\frac{d(H_D x_D)}{dt} = V_1 y_1 - L'_D x_D \quad (7.9)$$

tray  $j = 1, \dots, N_1$  in column section 1:

$$0 = L_{j-1} + V_{j+1} - L_j - V_j, \quad (7.10)$$

$$H_j \frac{dx_j}{dt} = L_{j-1} x_{j-1} + V_{j+1} y_{j+1} - L_j x_j - V_j y_j \quad (7.11)$$

middle vessel:

$$\frac{dH_M}{dt} = L_{N_1} - L'_M, \quad (7.12)$$

$$\frac{d(H_M x_M)}{dt} = L_{N_1} x_{N_1} - L'_M x_M \quad (7.13)$$

tray  $j = 1, \dots, N_2$  in column section 2:

$$0 = L_{j-1} + V_{j+1} - L_j - V_j, \quad (7.14)$$

$$H_j \frac{dx_j}{dt} = L_{j-1} x_{j-1} + V_{j+1} y_{j+1} - L_j x_j - V_j y_j \quad (7.15)$$

total reboiler:

$$\frac{dH_B}{dt} = L_{N_2} - V_B, \quad (7.16)$$

$$\frac{d(H_B x_B)}{dt} = L_{N_2} x_{N_2} - V_B y_B \quad (7.17)$$

The cyclic conventional (two-vessel) column shown in Figure 7.1 has only one column section and is described by Equations (7.8), (7.9), (7.10), (7.11), (7.16) and (7.17).

### Indirect level control

The liquid reflux out of the condenser and middle vessel ( $L_D$  and  $L_M$ , respectively) are given by the proportional controller in Eq. 7.5. In addition, we do not allow a vessel to be completely empty. If a vessel holdup decreases towards zero the liquid reflux out of that particular vessel is decreased, or, in the limit, turned off to accumulate material in the vessel. To achieve a soft “turn off” the liquid reflux determined by the controller is modified by an exponential function (Furlonge *et al.*, 1999):

$$L' = L \left[ 1 - \exp\left(-\frac{H}{H_{min}}\right) \right] \quad (7.18)$$

where  $L'$  is the manipulated liquid reflux (i.e.,  $L'_D$  and  $L'_M$  in Equations (7.8)-(7.9) and Equations (7.12)-(7.13),  $L$  is the controller-determined liquid reflux given by Equation (7.5),  $H$  is the liquid holdup in the current vessel and  $H_{min}$  is a selected minimum value of the liquid holdup.

**Vapor-liquid equilibrium** for component  $i = 1, \dots, n$

$$y_i P = x_i \gamma_i^L(T, \mathbf{x}) P_i^{sat}(T) \quad (7.19)$$

where  $P = 1$  atm in all the simulations presented in this article and

$$\sum_{i=1}^n y_i = 1 \quad (7.20)$$

The vapor pressures were calculated by the Antoine equation:

$$\log_{10} P_i^{sat} = A_i - \frac{B_i}{T + C_i} \quad (7.21)$$

where  $P_i^{sat}$  is in *mmHg* and  $T$  in  $^{\circ}C$ . The liquid activity coefficients were calculated by the Wilson equation:

$$\ln \gamma_i^L = 1 - \ln \left( \sum_{j=1}^n x_j \Lambda_{ij} \right) - \sum_{k=1}^n \left( \frac{x_k \Lambda_{ki}}{\sum_{j=1}^n x_j \Lambda_{kj}} \right), \quad (7.22)$$

$$\Lambda_{ij} = \frac{V_j}{V_i} \exp \left( \frac{-A_{ij}}{RT} \right) \quad (7.23)$$

where  $V_j$  is in  $\text{cm}^3/\text{mol}$ ,  $A_{ij}$  in  $\text{cal}/\text{mol}$  and  $T$  in  $K$ . We use parameters for the Antoine and Wilson equations and liquid molar volumes reported in Gmehling et al. (1977-1990), as listed in Table 7.19.

Table 7.19: Thermodynamic data for the example mixtures<sup>a</sup>

Class 0.0-1		Parameters for the Antoine Equation			$V_i$ [ $\frac{\text{cm}^3}{\text{mol}}$ ]
	A	B	C		
(1) Methanol	8.08097	1582.271	239.726	40.73	
(2) Ethanol	8.11220	1592.864	226.184	58.68	
(3) 1-Propanol	8.37895	1788.020	227.438	75.14	
<u>Binary Interaction Parameters for the Wilson Equation</u>					
	$A_{11} = 0$	$A_{12} = 135.8113$	$A_{13} = 397.4862$		
	$A_{21} = -132.0576$	$A_{22} = 0$	$A_{23} = 102.6706$		
	$A_{31} = -265.4397$	$A_{32} = -40.8745$	$A_{33} = 0$		
Class 1.0-1a		Parameters for the Antoine Equation			$V_i$ [ $\frac{\text{cm}^3}{\text{mol}}$ ]
	A	B	C		
(1) Acetone	7.63132	1566.69	273.419	74.05	
(2) Methanol	8.08097	1582.271	239.726	40.73	
(3) Water	8.01767	1715.70	234.268	18.01	
<u>Binary Interaction Parameters for the Wilson Equation</u>					
	$A_{11} = 0$	$A_{12} = -161.8813$	$A_{13} = 489.3727$		
	$A_{21} = 583.1054$	$A_{22} = 0$	$A_{23} = 19.2547$		
	$A_{31} = 1422.849$	$A_{32} = 554.0494$	$A_{33} = 0$		
Class 1.0-2		Parameters for the Antoine Equation			$V_i$ [ $\frac{\text{cm}^3}{\text{mol}}$ ]
	A	B	C		
(1) Benzene	6.87987	1196.760	219.161	89.41	
(2) Chloroform	6.95465	1170.966	226.232	80.67	
(3) Acetone	7.11714	1210.595	229.664	74.05	
<u>Binary Interaction Parameters for the Wilson Equation</u>					
	$A_{11} = 0$	$A_{12} = 49.6010$	$A_{13} = 34.7648$		
	$A_{21} = -161.8065$	$A_{22} = 0$	$A_{23} = -485.5470$		
	$A_{31} = 240.8594$	$A_{32} = 28.4509$	$A_{33} = 0$		

<sup>a</sup> From Gmehling et al. (1977-1990), *VLE Data Collection*, DECHEMA series, at atmospheric pressure.





## Chapter 8

# Extractive Batch Distillation: Column Schemes and Operation

*Preliminary version presented at AIChE Annual Meeting, Los Angeles, November 1997*

This chapter focuses on the use of extractive batch distillation for separating binary minimum-boiling homoazeotropic mixtures. We consider entrainers that are high-boiling, miscible and zeotropic with the original mixture components. We compare conventional extractive batch distillation and the middle vessel extractive batch distillation, both with semicontinuous entrainer feed. The effect of the column configuration on the operation is evaluated, and the performance of two principally different operating policies (simultaneous and sequential) for the middle vessel column are considered. Insight into continuous extractive distillation operation is extended to describe the instantaneous conditions during batch operation.

### 8.1 Introduction

Extractive distillation is widely used in the chemical and petrochemical industries, and continuous processes are well described in the literature (see for example Hoffman (1964), Van Winkle (1967) and Perry and Chilton (1973)). In this study we consider batch operation of the extractive distillation scheme for which the knowledge on design and operation is limited. The inherent dynamics of batch operation introduces new aspects to the extractive distillation process as compared to continuous operation.

Extractive distillation in the conventional batch column is shown in Figure 8.1. Kogan (1971) described a laboratory unit of extractive batch distillation and pointed out the disadvantage of increasing entrainer dilution of the still pot (reboiler) during the operation. In a series of pa-

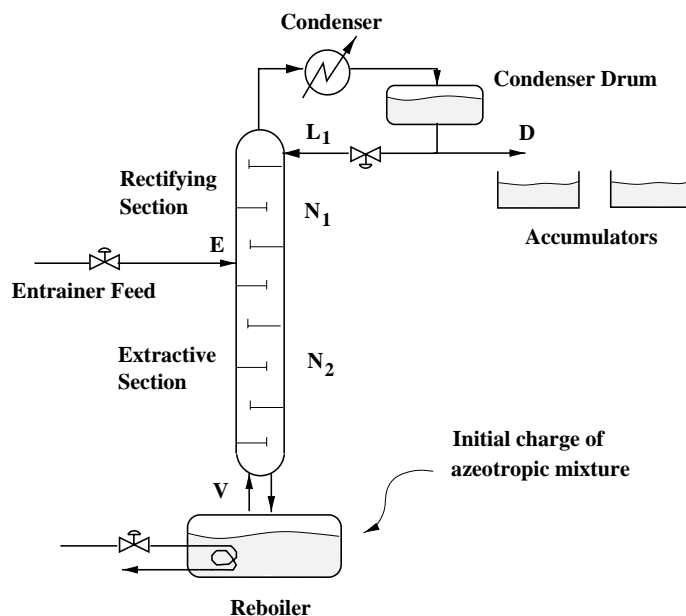


Figure 8.1: Conventional extractive batch distillation column.

pers, Yatim and Lang and coworkers (1993; 1994; 1995) gave experimental as well as dynamic simulation results on the operation of extractive distillation in the conventional batch column.

The column scheme in Figure 8.1 has two main disadvantages caused by accumulation of the entrainer in the reboiler: (i) operational problems due to filling, and (ii) decreased separation efficiency during operation. One potential way to overcome these problems is to use the middle vessel column shown in Figure 8.2, which closely resembles continuous extractive distillation except that the operation is batchwise (dynamic) and that the separation may be performed in one column rather than in a column sequence. The middle vessel implementation is potentially more energy efficient than the conventional scheme due to the combination of a rectifying-extraction section and a stripping section in one column.

Safrit *et al.* (1995; 1997b) studied extractive batch distillation in the middle vessel column for the separation of acetone and methanol using water as entrainer. Water was continuously removed as a bottom product and recycled to the process. They compared the separation performance of this process with the conventional extractive batch distillation column. The extractive middle vessel distillation column showed better performance with regard to energy consumption. The study also showed that the performance of the separation is sensitive to the entrainer feed flowrate, as known from continuous operation, and to the switching times between fractions in the batch operation. The constant product composition policy were considered, achieving a desired purity in the distillate and bottom product. They proposed an algorithm to “steer” the middle vessel

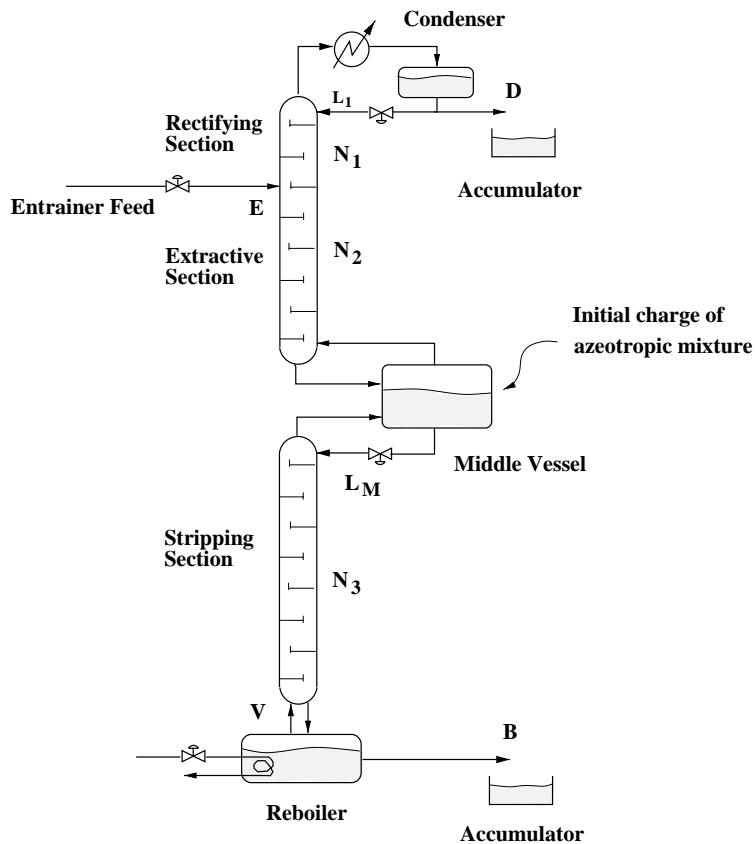


Figure 8.2: Middle vessel extractive batch distillation column (basic configuration with liquid and vapor flow through the middle vessel).

(liquid) composition by manipulating the reflux, reboil and entrainer feed flowrate so as to balance the two opposite directed effects of product removal.

Düssel and Stichlmair (1995) discussed the extractive distillation in the conventional batch column and its relation to the ternary VLE diagram distillation lines. In a succeeding paper, Warter *et al.* (1997) gave simulation results for conventional extractive batch distillation schemes with two different operating policies; constant reflux and constant distillate composition (both with constant entrainer feeding). They studied the influence of operating parameters such as reflux ratio and entrainer feed flowrate on the process performance for the mixture ethanol and water using ethylene glycol as entrainer. The same separation results in terms of purity and recovery were achieved with high entrainer flowrate and low reflux ratio as well as with low entrainer flowrate and high reflux ratio. The ethanol recovery was found to be sensitive to the purity of the entrainer feed. A high water impurity in the entrainer could be compensated by an increase in

the reflux ratio in order to achieve the same separation results. Köhler *et al.* (1995) provided an interesting industrial example of combined heteroazeotropic and extractive distillation performed in a conventional batch column and decanter.

Warter and Stichlmair (1999) studied extractive batch distillation in both the conventional column and the middle vessel column. The mixture system of ethanol and water using ethylene glycol as entrainer was considered. The middle vessel column was found to be superior to the conventional batch extractive distillation column in terms of energy demand. Furthermore, they suggested a modification of the middle vessel column arrangement where the liquid stream from the extractive section bypasses the middle vessel and enters directly the stripping section (see the liquid bypass configuration in Figure 8.17). This configuration had better performance in terms of separation performance and energy demand. They were able to achieve simultaneous ethanol and ethylene glycol production and pure water in the middle vessel at the end of operation. This is explained by the fact that ethylene glycol has very low volatility and thus remains almost completely in the liquid phase. Thus, negligible amounts of ethylene glycol enters the middle vessel in the vapor stream from the stripping section in this modification of the column.

Dynamic optimization of the complete extractive batch distillation process was reported by Mujtaba (1999). For the mixture acetone-methanol-water the best performance was found when the entrainer was introduced as a semicontinuous feed to the column section and not as a batch charge to the reboiler. They optimized piecewise constant reflux ratio and entrainer feed flowrate for each operating step (minimum time and maximum profit objective functions), but did not compare the results with previous work. Milani (1999) considered batch extractive distillation of acetone and methanol where the water entrainer was charged directly to the reboiler. Large quantities of the entrainer was needed in order to achieve high purity acetone in the distillate.

Previous studies on continuous extractive distillation have shown that there is a maximum as well as a minimum reflux ratio ( $L_1/D$ ) to make the separation feasible (Andersen *et al.*, 1995; Laroche *et al.*, 1993). High reflux (high internal flows) may be harmful in extractive distillation because it decreases the entrainer concentration in the extractive column section. If the desired purity of the distillate product requires high reflux one may have to purify the distillate fraction in a subsequent operation. Similarly, there is a maximum as well as a minimum entrainer feed ratio to make the separation feasible. Thus, there is a trade-off between the entrainer feed flowrate and the reflux and reboil ratios.

The entrainer load to the column is an important variable in effective separation. A very rough rule of thumb for continuous extractive distillation is to use 1 to 4 moles of entrainer per mole of feed (Schweitzer, 1997). However, the actual value must be determined by experiment or by computer simulation (and possibly optimization).

In this paper two main configurations are considered: (1) conventional extractive batch distillation column (also called an extractive batch rectifier); and (2) middle vessel extractive batch distillation column (an extractive batch rectifier and a batch stripper combined with a middle vessel). The columns are operated “open-loop”, that is, with no feedback control of compositions (or temperatures). These results are then rather sensitive to the operating parameters such as entrainer flowrate and reflux. The values were found by trial-and-error and are by no means optimal.

## 8.2 Mixtures studied

The following two mixture systems are studied in this paper:

System 1: ethanol (1) and water (2) + ethylene glycol entrainer (E); (easy separation)

System 2: acetone (1) and methanol (2) + water entrainer (E); (more difficult separation)

### System 1 (ethanol - water - ethylene glycol)

Extractive distillation of ethanol and water using ethylene glycol as an entrainer (System 1) is a classical example in the distillation literature. The mixture was chosen mainly because it is easy to find comparable examples in the distillation literature. This separation also represents a typical separation task in the fine- and specialty chemical industries. The residue curve map is shown in Figure 8.3. Ethanol and water form a minimum-boiling azeotrope rich in ethanol. The binary

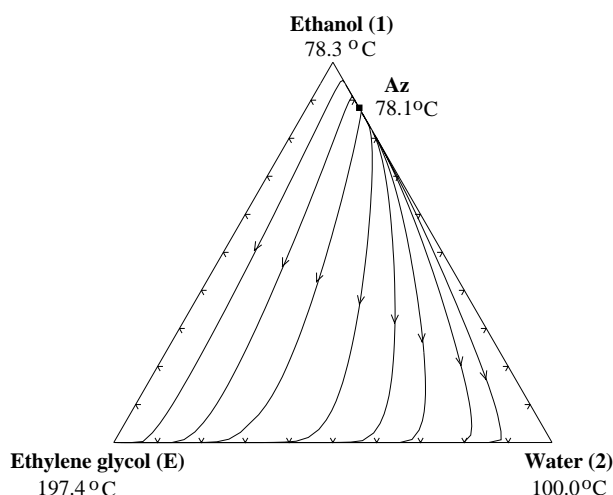


Figure 8.3: Residue curve map for the ternary azeotropic mixture ethanol, water and ethylene glycol (System 1) at 1 atm (from ASPEN PLUS<sup>TM</sup>).

azeotropic composition is 89.3 mole % ethanol at 1 atm (Horsley, 1973). By adding ethylene glycol, the relative volatility between ethanol and water becomes larger than one and separation into pure components by distillation is possible. Note the large boiling-point differences between the ethylene glycol entrainer (E) and the azeotrope constituents ethanol (1) and water (2):  $\Delta T_{E-1} = 119.1^\circ\text{C}$  and  $\Delta T_{E-2} = 97.4^\circ\text{C}$ . Hence, the separation of ethanol and water from ethylene glycol by distillation is relatively easy and requires only a few number of equilibrium trays and low reflux. Due to the very large relative volatility between ethanol and ethylene glycol

it is sufficient with only one or a few equilibrium trays in the rectifying section of the extractive distillation column.

### System 2 (acetone - methanol - water)

The importance and effect of the rectifying section and the reflux ratio are better illustrated by the acetone and methanol separation using water as entrainer (System 2). This is the standard industrial method for separating acetone from methanol using water as entrainer. Water has a greater affinity to methanol, the more polar of the pair, so the relative volatility of methanol is decreased. This allows the acetone to be distilled overhead. The residue curve map is shown in Figure 8.4. Acetone and methanol form a binary minimum-boiling azeotrope of about 78.5 mole

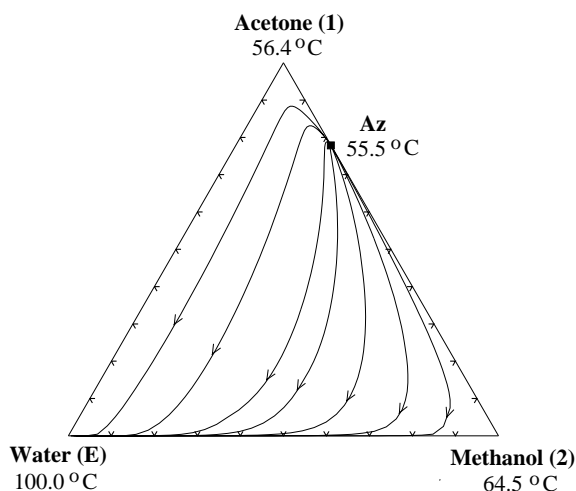


Figure 8.4: Residue curve map for the ternary azeotropic mixture acetone, methanol and water (System 2) at 1 atm (from ASPEN Plus<sup>TM</sup>).

% acetone. Water is miscible and zeotropic in the whole composition space. This system also has relatively large boiling-point differences between the water entrainer (E) and the azeotrope constituents acetone (1) and methanol (2):  $\Delta T_{E-1} = 43.9^\circ\text{C}$  and  $\Delta T_{E-2} = 35.5^\circ\text{C}$ . However, the binary system of acetone and water forms a *tangentially zeotropic mixture* (tangent pinch). This is shown in Figure 8.5 where we see that at high concentrations of acetone, the relative volatility between acetone and water is close to unity. Thus, nearly all the equilibrium stages required to separate acetone from water are due to the last purification part of high purity acetone. Even with a high reflux ratio and a large number of stages the distillate acetone will be contaminated with a small amount of water. Requiring acetone of high purity may, as discussed earlier, cause operational problems since high reflux may be harmful in extractive distillation. This problem can be circumvented by relaxing the water impurity demand in the acetone distillate product and instead purify the distillate in a separate step.

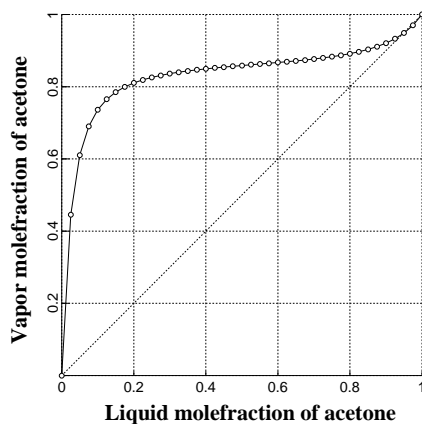


Figure 8.5: Vapor-liquid equilibrium diagram for the binary tangent pinch mixture acetone and water (System 2) at 1 atm (from ASPEN Plus<sup>TM</sup>).

### 8.3 Mathematical model and assumptions

In all simulations presented in this paper we assume that the columns operate under atmospheric pressure with no pressure drop in the column. We assume a total condenser with no sub-cooling. Negligible vapor holdup and constant molar liquid holdup on all trays and in the condenser are assumed. Furthermore, we assume perfect mixing and vapor-liquid equilibrium on all trays. Constant molar vapor flows in the column are used in all simulations (i.e. simplified energy balance). Ideal behavior in the vapor phase is assumed and the Antoine equation for the vapor pressure along with the Wilson activity coefficient model are used to describe the liquid phase. The thermodynamic model and mixture data used is described in Appendix A8.

The initial column compositions are equal to that of the original feed mixture in all the simulations presented in this paper. The vapor flow (boilup) in the column is constant and equal in all sections.

The resulting set of nonlinear algebraic and ordinary differential equations (DAE's) is stiff due to widely different time constants of the trays, reboiler and the middle vessel. The commercial software package SpeedUp (1993) was used for dynamic simulation.

## 8.4 Extractive batch distillation in the conventional column

### 8.4.1 Process description

Extractive distillation using a conventional batch column is illustrated in Figure 8.1. The configuration consists of two column sections: a rectifying section and an extractive section below the entrainer feed point. Thus, it may be called a *two-section* extractive batch distillation column. The products are removed as distillate in a sequential manner. For some mixture systems the rectifying section may be omitted.

The operating procedure for the conventional extractive batch distillation process used in this study is:

Step 1 *Startup*: Total reflux operation to build up column composition profile.

Step 2 *1st cut*: Production of first distillate product (component 1).  
Finite reflux with entrainer feeding. (Step 2 is the focus of this paper.)

Step 3 *Off-cut*: Removal of an off-cut distillate fraction (mixture of 1 and 2).  
Finite reflux without entrainer feeding.

Step 4 *2nd cut*: Production of second distillate product.  
Finite reflux without entrainer feeding.

Step 5 *Entrainer recovery*: Removal of an off-cut distillate fraction that contains all the residual second product (component 2) to achieve pure entrainer (E) in the reboiler.  
Finite reflux without entrainer feeding.

Step 6 *Entrainer discharge*: Removal of the recovered entrainer (E) from the reboiler for reuse, either by emptying the reboiler or by boiling-off the entrainer as a third distillate product.

To eliminate an off-cut between the first and second distillate product (Step 3), total reflux operation may be implemented to build up the concentration of the second distillate product component. Otherwise, off-cut from Step 3 may be recycled to a later batch operation, if needed.

In this study, we only consider constant reflux ratio and constant entrainer feed flowrate during the extractive distillation period (Step 2). The operating policy is open loop, that is, predefined values are used without feedback from the process.



### 8.4.2 Simulation results for System 1 (ethanol - water - ethylene glycol)

The original mixture feed composition is 65 mol% ethanol (1) and 35 mol% water (2). Ethylene glycol (E) is used as entrainer. The column specifications and initial conditions for the simulations are given in Table 8.1. The total liquid holdup in the column is less than 2 % of the total feed charge. The first distillate product (ethanol) is collected in the accumulator with an overall purity of 99.5 mole % ethanol and 0.5 mole % water. Ethylene glycol of 99.99 mole % purity is obtained in the reboiler at the end of operation.

Table 8.1: Column data and initial conditions for extractive batch distillation of ethanol and water using ethylene glycol as entrainer.

Total no. of trays	20 (excl. reboiler)
No. of trays per section	$N_1 = 2, N_2 = 18$
Total initial charge	$H_{F0} = 5.135$ kmol
Condenser holdup (constant)	$H_{D0} = 0.035$ kmol
Initial reboiler holdup	$H_{B0} = 5.000$ kmol
Tray holdup (constant)	$H_j = 0.005$ kmol
Boilup, vapor flow (constant)	$V_B = 5.0$ kmol/h

The results from five selected case studies are summarized in Table 8.2. The recovery of ethanol in Step 2 (1st cut) is seen to vary between 83.1 % and 93.0 %. Simulation results for Case 1 are shown in Figures 8.6 and 8.7.

Table 8.2: Operating conditions and simulation results for extractive batch distillation of ethanol and water using ethylene glycol as entrainer.

Effect studied	Operating conditions	Recovery
Case 1: <i>base case</i>	Entrainer flowrate, $E = 2.5$ kmol/hr	$\sigma_{ethanol} = 93.0$ %
	Reflux ratio, $R = 1.5$	
	Entrainer-to-vapor ratio, $E/V = 0.5$	$t_2 = 2.35$ hr
Case 2: <i>decrease R</i>	Entrainer flowrate, $E = 2.5$ kmol/hr	$\sigma_{ethanol} = 84.3$ %
	Reflux ratio, $R = 1.0$	
	Entrainer-to-vapor ratio, $E/V = 0.5$	$t_2 = 2.40$ hr
Case 3: <i>decrease R</i> <i>increase E</i>	Entrainer flowrate, $E = 3.0$ kmol/hr	$\sigma_{ethanol} = 84.8$ %
	Reflux ratio, $R = 1.0$	
	Entrainer-to-vapor ratio, $E/V = 0.6$	$t_2 = 2.54$ hr
Case 4: <i>decrease R</i> <i>decrease E</i>	Entrainer flowrate, $E = 2.0$ kmol/hr	$\sigma_{ethanol} = 83.1$ %
	Reflux ratio, $R = 1.0$	
	Entrainer-to-vapor ratio, $E/V = 0.4$	$t_2 = 2.52$ hr
Case 5: <i>increase E</i>	Entrainer flowrate, $E = 3.0$ kmol/hr	$\sigma_{ethanol} = 92.8$ %
	Reflux ratio, $R = 1.5$	
	Entrainer-to-vapor ratio, $E/V = 0.6$	$t_2 = 2.50$ hr

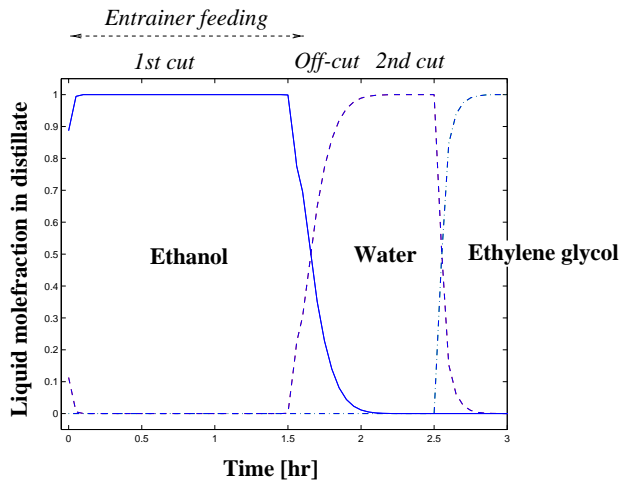


Figure 8.6: Batch extractive distillation separating ethanol and water using ethylene glycol as entrainer: Distillate product composition trajectory. Entrainer feeding is stopped at water breakthrough ( $t_2 = 1.56$  hours). Ethanol recovery 93.0 % (Case 1).

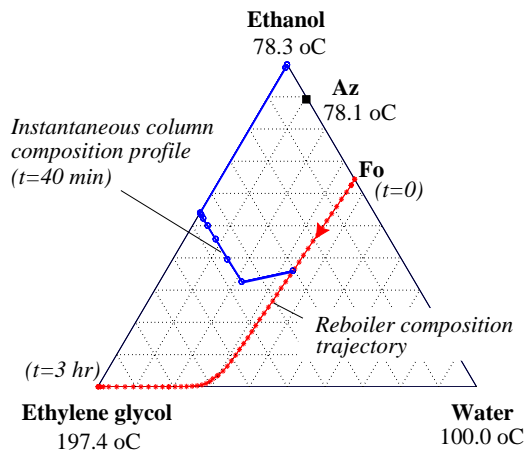


Figure 8.7: Liquid composition profile in the column at 40 minutes (1st cut) and reboiler composition change with time for the complete process corresponding to Figure 8.6 (Case 1).

Figure 8.6 shows the composition of the distillate as a function of time. The first distillate fraction (1st cut) is almost pure ethanol. Once the ethanol is exhausted in the reboiler still, there is a breakthrough of water in the distillate and entrainer feeding is stopped. The off-cut fraction is a mixture of ethanol and water. The second distillate fraction (2nd cut) is almost pure water. The column essentially separates a binary mixture of water and ethylene glycol during Step 4

(2nd cut). To obtain pure ethylene glycol in the reboiler at the end of operation (for reuse), we removed a second off-cut fraction of water and ethylene glycol as distillate (Step 5). Further, pure ethylene glycol could have been produced as a third distillate fraction (Step 6).

The size (amount of material) of the off-cuts depends on the sharpness of the separation between the products, which is dependent on the column holdup, relative volatility, reflux and number of theoretical trays.

Figure 8.7 shows the reboiler composition change during the operation. The initial change is almost linear because the column parameters and operating conditions give a constant distillate composition during the 1st cut (Step 2). Once the ethanol has been removed from the system the composition trajectories move along the edge of the composition diagram that belong to these components.

Figure 8.7 also shows a snapshot of the column profile at a time instant during the period with entrainer feeding (Step 2: 1st cut). It is similar to the profile in the rectifying and extractive sections of a continuous extractive distillation column (see Chapter 2). The distillate is nearly pure ethanol. The rectifying section of the column essentially separates ethanol from ethylene glycol during this step of the process. The profile lies on the binary edge between ethanol and ethylene glycol in the composition diagram. The profile in the extractive section is the part that goes inside the composition triangle in Figure 8.7. There are essentially three effects going on in this section: (i) mixing of the entrainer and the original feed, (ii) countercurrent flow of streams with different compositions, and, (iii) separation between ethanol and water (in the presence of the ethylene glycol entrainer). If the entrainer load is too low, i.e. insufficient separation of the azeotrope-forming components, the rectifying profile does not lie on the binary edge but inside the composition triangle.

For the given column parameters and operating conditions (entrainer load, internal flows) the separation between ethanol and water (in the presence of ethylene glycol) in the extractive section is complete. Therefore the distillate trajectory reaches the unstable node (ethanol) and follows the edges of the composition triangle during Step 2 (1st cut).

### Effect of reflux and entrainer load

From Table 8.2 we see that the ethanol recovery depends mostly on the reflux ratio. It seems like the reflux ratio mainly affects the amount of off-cut (Step 3). In our study, the reflux ratio was kept constant during the whole operation although the separation (recovery) would probably improve if the reflux ratio was increased after Step 2.

In Figure 8.8, we show graphically the recovery of ethanol as a function of the ratio between entrainer and vapor flow ( $E/V$ ). We see that increased entrainer load improves the ethanol recovery. The improvement is larger at low reflux ratios, and there seem to be a maximum entrainer feed flowrate  $E_{max}$ , for which an increase in the entrainer load does not improve the separation efficiency in the extractive section. (Obviously, there is also an  $E_{min}$  for which the separation in the extractive section is insufficient to meet the product specifications).

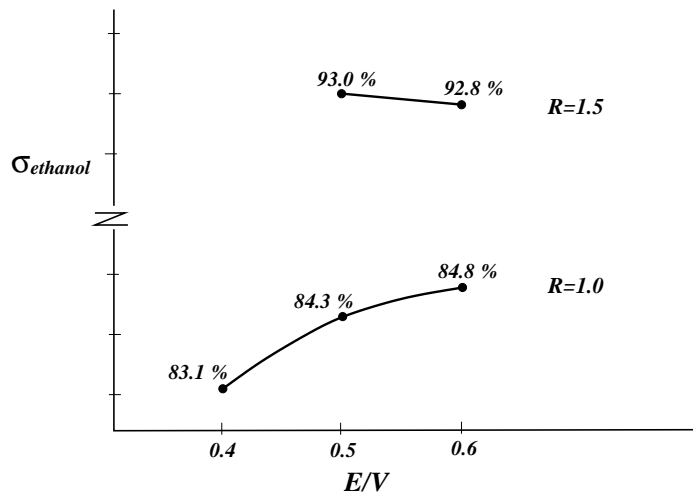


Figure 8.8: Recovery of ethanol as a function of entrainer-to-vapor flow ratio (data from Table 8.2).

Warter and Stichlmair (1999) did not find a maximum value  $E_{\max}$  in their study of extractive batch distillation of ethanol - water - ethylene glycol. However, our results are in accordance with Kjensgjord (1998) who also found that the lower limiting value  $E_{\min}$  decreases with increasing reflux ratio. The explanation is that there is a trade-off between internal flows ( $V$  and  $L$ ) and entrainer feed flow ( $E$ ). The separation between the original mixture components 1 and 2 in the extractive section is improved by an increase in the entrainer feed flowrate. The improvement is larger at low reflux ratios, and there seem to be a maximum entrainer feed flowrate for which an increase in the entrainer load does not improve the separation efficiency in the extractive section.

### Purpose of the rectifying section

The purpose of the rectifying section is to recycle the entrainer, that is, to separate ethanol (1) from ethylene glycol (E) during Step 2. Simulations show that for this particular mixture system, the separation in the rectifying section requires only one tray and no reflux (in Step 2). This illustrates that the mixture ethanol - water - ethylene glycol (System 1) is inadequate for studying the importance of the rectifying section in extractive batch distillation.

### 8.4.3 Simulation results for System 2 (acetone - methanol - water)

The original feed composition is 50 mol% acetone and 50 mol% methanol. Pure water is used as the entrainer. The column specifications and initial conditions are given in Table 8.3.

Table 8.3: Column data and initial conditions for the extractive batch distillation column separating acetone and methanol using water as entrainer.

Total no. of trays	20 (excl. reboiler)
No. of trays per section	$N_{rec} = 6, N_{ex} = 14$
Total initial charge	$H_{F0} = 5.385$ kmol
Condenser holdup (constant)	$H_{D0} = 0.035$ kmol
Initial reboiler holdup	$H_{B0} = 5.283$ kmol
Tray holdup (constant)	$H_j = 1/300$ kmol
Boilup, vapor flow (constant)	$V_B = 5.0$ kmol/h

The existence of a tangent pinch for the binary pair acetone and water (see Figure 8.5) makes it difficult to achieve water-free acetone (from simulations we learned that it was difficult to get more than 98.5 mole % acetone), but otherwise the separation between acetone-water is easy. Thus, we relax the water impurity specification of the acetone product, and use the following specifications:

*1st cut:* 96.0 mole % acetone with maximum 0.5-1.0 mol% methanol impurity;

*2nd cut:* 99.0 mol% methanol with maximum 1.0 mol% acetone impurity;

*Entrainer recovery:* 99.9 mol% water with maximum 0.1 mol% methanol impurity.

#### Startup procedures

During startup (Step 1) the column was operated at total reflux for 15 minutes. This time period was chosen somewhat arbitrary. Two alternative startup procedures were compared to see which one that yields the best overall separation results:

Startup procedure 1: Total reflux operation without entrainer feeding

Startup procedure 2: Total reflux operation with entrainer feeding

Startup procedure 2 was found to be the best. Here we build up both the column composition profile and the purity of distillate before any product removal. This avoids an off-spec distillate fraction at the beginning of the 1st cut (Step 2).

There is also the third option of skipping the total reflux operation and starting directly with Step 2 (finite reflux with entrainer feeding), but then there will be a greater loss of ethanol and methanol because of the need to remove an off-cut before the 1st cut.

In all simulations the column is operated with a constant entrainer flowrate until there is a methanol breakthrough in the acetone distillate product (or more precisely; when there is 96.0 mole % acetone in the accumulated distillate product). Then, ordinary distillation with a constant reflux ratio (equal to the ratio used during the entrainer feeding period) is performed.

We report five selected case studies where we use values of  $E$  and  $R$  which meet the purity specifications (trial-and-error approach). These values are by no means optimal for the process. Safrit and Westerberg (1997b) formulated this into an optimization problem (variables  $E$  and  $R$  and profit function), but there are no studies reported on how to implement such an optimal operating policy.

The results from the dynamic simulations are summarized in Table 8.4 (Cases 1-5), and more detailed results are shown in Figures 8.9-8.14 (Cases 2, 3 and 5).

Table 8.4: *Operating conditions and simulation results for extractive batch distillation of acetone and methanol using water as entrainer.*

Effect studied	Operating conditions	Recovery
Case 1: <i>startup 1</i>	Entrainer flowrate, $E = 3.5$ kmol/hr	$\sigma_{acetone} = 83.9$ %
	Reflux ratio, $R = 4$	
	Entrainer-to-vapor ratio, $E/V = 0.7$	$t_2 = 2.35$ hr
Case 2: <i>startup 2</i>	Entrainer flowrate, $E = 3.5$ kmol/hr	$\sigma_{acetone} = 85.6$ %
	Reflux ratio, $R = 4$	
	Entrainer-to-vapor ratio, $E/V = 0.7$	$t_2 = 2.40$ hr
Case 3: <i>increase E startup 2</i>	Entrainer flowrate, $E = 6.0$ kmol/hr	$\sigma_{acetone} = 90.6$ %
	Reflux ratio, $R = 4$	
	Entrainer-to-vapor ratio, $E/V = 1.2$	$t_2 = 2.54$ hr
Case 4: <i>increase E startup 2</i>	Entrainer flowrate, $E = 8.0$ kmol/hr	$\sigma_{acetone} = 90.0$ %
	Reflux ratio, $R = 4$	
	Entrainer-to-vapor ratio, $E/V = 1.2$	$t_2 = 2.52$ hr
Case 5: <i>further increase E startup 2</i>	Entrainer flowrate, $E = 10.0$ kmol/hr	$\sigma_{acetone} = 89.1$ %
	Reflux ratio, $R = 4$	
	Entrainer-to-vapor ratio, $E/V = 2.0$	$t_2 = 2.50$ hr

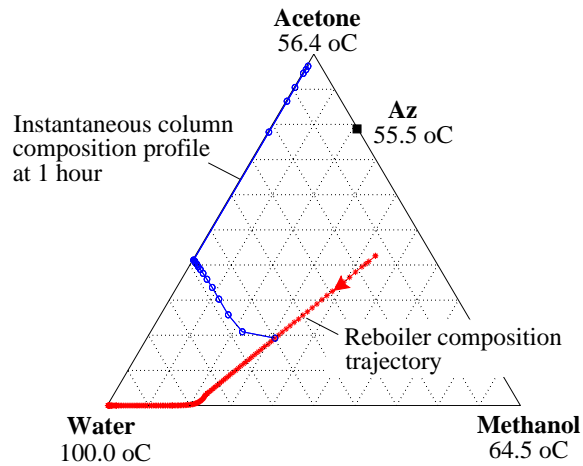


Figure 8.9: Extractive batch distillation of acetone and methanol using water as entrainer. Liquid composition profile in the column at 1 hour and reboiler composition trajectory for the complete process (Case 2 in Table 8.4).

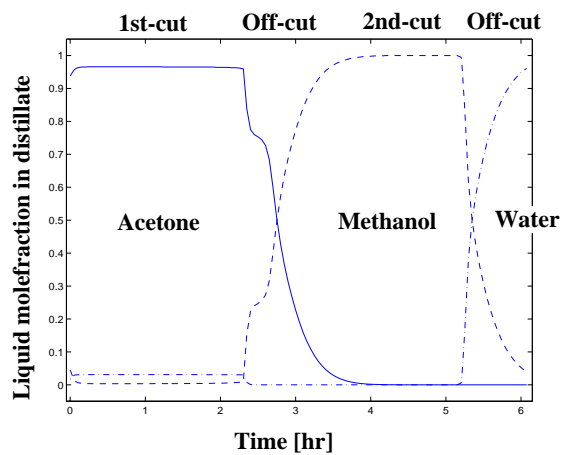


Figure 8.10: Distillate composition trajectory corresponding to Figure 8.9. Entrainer feeding stopped at methanol breakthrough in acetone product ( $t_2 = 2.40$  hours). Acetone recovery 85.6 % (Case 2).

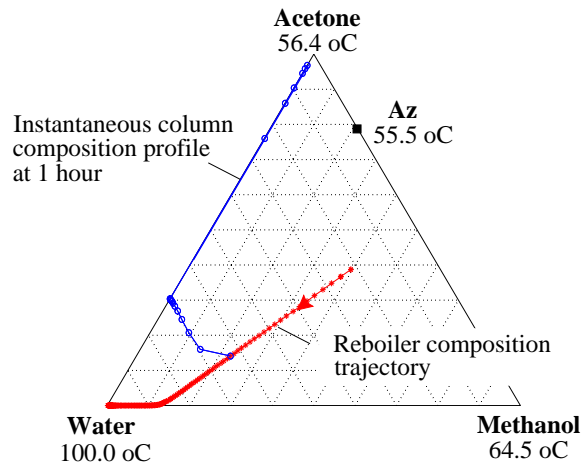


Figure 8.11: Increased entrainer load improves acetone recovery: Extractive batch distillation of acetone and methanol using water as entrainer. Liquid composition profile in the column at 1 hour and reboiler composition trajectory for the complete process (Case 3).

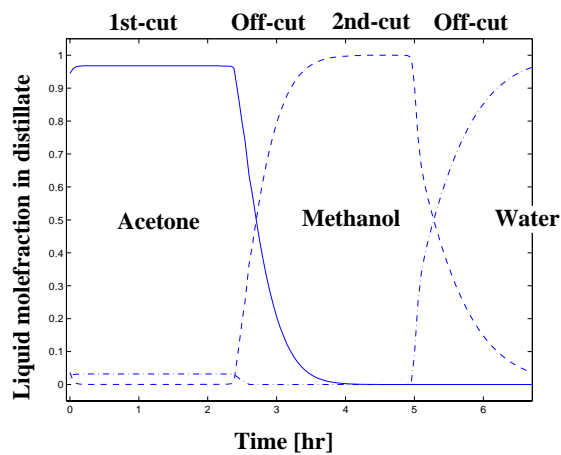


Figure 8.12: Increased entrainer load improves acetone recovery: Distillate composition trajectory corresponding to Figure 8.11. Entrainer feeding stopped at methanol breakthrough in acetone product ( $t_2 = 2.54$  hours). Acetone recovery 90.6 % (Case 3).



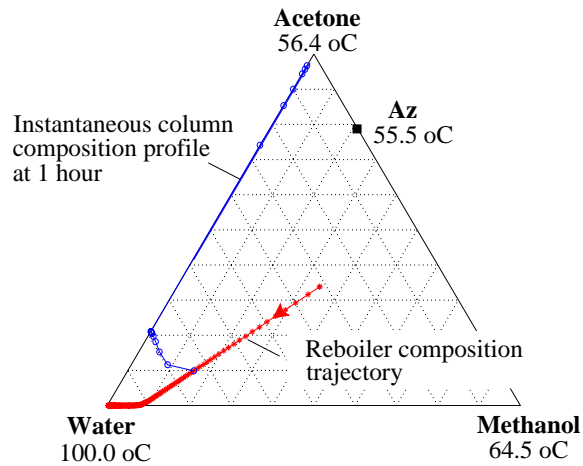


Figure 8.13: An even further increase in entrainer load reduces acetone recovery: Extractive batch distillation of acetone and methanol using water as entrainer. Liquid composition profile in the column at 1 hour and reboiler composition trajectory for the complete process (Case 5).

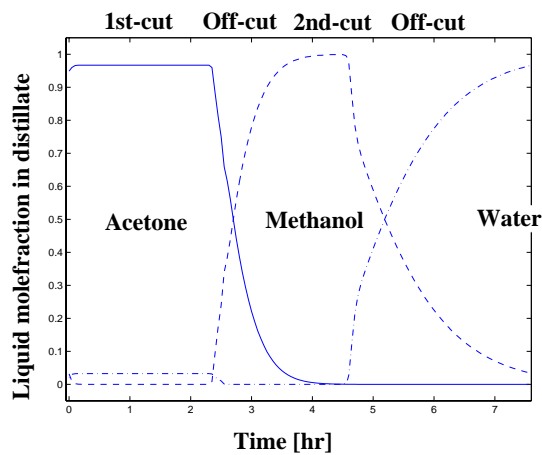


Figure 8.14: An even further increase in entrainer load reduces acetone recovery: Distillate composition trajectory corresponding to Figure 8.13. Entrainer feeding stopped at methanol breakthrough in acetone product ( $t_2 = 2.50$  hours). Acetone recovery 89.1 % (Case 5).

### Degradation of column profile

In extractive distillation using a conventional batch column, the reboiler residue is gradually enriched in water during the extractive distillation period (Step 2), as illustrated in Figure 8.15. This causes a “degradation” of the column profile which decreases the efficiency of the separa-

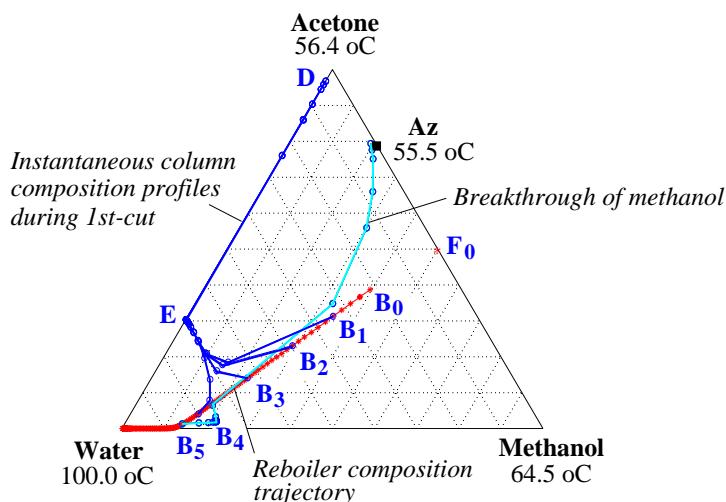


Figure 8.15: Degradation of column profile during 1st cut: Liquid composition profiles at  $t_1=12$  min,  $t_2=30$  min,  $t_3=1$  hr,  $t_4=2$  hr and  $t_5=2.5$  hr. Entrainer feeding stopped at methanol breakthrough in distillate product ( $t_5=2.5$  hr) (Case 3).

ration in the extractive section. This is different from continuous extractive distillation where the strongly curved profile in the extractive section is maintained (steady-state operation). The original mixture of acetone and methanol is marked by  $F_0$  in Figure 8.15. The resulting composition in the reboiler at the end of Step 1 (with startup procedure 2) is marked by  $B_0$  ( $x_{B_0} = [0.387, 0.396, 0.217]$ ). During the extractive distillation step (Step 2), the reboiler product gets enriched in the water entrainer, marked by  $B_1, B_2, \dots, B_5$ . When the reboiler composition has reached  $B_5$  (at 2.5 hours in Figure 8.15), the instantaneous composition profile along the column is shifted and a binary fraction of acetone and methanol is achieved in the distillate. When all of the acetone has been removed as distillate product, the composition of the reboiler reaches the binary edge of water and methanol and the column essentially performs a binary separation of methanol and water.

### Effect of entrainer load

Figure 8.16 shows the effect of the entrainer feed flowrate on the acetone recovery. As expected, there is a optimum in the entrainer feed flow (see previous discussion in Section 8.4).

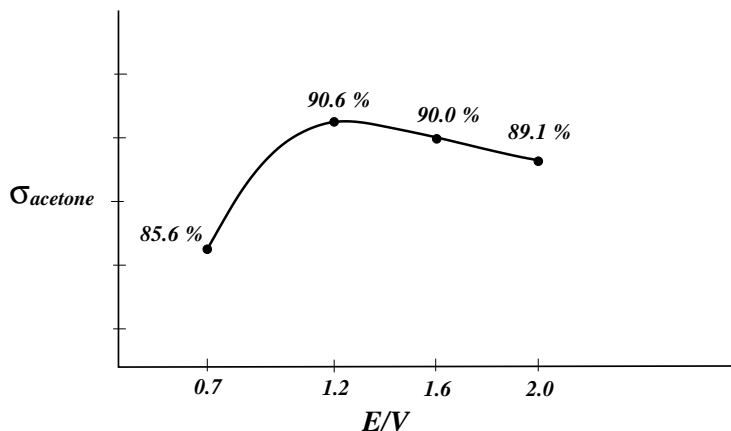


Figure 8.16: Recovery of acetone as a function of entrainer-to-vapor flow ratio (data from Table 8.4 with  $R=4$ ).

For a lower reflux ratio ( $R=3$ ) and entrainer flowrate as in Case 3 ( $E=6.0$  kmol/hr in Table 8.4) we obtained an acetone recovery of 84.3 %.

### Entrainer purity

The entrainer purity was found to be important for the separation, that is, the acetone recovery was sensitive to the methanol impurity of the water entrainer feed. We used the same conditions as for Case 3 in Table 8.4 and computed the acetone recovery ( $\sigma_{acetone}$ ) for three cases:

- a) Pure water (0 mole % methanol):  $\sigma_{acetone} = 90.6$  %
- b) 0.1 mole % methanol:  $\sigma_{acetone} = 90.1$  %
- c) 0.5 mole % methanol:  $\sigma_{acetone} = 57.3$  %

From this we conclude that the acetone recovery is sensitive to entrainer purity, and that it is acceptable to allow for about 0.1 mole % methanol impurity. (It was an additional 48 minutes to purify the entrainer reboiler residue from 99.5 mole % to 99.9 mole %.)

#### 8.4.4 Summary: Extractive batch distillation

The simulation results can be summarized as follows:

- Increased entrainer load gives better separation of the azeotrope-forming components 1 and 2 in the extractive section (here: less methanol impurity in the acetone distillate product).
- Increased reflux gives better separation of the entrainer and the azeotrope-forming component 1 in the rectifying section (here: less water in the acetone distillate product).
- These two effects need to be balanced as increased reflux results in less relative entrainer load. For large entrainer flowrates there was no further advantage in terms of separation and a large amount of the entrainer was accumulated in the reboiler.

### 8.5 Extractive batch distillation in the middle vessel column

#### 8.5.1 Process description

Extractive distillation in a middle vessel batch column is illustrated in Figure 8.2. The original mixture to be separated may be initially charged to the middle vessel or distributed to both the reboiler and the middle vessel. The middle vessel configuration allows for simultaneous removal of distillate and bottom product. In addition, the middle vessel may be gradually purified to retrieve a product at the end of operation. The configuration consists of three column sections: a rectifying section, an extractive section and a stripping section connected by a middle vessel (holdup tank). The rectifying section serves to separate acetone (1) from water (E), the extractive section to extract methanol (2) from the original feed mixture with the help of water (E), and the stripping section to strip acetone (1) out of the bottom product (possibly E).

The operating procedure for the middle vessel extractive batch distillation process used in this study is:

Step 1 *Startup*: Total reflux (and reboil) operation to build up the column composition profile.

Step 2 *1st cut*: Production of the first distillate product (component 1) and removal of bottom product. Finite reflux with continuous entrainer feeding. (Step 2 is the focus of this paper.)

Step 3 *Off-cut*: Removal of an off-cut fraction (either as distillate or bottom product or both) to purify component 2 in the middle vessel. Finite reflux and reboil without entrainer feeding.

Step 4 *2nd cut*: Production of second distillate or bottom product.  
Finite reflux without entrainer feeding.

### Modifications of the middle vessel configuration

The configuration of the vapor and liquid flows to and from the middle vessel is of major importance in the extractive distillation scheme. We considered the three alternative configurations illustrated in Figure 8.17:

1. *Basic middle vessel configuration*: both vapor and liquid flow through the middle vessel (Safrit *et al.*, 1995; Safrit and Westerberg, 1997b).
2. *Vapor bypass middle vessel configuration*: only liquid flows through the middle vessel (Wittgens *et al.*, 1996; Skogestad *et al.*, 1997; Hilmen *et al.*, 1997).
3. *Liquid bypass middle vessel configuration*: only vapor flow through the middle vessel (Warter and Stichlmair, 1999).

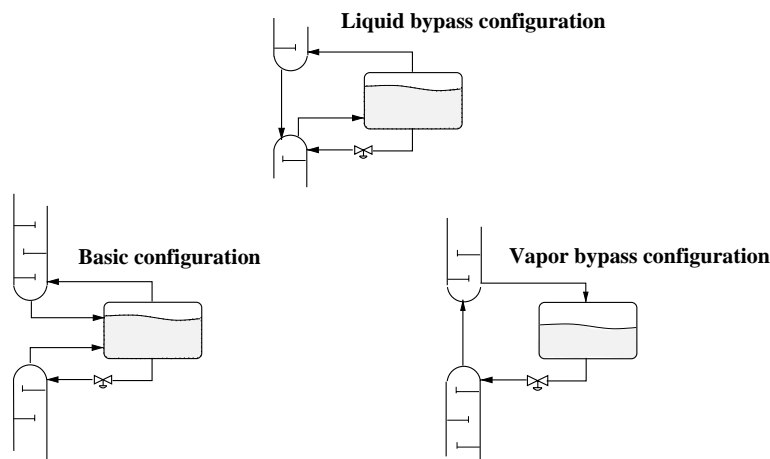


Figure 8.17: Alternative middle vessel configurations for extractive batch distillation.

The vapor bypass configuration (only liquid flow through middle vessel) has been used for the multivessel batch distillation in Chapter 6 and Chapter 7. In this case, the difference between the basic and the vapor bypass configuration is minor (at most one equilibrium tray). However, this is not the case for the extractive distillation scheme where the heavy entrainer is continuously fed above the middle vessel. Warter and Stichlmair (1999) found that for extractive distillation the liquid bypass configuration had the best performance and this is confirmed in this study.

4. *“Long” liquid bypass middle vessel configuration*: where the liquid bypass is returned further down the stripping section (not shown).

We propose this fourth configuration as a possible scheme to avoid that entrainer enters the middle vessel through the vapor phase. This scheme offers the possibility of achieving a pure middle vessel product, but it has not been considered in the simulations presented in this study.

### Separation schemes

There are two principally different ways of operating the extractive middle vessel column:

Scheme I: Simultaneously producing acetone (1) and water (E) with methanol (2) accumulated in the middle vessel;

Scheme II: Producing acetone (1) distillate only and removing a fraction of methanol (2) and water (E) in the bottom (2 + E) to be separated in a second operation.

These alternative separation schemes are illustrated in Figure 8.18.

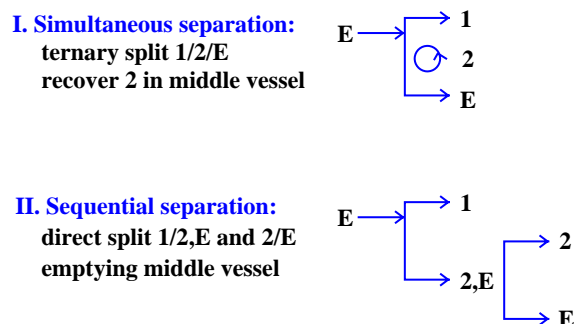


Figure 8.18: Separation schemes for the separation of an original binary mixture 1 and 2 using  $E$  as entrainer in the extractive middle vessel batch distillation column.

Scheme I is attractive since it requires only a single operation. However, it may not be optimal in terms of product recovery and minimum batch time.

Scheme II is very similar to continuous extractive distillation scheme with a direct sequence of two columns.

The main problem with the basic and vapor bypass configurations is that entrainer must accumulate in the middle vessel during Step 2 (entrainer feeding). This follows from a component balance for entrainer in the middle vessel. For the “best” case where we neglect the volatility of the entrainer in the basic configuration, we get:

$$\frac{d}{dt}(x_{EM} H_M) = E - x_{EM} L_M \quad (8.1)$$

where  $x_{EM}$  is the molefraction of entrainer in the middle vessel. If  $E > L_M$ , then the amount of entrainer accumulated will increase steadily. If  $E < L_M$ , then the amount will increase until we reach a value where  $E = x_{EM} L_M$ , i.e. where  $x_{EM} = E/L_M$ . (This simple analysis which gives the “unavoidable” accumulation of entrainer in the middle vessel may be used to conclude that some earlier claims in the literature about simultaneous separation into pure products in the basic configuration must be incorrect.)

### 8.5.2 Simulation results with simultaneous separation (Scheme I)

The original mixture feed composition is 50 mol% acetone and 50 mol% methanol. Pure water is used as the entrainer. The column specifications and initial conditions are given in Table 8.5.

Table 8.5: Column data and initial conditions for the middle vessel extractive batch distillation column separating acetone and methanol using water as entrainer.

Total no. of trays	30 (excl. reboiler)
No. of trays per section	$N_1 = 6, N_2 = 14, N_3 = 10$
Total initial charge	$H_{F0} = 5.385$ kmol
Condenser holdup (constant)	$H_{D0} = 0.035$ kmol
Initial middle vessel holdup	$H_{M0} = 5.125$ kmol
Reboiler holdup (constant)	$H_{B0} = 0.035$ kmol
Tray holdup (constant)	$H_j = 1/300$ kmol
Boilup, vapor flow (constant)	$\dot{V}_B = 5.0$ kmol/h

The operating conditions are chosen to be comparable with the parameters used for the conventional batch extractive distillation presented in the previous section (Case 3 in Table 8.4). The values are by no means optimal for the operation of the extractive middle vessel batch distillation column. The product specifications are the same.

The results from dynamic simulation of selected cases are summarized in Table 8.6 where we see that the liquid bypass configuration is superior in terms of acetone recovery.

Table 8.6: Operating conditions and simulation results for middle vessel extractive batch distillation of acetone and methanol using water as entrainer.

Configuration	Operating conditions	Recovery
Liquid bypass	Entrainer flowrate, $E = 6.0$ kmol/hr	$\sigma_{acetone} = 93.3$ %
	Reflux ratio, $R = 4$	
	Entrainer-to-vapor ratio, $E/V = 1.2$	
	$L_M = 1.0$ kmol/hr and $B = 6.0$ kmol/hr	
Basic	Entrainer flowrate, $E = 6.0$ kmol/hr	$\sigma_{acetone} = 90.3$ %
	Reflux ratio, $R = 4$	
	Entrainer-to-vapor ratio, $E/V = 1.2$	
	$L_M = 7.5$ kmol/hr and $B = 2.5$ kmol/hr	
Vapor bypass	Entrainer flowrate, $E = 6.0$ kmol/hr	$\sigma_{acetone} = 46.4$ %
	Reflux ratio, $R = 4$	
	Entrainer-to-vapor ratio, $E/V = 1.2$	
	$L_M = 7.5$ kmol/hr and $B = 2.5$ kmol/hr	

For the liquid bypass configuration we used the following procedure (see also Table 8.6):

Step 1 *Startup*: with bottom removal:  $R=\infty$ ,  $E=B=6.0$  kmol/hr,  $L_M=0$ ;

Step 2 *Distillate 1st cut*:  $R=4$ ,  $E=B=6.0$  kmol/hr,  $L_M=D=1.0$  kmol/hr (until  $t_2 = 2.62$  hr);

Step 3 *Distillate off-cut*:  $R=4$ ,  $E=0$ ,  $L_M=2.0$  kmol/hr,  $B=1.0$  kmol/hr (until  $t_3 = 2.95$  hr);

Step 4 *Only bottom product removal*:  $R=\infty$ ,  $E=0$ ,  $L_M=1.0$  kmol/hr,  $B=1.0$  kmol/hr (until  $t_4 = 4.84$  hr);

Note that we remove a bottom product during startup (because the level in the reboiler was constant). This results in some loss of acetone in the bottom flow (about 3 % of the initial methanol charge). In Step 2 we used  $L_M = D$  and  $B = E$ , that is, the amount in the middle vessel decreases according to what is removed as distillate.

The results for the liquid bypass configuration are illustrated in Figures 8.19 - 8.22. We were unable to obtain simultaneous production of acetone distillate and pure water entrainer bottom product.

For the basic and vapor bypass configurations it is even more difficult to choose reasonable values for the operating parameters. We used  $L_M > E$  ( $L_{M,\min}=V$ ) and tried several values. In addition to the two cases shown in Table 8.6, simulations with  $L_M = 11$  kmol/hr ( $B=E$ ) yield 82.4 % acetone recovery with the basic configuration and 68.4 % acetone recovery with the vapor bypass configuration.

We conclude that simultaneous separation (Scheme I) is difficult to achieve. However, if we allow for a separate step to purify the bottom product (Scheme II) then the purity specifications are easily achieved.



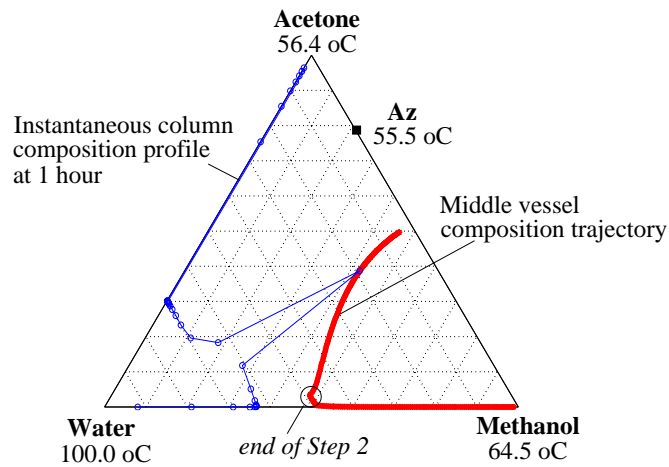


Figure 8.19: Extractive middle vessel batch distillation with liquid bypass configuration attempting simultaneous separation (Scheme I). Operating conditions given in Table 8.6.

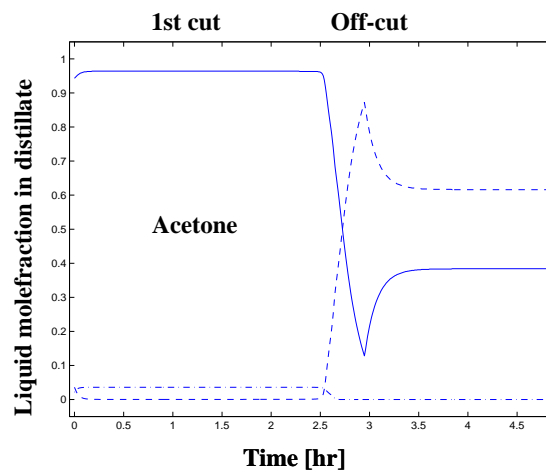


Figure 8.20: Distillate composition trajectory for liquid bypass configuration corresponding to Figure 8.19. Entrainer feeding stopped at methanol breakthrough in acetone product ( $t_2 = 2.62$  hr).

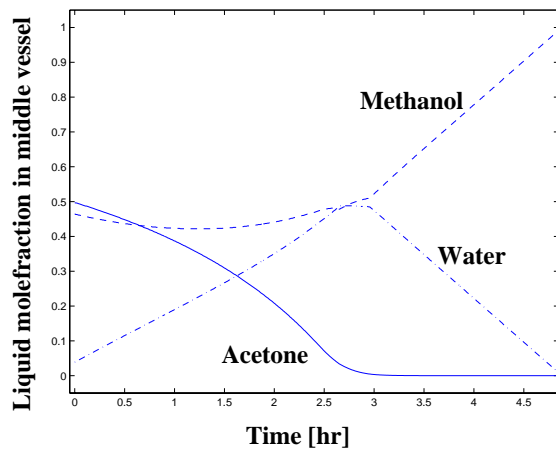


Figure 8.21: Middle vessel composition trajectory for liquid bypass configuration corresponding to Figure 8.19.

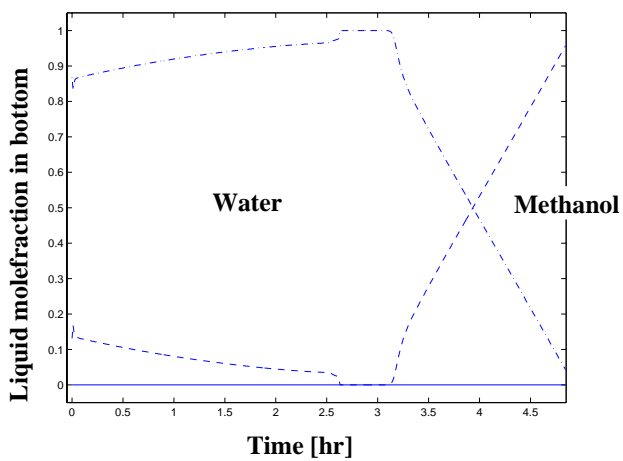


Figure 8.22: Bottom product composition trajectory for liquid bypass configuration corresponding to Figure 8.19.

### 8.5.3 Summary: Extractive middle vessel batch distillation

The middle vessel extractive batch distillation column solves the previously mentioned problem of entrainer accumulation in the reboiler (feed vessel) of the conventional batch column configuration. The volume of the middle vessel can be kept constant or even decrease with time due to the removal of material in the stripping section of the column. In addition, the batch extractive middle vessel column is potentially more energy efficient due to the multieffect nature of combining a rectifying-extraction section and a stripper section in one column (see Chapter 6), even when compared to continuous extractive distillation (comparable to a direct sequence of two columns). However, several aspects of extractive distillation in batch columns remains unanswered such as optimal policy for the entrainer feeding, required quality of the entrainer feed (purity, temperature), entrainer feed tray location, reflux policy and others.

In particular, it is difficult to find (open loop) values for the operating parameters. This gives an incentive to consider feedback control strategies for the extractive middle vessel batch distillation column.

## 8.6 Conclusion

In this study we have focused on the use of extractive distillation in batch columns for separating homogeneous minimum-boiling azeotropic mixtures. The influence of operating parameters such as reflux ratio, entrainer feed flowrate and entrainer purity on the separation performance have been explored in a dynamic simulation study.

The extractive middle vessel batch distillation column with the liquid bypass configuration was found to have the best performance. Our study confirms that it is advantageous to avoid mixing (and accumulation) of the entrainer in the middle vessel during the extractive distillation operation.

Extractive distillation in batch columns has to the authors knowledge not been implemented industrially. This is probably due operational problems (filling of reboiler) in the conventional column. The middle vessel batch column is more suited for the extractive distillation process, but there is a need for experimental verification and implementation (pilot-scale testing) of practical operating and control policies.

## Appendix 8A

The vapor- liquid equilibrium calculations are based on the following equations:

$$y_i P = x_i \gamma_i^L (T, \mathbf{x}) P_i^{sat} (T)$$

and

$$\sum_{i=1}^n y_i = 1$$

where  $P = 1$  atm in all the simulations presented in this paper. The vapor pressures were calculated by the Antoine equation:

$$\ln P_i^{sat} = A_i - \frac{B_i}{T + C_i}$$

where  $P_i^{sat}$  is in  $Pa$  and  $T$  in  $K$ . The liquid activity coefficients were calculated by the Wilson equation:

$$\ln \gamma_i = 1 - \ln \left( \sum_{j=1}^{n_c} x_j \Lambda_{ij} \right) - \sum_{k=1}^{n_c} \left( \frac{x_k \Lambda_{ki}}{\sum_{j=1}^{n_c} x_j \Lambda_{kj}} \right)$$

$$\Lambda_{ij} = \frac{V_j}{V_i} \exp \left( \frac{-A_{ij}}{RT} \right)$$

where  $V_j$  is in  $cm^3/mol$ ,  $A_{ij}$  in  $cal/mol$  and  $T$  in  $K$ . Parameters for the Antoine and Wilson equations for the example mixtures used in the simulations presented in this article are given in Table 8.7.

Table 8.7: Thermodynamic Data for the Example Mixtures<sup>a</sup>

<u>Parameters for the Antoine Equation</u>				
	A	B	C	$V_i [\frac{cm^3}{mol}]$
(1) Ethanol	23.5807	3673.81	-46.681	58.69
(2) Water	23.2256	3835.18	-45.343	18.01
(3) Ethylene glycol	25.1431	6022.18	-28.250	55.92
<u>Binary Interaction Parameters for the Wilson Equation</u>				
	$A_{11} = 0$	$A_{12} = 393.1971$	$A_{13} = -129.2043$	
	$A_{21} = 926.263$	$A_{22} = 0$	$A_{23} = 1266.0109$	
	$A_{31} = 1539.4142$	$A_{32} = -1265.7398$	$A_{33} = 0$	
<u>Parameters for the Antoine Equation</u>				
	A	B	C	$V_i [\frac{cm^3}{mol}]$
(1) Acetone	21.3009	2801.53	-42.875	74.04
(2) Methanol	23.4999	3643.31	-33.434	40.73
(3) Water	23.2256	3835.18	-45.343	18.01
<u>Binary Interaction Parameters for the Wilson Equation</u>				
	$A_{11} = 0$	$A_{12} = -161.8813$	$A_{13} = 489.3727$	
	$A_{21} = 583.1054$	$A_{22} = 0$	$A_{23} = 19.2547$	
	$A_{31} = 1422.849$	$A_{32} = 554.0494$	$A_{33} = 0$	

<sup>a</sup> From Gmehling et al. (1977-1990), *VLE Data Collection*, DECHEMA series, at atmospheric pressure.



## Chapter 9

# Control Strategies for Extractive Middle Vessel Batch Distillation

A novel control structure for batch extractive distillation using the middle vessel column is proposed. Tight composition control and simultaneous production of distillate product and entrainer recovery are obtained with simple single loop PI controllers.

### 9.1 Introduction

This study focuses on control strategies for the extractive batch distillation in the middle vessel column shown in Figure 9.1. The entrainer feed (E) and the liquid flow from the middle vessel ( $L_M$ ) provide extra degrees of freedom compared to conventional distillation. Warter and Stichlmair (1999) proposed a modification where the entrainer-rich liquid stream from the extractive section bypasses the middle vessel and enters the stripping section directly. This modification, hereafter called the *liquid bypass configuration*, avoids unnecessary mixing and accumulation of the high-boiling entrainer into the middle vessel, and is the one studied in this paper.

The use of constant entrainer feed flowrate (E) and constant reflux ( $L_1$  and  $L_M$ ) considered in Chapter 8 is inherently an open loop strategy that results in changes in the distillate and bottom product compositions. We were not able to find (open loop) operating conditions for a simultaneous distillate and bottom product removal that satisfied the product specifications (Scheme I) in Chapter 8. In this paper we consider a feedback control strategy to simplify operation and avoid over-fractionation.

Batch extractive distillation has been studied experimentally and by simulations in a series of papers by Lang, Lelkes and Yatim *et al.* (1993; 1994; 1995; 1998a; 1998b; 1998c), Safrit *et al.* (1995; 1997b), Warter and Stichlmair (1999) and others (referenced in Chapter 8). These

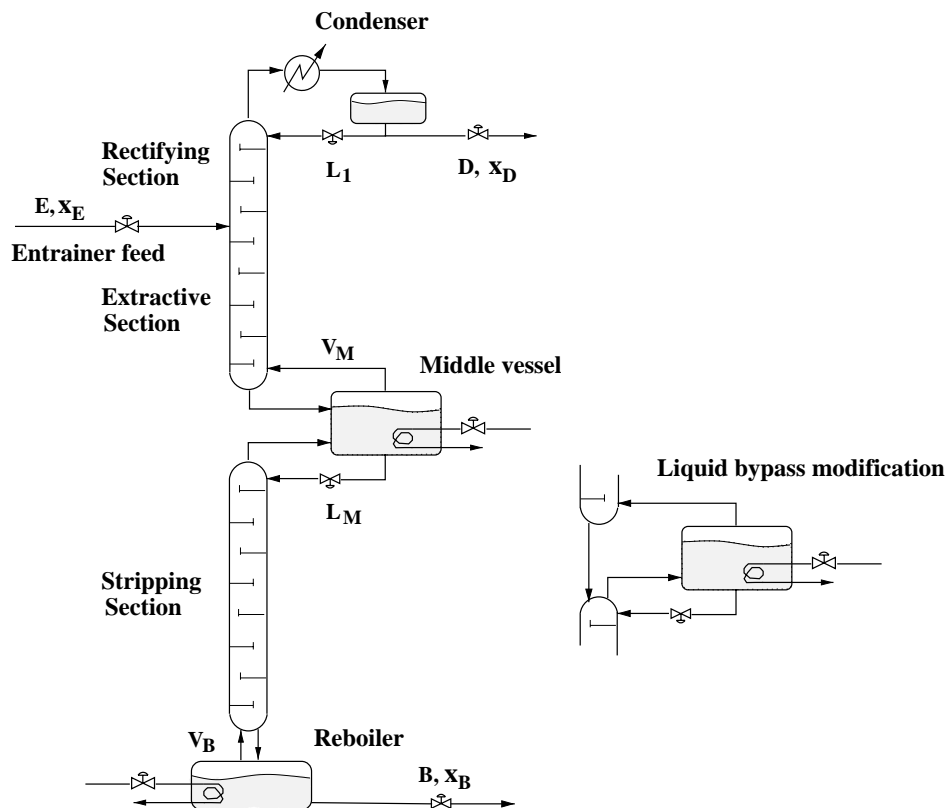


Figure 9.1: Extractive middle vessel batch distillation column. To the right is the liquid bypass configuration proposed by Warter *et al.* (1999).

open loop studies have identified operating parameters that influence the separation performance. Amongst these are the entrainer feed flowrate (most important), reflux ratio, entrainer feed purity and temperature. Column design parameters like entrainer feed tray location and middle vessel configuration are also found to be important.

Hilmen *et al.* (1997) were the first to propose a control strategy for extractive batch distillation in the middle vessel column. In the present paper, these considerations are extended to include the liquid bypass configuration proposed by Warter and Stichlmair (1999), which was shown to have the the best separation performance for extractive distillation in the middle vessel batch column.

Recently, Phimister and Seider (2000b) proposed a DB-control configuration for extractive distillation in the middle vessel column (where the distillate flow is used to control the distillate purity and the bottom flow is used to control the bottom purity by single loop P-controllers and the entrainer flowrate is constant). However, they used the vapor bypass configuration (that is,



only liquid flows through the middle vessel) which was found to be inferior in Chapter 8.

Farschman and Diwekar (1996), Barolo *et al.* (1998) and Phimister and Seider (2000a) evaluated various control configurations for the middle vessel batch distillation column separating ideal ternary mixtures. Farschman and Diwekar (1996) use the ratio of the vapor flow in the rectifying section to the vapor flow in the stripping section as a control parameter (this ratio  $q$  was proposed by Davidyan *et al.* (1994) as discussed in Chapter 6). They showed that the middle vessel provides a decoupling of the two-end control loops. This middle vessel decoupling effect between the attached column sections was also pointed out by Barolo *et al.* (1996a) and Barolo *et al.* (1996b).

An indirect level control strategy was proposed for the multivessel batch distillation column (Skogestad *et al.*, 1997), and our proposed control strategy is similar to this.

The literature on control of extractive distillation in continuous columns is extensive and was reviewed by Jacobsen *et al.* (1991). Andersen *et al.* (1995) considered integrated design and control of continuous extractive distillation columns. They show that a simpler control situation can be obtained by increasing the entrainer feed flow above its economically optimum.

## 9.2 Important considerations for control

An analysis of the middle vessel batch distillation columns reveals some important considerations for control:

1. The entrainer feed flowrate determines the separation efficiency between the original mixture components 1 and 2 in the extractive section. There is a minimum entrainer feed flowrate necessary to “break” the azeotrope  $A_{12}$ .
2. High reflux “weakens” the effect of the entrainer (E). There is a minimum and a maximum reflux ratio in order to achieve acceptable separation between component 1 and E in the rectifying section (1/E split) and between component 1 and 2 in the extractive section (1/2 split with help of E).
3. Entrainer may accumulate in the feed vessel (reboiler or middle vessel).
4. The middle vessel decouples the extractive section and the stripping section. However, this decoupling is less with the liquid bypass configuration.
5. Because the entrainer dominates the liquid phase in the extractive section during the entrainer feeding period, it is difficult to use temperature measurements to infer compositions in this section.
6. Temperature is not a unique indicator of the composition for multicomponent mixtures. This may cause difficulties in using temperature measurements to infer composition even in the stripping section of the extractive middle vessel column.

7. The liquid load (internal liquid flow) is higher in the stripping section than in the rectifying section and, for some cases, in the extractive section. This may cause difficulties in achieving high purity of the bottom product (entrainer recovery). It may be necessary to have a higher vapor flowrate in the stripping section of the column.

In continuous extractive distillation the entrainer-to-feed flow ratio ( $E/F$ ) is usually held constant, although some authors propose to keep the entrainer-to-distillate flow ratio ( $E/D$ ) constant (Westerberg and Wahnschafft, 1996). In most continuous extractive distillation processes, the entrainer flowrate ( $E$ ) is not used for control. However, due to the transient behavior of batch operation it seems more pertinent to use the entrainer flowrate ( $E$ ) for composition control in the extractive batch distillation column.

In order to minimize the time consumption of the batch distillation, maximum boilup (constant vapor flow in all three column sections) was used in the simulations presented in this study.

### 9.3 Two-point composition control

We propose the following feedback control strategy for the extractive middle vessel batch distillation column (see Figure 9.2) during the entrainer feeding period:

- Liquid reflux ( $L_1$ ) is used to control the  $1/E$  split in the rectifying section;
- Entrainer feed flowrate ( $E$ ) is used to control the  $1/2$  split in the extractive section;
- Liquid flow out of middle vessel ( $L_M$ ) is used to control the  $2/E$  split in the stripping section;
- Distillate flowrate ( $D$ ) is used to control the level in condenser drum;
- Bottom flowrate ( $B$ ) is used to control the level in reboiler.

Note that it may be possible to change the “pairings”, but the above proposal gives the most “direct” effect in terms of composition control. Due to lack of composition measurements, we propose to use the reflux ( $L_1$ ) to control the column *temperature* near the middle of the rectifying section. (Alternatively, the reflux ratio ( $R = L_1/D$ ) may be held constant within its allowed range (minimum and maximum value.) Similarly, the liquid flow from the middle vessel ( $L_M$ ) is used to control the *temperature* in the stripping section below ( $T_2$ ). This also indirectly adjusts the middle vessel holdup and there is no need for level control (same strategy as used in Chapter 7). We do not recommend using a temperature measurement for adjusting the entrainer flowrate since the temperature in the extractive section is dominated by the entrainer and thus insensitive to the split between component 1 and 2. We therefore propose to measure the split between 1 and 2 by measuring the amount of component 2 (impurity) in the distillate ( $x_{D2}$ ). An alternative is to use a more direct composition measurement of the methanol in the extractive section, but this is less practical.

In the Figure 9.2 we also show by the dotted line a possible modification where the liquid bypass is returned further down in the stripping section. However, this modification has not been simulated.

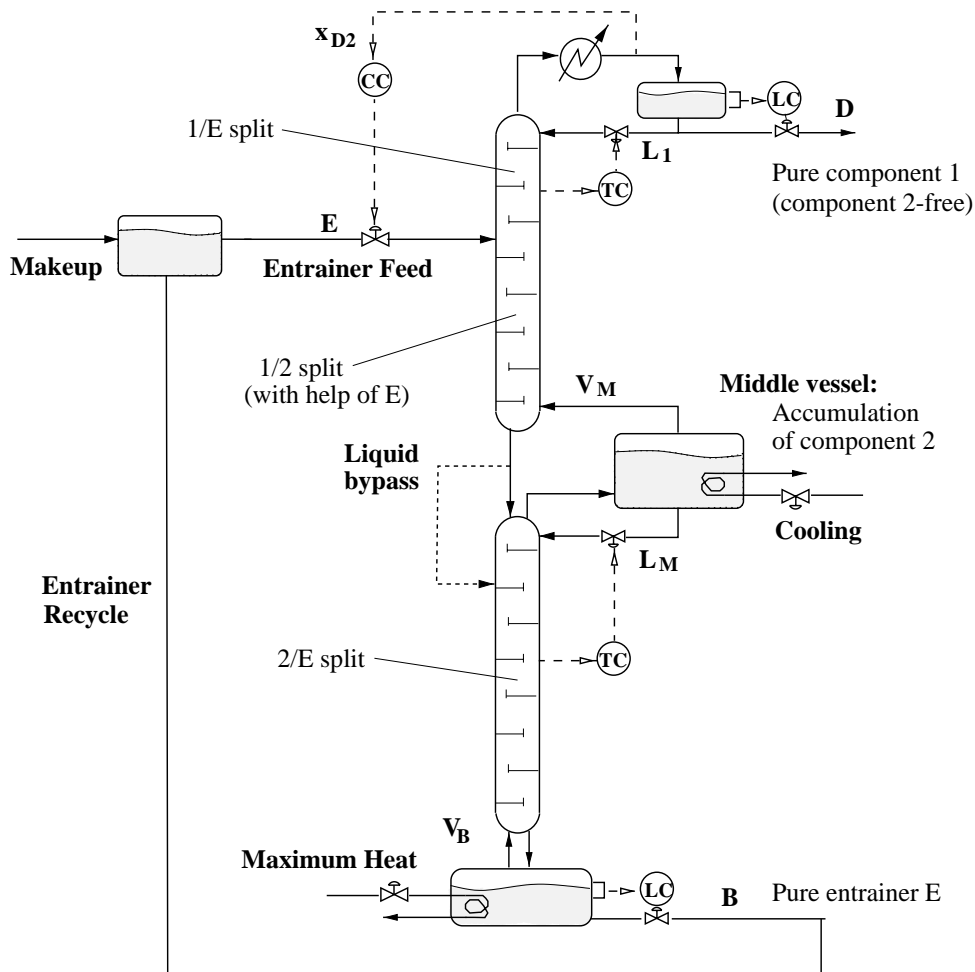


Figure 9.2: Proposed control structure for two-point composition control of the extractive middle vessel batch distillation column with the liquid bypass configuration. Simultaneous separation (Scheme I) with entrainer recycle is illustrated. The alternative liquid bypass (dotted line) is a possible modification to avoid entrainer accumulation in the middle vessel, but was not considered in the simulations.

## 9.4 Simulation model

The mathematical model is based on the same assumptions as the model described in Chapter 8. The model with PI control was implemented in SpeedUp (1993) and the input file is included in Appendix A in the back of the thesis.

## 9.5 Closed loop simulation results

In this study we consider the mixture acetone (1) - methanol (2) - water (E) (System 2 in Chapter 8). The original mixture feed composition was 50 mol% acetone and 50 mol% methanol. Pure water was used as entrainer. The column specifications and initial conditions for the simulations are given in Table 9.1.

Table 9.1: Column data and initial conditions for the middle vessel extractive batch distillation column separating acetone and methanol using water as entrainer.

Total no. of trays	30 (excl. reboiler)
No. of trays per section	$N_1 = 6, N_2 = 14, N_3 = 10$
Total initial charge	$H_{F0} = 5.385$ kmol
Condenser holdup (constant)	$H_{D0} = 0.035$ kmol
Initial middle vessel holdup	$H_{M0} = 5.125$ kmol
Reboiler holdup (constant)	$H_{B0} = 0.035$ kmol
Tray holdup (constant)	$H_j = 1/300$ kmol

We used the same product specifications as in Chapter 8:

*Acetone:* 96.0 mol % acetone (maximum 0.1 mol % methanol and 3 mol % water impurity);

*Methanol:* 99.0 mol % methanol (maximum 1.0 mol % acetone impurity);

*Entrainer recovery:* 99.9 mol % water (maximum 0.1 mol % methanol impurity).

For all the simulations in this study we use constant vapor flow in the stripping section ( $V_B$ ), and constant vapor flow in the extractive and rectifying sections ( $V_M$ ). The extractive section determines the minimum vapor flow in the column  $V_{\min}$ . We have considered two cases:

- *Equal vapor flows:*  $V_B = V_M = 5$  kmol/hr;
- *Different vapor flows:*  $V_B = 7$  kmol/hr and  $V_M = 5$  kmol/hr (with cooling in the middle vessel).

The cooling introduces an extra degree of freedom which may be necessary to achieve a pure bottom product.

The control parameters for the PI-controllers used in the simulations are given in Table 9.2.

Table 9.2: Control parameters used in simulations of extractive middle vessel batch distillation with liquid bypass configuration in Figure 9.2.

CC-loop:	$K_{C1} = 1000, \tau_{I,1} = 0.25$
$x_{D2} \longleftrightarrow E$	$x_{D2,sp} = 0.001, E_{\max} = 10 \text{ kmol/hr}$
TC-loop:	$K_{C2} = 0.25, \tau_{I,2} = 0.15$
$T_2 \longleftrightarrow L_M$	$T_{2,sp}$ specified in Table 9.3, $L_{M,\min} = 0$

Step 1 *Startup*: The column is operated at total reflux ( $D=B=0$ ) and  $L_M=0$  with constant entrainer flowrate  $E = 6 \text{ kmol/hr}$  in 15 minutes (that is, the middle vessel and reboiler holdup increase). After the startup period the reboiler holdup is pure water with  $H_{B1} = 1.035 \text{ kmol}$  and the middle vessel holdup is  $H_{M1} = 5.715 \text{ kmol}$ .

Step 2 *Extractive distillation operation*: The controllers are switched on (manipulating the entrainer flowrate  $E$  and the liquid flow out of the middle vessel  $L_M$ ) in order to drive the distillate composition and bottom entrainer composition to their desired values. The entrainer feeding is stopped when the impurity of the distillate product exceeds a pre-specified maximum value (at time  $t_2$ ).

Step 3 *Ordinary distillation*: The column is operated without entrainer feed as an ordinary middle vessel batch distillation column with feedback control to separate the residual material in the system. The setpoints  $x_{D2,sp}$  and  $T_{2,sp}$  in Table 9.2 are changed accordingly.

The results of the *closed loop extractive distillation operation* (Step 2) are summarized in Table 9.3. The two different separation schemes described in Chapter 8 (I: simultaneous and II: sequential) were implemented by changing the temperature set-point in the stripping section  $T_{2,sp}$  (that determines the 2/E split). We only show the results for the extractive distillation operation (Step 2) as this is the crucial part of the separation. Step 3 is ordinary distillation separating methanol and water in the middle vessel column.

For the simultaneous separation (Scheme I), we found that the vapor flow must be higher in the stripping section than in extractive and rectifying sections in order to obtain the specified water purity in the bottom product (Case 1: acetone recovery 86.0 %). Operation with equal vapor flows and parameters in Case 2 did not obtain pure water in the bottom product during the whole Step 2 (see Figure 9.12b). In both cases, there must be a period without entrainer feeding where the middle vessel product (methanol) is purified by ordinary distillation, but this could possibly have been avoided by using the alternative liquid bypass configuration shown in Figure 9.2.

From Figure 9.6 we see that the entrainer flowrate is almost constant during Step 2: The entrainer load is high initially ( $E_{\max}$ ), then almost constant at about 5.2 kmol/hr (moderately increasing) with a rapid increase towards the end of the extractive distillation period ( $E_{\max}$ ). This indicates

Table 9.3: Operating conditions and simulation results for control of extractive middle vessel batch distillation with liquid bypass configuration.

Separation scheme	Operating conditions	Recovery
Case 1: <i>I: simultaneous different vapor flows</i>	Reflux ratio, $R = 4$ $T_{2,sp} = 77.0^\circ C$ $V_B = 7 \text{ kmol/hr}, V_M = 5 \text{ kmol/hr}$	$\sigma_{acetone} = 86.0 \%$ $t_2 = 2.41 \text{ hr}$
Case 2: <i>I: attempt simultaneous equal vapor flows</i>	Reflux ratio, $R = 4$ $T_{2,sp} = 77.0^\circ C$ $V_B = 5 \text{ kmol/hr}, V_M = 5 \text{ kmol/hr}$	$\sigma_{acetone} = 86.7 \%$ $t_2 = 2.43 \text{ hr}$
Case 3: <i>II: sequential equal vapor flows</i>	Reflux ratio, $R = 4$ $T_{2,sp} = 70.0^\circ C$ $V_B = 5 \text{ kmol/hr}, V_M = 5 \text{ kmol/hr}$	$\sigma_{acetone} = 99.3 \%$ $t_2 = 2.79 \text{ hr}$
Case 4: <i>II: sequential different vapor flows</i>	Reflux ratio, $R = 4$ $T_{2,sp} = 70.0^\circ C$ $V_B = 7 \text{ kmol/hr}, V_M = 5 \text{ kmol/hr}$	$\sigma_{acetone} = 99.4 \%$ $t_2 = 2.79 \text{ hr}$

Startup period (15 min):  $E = 6 \text{ kmol/hr}, D = B = L_M = 0$

that it may be acceptable with constant entrainer feed flowrate for batchwise extractive distillation in the middle vessel column (similar to continuous columns).

From Figure 9.7 we see that the liquid flow out of the middle vessel increases to a value twice the distillate flow (Case 1:  $D = 1 \text{ kmol/hr}$ ). The middle vessel holdup is decreased during the whole extractive distillation operation (Step 2). The bottom flowrate (B) is governed by varying entrainer feed flowrate (proportionally by mass balance).

For the sequential separation (Scheme II), the separation between 2 and E in the stripping section is not important (that is, a mixture of 2 and E is removed in the bottom similar to the continuous extractive distillation scheme) and the vapor flow may be equal in all sections. In Case 4, the entrainer flowrate reaches saturation  $E_{\max} = 10 \text{ kmol/hr}$ . The entrainer does practically not accumulate in the middle vessel even though the entrainer load is higher (see Figure 9.17) and the acetone recovery is greatly improved (Case 4: acetone recovery 99.4 %).

9.5.1 Closed loop simulation results (Scheme I: simultaneous)

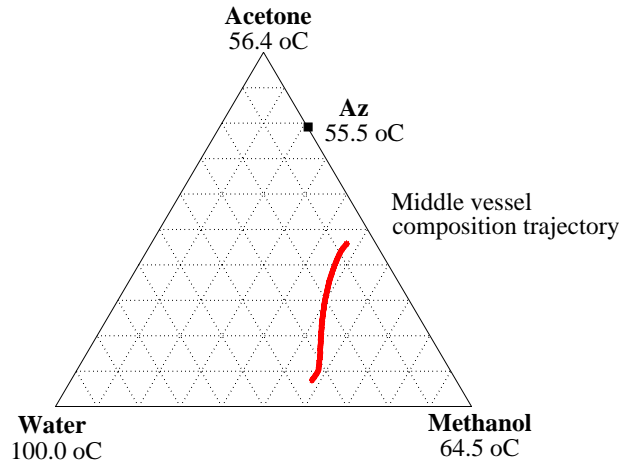


Figure 9.3: Control of extractive middle vessel batch distillation with liquid bypass configuration. Middle vessel composition trajectory for the entrainer feeding period (Step 2) of the extractive distillation process (Case 1).

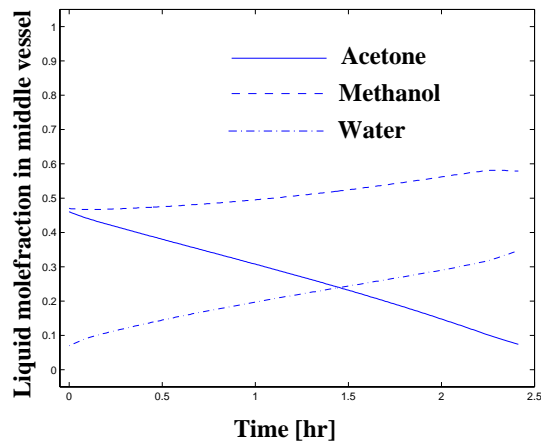
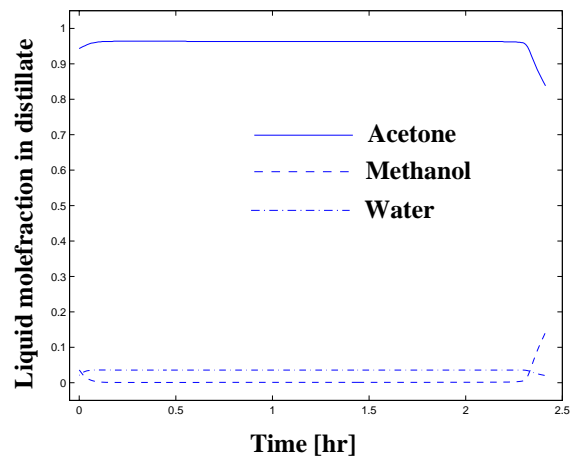
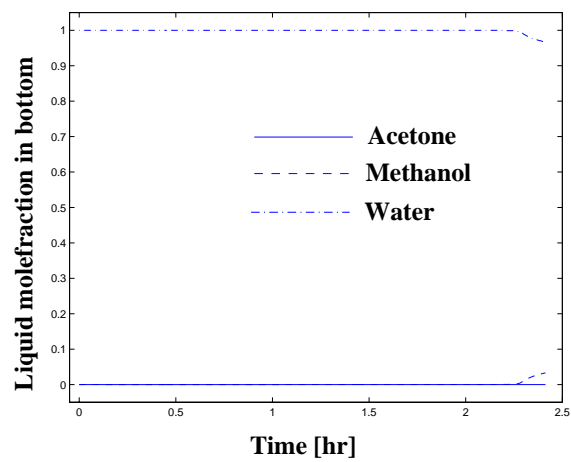


Figure 9.4: Middle vessel composition trajectory corresponding to Figure 9.3. Water and methanol accumulate in the middle vessel during entrainer feeding (Case 1).



(a) Distillate product composition



(b) Bottom product composition

Figure 9.5: Distillate and bottom product composition trajectories corresponding to Figure 9.3. Simultaneous production of acetone and water during the whole entrainer feeding period (Step 2) of the extractive distillation process (Case 1).



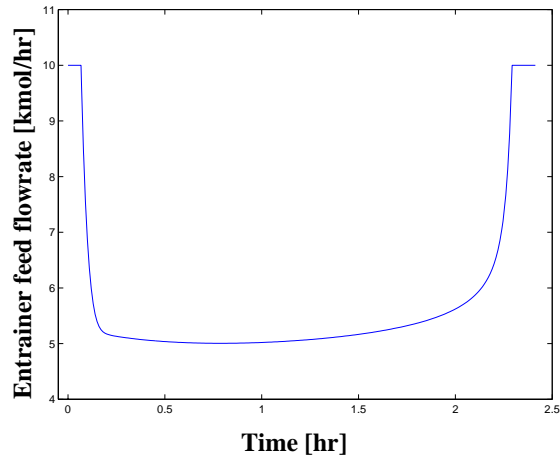


Figure 9.6: Entrainer feed flowrate  $E$  during the entrainer feeding period (Step 2) of the extractive distillation process with liquid bypass configuration (Case 1).

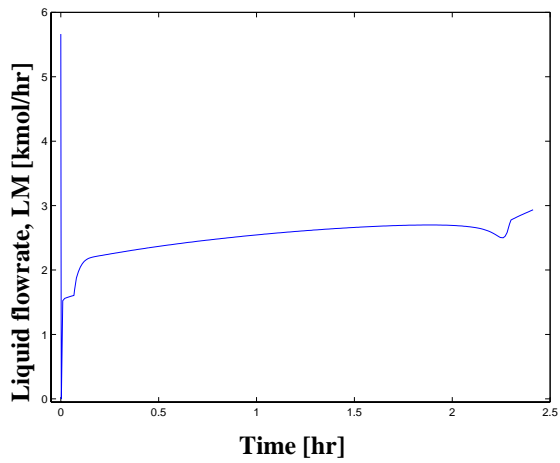


Figure 9.7: Liquid flow out of middle vessel  $L_M$  during the entrainer feeding period (Step 2) of the extractive distillation process with liquid bypass configuration (Case 1).

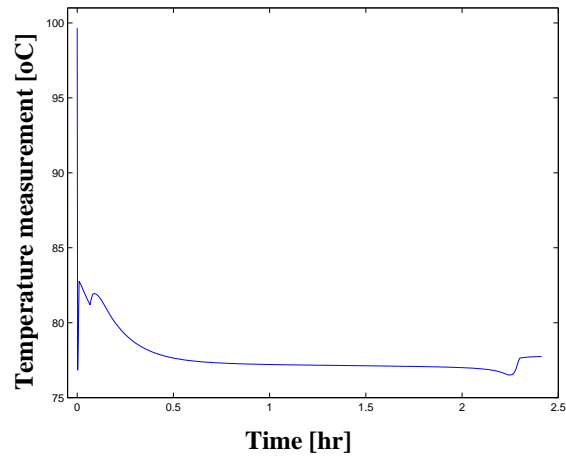


Figure 9.8: Temperature measurement on tray in stripping section  $T_2$  during the entrainer feeding period (Step 2) of the extractive distillation process with liquid bypass configuration (Case 1).

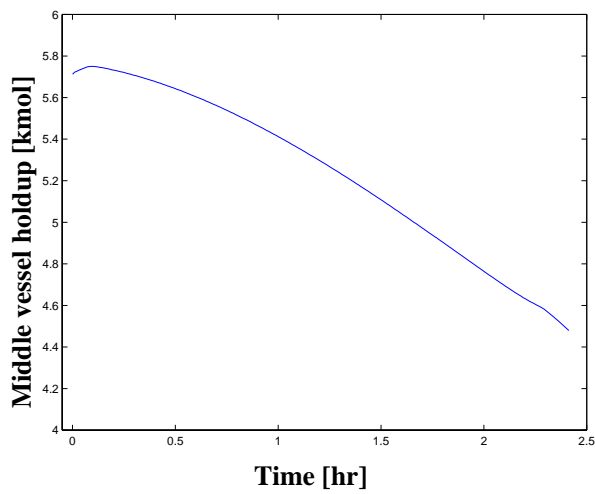


Figure 9.9: Middle vessel holdup  $H_M$  during the entrainer feeding period (Step 2) of the extractive distillation process with liquid bypass configuration (Case 1).

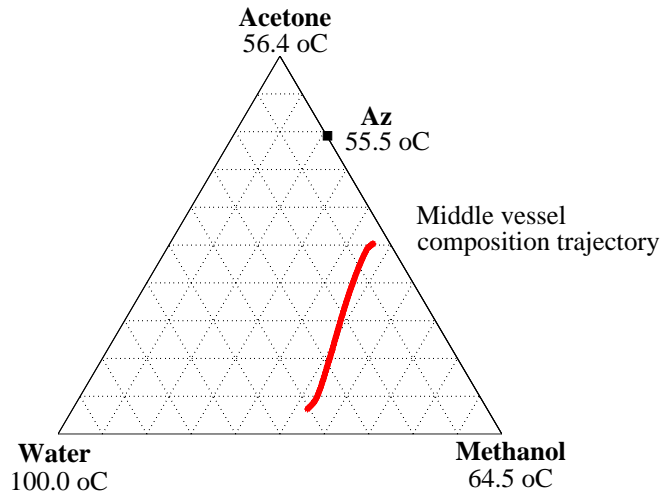


Figure 9.10: Control of extractive middle vessel batch distillation with liquid bypass configuration. Middle vessel composition trajectory for the entrainer feeding period (Step 2) of the extractive distillation process (Case 2).

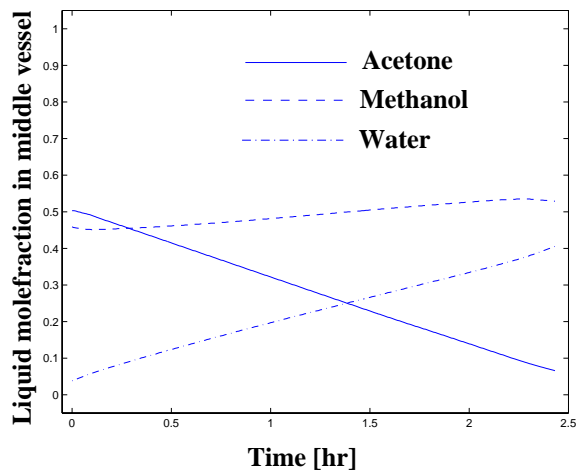
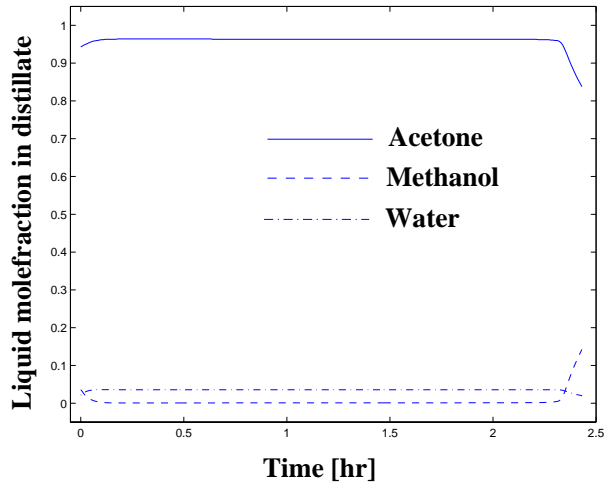
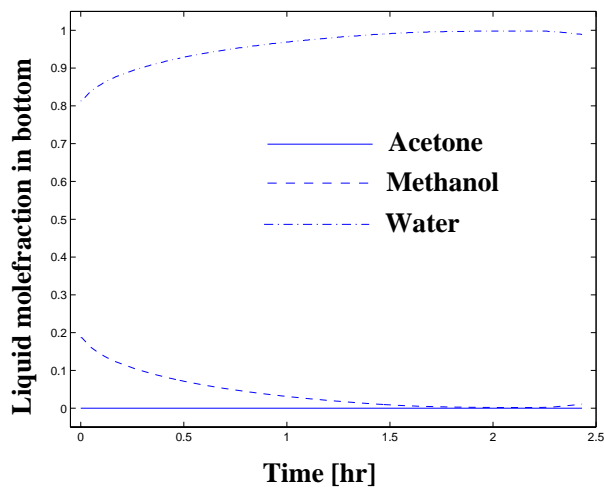


Figure 9.11: Middle vessel composition trajectory corresponding to Figure 9.10 (Case 2).



(a) Distillate product composition



(b) Bottom product composition

Figure 9.12: Distillate and bottom product composition trajectories corresponding to Figure 9.10. The separation in the stripping section is insufficient, that is, the bottom product is not pure water during the whole entrainer feeding period (Case 2).

### 9.5.2 Closed loop simulation results (Scheme II: sequential)

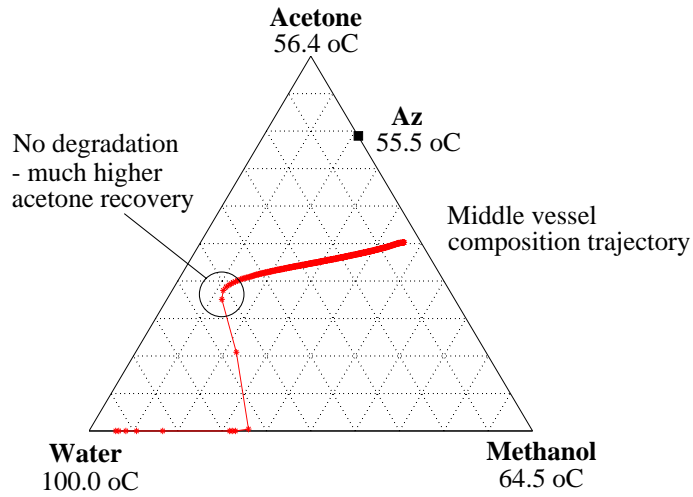


Figure 9.13: Control of extractive middle vessel batch distillation with liquid bypass configuration. Middle vessel composition trajectory for the entrainer feeding period (Step 2) of the extractive distillation process. The composition profile in the column does not degrade during entrainer feeding (Case 3).

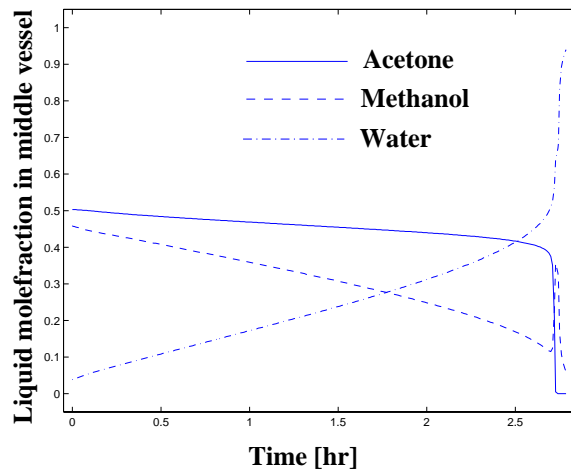
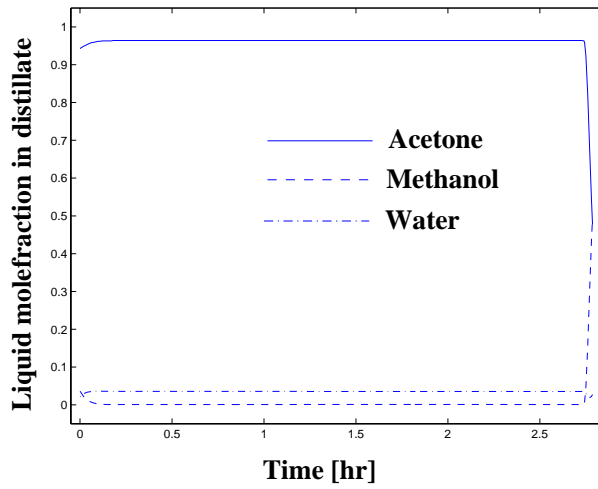
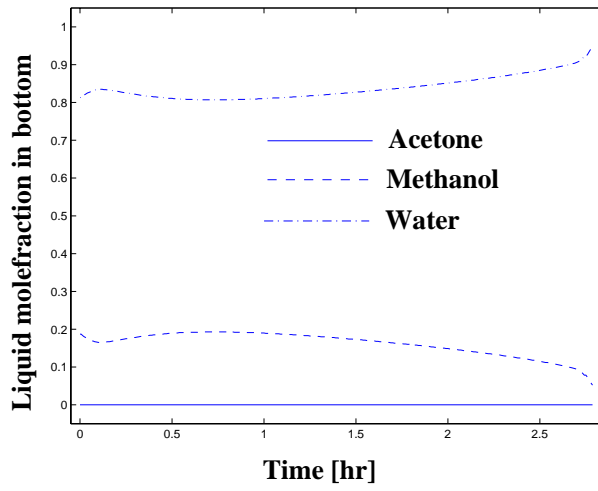


Figure 9.14: Middle vessel composition trajectory corresponding to Figure 9.13. Water accumulates in the middle vessel and methanol is removed from the middle vessel during entrainer feeding (Case 3).



(a) Distillate product composition



(b) Bottom product composition

Figure 9.15: Distillate and bottom product composition trajectories corresponding to Figure 9.13. Production of acetone distillate product and a fraction of methanol and water in the bottom product (Case 3).

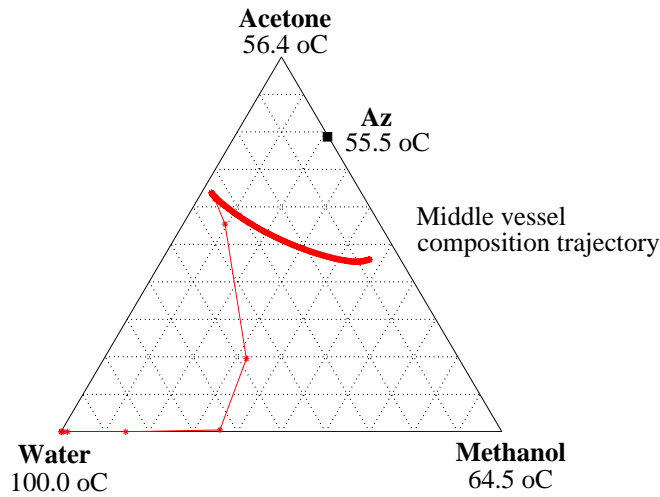


Figure 9.16: Control of extractive middle vessel batch distillation with liquid bypass configuration. Middle vessel composition trajectory for the entrainer feeding period (Step 2) of the extractive distillation process (Case 4).

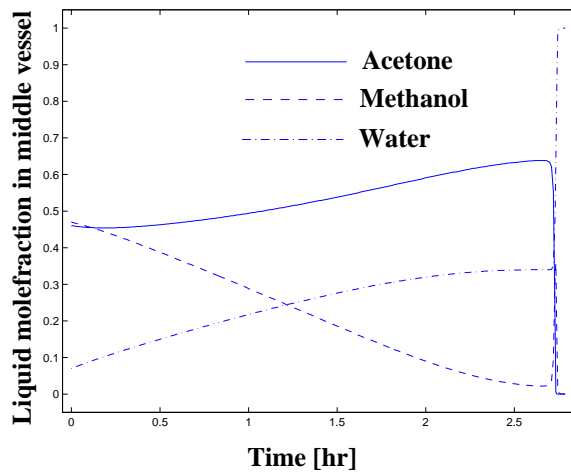
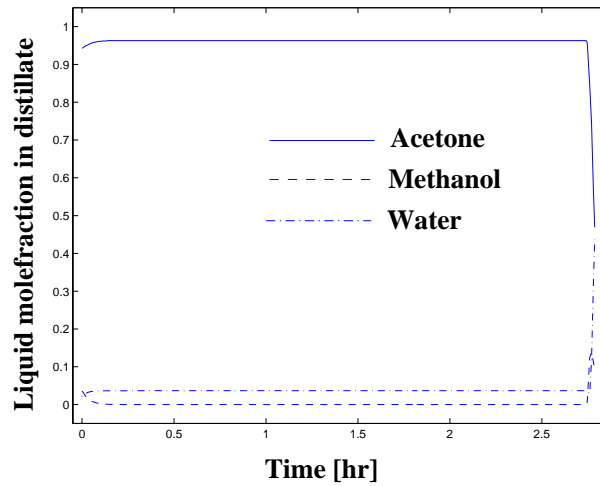
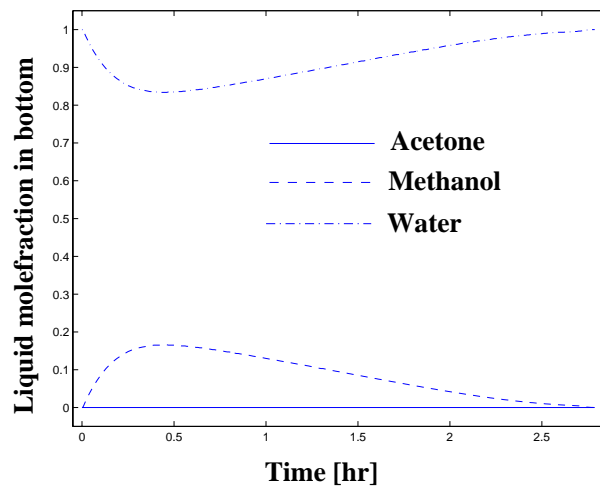


Figure 9.17: Middle vessel composition trajectory corresponding to Figure 9.16. Very little water accumulates in the middle vessel and methanol is removed from the middle vessel during entrainer feeding (Case 4).



(a) Distillate product composition



(b) Bottom product composition

Figure 9.18: Distillate and bottom product composition trajectories corresponding to Figure 9.16 (Case 4).



## 9.6 Discussion and further work

The sequential separation (Scheme II) in the middle vessel column has significantly higher acetone recovery than in the conventional extractive distillation column studied in Chapter 8 (for  $R=4$  the maximum recovery was about 90.6 % in this column). The simultaneous separation (Scheme I) in the middle vessel column has less acetone recovery than in the conventional extractive distillation column. However, extractive batch distillation in the middle vessel column configuration allows direct entrainer recycle and possible time (energy) savings.

It would be interesting to compare the time consumption for the complete extractive distillation process (including the methanol and water entrainer recovery Step 3) for the two alternative separation schemes (simultaneous and sequential) in the middle vessel column. The simultaneous separation scheme *may* have the advantage of time (energy) savings in addition to the possibility of direct entrainer recycle, but with less acetone recovery.

Warter and Stichlmair (1999) report for the mixture ethanol and water using ethylene glycol as entrainer (System 1 in Chapter 8) that they were able to achieve a pure middle vessel product (water) at the end of the extractive distillation operation (Step 2) in the liquid bypass configuration. This is probably because the ethylene glycol entrainer in this mixture system has very low volatility and the vapor flow from the stripping section is essentially entrainer-free. To obtain an entrainer-free middle vessel product in other cases we propose to introduce the liquid bypass further down in the stripping section.

## 9.7 Conclusion

A novel control structure for batch extractive distillation in the middle vessel column is proposed. Tight composition control and simultaneous production of distillate product and entrainer recovery are obtained with simple single loop PI controllers. Simultaneous production of acetone distillate and water bottom product required a higher vapor flow in the stripping section than in the extractive section. The highest acetone recovery was obtained with sequential separation (Scheme II) in the middle vessel column.



## **Part III**

# **Conclusions**



## Chapter 10

# Practical Implications, Conclusions and Suggestions for Future Work

Here we provide brief guidelines on how to approach azeotropic mixtures separation tasks and summarize overall conclusions derived from this thesis. For more detailed descriptions and conclusions we refer to the individual chapters in the thesis.

### 10.1 Practical implications

The main objective of this section is to provide some simple practical guidelines for industrialists. We also recommend the handbooks by Drew (1997), Schweitzer (1997) and Rousseau (1987).

#### *Introduction: Solvent recovery in fine- and specialty chemical industry*

Recovery and reuse of solvents are critical today because of solvent shortages, high prices and air and water pollution regulations. Liquid solvents contaminated with chemicals, dirt or other solvents must be purified to make it suitable for reuse. Purification is usually accomplished by distillation. Many processes involve use of multiple solvents which become mixed in use. Where more than three solvents are present, batch distillation is usually more desirable than continuous (Drew, 1975).

The solvent recovery system is typically developed for multicomponent liquid mixtures, varying feed compositions and difficult separation (azeotropes, close-boiling components and high purity requirements). The best process would usually be that which produces the highest recovery of quality solvent at the lowest equipment and operating costs, while satisfying pollution-control and safety constraints.

Complete separation of multicomponent azeotropic mixtures may be very difficult and sometimes an azeotrope fraction is an acceptable product. Examples of such mixtures from industry are THF (tetrahydrofuran) - MEK (methyl ethyl ketone) - toluene; methanol - ethanol - propanol; and benzene - toluene - xylene (Schweitzer, 1997). In the worst cases, it may only be possible to take fractions by boiling-point range, reusing as much as possible and incinerating or selling the rest. Having said this, there are “azeotrope-breaking” processes that separate these mixtures into pure components, and some of these processes are developed in particular for solvent recovery in fine- and specialty chemical industries.

Specifications for recovered solvents which normally can be met economically are listed by Drew (1975) are: water content of solvent; 0.05-0.5 %, cross mixing of solvents; 0.5-5%, and organic content of waste water; 10 to 100 parts/million. Usually, this means the recovered solvent will meet manufacturer’s specifications for industrial-solvent grades.

### ***How to approach and analyze the separation task***

There is no standard procedure by which separation processes are chosen. However, there are certain guidelines that are usually followed (Rousseau, 1987):

1. Define the problem. Usually, this entails establishing product purity and recovery specifications.
2. Determine which separation methods are capable of accomplishing the separation.

The general approach for the development of a liquid mixture separation process is illustrated in Figure 10.1. The first task is often to assess the vapor-liquid-liquid equilibrium behavior of the

#### **Separation system process development**

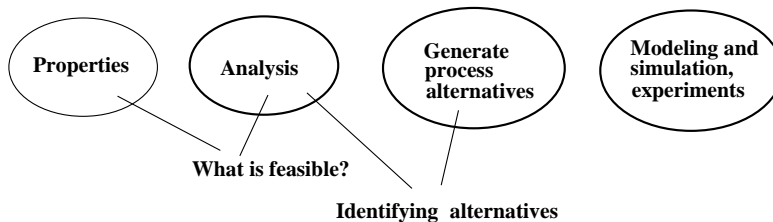


Figure 10.1: *Development of separation systems.*

species to be separated (Westerberg and Wahnschafft, 1996). Experimental data is the only assure way to predict the behavior, and many such data are currently available. Horsley (1973), for example, has compiled a listing of known azeotropes. Available data for ternary or higher mixtures

over the concentration range of interest are seldom adequate (Stichlmair and Fair, 1998). Westerberg and Wahnschafft (1996) give a way to determine if the multicomponent mixture displays highly nonideal behavior (from flash calculations) based on binary pair infinite dilution  $K$ -values (see also Chapter 3, Section 3.8). The hydrogen-bonding guidelines given by Berg (1969) based on specific molecular groups are also useful for predicting deviation from ideality.

If the mixture displays azeotropic or heterogeneous behavior, the separation systems will be very different from the distillation systems for fairly ideal mixtures (Westerberg, 1997).

Generally, if the mixture in question is heterogeneous or multiphase, phase separation of the existing phases should be carried out before any homogeneous separation, as recommended by Smith (1995). For example, pretreatment by filtration or decantation may be adequate if the given mixture is contaminated with solids and tars.

The next step after this property assessment is to generate separation process alternatives. This may be done by “property difference analysis” described by, for example, Jaksland and Gani (1995; 1997). The property differences of the mixture components indicate what separation unit operation that is most tangible for the given separation task.

A binary homoazeotropic mixture is inherently impossible to separate by ordinary distillation at the system pressure. Unless pressure variation can be utilized, which is the first thing to evaluate, special methods are required, such as heteroazeotropic or extractive distillation or hybrid processes that combine membranes and distillation, for example. For these the entrainer-addition distillation methods we need to search for candidate entrainers that gives (ternary) VLE diagrams that are promising for these separation schemes (Chapter 2).

If the mixture has more than three components, we need to analyze each binary pair and also the ternary combinations of the components. This gives us useful information on how to separate the mixture as a whole.

To determine the mixture’s VL(L)E behavior there are many commercial software packages available, for example DISTILL from HyproTech and SPLIT from AspenTech. The physical properties can be obtained from databanks or by physical property estimation packages. From plots of the phase behavior such as T-x,y diagrams for each binary pair in the mixture, we can see whether the mixture displays azeotropic and/or heterogeneous behavior. Azeotropic data handbooks (e.g. Horsley (1973) and Gmehling *et al.* (1994)) which often provide azeotrope composition and boiling point at given pressures are also useful in determining whether there are any azeotropes appearing. A step-by-step approach with examples is given by Westerberg and Wahnschafft (1996) and Westerberg (1997).

Phase diagram analysis such as plot of distillation lines or residue curves on a composition diagram is an excellent tool for gaining insights into the complex behavior of nonideal ternary mixtures. Some uses for industrial mixtures are illustrated by, for example, Wasylkiewicz *et al.* (1999b) and in Chapter 2 of this thesis.

From the binary VL(L)E information we recommend drawing composition triangles (either by hand or by using the mentioned software packages) which include:

- location and boiling temperature of the pure components and azeotropes;
- sketch of residue curves or distillation lines near the singular points with arrows indicating increasing temperature.

The ternary mixture has one of the 26 possible topological VLE diagram structures given in Figure 3.21. See also Table 3.8 for a quick look-up on possible structure classes based solely on the binary information. In most cases the topological structure can be determined based solely on this information (see Chapter 3). Usually the existence of azeotropes split the VLE diagram into distillation regions that limit the possibility of separating the mixture by ordinary distillation. One should:

- localize the feed composition of the mixture in question;
- as a first approximation use the  $\infty/\infty$  approach or  $\infty/N$  approach described in Chapter 2 to predict the product areas for this feed.

If separation into (relatively) pure components is not possible by ordinary distillation, then we need to consider special methods for separating the mixture. Chapter 2 gives an overview of various “azeotrope-breaking” methods and industrial processes.

## 10.2 Conclusions

The thesis offers a critical evaluation of azeotropic distillation theory and puts the large number of publications into perspective. Useful knowledge from the Russian distillation research community has been included through the cooperation with the thesis co-advisor Dr. Valeri N. Kiva.

The main contributions of this thesis are summarized below:

**Chapter 2:** Gives an introduction and overview of azeotropic mixtures separation, and illustrates the use of azeotropic phase equilibrium diagrams for the development of entrainer-addition distillation systems. The powerful process of combined heteroazeotropic and extractive distillation is given as an example that is normally excluded by entrainer selection criteria given in recent textbooks and encyclopedia.

**Chapter 3:** Provides a survey on azeotropic phase equilibrium diagrams with critical evaluation of the published literature in this field of research. The specific contributions are given in the introductory pages of the chapter.

**Chapter 4:** Presents the simplifying concept of elementary topological cells of ternary VLE diagrams. This abstraction of the structural VLE diagrams greatly reduces the number structures



that need to be analyzed in order to reveal the qualitative characteristics of any ternary azeotropic mixture. Statistics on the physical existence (occurrence) of azeotropic mixtures are also included.

**Chapter 5:** Examines the effect of column holdup in residue curve map prediction of batch distillation products and off-cuts. Even though column holdup was found to affect the distillate product sequence, the quick analysis based on residue curve maps and simple models of batch distillation neglecting tray holdup can be recommended if used with care.

**Chapter 6:** Gives an introduction to batch distillation in general, and provides a comparison of the time consumption of the cyclic and the closed middle vessel batch distillation for separating ternary ideal mixtures. Time savings of up to 50 % were found for the middle vessel column for difficult (low relative volatility) separations. The middle vessel column performs best for feeds which are rich in light and heavy components as opposed to some previous claims in the literature.

**Chapter 7:** Determines the use VLE diagram information, such as distillation lines and isotherms, as a graphical tool for operation and control considerations in cyclic and closed middle vessel batch distillation of ternary azeotropic mixtures.

**Chapter 8:** Extends extractive distillation insight to batch distillation operation in the conventional and middle vessel batch columns. The influence of column design and extractive distillation operating parameters on the separation performance has been determined. The middle vessel column with the liquid bypass configuration was found to have the best performance.

**Chapter 9:** Presents a novel control strategy for extractive batch distillation in the middle vessel column with the liquid bypass configuration. Tight composition control and simultaneous production of distillate product and entrainer bottom product are obtained during the entrainer feeding period, but an additional step to purify the middle vessel product was found to be unavoidable. A refinement of the liquid bypass configuration that may avoid entrainer accumulation in the middle vessel is proposed.

## 10.3 Suggestions for future work

Some directions for future work may include:

**Further extension** of continuous azeotropic distillation insights to batch operation. In particular, the close resemblance between continuous distillation and the middle vessel column makes the extension for this batch column operation easier. Recently, the research groups of Stichlmair and coworkers (TU Munich) and Barton and coworkers (MIT Boston) have pursued this topic (see reference list).

**Analysis** of the batch distillation behavior for mixtures of Cell III (and Cell IV) and possible multiplicity (see Chapter 7) remains an unsolved problem.

**Heteroextractive batch distillation** is a powerful method of separating azeotropic mixtures that is almost unexplored. We propose to investigate a heteroazeotropic or combined het-

eroazeotropic and extractive batch distillation system in the middle vessel column where the heteroazeotrope is removed as distillate or intermediate product and separated by decantation (see Chapter 7).

**Membrane-distillation hybrids** have the potential to become an attractive method of separating azeotropic mixtures, especially in pharmaceutical and fine chemical production where other separation methods based on the addition of an entrainer are ruled out since they introduce new chemical components to the mixture system. The often mentioned disadvantage of limiting capacity of the membrane units (pervaporation) is not necessary an issue in such small-scale chemicals production. In addition, membrane distillation hybrids may be competitive simply because membranes are less energy intensive than distillation.

**Reactive distillation-membrane hybrids** The production of esters by the reaction of acids and alcohols is a commonly used process in the chemical industry. Water is generated in the process, and its removal increases the yield of ester (e.g. Sørensen (1994)). If the ester is fairly none-volatile (has a high boiling point), water can be removed by heating the reaction mixture so that the lower boiling alcohol evaporates with the water while the higher boiling ester remains in the reactor. Water and alcohol may then be separated in a ordinary distillation column, though this is possible only up to the azeotropic composition. Augmenting the distillation with vapor permeation seems to be a promising choice for these processes (Sulzer, 1998). The dehydrated alcohol from the membrane-unit can be recycled back to the reactor, enabling complete reaction of the feed acid. The ester separation is simplified too, since the ester has only to be separated from the alcohol.

**Occurrence of classes** There is a need for an updated list of the natural occurrence of the various ternary mixture classes based. This may include theoretical predictions e.g. based on binary azeotropic data collected in Gmehling *et al.* (1994) (based on data from Lecat 1918, Lecat 1949, Ogorodnikov *et al.* 1971, Horsley 1973 and the Dortmund Data Bank, Gmehling *et al.* 1977). This azeotropic data book reports to comprise more than 18 800 systems involving approximately 1 700 compounds, in which approximately 47 % of the systems show azeotropic behavior. In particular, it would be interesting to check the possible existence of classes for which occurrence is not reported (e.g. Serafimov's class 3.0-1a).





# Note Concerning the References

The following three Russian scientific journals have been published in English-language editions since about 1957:

*Theoretical Foundations of Chemical Engineering*

English edition of *Teoreticheskie Osnovy Khimiceskoj Technologii*, Maik nauka, Interperiodica Publ., Moscow. A comprehensive journal covering all aspects of theoretical and applied research in chemical engineering. Published 6 times per year.

*Russian Journal of Physical Chemistry*

English edition of *Zurnal Fiziceskoj Khimii*, Akademija Nauk SSSR, Moscow. Published monthly by The British Library Document Supply Centre in cooperation with the Royal Society of Chemistry, London.

*Russian Journal of Applied Chemistry*

English edition of *Zurnal Prikladnoi Khimii*, Akademija Nauk SSSR, Moscow. Previously *Journal of Applied Chemistry of the USSR* (until 1992). Published monthly by Consultants Bureau, New York.

The papers in the English-language editions are translations of papers originally written in Russian. The translations are often poor and the titles sometimes inadequate and ambiguous. Therefore, we have given corrected English titles in square brackets for some of the references. For example, we have added corrected words in brackets in the subtitle of Serafimov (1968*b*): “II. The Form [*Pattern*] of Distillation Lines [*Residue Curves*] in the Region of Singular Points for Four-Component Mixtures” to show that the Russian term “distillation line” is what is “residue curve” in most English-language publications.

Furthermore, the page numbers refer to the page numbering in the English edition, whereas the page numbers given in brackets correspond to the page numbering in the *original* Russian edition of the journals. If a reference is only available in Russian language this is marked by (in Russian). This also applies to other references that are not available in English-language translations.



# References

- Ahmad, B.S. (1997). Synthesis of Batch Processes with Integrated Solvent Recovery. PhD thesis. Massachusetts Institute of Technology, Boston, USA.
- Ahmad, B.S. and P.I. Barton (1994). Solvent recovery Targeting for Pollution Prevention in Pharmaceutical and Specialty Chemical Manufacturing. *AIChE Symp. Series* **90**(303), 59–73.
- Ahmad, B.S. and P.I. Barton (1996). Homogeneous Multicomponent Azeotropic Batch Distillation. *AIChE J.* **42**(2), 3419–3433.
- Ahmad, B.S., Y. Zhang and P.I. Barton (1998). Product Sequences in Azeotropic Batch Distillation. *AIChE J.* **44**(5), 1051–1070.
- Andersen, H.W., L. Laroche and M. Morari (1995). Effect of Design on the Operation of Homogeneous Azeotropic Distillation. *Comp. Chem. Eng.* **19**(1), 105–122.
- Babich, S.V. (1972). Development of the Separation Technology for Light Fraction of the Gasoline Oxidate by Means of Thermodynamic-Topological Analysis (in Russian). PhD thesis. Lomonosov Institute of Fine Chemical Technology, Moscow, Russia.
- Baburina, L.V., V.M. Platonov and M.G. Slin'ko (1983). Thermodynamic Investigation of Phase Diagrams of Ternary Azeotropic Mixtures (in Russian). *Doklady Akademii nauk SSSR* **269**(1), 129–133.
- Baburina, L.V., V.M. Platonov and M.G. Slin'ko (1988). Classification of Vapor-Liquid Equilibrium Diagrams for Homogeneous Azeotropic Mixtures. *Theor. Found. Chem. Eng.* **22**(4), 390–396 [535–542].
- Balashov, M.I., A.V. Grishunin, A.V. Ryazanova and L.A. Serafimov (1970). On the Investigation of Continuous and Batch Distillation Regions (in Russian). *Book: Physical-Chemical Foundations of Distillation, Moscow Lomonosov Institute of Fine Chemical Technology, Moscow*, 205–215.
- Barolo, M. and G.B. Guarise (1996). Batch Distillation of Multicomponent Systems with Constant Relative Volatilities. *Trans. IChemE* **74**(Part A), 863–871.

- Barolo, M., G.B. Guarise, N. Ribon, S.A. Rienzi, A. Trotta and S. Macchietto (1996a). Some Issues in the Design and Operation of a Batch Distillation Column with a Middle Vessel. *Comp. Chem. Engng.* **20**(Suppl.), S37–S42.
- Barolo, M., G.B. Guarise, S.A. Rienzi, A. Trotta and S. Macchietto (1996b). Running Batch Distillation in a Column with a Middle Vessel. *Ind. Eng. Chem. Res.* **35**(12), 4612–4618.
- Barolo, M., G.B. Guarise, S.A. Rienzi and A. Trotta (1998). Understanding the Dynamics of a Batch Distillation Column with a Middle Vessel. *ESCAPE-8, Brugge, Belgium, May 24-27, 1998, Supplement to Comp. Chem. Engng.* **22**(Supplement), S37–S44.
- Bauer, M.H. and J. Stichlmair (1995). Synthesis and Optimization of Distillation Sequences for the Separation of Azeotropic Mixtures. *Comp. Chem. Eng.* **19**, S15–S20.
- Bekiaris, N. and M. Morari (1996). Multiple Steady States in Distillation:  $\infty/\infty$  Predictions, Extensions, and Implications for Design, Synthesis, and Simulation. *Ind. Eng. Chem. Res.* **35**, 4264–4280.
- Bekiaris, N., G.A. Meski, G.A. Raudu and M. Morari (1993). Multiple Steady States in Homogeneous Azeotropic Distillation. *Ind. Eng. Chem. Res.* **32**(9), 2023–2038.
- Benedict, M. and D.R. Rubin (1945). Extractive and Azeotropic Distillation I. Theoretical Aspects. *Trans. Am. Inst. Chem. Eng.* **41**, 353–370.
- Berg, L. (1969). Azeotropic and Extractive Distillation: Selecting the Agent for Distillation. *Chem. Eng. Prog.* **65**(9), 52–57.
- Bergdorf, J. (1991). Case Study of Solvent Dehydration in Hybrid Processes with and without Pervaporation. *Proc. Fifth International Conference on Pervaporation Processes in the Chemical Industry*. Heidelberg (GE), 362–382.
- Bernot, C. (1990). Design and Synthesis of Multicomponent Batch Distillation. PhD thesis. University of Massachusetts, Amherst, USA.
- Bernot, C., M.F. Doherty and M.F. Malone (1990). Patterns of Composition Change in Multicomponent Batch Distillation. *Chem. Eng. Sci.* **45**(5), 1207–1221.
- Bernot, C., M.F. Doherty and M.F. Malone (1991). Feasibility and Separation Sequencing in Multicomponent Batch Distillation. *Chem. Eng. Sci.* **46**(5/6), 1311–1326.
- Biegler, L.T., I.E. Grossmann and Westerberg A.W. (1997). *Systematic Methods of Chemical Process Design*. Prentice Hall, NJ.
- Bogdanov, V.S. and V.N. Kiva (1977). Localization of Single [Unity] K- and  $\alpha$ -Lines in Analysis of Liquid-Vapor Phase Diagrams. *Russ. J. Phys. Chem.* **51**(6), 796–798 [1349–1352].
- Bortolini, P. and G.B. Guarise (1970). A New Method of Batch Distillation (in Italian). *Quad. Ing. Chim. Ital.* **6**, 1–9.



- Bossen, B.S., S.B. Jørgensen and R. Gani (1993). Simulation, Design, and Analysis of Azeotropic Distillation Operations. *Ind. Eng. Chem. Res.* **32**(4), 620–633.
- Boyarinov, A.I., V.N. Vetokhin, T.N. Gartman, V.V. Kafarov and D.N. Motyl' (1974). Calculation of the Limits of Distillation Regions [Calculation of Residue Curve Boundaries]. *Russ. J. Phys. Chem.* **48**(2), 299–302.
- Brignole, E.A., S. Bottini and R. Gani (1986). A Strategy for the Design and Selection of Solvents for Separation Processes. *Fluid Phase Equilibria* **29**, 125–132.
- Brown, W.D. (1963). Economics of Recovering Acetic Acid. *Chem. Eng. Prog.* **59**(10), 65–68.
- Bushmakina, I.N. and I. Kish (1957a). Isobaric Liquid-Vapor Equilibrium in a Ternary System with an Azeotrope of the Saddlepoint Type. *Russ. J. Appl. Chem.* **30**(2), 205–215 [200–211].
- Bushmakina, I.N. and I.N. Kish (1957b). "Separating Lines" of Distillation and Rectification of Ternary Systems [Residue Curve Boundaries and Distillation of Ternary Mixtures]. *Russ. J. Appl. Chem.* **30**(4), 595–600 [561–567].
- Bushmakina, I.N. and P.Ya. Molodenco (1957). The Choice of Entrainer for Azeotropic Rectification (in Russian). *Vestnik of Leningrad State University, Ser. Physics and Chemistry* **10**, 68–92.
- Castillo, F.J.L., D.Y.C. Thong and G.P. Towler (1998). Homogeneous Azeotropic Distillation. 1. Design Procedure for Single-Feed Column at Nontotal Reflux. *Ind. Eng. Chem. Res.* **37**, 987–997.
- Chang, T. and T.T. Shih (1989). Development of an Alternative Distillation Scheme for Purification of Tetrahydrofuran. *Fluid Phase Equilibria* **52**, 161–168.
- Cheong, W. and P.I. Barton (1999a). Azeotropic Distillation in a Middle Vessel Batch Column. 1. Model Formulation and Linear Separation Boundaries. *Ind. Eng. Chem. Res.* **38**(4), 1504–1530.
- Cheong, W. and P.I. Barton (1999b). Azeotropic Distillation in a Middle Vessel Batch Column. 2. Nonlinear Separation Boundaries. *Ind. Eng. Chem. Res.* **38**(4), 1531–1548.
- Cheong, W. and P.I. Barton (1999c). Azeotropic Distillation in a Middle Vessel Batch Column. 3. Model Validation. *Ind. Eng. Chem. Res.* **38**(4), 1549–1564.
- Christensen, F.M. and S.B. Jørgensen (1987). Optimal Control of Binary Batch Distillation with Recycled Waste Cut. *Chem. Engng. J.* **34**, 57–64.
- Davidyan, A.G., V.N. Kiva and V.M. Platonov (1991a). Batch Rectification in a Two-Section Column with a Central Reservoir [Middle Vessel] for Identical Vapor Flows in the Sections. *Theor. Found. Chem. Eng.* **25**(6), 771–782.

- Davidyan, A.G., V.N. Kiva and V.M. Platonov (1991b). Separation of Binary Mixtures in Two-Section Column with Central Reservoir [*Middle Vessel*]. *Theor. Found. Chem. Eng.* **25**(4), 467–475.
- Davidyan, A.G., V.N. Kiva and V.M. Platonov (1992a). Batch Fractionation of Multi-component Mixtures in Two-Section Column with Central Reservoir [*Middle Vessel*]. *Theor. Found. Chem. Eng.* **26**(4), 467–477.
- Davidyan, A.G., V.N. Kiva and V.M. Platonov (1992b). Batch-Type Fractionation in Two-Section Column with Central Reservoir [*Middle Vessel*] and Different Vapor Flow Rates in Sections. *Theor. Found. Chem. Eng.* **26**(2), 163–172.
- Davidyan, A.G., V.N. Kiva and V.M. Platonov (1993). The Minimal-Reflux Regime in a Rectification Column with a Middle Reservoir [*Middle Vessel*]. *Theor. Found. Chem. Eng.* **27**(4), 373–380.
- Davidyan, A.G., V.N. Kiva, G.A. Meski and M. Morari (1994). Batch Distillation with a Middle Vessel. *Chem. Eng. Sci.* **49**(18), 3033–3051.
- Diwekar, U.M. (1995). *Batch Distillation. Simulation, Optimal Design and Control*. Series in Chem. and Mech. Eng., Taylor & Francis.
- Doherty, M.F. (1985). The Presynthesis Problem for Homogeneous Azeotropic Distillation Has a Unique Explicit Solution. *Chem. Eng. Sci.* **40**(10), 1885–1889.
- Doherty, M.F. and G.A. Calderola (1985). Design and Synthesis of Homogenous Azeotropic Distillations 3. The Sequencing of Columns for Azeotropic and Extractive Distillation. *Ind. Eng. Chem. Fundam.* **24**(4), 474–485.
- Doherty, M.F. and J.D. Perkins (1978a). On the Dynamics of Distillation Processes I. The Simple Distillation of Multicomponent Non-Reacting, Homogeneous Liquid Mixtures. *Chem. Eng. Sci.* **33**, 281–301.
- Doherty, M.F. and J.D. Perkins (1978b). On the Dynamics of Distillation Processes II. The Simple Distillation of Model Solutions. *Chem. Eng. Sci.* **33**, 569–578.
- Doherty, M.F. and J.D. Perkins (1979a). On the Dynamics of Distillation Processes III. The Topological Structure of Ternary Residue Curve Maps. *Chem. Eng. Sci.* **34**, 1401–1414.
- Doherty, M.F. and J.D. Perkins (1979b). The Behaviour of Multicomponent Azeotropic Distillation Processes. *Inst. Chem. E. Symp. Ser.* **56**, 4.2/21–4.2/48.
- Doherty, M.F. and J.F. Knapp (1993). *Distillation, Azeotropic and Extractive*. Vol. 8. fourth ed.. Kirk-Othmer Enc. Chem. Tech.
- Drew, J.W. (1975). Design for Solvent Recovery. *Chem. Eng. Prog.* **71**(2), 92–99.
- Drew, J.W. (1997). Solvent Recovery. *Handbook of Separation Techniques for Chemical Engineers*.

- Düssel, R. and J. Stichlmair (1995). Separation of Azeotropic Mixtures by Batch Distillation Using an Entrainer. *Comp. Chem. Eng.* **19**(Suppl.), S113–S118.
- Esbjerg, K., T.R. Andersen, D. Müller, W. Marquardt and S.B. Jørgensen (1998). Static Multiplicities in Heterogeneous Azeotropic Distillation Sequences. *DYCOPS-5, 5th IFAC Symposium on Dynamics and Control of Process Systems, Corfu, Greece, June 8-10, 1998*, 393–398.
- Ewell, R.H. and L.M. Welch (1945). Rectification in Ternary Systems Containing Binary Azeotropes. *Ind. Eng. Chem. Res.* **37**(12), 1224–1231.
- Ewell, R.H., J.M. Harrison and L. Berg (1944). Azeotropic Distillation. *Ind. Eng. Chem. Res.* **36**(10), 871–875.
- Fair, J.R. (1987). Distillation: Whither, Not Whether. *I. Chem. E. Symposium Series* **104**, A613–A627.
- Farschman, C.A. and U. Diwekar (1996). Dual Composition in a Novel Batch Distillation Column. AIChE Annual Meeting, Chicago, November, 1996.
- Fidkowski, Z.T., M.F. Doherty and M.F. Malone (1993). Feasibility of Separations for Distillation of Nonideal Ternary Mixtures. *AIChE J.* **39**(8), 1303–1321.
- Fien, G.-J.A.F. and Y.A. Liu (1994). Heuristic Synthesis and Shortcut Design of Separation Processes Using Residue Curve Maps: A Review. *Ind. Eng. Res.* **33**, 2505–2522.
- Flemming, H.L. and C.S. Slater (1992). *Membrane Handbook*. Chapman & Hall, London.
- Foucher, E.R., M.F. Doherty and M.F. Malone (1991). Automatic Screening of Entrainers for Homogeneous Azeotropic Distillation. *Ind. Eng. Chem. Res.* **30**, 760–772.
- Furlonge, H.I., C.C. Pantelides and E. Sørensen (1999). Optimal Operation of Multivessel Batch Distillation Columns. *AIChE J.* **45**(4), 781–801.
- Furter, W.F. (1968). Salt Effect in Distillation: A Technical Review. *Chem. Eng.*
- Furtzer, I.A. (1994). Synthesis of Entrainers in Heteroazeotropic Distillation Systems. *Canadian J. Chem. Eng.* **72**, 358–364.
- Gmehling, J., J. Menke, J. Krafczyk and K. Fischer (1994). *Azeotropic Data, Part I and Part II*. VCH-Publishers, Weinheim, New York.
- Gmehling, J., U. Onken and W. Arlt (1977-1990). *Vapor-Liquid Equilibrium Data Collection*. Vol. I/1-8. DECHEMA Chemistry Data Series. Frankfurt/Main, Germany.
- Gmehling, J. and C. Möllmann (1998). Synthesis of Distillation Processes Using Thermodynamic Models and the Dortmund Data Bank. *Ind. Eng. Chem. Res.* **37**(8), 3112–3123.
- Goldblatt, M.E. and C.H. Gooding (1986). An Engineering Analysis of Membrane-Aided Distillation. *AIChE Symp. Series* **82**(248), 51–69.

- Guerreri, G. (1992). Membrane Alcohol Separation Process - Integrated Pervaporation and Fractional Distillation. *Trans. IChemE.* **70**(A), 501–508.
- Gurikov, Y.V. (1958). Structure of the Vapor-Liquid Equilibrium Diagrams of Ternary Homogeneous Solutions (in Russian). *Russ. J. Phys. Chem.* **32**(9), 1980–1996. Abstract in English.
- Güttinger, T.E. and M. Morari (1996). Multiple Steady States in Homogeneous Separation Sequences. *Ind. Eng. Chem. Res.* **35**(12), 4597–4611.
- Güttinger, T.E. and M. Morari (1997). Predicting Multiple Steady States in Distillation: Singularity Analysis and Reactive Systems. *PSE '97-ESCAPE-7, 25-29 May, 1997, Trondheim, Norway, Supplement to Computers Chem. Engng.* **21**, S995–S1001. See C97-2.
- Haase, R. (1949). Zur Thermodynamik flüssiger Dreistoffgemische (in German). *Z. Naturforsch.* **4a**, 342–352.
- Haase, R. (1950a). Verdampfungsgleichgewichte von Mehrstoffgemischen: VI. Ternare Systeme mit Mischungslücke (in German). *Z. Naturforsch* **5a**(2), 109–124.
- Haase, R. (1950b). Verdampfungsgleichgewichte von Mehrstoffgemischen: VII. Ternären Azeotropen Punkte (in German). *Z. Phys. Chemie* **195**, 362–385.
- Haase, R. and H. Lang (1951). Rektifikationslinien Ternärer Systeme (in German). *Chem. Ing. Tech.* **23**(13), 313–336.
- Halvorsen, I.J. and S. Skogestad (1999). Use of Short-Cut Methods to Analyse Optimal Operation of Petlyuk Distillation Columns. *PRES'99, 2nd Conference on Process Integration, Modelling and Optimization for Energy Saving and Pollution Reduction, May 31 - June 2, 1999, Budapest, Hungary.*
- Hasebe, S., B. Abdul Aziz, I. Hashimoto and T. Watanabe (1992). Optimal Design and Operation of Complex Batch Distillation Column. *Proc. IFAC Workshop on Interactions Between Process Design and Process Control* (Pergamon Press, Ed.). Oxford (UK), 177–182.
- Hasebe, S., M. Noda and I. Hashimoto (1997). Optimal Operation Policy for Multi-Effect Batch Distillation System. *PSE'97-ESCAPE-7, 25-29 May 1997, Trondheim, Norway, Suppl. to Comp. Chem. Eng.* **21**, S1221–S1226.
- Hasebe, S., T. Kurooka and I. Hashimoto (1995). Comparison of the Separation Performances of a Multi-Effect Batch Distillation System and a Continuous Distillation System. *Proc. IFAC Symp. DYCORDER+ '95, Elsingore, Denmark, published by Pergamon Press*, 249–254.
- Hilmen, E.K., S. Skogestad, M.F. Doherty and M.F. Malone (1997). Intergrated Design, Operation and Control of Batch Extractive Distillation with a Middle Vessel. Presented at AIChE Annual Meeting, Los Angeles, CA, November, 1997.
- Hoffman, E.J. (1964). *Azeotropic and Extractive Distillation*. Vol. IV. Intersci. Lib. Chem. Engng. and Processing, John Wiley & Sons, Inc.

- Hömmerich, U. and R. Rautenbach (1998). Design and Optimization of Combined Pervaporation/Distillation Processes for the Production of MTBE. *J. Membrane Sci.* **146**, 53–64.
- Horsley, L.H. (1973). *Azeotropic Data - III*. Advances in Chemistry Series 116, Ed. R.F. Gould, American Chemistry Society, Washington, DC.
- Humphrey and Seibert (1992). New Horizons. *Chem. Eng.*, 86–98.
- Jacobsen, E.W., L. Laroche and M. Morari (1991). Robust Control of Homogeneous Azeotropic Distillation Columns. *AIChE J.* **37**(12), 1810–1824.
- Jaksland, C.A., G. Hytoft and R. Gani (1997). Computer-Aided Process Design and Optimization with Novel Separation Units. *Appl. Thermal Eng.* **17**(8-10), 973–980.
- Jaksland, C.A., R. Gani and K.M. Lien (1995). Separation Process Design and Synthesis Based on Thermodynamic Insights. *Chem. Eng. Sci.* **50**(3), 511–530.
- Julka, V. and M.F. Doherty (1993). Geometric Nonlinear Analysis of Multicomponent Nonideal Distillation: A Simple Computer-Aided Design Procedure. *Chem. Eng. Sci.*, 1367–1391.
- King, C.J. (1980). *Separation Processes*. 2nd ed.. Mc-Graw Hill.
- Kiva, V.N. and B.M. Alukhanova (1997). Multiple Steady States of Distillation and Its Realization. *PSE '97-ESCAPE-7, 25-29 May, 1997, Trondheim, Norway, Supplement to Computers Chem. Engng.* **21**, S541–S546.
- Kiva, V.N. and L.A. Serafimov (1973). Rules that Govern the Composition Trajectories of Simple Distillation of Ternary Mixtures [Non-local Rules of the Movement of Process Lines for Simple Distillation in Ternary Systems]. *Russ. J. Phys. Chem.* **47**(3), 638–642.
- Kiva, V.N. and L.A. Serafimov (1973c). Batch Distillation of Ternary Mixtures at Constant Reflux Ratio, II. Analysis of the Dynamic System of the Distillate and the Splitting into Regions of Distillation. *Russ. J. Phys. Chem.* **47**(3), 634–637.
- Kiva, V.N. and L.A. Serafimov (1975). Structure of Phase Vapor-Liquid Diagrams of Ternary Mixtures and Rectification Boundaries. *CHISA'75, Prague, 1975, Lecture Summaries H-2*, 26.
- Kiva, V.N. and L.A. Serafimov (1976a). Localization of Boundaries for Batch Distillation of Ternary Mixtures. *Russ. J. Phys. Chem.* **50**(10), 2481–2483.
- Kiva, V.N. and L.A. Serafimov (1976b). Regions of Continuous Distillation of Ternary Mixtures and Location of Their Boundaries I. Conditions of Total Reflux. *Russ. J. Phys. Chem.* **50**(4), 526–528 [882–885].
- Kiva, V.N., I.M. Marchenco and Yu.N. Garber (1993). Possible Compositions of the Products of Ternary–Mixture Rectification with a Binary Saddle. *Theor. Found. Chem. Eng.* **27**(4), 336–342.

- Kiva, V.N., V.V. Starostin, V.A. Cherepakhina and V.S. Timofeev (1988). Separation of Mixtures by Rectification Redistribution. *Soviet Chemical Industry* **20**(9), 45–47.
- Kjensgjord, E. (1998). Modelling and Optimisation of Batch Extractive Distillation. Norwegian University of Science and Technology: Diploma work.
- Knapp, J.P. and M.F. Doherty (1990). Thermal Integration of Homogeneous Azeotropic Distillation Sequences. *AIChE J.* **36**(7), 969–984.
- Knapp, J.P. and M.F. Doherty (1994). Minimum Entrainer Flow for Extractive Distillation: a Bifurcation Theoretic Approach. *AIChE J.* **40**(2), 243–268.
- Knauf, R., U. Meyer-Blumenroth and J. Semel (1998). Membrane Processes in the Chemical Industry [in German]. *Chem. Ing. Tech.* **70**, 1265–1270.
- Kogan, L.V. and V.V. Kafarov (1977a). Determination of the Boundaries of Rectification Regions. Communication I.. *Russ. J. Appl. Chem.* **50**(2), 302–305 [323–326].
- Kogan, L.V. and V.V. Kafarov (1977b). Determination of the Boundaries of Rectification Regions. Communication II.. *Russ. J. Appl. Chem.* **50**(2), 306–309 [326–329].
- Kogan, V.B. (1971). *Azeotropic and Extractive Distillation (in Russian)*. Vol. 2nd edition. Chemistry Publishing Co., Leningrad.
- Köhler, J., H. Haverkamp and N. Schadler (1995). Discontinuous Rectification of Azeotropic Mixtures with Use of Auxiliary Substances (in German). *Chem. Ing. Tech.* **67**(8), 967–971.
- Komarova, L.F., L.A. Serafimov and Yu.N. Garber (1974). Classification of Ternary Mixtures with Biazeotropic Constituents. *Russ. J. Phys. Chem.* **48**(6), 1391–1396 [817–818].
- Kunesh, J.G., H.Z. Kister, M.J. Lockett and J.R. Fair (1995). Distillation: Still Towering Over Other Options. *Chem. Eng. Prog.* **18**(Oct.), 43–54.
- Kushner, T.M., G.V. Shul'ga and L.A. Serafimov (1992). Evolution of VLE diagrams of Biazeotropic Binary Mixtures with Variation of Pressure. In *Paper Collection "Problems of thermodynamics of heterogeneous systems and the theory of interfacial effects", Issue 9, St.Petersburg University, St.Petersburg*, 64–81.
- Lang, P., H. Yatim, P. Moszkowicz and M. Otterbein (1994). Batch Extractive Distillation Under Constant Reflux Ratio. *Comp. Chem. Eng.* **18**(11/12), 1057–1069.
- Lang, P., Z. Lelkes, P. Moszkowicz, M. Otterbein and H. Yatim (1995). Different Operational Policies for the Batch Extractive Distillation. *Comp. Chem. Engng.* **19**(Suppl.), S645–S650.
- Laroche, L., N. Bekiaris, H.W. Andersen and M. Morari (1992a). Homogeneous Azeotropic Distillation: Separability and Flowsheet Synthesis. *Ind. Eng. Chem. Res.* **31**(9), 2190–2209.
- Laroche, L., N. Bekiaris, H.W. Andersen and M. Morari (1992b). The Curious Behavior of Homogeneous Azeotropic Distillation - Implications for Entrainer Selection. *AIChE J.* **38**(9), 1309–1328.

- Laroche, L., N. Bekiaris, H.W. Andersen and M. Morari (1993). Homogeneous Azeotropic Distillation: Comparing Entrainers. *Can. J. Chem. Eng.* **69**(Dec.), 1302–1319.
- Lecat, M. (1949). *Tables Azéotropiques, Azéotropes Binaries Orthobares*. Brussels.
- Lelkes, Z., P. Lang and M. Otterbein (1998b). Feasibility and Sequencing Studies for Homoazeotropic Distillation in a Batch Rectifier with Continuous Entrainer Feeding. *Comput. Chem. Eng.* **22**(Suppl.), S653–S656.
- Lelkes, Z., P. Lang, B. Benadda and P. Moszkowicz (1998a). Feasibility of Extractive Distillation in a Batch Rectifier. *AIChE J.* **44**(4), 810–822.
- Lelkes, Z., P. Lang, P. Moszkowicz, B. Benadda and M. Otterbein (1998c). Batch Extractive Distillation: The Process and the Operational Policies. *Chem. Eng. Sci.* **53**(7), 1331–1348.
- Lestak, F. and C. Collins (1997). Advanced Distillation Saves. *Chem. Engng.* **July**, 72–76.
- Levy, S.G. and M.F. Doherty (1986). Design and Synthesis of Homogeneous Azeotropic Distillations. 4. Minimum Reflux Calculations for Multiple-Feed Columns. *Ind. Eng. Chem. Fundam.* **25**, 269–279.
- Levy, S.G., D.B. Van Dongen and M.F. Doherty (1985). Design and Synthesis of Homogeneous Azeotropic Distillations. 2. Minimum Reflux Calculations for Nonideal and Azeotropic Columns. *Ind. Eng. Chem. Fundam.* **24**(4), 463–474.
- Li, W. and X. Xu (1998). Separation of Acetone/Water by Modified  $\gamma$ -Alumina Membrane via a New Method. *J. Membrane Sci.* **149**, 21–27.
- Malenko, Yu.I. (1970). Physicochemical Analysis of Distillation Diagrams. II. Quaternary Mixtures. *Russ. J. Phys. Chem.* **44**(7), 916–918 [1631–1636].
- Malesinski, W. (1965). *Azeotropy and Other Theoretical Problems of Vapor-Liquid Equilibrium*. Interscience, New York.
- Marchenko, I.M., V.N. Kiva and Yu.N. Garber (1992). Technological Aspects of Tie-Line Transferability in the Distillation of Class 1.0-2 Systems. *Russ. J. Appl. Chem.* **65**(2), 336–340 [279–283].
- Matsuyama, H. and H. Nishimura (1977). Topological and Thermodynamic Classification of Ternary Vapor-Liquid Equilibria. *J. Chem. Eng. Jpn.* **10**(3), 181–187.
- Meski, G.A. and M. Morari (1995). Design and Operation of a Batch Distillation with a Middle Vessel. *Comp. Chem. Eng.* **19**(Suppl.), S597–S602.
- Meski, G.A., M. Han, N. Bekiaris and M. Morari (1998). Optimality for Batch Distillation Configurations. *IFAC Symposium DYCOPS-5, Corfu, Greece, 8-19 June 1998*, 387–392.
- Milani, S.M. (1999). Optimization of Solvent Feed Rate for Maximum Recovery of High Purity Top Product in Batch Extractive Distillation. *Trans. IChemE.* **77**(Part A), 469–470.

- Mujtaba, I.M. (1999). Optimization of Batch Extractive Distillation Processes for Separating Close Boiling and Azeotropic Mixtures. *Trans. IChemE*. **77**(Part A), 588–596.
- Mujtaba, I.M. and S. Macchietto (1998). Holdup Issues in Batch Distillation - Binary Mixtures. *Chem. Engng. Sci.* **53**(14), 2519–2530.
- Müller, E. (1988). *Liquid-Liquid Extraction*. Vol. B3. Ullmann's Enc. Ind. Chem.
- Nikolaev, E.S., V.N. Kiva, A.S. Mozzhukhin and L.A. Serafimov (1979). Use of Functional Operators to Determine Continuous Distillation Regions. *Theor. Found. Chem. Eng.* **13**(4), 493–498.
- Ognisty, T.P. (1995). Analyze Distillation Columns With Thermodynamics. *Chem. Eng. Prog.*, 40–46.
- Ostwald, W. (1902). *Lehrbuch der Allgemeinen Chemie. Verwandtschaftslehre. Erste Teil (In German)*. Verlag von Wilhelm Engelmann, Leipzig, Germany.
- Pelkonen, S., R. Kaesemann and A. Górak (1997). Distillation Lines for Multicomponent Separation in Packed Columns: Theory and Comparison with Experiment. *Ind. Eng. Chem. Res.* **36**, 5392–5398.
- Perry, R.H. (1997). *Perry's Chemical Engineers' Handbook*. Chem. Engng. Series. 7th ed.. Green, D.W. and Maloney, J.O. (Eds.), McGraw Hill, Inc., New York.
- Perry, R.H. and C.H. Chilton (1963). *Chemical Engineers' Handbook*. Chem. Engng. Series. 4th ed.. McGraw Hill, Inc., New York.
- Perry, R.H. and C.H. Chilton (1973). *Chemical Engineers' Handbook*. Chem. Engng. Series. 5th ed.. McGraw Hill, Inc., New York.
- Peterson, E.J. and L.R. Partin (1997). Temperature Sequences for Categorizing All Ternary Distillation Boundary Maps. *Ind. Eng. Chem. Res.* **36**(5), 1799–1811.
- Petlyuk, F.B. (1978). Rectification of Zeotropic, Azeotropic and Continuous Mixtures in Simple and Complex Infinite Columns with Finite Reflux. *Theor. Found. Chem. Eng.* **12**, 671–678.
- Petlyuk, F.B. and L.A. Serafimov (1983). *Multicomponent Distillation. Theory and Design (in Russian) [Mnogokomponentnaya Rektifikatsiya: Teriyo I. Raschet]*. Chemistry Publishing Co, Moscow.
- Petlyuk, F.B. and R.Yu. Danilov (2000). Synthesis of Separation Flowsheets for Multicomponent Azeotropic Mixtures on the Basis of the Distillation Theory. Presynthesis: Prediction of Feasible Product Compositions. *Theor. Found. Chem. Eng.* **34**(3), 265–285.
- Petlyuk, F.B. and V.S. Avet'yan (1971). Investigation of the Rectification of Three-Component Mixtures with Infinite Reflux. *Theor. Found. Chem. Eng.* **5**(4), 499–507.



- Petlyuk, F.B., V.Ya. Kievski and L.A. Serafimov (1975a). Thermodynamic and Topologic Analysis of the Phase Diagram of Polyazeotropic Mixtures. I. Algorithm for Construction of Structural Graphs for Azeotropic Ternary Mixtures. *Russ. J. Phys. Chem.* **69**(12), 3105–3108.
- Petlyuk, F.B., V.Ya. Kievski and L.A. Serafimov (1975b). Thermodynamic and Topologic Analysis of the Phase Diagram of Polyazeotropic Mixtures. I. Definition of Distillation Regions Using a Computer [*Computer-Aided Determination of Distillation Regions*]. *Russ. J. Phys. Chem.* **69**(12), 3102–3104.
- Petlyuk, F.B., V.Ya. Kievski and L.A. Serafimov (1977a). Thermodynamic-Topological Analysis of VLE Diagrams for Multicomponent Mixtures. III. Algorithm of Structure Graph Drawing for Four-Component Mixtures. *Russ. J. Phys. Chem.* **71**(2), 315–318.
- Petlyuk, F.B., V.Ya. Kievski and L.A. Serafimov (1978). Thermodynamic-Topological Analysis of VLE Diagrams for Multicomponent Mixtures. IV. Use of the Structure Matrix for Analysis of Feasible Separations of the Wood Pyrolysis Product. *Russ. J. Phys. Chem.* **72**(5), 1145–1148.
- Petlyuk, F.B., V.Ya. Kievskii and L.A. Serafimov (1977b). A Combined Thermodynamic and Topological Analysis of Phase Equilibrium Diagrams for Polyazeotropic Systems - V. The Use of the Phase Equilibrium Model in Combined Thermodynamic and Topological Analysis. *Russ. J. Phys. Chem.* **51**, 338–340.
- Petlyuk, F.B., V.Ya. Kievski and L.A. Serafimov (1977c). Method for the Isolation of the Regions of Rectification of Polyazeotropic Mixtures Using an Electronic Computer [*Computer-Aided Determination of Distillation Regions for Multicomponent Mixtures*]. *Theor. Found. Chem. Eng.* **11**(1), 3–10.
- Pettersen, T. and K. Lien (1995). Design of Hybrid Distillation and Vapor Permeation Processes. *J. Membrane Sci.* **99**, 21–03.
- Pham, H.N. and M.F. Doherty (1990a). Design and Synthesis of Heterogeneous Azeotrope Distillation-I. Heterogeneous Phase Diagrams. *Chem. Eng. Sci.* **45**(7), 1823–1836.
- Pham, H.N. and M.F. Doherty (1990b). Design and Synthesis of Heterogeneous Azeotrope Distillation-II. Residue Curve Maps. *Chem. Eng. Sci.* **45**(7), 1837–1844.
- Pham, H.N. and M.F. Doherty (1990c). Design and Synthesis of Heterogeneous Azeotrope Distillation-III. Column Sequences. *Chem. Eng. Sci.* **45**(7), 1845–1854.
- Phimister, J.R. and W.D. Seider (2000a). Distillate-Bottoms Control of Middle-Vessel Distillation Columns. *Ind. Eng. Chem. Res.* **39**, 1840–1849.
- Phimister, J.R. and W.D. Seider (2000b). Semicontinuous, Middle-Vessel, Extractive Distillation. *Comp. Chem. Engng.* **24**, 879–885.

- Pöllmann, P. and E. Blass (1994). Best Products of Homogeneous Azeotropic Distillations. *Gas Sep. Purif.* **8**(4), 194–228.
- Pöllmann, P., M.H. Bauer and E. Blass (1996). Investigation of Vapour-Liquid Equilibrium of Non-Ideal Multicomponent Systems. *Gas Sep. Purif.* **10**(4), 225–241.
- Pratt, H.R.C. (1967). *Countercurrent Separation Processes*. Elsevier Publishing Company, Amsterdam.
- Pressly, T.G. and K.M. Ng (1998). A Break-Even Analysis of Distillation-Membrane Hybrids. *AIChE. J.* **44**(1), 93–105.
- Pretel, E.J., P.A. Lopez, S.B. Bottini and E.A. Brignole (1994). Computer-Aided Molecular Design of Solvent for Separation Processes. *AIChE. J.* **40**(8), 1349–1360.
- Prigogine, I. and R. Defay (1954). *Chemical Thermodynamics*. Longmans & Green, London.
- Rautenbach, R. and J. Vier (1995). Design and Analysis of Combined Distillation/Pervaporation Processes. *Proc. Seventh International Conference on Pervaporation Processes in the Chemical Industry, Reno (NV)*, 70–85.
- Rautenbach, R. and R. Albrecht (1989). *Membrane Processes*. John Wiley, New York.
- Rautenbach, R., S. Klatt and J. Vier (1992). State of the Art of Pervaporation - 10 Years of Industrial PV. *Proc. 6th International Conference on Pervaporation Processes in the Chemical Industry, Ottawa*, 2–15.
- Reinders, W. and C.H. de Minjer (1940). Vapour-Liquid Equilibria in Ternary Systems I. The Course of the Distillation Lines. *Rec. Trav. Chem.* **59**, 207–230.
- Reinders, W. and C.H. DeMinjer (1940a). Vapour-Liquid Equilibria in Ternary Systems. II. The System Acetone-Chloroform-Benzene. *Rec. Trav. Chem.* **59**, 369–391.
- Reinders, W. and C.H. DeMinjer (1940b). Vapour-Liquid Equilibria in Ternary Systems. III. The Course of the Distillation Lines in the System Acetone-Chloroform-Benzene. *Rec. Trav. Chem.* **59**, 392–406.
- Reinders, W. and C.H. DeMinjer (1947a). Vapour-Liquid Equilibria in Ternary Systems. IV. The System Water-Acetone-Trichloroethene. *Rec. Trav. Chem.* **66**(9/10), 552–563.
- Reinders, W. and C.H. DeMinjer (1947b). Vapour-Liquid Equilibria in Ternary Systems. V. The System Water-Formic Acid-Metaxylene. *Rec. Trav. Chem.* **66**(9/10), 564–572.
- Reinders, W. and C.H. DeMinjer (1947c). Vapour-Liquid Equilibria in Ternary Systems. VI. The System Water-Acetone-Chloroform. *Rec. Trav. Chem.* **66**(9/10), 573–604.
- Reshetov, S.A. (1998). Private communications. Karpov Institute of Physical Chemistry, Moscow.

- Reshetov, S.A., I.B. Zhvanetskij and E.V. Orlova (1999). Modeling of Continuous Distillation of Ternary Mixtures with Phase Diagrams Containing One-Side Unity  $\alpha$ -Lines. *Theor. Found. Chem. Eng.* **33**(2), 149–155.
- Reshetov, S.A., V.Yu. Sluchnikov, V.S. Ryzhova and I.B. Zhvanetskij (1990). Diagrams of K-Ordering Regions with an Arbitrary Number of Unitary  $\alpha$ -Lines [*Univolatility Lines*]. *Russ. J. Phys. Chem.* **64**(9), 1344–1347 [2498–2503].
- Rev, E. (1992). Crossing of Valleys, Ridges, and Simple Boundaries by Distillation in Homogeneous Ternary Mixtures. *Ind. Eng. Chem. Res.* **31**(3), 893–901.
- Robinson, C.S. and E.R. Gilliland (1950). *Elements of Fractional Distillation*. Vol. 4. McGraw Hill, Inc., New York.
- Robinson, E.R. (1970). Optimal control of an industrial batch distillation column. *Chem. Eng. Sci.*, 921–928.
- Rooks, R.E., V. Julka, M.F. Doherty and M.F. Malone (1998). Structure of Distillation Regions for Multicomponent Azeotropic Mixtures. *AIChE Journal* **44**(6), 1382–1391.
- Rousseau, R.W. (1987). Handbook of Separation Process Technology. *Book*; Wiley, New York.
- Safrit, B.T. (1996). Synthesis of Azeotropic Batch Distillation Separation Systems. PhD thesis. Carnegie Mellon University, Pittsburgh, USA.
- Safrit, B.T. and A.W. Westerberg (1997a). Algorithm for Generating the Distillation Regions for Azeotropic Multicomponent Mixtures. *Ind. Eng. Chem. Res.* **36**, 1827–1840.
- Safrit, B.T. and A.W. Westerberg (1997b). Improved Operational Policies for Batch Extractive Distillation Columns. *Ind. Eng. Chem. Res.* **36**, 436–443.
- Safrit, B.T. and A.W. Westerberg (1997c). Synthesis of Azeotropic Batch Distillation Systems. *Ind. Eng. Chem. Res.* **36**, 1841–1854.
- Safrit, B.T., A.W. Westerberg, U. Diwekar and O.M. Wahnschafft (1995). Extending Continuous Conventional and Extractive Distillation Feasibility Insights to Batch Distillation. *Ind. Eng. Chem. Res.* **34**, 3257–3264.
- Schreinemakers, F.A.H. (1901a). Dampfdrucke Ternärer Gemische. Theoretischer Teil: Dritte Abhandlung (In German). *Z. Phys. Chem.* **36**(6), 710–740.
- Schreinemakers, F.A.H. (1901b). Dampfdrucke ternärer Gemische. Theoretischer Teil: Erste Abhandlung (In German). *Z. Phys. Chem.* **36**(3), 257–289.
- Schreinemakers, F.A.H. (1901c). Dampfdrucke Ternärer Gemische. Theoretischer Teil: Zweite Abhandlung (In German). *Z. Phys. Chem.* **36**(4), 413–449.
- Schreinemakers, F.A.H. (1902). Einige Bemerkungen über Dampfdrucke Ternärer Gemische (In German). *Z. Phys. Chem.* **43**, 671–685.

- Schweitzer, P.A. (1979). Handbook of Separation Techniques for Chemical Engineers. *Book; McGraw-Hill*. Section 1.3.
- Schweitzer, P.A. (1997). Handbook of Separation Techniques for Chemical Engineers. *Book; McGraw-Hill*.
- Seader, J.D. and E.J. Henley (1998). *Separation Process Principles*. John Wiley & Sons, Inc., New York.
- Serafimov, L.A. (1968a). Separation Technology of Azeotropic Mixtures (in Russian). *Book: Azeotropy and Polyazeotropy, Chapter XXI (additional chapter in Russian edition), W. Świątosławski (Ed.), Chemistry Publishing Co., Moscow, 186–224*.
- Serafimov, L.A. (1968b). The Azeotropic Rule and the Classification of Multicomponent Mixtures. II. The Form [*Behavior*] of Distillation Lines [*Residue Curves*] Near Four-Component Singular Points. *Russ. J. Phys. Chem.* **42**(1), 130–131 [248–252].
- Serafimov, L.A. (1968c). The Azeotropic Rule and the Classification of Multicomponent Mixtures. III. Distribution of Singular Points in the Phase Diagram for Liquid-Vapor Equilibrium in Four-Component Mixtures. *Russ. J. Phys. Chem.* **42**(1), 132–135 [252–256].
- Serafimov, L.A. (1968d). Theoretical Principles of Distillation Sequences Design and Synthesis for Nonideal Multicomponent Mixtures (in Russian). PhD thesis. Lomonosov Institute of Fine Chemical Technology, Moscow.
- Serafimov, L.A. (1969a). The Azeotropic Rule and the Classification of Multicomponent Mixtures. IV. Principal Equations for the Calculation of Liquid-Vapor Phase Equilibrium Diagrams for Four-Component Mixtures. *Russ. J. Phys. Chem.* **43**(3), 621–624.
- Serafimov, L.A. (1969b). The Azeotropic Rule and the Classification of Multicomponent Mixtures V. Analysis of Liquid-Vapor Phase Equilibrium Diagrams for Quaternary Mixtures. *Russ. J. Phys. Chem.* **43**(5), 749–751 [1343–1346].
- Serafimov, L.A. (1969c). The Azeotropic Rule and the Classification of Multicomponent Mixtures VI. n-Component Mixtures. *Russ. J. Phys. Chem.* **43**(7), 981–983.
- Serafimov, L.A. (1970a). General Principles of the Course of Unidistribution Lines in Vapor-Liquid Equilibrium Diagrams of Ternary Mixtures. *Physical-Chemical Foundations of Rectification*, *Collection of papers by Moscow Lomonosov Institute of Fine Chemical Technology, MITChT, Moscow, 20–30*.
- Serafimov, L.A. (1970b). The Azeotropic Rule and the Classification of Multicomponent Mixtures VII. Diagrams for Ternary Mixtures. *Russ. J. Phys. Chem.* **44**(4), 567–571 [1021–1027].
- Serafimov, L.A. (1971a). The Azeotropic Rule and the Classification of Multicomponent Mixtures. IX. Tangential Azeotropy and Correlation Between the General Relation Between Singular Points of Various Types. *Russ. J. Phys. Chem.* **45**(6), 831–833 [1473–1476].

- Serafimov, L.A. (1971*b*). The Azeotropic Rule and the Classification of Multicomponent Mixtures. VIII. The General Relations of Tangential Azeotropy. *Russ. J. Phys. Chem.* **45**(5), 638–642 [1140–1147].
- Serafimov, L.A. (1971*c*). The Azeotropic Rule and the Classification of Multicomponent Mixtures. X. Doubly Tangential Azeotropes. *Russ. J. Phys. Chem.* **45**(6), 918–921 [1620–1625].
- Serafimov, L.A. (1971*d*). The Azeotropic Rule and the Classification of Multicomponent Mixtures. XI. Tangential Azeotropy for Three-Component Systems and Chains of Topological Structures. *Russ. J. Phys. Chem.* **45**(10), 1388–1389 [2448–2450].
- Serafimov, L.A. (1987). Thermodynamic Topological Analysis and Separation of Multicomponent Polyazeotropic Mixtures. *Theor. Found. Chem. Eng.* **21**(1), 44–54.
- Serafimov, L.A. (1996). Thermodynamic and Topological Analysis of Liquid-Vapor Phase Equilibrium Diagrams and Problems of Rectification of Multicomponent Mixtures. *Book: Mathematical Methods in Contemporary Chemistry, S.I. Kuchanov (Ed.) Gordon and Breach Publishers, Amsterdam*, 557–605.
- Serafimov, L.A. and A.K. Frolkova (1997). Fundamental Principle of Concentration-Field Redistribution Between Separation Regions as a Basis for the Design of Technological Systems. *Theor. Found. Chem. Eng.* **31**(2), 159–166.
- Serafimov, L.A., L.F. Komoarova and Yu.N. Garber (1974). Classification of VLE Diagrams for Ternary Mixtures with Biazeotropic Constituents. *Russ. J. Phys. Chem.* **48**(6), 1391.
- Serafimov, L.A., T.M. Kushner and T.V. Cheluskina (1996). Thermodynamic-Topological Analysis of VLE Diagrams for Ternary Mixtures with Two Ternary Azeotropes. *In Papers Collection: Problems of Thermodynamics of Heterogeneous Systems and the Theory of Interfacial Effects*, Issue 10, St.Petersburg University, St.Petersburg, 26–55.
- Serafimov, L.A., V.S. Timofeyev and M.I. Balashov (1973). Rectification of Multicomponent Mixtures II. Local and General Characteristics of the Trajectories of Rectification Processes at Infinite Reflux Ratio. *Acta Chemica Acad. Sci. Hung.* **75**(2), 193–211.
- Serafimov, L.A., V.T. Zharov and V.S. Timofeyev (1971). Rectification of Multicomponent Mixtures I. Topological Analysis of Liquid-Vapor Phase Equilibrium Diagrams. *Acta Chemica Acad. Sci. Hung.* **69**(4), 383–396.
- Serafimov, L.A., Yu.E. Gol'berg, T.A. Vitman and V.N. Kiva (1972). Properties of Univolatility Sets and Its Location in the Concentration Space (in Russian). *In book: "Chemistry. Collection of the Scientific Works of Ivanovo Energetic Institute"*, Ivanovo-Vladimir, Issue 14, 166–179.
- Skogestad, S. (1992). Dynamics and Control of Distillation Columns – A Critical Survey. *IFAC Symposium Dycord+ '92, Maryland, Apr. 27-29, 1992*.

- Skogestad, S., B. Wittgens, R. Litto and E. Sørensen (1997). Multivessel Batch Distillation. *AIChE J.* **43**(4), 971–978.
- Sluchenkov, V.Yu., S.A. Reshetov and I.B. Zhvanetskij (1990). Unit  $\alpha$ -Lines in Three-Component Systems with a Ternary Azeotrope [Univolatility Lines in Ternary Mixtures with Ternary Azeotropes]. *Russ. J. Phys. Chem.* **64**(5), 737–739 [1381–1384].
- Smith, R. (1995). *Chemical Process Design*. McGraw-Hill, Inc.
- Sobolev, D.M., I.L. Shul'gin, V.A. Lovchikov, Yu.I. Malenko and P.G. Romankov (1980). Boundaries of Distillation Regions. *Russ. J. Phys. Chem.* **53**(11), 2566–2567.
- Sørensen, E. (1994). Studies on Optimal Operation and Control of Batch Distillation Columns. 1994:62. Norwegian Institute of Technology.
- Sørensen, E. (1997). Alternative Ways of Operating a Batch Distillation Column. *Distillation and Absorption '97, IChemE Symposium, Maastricht, The Netherlands, 8-10 September, 1997*, 643–652.
- Sørensen, E. (1999). A Cyclic Operating Policy for Batch Distillation - Theory and Practice. *Comp. Chem. Eng.* **23**(4-5), 533–542.
- Sørensen, E. and M. Prenzler (1997). A Cyclic Operating Policy for Batch Distillation - Theory and Practice. *PSE '97-ESCAPE-7, 25-29 May, 1997, Trondheim, Norway, Supplement to Computers Chem. Engng.* **21**, S1215–S1220.
- Sørensen, E. and S. Skogestad (1994). Optimal Operating Policies of Batch Distillation with Emphasis on the Cyclic Operating Policy. *PSE'94, 5th International Symposium on Process Systems Engineering, 30 May - 3 June 1994*, 449–456.
- Sørensen, E. and S. Skogestad (1996). Comparison of Inverted and Regular Batch Distillation. *Chem. Eng. Sci.* **51**(22), 4949–4962.
- SpeedUp (1993). SPEEDUP User Manual. Aspen Technologies, Prosys Technology Ltd.
- Stichlmair, J. (1988). *Distillation and Rectification*. Vol. B3. Ullmann's Enc. Ind. Chem.
- Stichlmair, J. and J.R. Fair (1998). *Distillation: Principles and Practices*. Wiley, New York.
- Stichlmair, J.G., J.-R. Fair and J.L. Bravo (1989). Separation of Azeotropic Mixtures via Enhanced Distillation. *Chem. Eng. Prog.* **85**(1), 63–69.
- Storonkin, A.V. (1967). Thermodynamics of Heterogeneous Systems (in Russian). *Leningrad University Publishing Dept, Leningrad*.
- Storonkin, A.V. and N.A. Smirnova (1963). The Thermodynamics of Multicomponent Heterogeneous Systems. VI. Distillation Curves in the Miscibility Gap of Ternary Systems. *Russ. J. Phys. Chem.* **37**(3), 601–607.

- Sulzer (1998). Sultzer Technical Review. *Webpages*.
- Swietoslawski, W. (1963). *Azeotropy and Polyazeotropy*. Oxford Pergamon Press.
- Tassios, D.P. (1972). Preface. *Extractive and Azeotropic Distillation*. Advances in Chemistry Series 115. American Chemistry Society, Washington DC.
- Tester, J.W. and M. Modell (1997). *Thermodynamics and Its Applications*. Third Ed., Prentice Hall, NJ.
- Thong, D.Y.-C., F.J.L. Castillo and G.P. Towler (2000). Distillation Design and Retrofit Using Stage-Composition Lines. *Chem. Eng. Sci.* **55**, 625–640.
- Timofeev, V.S, L.A. Serafimov and V.V. Beregovyh (1970). Properties of the Vapor-Liquid Equilibrium Diagrams of Heterogeneous Mixtures (in Russian). "Physiochemical Foundations of Rectification", *Collection of papers by Moscow Lomonosov Institute of Fine Chemical Technology, MITChT, Moscow*, 30–39.
- Treybal, R.E. (1963). *Liquid-Liquid Extraction*. McGraw-Hill, New York.
- Treybal, R.E. (1970). A Simple Method of Batch Distillation. *Chem. Eng.*, 95–98.
- Van Dongen, D.B. and M.F. Doherty (1984). On the Dynamics of Distillation Processes V. The Topology of the Boiling Temperature Surface and Its Relation to Azeotropic Distillation. *Chem. Eng. Sci.* **39**(5), 883–892.
- Van Dongen, D.B. and M.F. Doherty (1985a). Design and Synthesis of Homogenous Azeotropic Distillations 1. Problem Formulation for a Single Column. *Ind. Eng. Chem. Fund.* **24**(4), 454–463.
- Van Dongen, D.B. and M.F. Doherty (1985b). On the Dynamics of Distillation Processes VI. Batch Distillation. *Chem. Eng. Sci.* **40**(11), 2087–2093.
- Van Winkle, M. (1967). *Distillation*. Chem. Eng. Series. McGraw Hill, Inc.
- Vitman, T.A. and V.T. Zharov (1971a). Vapor-Liquid Equilibrium in the System Cyclohexane-Acetone-Isopropyl Alcohol-Benzene-Toluene. *Russ. J. Phys. Chem.* **45**(1), 79–80 [147–149].
- Vitman, T.A. and V.T. Zharov (1971b). Vapor-Liquid Equilibrium in the System Cyclohexane-Acetone-Isopropyl Alcohol-Toluene. *Russ. J. Phys. Chem.* **45**(1), 78–79 [145–147].
- Vogelpohl, A. (1999). On the Relation between Ideal and Real Systems in Ternary Distillation. *Trans. IChemE* **77**(9), 487–492.
- Wahnschafft, O.M. (1997). Advanced Distillation Synthesis Techniques for Nonideal Mixtures are Making Headway in Industrial Applications. *Distillation and Absorption '97, IChemE Symposium, Maastricht, The Netherlands, 8-10 September, 1997*, 613–623.

- Wahnschafft, O.M. and A.W. Westerberg (1993). The Product Composition Regions of Azeotropic Distillation Columns, 2. Separability in Two-Feed Column and Entrainer Selection. *Ind. Eng. Chem. Res.* **32**, 1108–1120.
- Wahnschafft, O.M., J.-P. le Rudulier and A.W. Westerberg (1993). A Problem Decomposition Approach for the Synthesis of Complex Separation Processes with Recycles. *Ind. Eng. Chem. Res.* **32**(6), 1121–1141.
- Wahnschafft, O.M., J.W. Koehler, E. Blass and A.W. Westerberg (1992). The Product Composition Regions of Single-Feed Azeotropic Distillation Columns. *Ind. Eng. Chem.* **31**(10), 2345–2362.
- Walas, S.M. (1985). *Phase Equilibria in Chemical Engineering*. Butterworth Publishers.
- Warter, M. and J. Stichlmair (1999). Batchwise Extractive Distillation in a Column with a Middle Vessel. *Comp. Chem. Eng. Suppl.*, S915–S918.
- Warter, M. and J. Stichlmair (2000). Batch Distillation of Azeotropic Mixtures in a Column with a Middle Vessel. *European Symposium on Computer Aided Process Engineering - 10, ESCAPE-10, Florence, Italy, May 7-10 2000*, 691–696.
- Warter, M., R. Düssel and J. Stichlmair (1997). To the Separation of Azeotropic Mixtures by Batchwise Extractive Distillation. Presented at *Dist. & Abs.'97*, Maastricht, The Netherlands, 8-10 September, 1997.
- Wasykiewicz, S.K., L.C. Kobylka and F.J.L. Castillo (1999a). Design and Synthesis of Distillation Sequences for the Separation of Multicomponent Azeotropic Mixtures. *III Sympozjum Destylacja, Absorpcja i Ekstrakcja Szklarska Poreba, 13-15 wrzesien 1999*, 83–91.
- Wasykiewicz, S.K., L.C. Kobylka and M.A. Satyro (1999b). Designing Azeotropic Distillation Columns. *Chem. Eng.*, 80–85.
- Westerberg, A.W. (1997). Separating Azeotropic Mixtures. *Systematic Methods of Chemical Process Design*, L.T. Biegler, I.E. Grossmann and A.W. Westerberg (Eds.), Prentice Hall, NJ, 455–494.
- Westerberg, A.W. and O.M. Wahnschafft (1996). Synthesis of Distillation-Based Separation Systems. *Advances in Chemical Engineering*, J.L. Anderson (Ed.), New York: Academic Press **23**, 63–170.
- Widagdo, S. and W.D. Seider (1996). Journal Review: Azeotropic Distillation. *AIChE J.* **42**(1), 96–128.
- Widagdo, S., W.D. Seider and D.H. Sebastian (1992). Dynamic Analysis of Heterogeneous Azeotropic Distillation. *AIChE J.* **38**(8), 1229–1242.
- Wijesinghe, A.M.J.C. (1985). Development of Industrial Complexes of Special Rectification Techniques for Solvent Recovery (in Russian). PhD thesis. M.V. Lomonosov Institute of Fine Chemical Engineering, Moscow, USSR.



- Wilson, R.Q., W.H. Mink, H.P. Munger and J.W. Clegg (1955). Dehydration of Hydrazine by Azeotropic Distillation. *AIChE J.* **1**(2), 220–224.
- Wittgens, B. and S. Skogestad (1997). Multivessel Batch Distillation - Experimental Verification. *Proc. Distillation & Absorption '97, Maastricht, September, IChemE Symposium Series* **142**, 239–248.
- Wittgens, B. and S. Skogestad (1998). Multivessel Batch Distillation - Potential Energy Savings. *IFAC Symposium DYCOPS-5, Corfu, Greece, 8-19 June 1998*, 515–520.
- Wittgens, B., R. Litto, E. Sørensen and S. Skogestad (1996). Total Reflux Operation of Multivessel Batch Distillation. *Comp. Chem. Engng.* **S20**, S1041–S1046.
- Yamakita, Y., J. Shiozaki and H. Matsuyama (1983). Consistency Test of Ternary Azeotropic Data by Use of Simple Distillation. *J. Chem. Eng. Jpn.* **16**(2), 145–146.
- Yatim, H., P. Moszkowicz and P. Otterbein, M. and Lang (1993). Dynamic Simulation of a Batch Extractive Distillation Process. *Comp. Chem. Eng.* **17**(Suppl.), S57–S62.
- Zharov, V.T. (1967). Free Evaporation of Homogeneous Multicomponent Solutions. *Russ. J. Phys. Chem.* **41**(11), 1539–1543.
- Zharov, V.T. (1968a). Evaporation of Homogeneous Multicomponent Solutions III. Behavior of Distillation Lines [Residue Curves] Near Singular Points. *Russ. J. Appl. Chem.* **42**(2), 195–198 [366–372].
- Zharov, V.T. (1968b). Free Evaporation of Homogeneous Multicomponent Solutions II. Four-Component Systems. *Russ. J. Appl. Chem.* **42**(1), 58–61 [116–122].
- Zharov, V.T. (1968c). Phase Transformations [Distillation Lines] and Rectification of Multicomponent Solutions. *Russ. J. Appl. Chem.* **41**(12), 2530–2536.
- Zharov, V.T. (1969a). Non-Local Relations in Vapor-Liquid Equilibrium Diagrams for Multicomponent Systems. *Russ. J. Phys. Chem.* **43**(11), 1563–1567 [2784–2791].
- Zharov, V.T. (1969b). Phase Representations [Distillation Lines] and Rectification of Many-Component Solutions - II. *Russ. J. Appl. Chem.* **42**(1), 94–98.
- Zharov, V.T. and A.V. Storonkin (1969). Local Rules in the Vicinity of a Multicomponent Azeotrope. *Russ. J. Phys. Chem.* **43**(5), 628–631 [1126–1131].
- Zharov, V.T. and L.A. Serafimov (1975). *Physicochemical Foundations of Simple Distillation and Rectification (in Russian)*. Chemistry Publishing Co., Leningrad.
- Zhvanetskij, I.B., S.A. Reshetov and V.Yu. Sluchenkov (1988). Classification of the K-Order Regions on the Distillation Line Diagram [Residue Curve Maps] for a Ternary Zeotropic System. *Russ. J. Phys. Chem.* **62**(7), 996–998 [1944–1947].

- Zhvanetskij, I.B., S.A. Reshetov and V.Yu. Sluchenkov (1989). Classification of the Diagram for the K-Ordering Regions [*Ternary Azeotropic Systems with Two and Three Binary Azeotropes*]. *Russ. J. Phys. Chem.* **63**(6), 914–916 [1653–1657].
- Zhvanetskij, I.B., S.A. Reshetov, V.Yu. Sluchenkov, E.V. Orlova and B.M. Alukhanova (1993). Diagrams of K-Ordered Regions of Three-Component [*Azeotropic*] Systems. *Theor. Found. Chem. Eng.* **27**(2), 99–106 [112–120].